TESE DE DOUTORAMENTO

DEVELOPMENT OF FAST METHODOLOGY FOR ANALYSIS AND SPECIATION OF MERCURY AND ARSENIC IN FOODSTUFF

Bedigama Kankanamge Kolita Kamal Jinadasa

ESCOLA DE DOCTORADO INTERNACIONAL

PROGRAMA DE DOUTORAMENTO EN CIENCIA E TECNOLOXÍA QUÍMICA

SANTIAGO DE COMPOSTELA

2020

USC
UNIVERSIDADE
DE SANTIAGO
DE COMPOSTELA

DECLARACIÓN DO AUTOR/A DA TESE

DEVELOPMENT OF FAST METHODOLOGY FOR ANALYSIS AND SPECIATION OF MERCURY AND ARSENIC IN FOODSTUFF

D./ Bedigama Kankanamge Kolita Kamal Jinadasa

Presento a miña tese, seguindo o procedemento axeitado ao Regulamento, e declaro que:

1) A tese abarca os resultados da elaboración do meu traballo.
2) De selo caso, na tese faise referencia ás colaboracións que tivo este traballo.
3) A tese é a versión definitiva presentada para a súa defensa e coincide coa versión enviada en formato electrónico.
4) Confirmo que a tese non incorre en ningún tipo de plaxio doutros autores nin de traballos presentados por min para a obtención doutros títulos.

En .Santiago de Compostela, 22 de xuño de 2020

Asdo. Bedigama Kankanamge Kolita Kamal Jinadasa

USC
UNIVERSIDADE
DE SANTIAGO
DE COMPOSTELA

AUTORIZACIÓN DO DIRECTOR / TITOR DA TESE

DEVELOPMENT OF FAST METHODOLOGY FOR ANALYSIS AND SPECIATION OF MERCURY AND ARSENIC IN FOODSTUFF

D. Antonio Moreda Piñeiro
Dna. Elena María Peña Vázquez

INFORMA/N:

Que a presente tese, correspóndese co traballo realizado por D. Bedigama Kankanamge Kolita Kamal Jinadasa, baixo a miña dirección, e autorizo a súa presentación, considerando que reúne os requisitos esixidos no Regulamento de Estudos de Doutoramento da USC, e que como director desta non incorre nas causas de abstención establecidas na Lei 40/2015.

De acordo co artigo 41 do Regulamento de Estudos de Doutoramento, declara tamén que a presente tese de doutoramento é idónea para ser defendida en base á modalidade de COMPENDIO DE PUBLICACIÓNS, nos que a participación do/a doutorando/a foi decisiva para a súa elaboración.

A utilización destes artigos nesta memoria, está en coñecemento dos coautores, tanto doutores como non doutores. Ademais, estes últimos teñen coñecemento de que ningún dos traballos aquí reunidos poderá ser presentado en ningunha outra tese de doutoramento.

En Santiago de Compostela, 22 de xuño de 2020

Asdo. D. Antonio Moreda Piñeiro

Asdo. Dna. Elena María Peña Vázquez

USC
UNIVERSIDADE
DE SANTIAGO
DE COMPOSTELA

“IF YOU CAN FIND A WAY WITHOUT ANY OBSTACLES,

IT PROBABLY LEADS NOWHERE”

Che Guevara

USC
UNIVERSIDADE
DE SANTIAGO
DE COMPOSTELA

ACKNOWLEDGEMENTS

USC
UNIVERSIDADE
DE SANTIAGO
DE COMPOSTELA

I am grateful to everyone who has helped me in my struggle to achieve my dream of becoming a Ph.D. I would like to thank Professor Antonio Moreda-Piñeiro for his counsel and seemingly boundless patience. Over the years he has inspired me when I became discouraged and rallied me when I became complacent. I would also like to thank Professor Elena Peña-Vázquez for her confidence and for always demanding perfection. Under her supervision, I have no doubt become a superior researcher; more confident and, at the same time, continuously skeptical.

Additional thanks to Professor Pilar Bermejo-Barrera for her aid in initiating this journey, Dr. Paloma Herbello Hermelo for her assistance, and the staff of the GETEE research group especially Professor María Raquel Domínguez González, Professor María Carmen Barciela Alonso and Professor Manuel Aboal Somoza for their outstanding work. Many thanks go to my fellow students and friends who have provided friendship and support, and with whom I have shared laughter, frustration, and companionship.

I cannot begin to express my gratitude to my family for all the love, support, encouragement, and prayers they have sent my way along this journey. To my parents, thank you for being my champions throughout the past years. I bow in ovation to my wife, son (Gishan), and daughter (Senumi) for their care and kindness. The three noble ones stood by me all through with patience and tolerance. My words of thanks cannot compensate for their contribution, yet with all humanity, I thank them for their noble gesture and splendid support.

USC
UNIVERSIDADE
DE SANTIAGO
DE COMPOSTELA

INDEX

USC
UNIVERSIDADE
DE SANTIAGO
DE COMPOSTELA

Abbreviations i
Abstract vii

I. INTRODUCTION 1

1. ARSENIC AND MERCURY EXTRACTION AND DETECTION IN FOODSTUFF 3
1.1. INTRODUCTION 5
1.2. MERCURY 6
1.3. ARSENIC 9
1.4. FOOD SAMPLE PREPARATION FOR Hg AND As ANALYSIS 10
1.4.1. Sample preparation for total mercury determination 11
1.4.2. Extraction methods for mercury speciation 13
1.4.3. Sample preparation methods for total arsenic determination 15
1.4.4. Extraction methods for arsenic speciation 17
1.5. REFERENCES 20

2. NEW ADSORBENTS BASED ON IMPRINTED POLYMERS AND COMPOSITE NANOMATERIALS FOR ARSENIC AND MERCURY SCREENING/SPECIATION: A REVIEW 39
2.1. INTRODUCTION 41
2.2. MOLECULARLY/IONIC IMPRINTING TECHNOLOGY 44
2.2.1. Ionic imprinted polymers 46
2.2.1.1. Vinylated and non-vinylated monomers for mercury ions 47
2.2.1.2. Vinylated and non-vinylated monomers for inorganic arsenic ions 49
2.2.1.3. Template removal procedures 55
2.3. NANOMATERIALS FOR Hg AND As DETERMINATION 55
2.3.1. Silver and gold nanoparticles 56
2.3.2. Quantum dots and carbon dots 57
2.3.2.1. Nanoprobes based on quantum dots 60
2.3.2.2. Nanoprobes based on carbon dots 63
2.3.3. Molecularly/ionic imprinted polymer - quantum dots composites 64
2.4. CONCLUSIONS 66
2.5. ACKNOWLEDGMENTS 66
2.6. REFERENCES 67

II. OBJECTIVES 81

III. RESULTS AND DISCUSSION 85

CHAPTER 1. SYNTHESIS AND APPLICATION OF A SURFACE IONIC IMPRINTING POLYMER ON SILICA-COATED Mn-DOPED ZnS QUANTUM DOTS AS A CHEMOSENSOR FOR THE SELECTIVE QUANTIFICATION OF INORGANIC ARSENIC IN FISH 87
1.1. INTRODUCTION 90
1.2. MATERIALS AND METHODS 92
1.2.1. Reagents 92
1.2.2. Instrumentation 93
1.2.3. Synthesis of IIP@ZnS:Mn QDs 94
1.2.4. Phosphorescence measurements 96
1.2.5. Analysis of samples 96
1.3. RESULTS AND DISCUSSION 97
1.3.1. Preparation and characterization of IIP/NIP@ZnS:Mn QDs 97
1.3.2. Variables affecting the RTP quenching by inorganic arsenic species 100
1.3.2.1. Effect of the interaction time between inorganic As and IIP-QDs 100
1.3.2.2. Effect of the pH 101
1.3.2.3. Effect of the IIP-QDs concentration 101
1.3.2.4. Interaction between IIP-QDs and As (III) and As (V) species 102
1.3.3. Imprinting effect and selectivity 104
1.3.4. Analytical performances 107
1.3.4.1. Calibration and matrix effect 107
1.3.4.2. Limit of detection and limit of quantification 107
1.3.4.3. Precision and accuracy 108
1.3.5. Applications 109
1.4. CONCLUSIONS 110
1.5. ACKNOWLEDGMENTS 111
1.6. REFERENCES 112
1.7 ELECTRONIC SUPPLEMENTARY INFORMATION (ESI) 117

CHAPTER 2. IONIC IMPRINTED POLYMER SOLID-PHASE EXTRACTION FOR INORGANIC ARSENIC SELECTIVE PRE-CONCENTRATION IN FISHERY PRODUCTS BEFORE HIGH-PERFORMANCE LIQUID CHROMATOGRAPHY – INDUCTIVELY COUPLED PLASMA-MASS SPECTROMETRY SPECIATION .. 121
2.1. INTRODUCTION 124
2.2. MATERIAL AND METHODS 127
2.2.1. Instrumentation 127
2.2.2. Reagents 127
2.2.3. Sample pre-treatments 129
2.2.4. Synthesis of As-ion imprinted polymer 130

2.2.5. Extraction (SPE) and quantification (HPLC-ICP-MS) of As species... 130
2.3. RESULTS AND DISCUSSION ... 132
2.3.1. IIP synthesis and characterization ... 132
2.3.2. Optimization of IIP-SPE parameters ... 134
2.3.2.1. Loading conditions ... 135
2.3.2.2. Elution conditions ... 136
2.3.2.3. Breakthrough volume and sample (fish extract) volume ... 136
2.3.3. Imprinting effect and selectivity ... 139
2.3.4. Analytical performances ... 141
2.3.4.1. Calibration ... 141
2.3.4.2. Limit of detection and limit of quantification ... 142
2.3.4.3. Precision and accuracy ... 142
2.3.5. Application ... 145
2.4. CONCLUSIONS ... 146
2.5. ACKNOWLEDGMENTS ... 146
2.6. REFERENCES ... 147
2.7. ELECTRONIC SUPPLEMENTARY INFORMATION (ESI) ... 152

CHAPTER 3. IONIC IMPRINTED POLYMER - VORTEX-ASSISTED DISPERSIVE MICRO-SOLID PHASE EXTRACTION FOR INORGANIC ARSENIC SPECIATION IN RICE BY HPLC-ICP-MS ... 155
3.1. INTRODUCTION ... 158
3.2. MATERIALS AND METHODS ... 160
3.2.1. Instrumentation ... 160
3.2.2. Reagents ... 160
3.2.3. Synthesis of the ionic imprinted polymer ... 161
3.2.4. Rice samples ... 162
3.2.5. Microwave assisted acid digestion ... 162
3.2.6. Ultrasound assisted extraction (UAE) ... 162
3.2.7. Vortex-assisted dispersive micro-solid phase extraction (VA-D-μ-SPE) ... 163
3.2.8. ICP-MS and HPLC-ICP-MS measurements ... 163
3.3. RESULTS AND DISCUSSION ... 165
3.3.1. Optimization of VA-D-μ-SPE ... 165
3.3.1.1. Rice extract pH and loading vortex stirring time and speed ... 165
3.3.1.2. Eluting vortex stirring time and speed ... 168
3.3.1.3. Effect of the IIP sorbent amount ... 168
3.3.2. Optimization of ultrasound-assisted extraction (UAE) ... 168
3.3.3. Imprinting effect and cross-reactivity (IIP selectivity) studies ... 170

3.3.4. Analytical performances of the UAE-VA-D-μ-SPE method 171
3.3.4.1. Calibration and matrix effect 171
3.3.4.2. Limit of detection (LOD) and limit of quantification (LOQ) 173
3.3.4.3. Precision and accuracy 173
3.3.4.4. IIP reusability 175
3.3.5. Application 175
3.4. CONCLUSIONS 176
3.5. ACKNOWLEDGEMENTS 177
3.6. REFERENCES 178
3.7. ELECTRONIC SUPPLEMENTARY INFORMATION (ESI) 184

CHAPTER 4. A PHENOBARBITAL CONTAINING POLYMER/ SILICA COATED QUANTUM DOT COMPOSITE FOR THE SELECTIVE RECOGNITION OF MERCURY SPECIES IN FISH SAMPLES USING A ROOM TEMPERATURE PHOSPHORESCENCE QUENCHING ASSAY 189
4.1. INTRODUCTION 192
4.2. MATERIAL AND METHODS 195
4.2.1. Reagents 195
4.2.2. Instrumentation 196
4.2.3. Ph-QDs synthesis 196
4.2.4. Analysis of fish samples 197
4.2.4.1. Ultrasound assisted acid extraction 198
4.2.4.2. Microwave assisted acid digestion 199
4.2.4.3. RTP measurements 199
4.2.4.4. ICP-MS measurements 200
4.3. RESULTS AND DISCUSSION 201
4.3.1. Ph-QDs characterization 201
4.3.2. RTP operating conditions 202
4.3.2.1. Effect of interaction time 202
4.3.2.2. Effect of the pH 203
4.3.2.3. Effect of Ph-QD concentration 204
4.3.3. Selectivity. Quenching effect from coexisting ions and compounds 206
4.3.4. Method validation 206
4.3.4.1. Calibration and matrix effect 206
4.3.4.2. Limit of detection and limit of quantification 208
4.3.4.3. Precision and accuracy 208
4.3.4.4. Comparison to other QD-based chemosensors for mercury detection 209
4.3.5. Application 210

4.4. CONCLUSIONS 212
4.5. ACKNOWLEDGMENTS 212
4.6. REFERENCES 213
4.7. ELECTRONIC SUPPLEMENTARY INFORMATION (ESI) 218

CHAPTER 5. MOLECULARLY IMPRINTED POLYMER-SOLID PHASE EXTRACTION AND HIGH- PERFORMANCE LIQUID CHROMATOGRAPHY - INDUCTIVELY COUPLED PLASMA MASS SPECTROMETRY FOR MERCURY SPECIATION IN SEAWEED 221
5.1. INTRODUCTION 224
5.2. MATERIALS AND METHODS 226
5.2.1. Reagents 226
5.2.2. Instrumentation 228
5.2.3. Preparation of the MIPs 228
5.2.4. Ultrasound assisted extraction of mercury species from seaweed . 230
5.2.5. MIP-based solid phase extraction procedure 230
5.2.6. Determinations by HPLC-ICP-MS and ICP-MS 231
5.3. RESULTS AND DISCUSSION 232
5.3.1. MIP-based solid phase extraction 232
5.3.1.1. Loading conditions: extract pH and loading flow rate 232
5.3.1.2. Eluting conditions: eluting flow rate and volume of the eluting solution 235
5.3.2. Breakthrough volume, mass capacity and reusability 235
5.3.3. Cross-reactivity 237
5.3.4. Calibration and matrix effect 239
5.3.5. Limit of detection and limit of quantification 239
5.3.6. Repeatability, reproducibility, and accuracy 240
5.3.7. Applications 241
5.4. CONCLUSIONS 242
5.5. ACKNOWLEDGMENTS 243
5.6. REFERENCES 244
5.7. ELECTRONIC SUPPLEMENTARY INFORMATION (ESI) 251

IV. CONCLUSIONS 253

V. ANNEX I. RESUMEN Y DISCUSIÓN 259

VI. ANNEX II. LIST OF PUBLICATIONS 271

USC
UNIVERSIDADE
DE SANTIAGO
DE COMPOSTELA

ABBREVIATIONS

USC
UNIVERSIDADE
DE SANTIAGO
DE COMPOSTELA

AA-D-μ-SPE	Air-assisted dispersive micro-solid phase extraction
AAS	Atomic absorption spectrometry
AFS	Atomic fluorescence spectrometry
AIBN	Azo n-n'-bis isobutyronitrile
APTES	3-aminopropyltriethoxysilane
As	Arsenic
AsB	Arsenobetaine
AsC	Arsenocholine
AsL	Arsenolipids
AsS	Arsenosugars
ATR	Attenuated total reflectance
ATSDR	Agency for Toxic Substances and Disease Registry
CDs	Carbon dots
CE	Capillary electrophoresis
CFM	Cyclic functional monomer
CL	Chemiluminescence
CNQDs	Carbon nitride quantum dots
CNS	Central nervous system
CONTAM	Panel on Contaminants in the Food Chain
CPE	Cloud point extraction
CRM	Certified reference material
DCP	Direct current argon plasma
DLLME	Dispersive liquid-liquid microextraction
DMA	Dimethyl arsinic acid
DMF	N,N-dimethylformamide
DVB	Divinylbenzene
dw	Dry weight
EDTA	Ethylenediaminetetraacetic acid
EFSA	European Food Safety Authority
ETAAS	Electrothermal atomic absorption spectrometry
EU	European Union
FAO	Food and Agriculture Organization
FTIR	Fourier transform infrared spectrometry
GC	Gas chromatography
Hg	Mercury

HPLC	High-performance liquid chromatography
IARC	International Agency for Research on Cancer
iAs	Inorganic arsenic
ICP MS	Inductively coupled plasma mass spectrometry
ICPOES	Inductively coupled plasma optical emission spectrometry
IIP	Ionic imprinted polymer
JECFA	Joint Expert Committee on Food Additives
KED	Kinetic energy discrimination
LOD	Limit of detection
LOQ	Limit of quantification
LPME	Liquid phase microextraction
μ-SPE	Micro-solid phase extraction
MAA	Methacrylic acid
MeHg	Methyl mercury
MIP	Molecularly imprinted polymer
MIT	Molecular imprinting technique
ML	Maximum levels
MMA	Monomethyl arsenic acid
MPA	Mercaptopropionic acid
MPCs	Maximum permissible concentrations
MRL	Maximum residue level
MSPE	Magnetic solid phase extraction
MWCNTs	Multiwall carbon nanotubes
NAA	Neutron activation analysis
NIP	Non-imprinted polymers
NPs	Nanoparticles
PEG	Polyethylene glycol
PMT	Photomultiplier tube
PTDI	Provisional tolerable daily intake
PTWI	Provisional tolerable weekly intake
QDs	Quantum dots
RfD	Reference dose
RSD	Relative standard deviation
RTP	Room temperature phosphorescence
SEM	Scanning electron microscopy

SPE	Solid phase extraction
SPME	Solid phase microextraction
tAs	Total arsenic
TEM	Transmission electron microscopy
TEM-EDS	Transmission electron microscopy-energy-dispersive
TEOS	Tetraethyl orthosilicate
TETRA	Tetramethylammonium ion
tHg	Total mercury
TMAH	Tetramethylammonium hydroxide
TMAO	Trimethyl arsine oxide
TWI	Tolerable weekly intake
UA-D-μ-SPE	Ultrasound-assisted dispersive micro-solid phase extraction
UAE	Ultrasound-assisted extraction
USEPA	United States Environmental Protection Agency
USFDA	Food and Drug Administration of the United States
UV	Ultraviolet
VA-D-μ-SPE	Vortex-assisted dispersive micro-solid phase extraction
WHO	World Health Organization
ww	Wet weight
XAS	X-ray absorption spectroscopy
XRD	X-ray diffraction spectrometry
XRF	X-ray fluorescence

USC
UNIVERSIDADE
DE SANTIAGO
DE COMPOSTELA

ABSTRACT

USC
UNIVERSIDADE
DE SANTIAGO
DE COMPOSTELA

Abstract

Ingestion of toxic metals (and metalloids) through food consumption is the most important route of exposure of heavy metals for humans. Globalization and international trade of food sources, coupled with natural and anthropogenic events of metal contamination, have increased the significance of foodborne metallic exposure in both developed and developing countries. However, measures taken to decrease metal contamination have also been successful and resulted in reduced metal exposure. Mercury (Hg) and arsenic (As) are two of the main contaminants in foodstuff such as seafood and rice. The knowledge from the total concentrations of these metals is not enough for assessing the health risk because toxicity and bioavailability of metals depend on the concentration and chemical form of the element. Metal speciation studies are therefore of great importance.

Sample preparation is a critical step that affects the quality of the results of an analytical process, and it is currently one of the main research trends in Analytical Chemistry. Interests in sample preparation are nowadays focused on miniaturization of well-established extraction techniques and on the development of fast screening methodologies. These new procedures are generally simpler, faster, and greener than conventional ones, and they offer enhanced selectivity to the target analyte, and a significant reduction of sample amount, extraction solvent volumes, and analysis time. Moreover, these novel methods are also responsible of dramatically reducing the cost of analysis, avoiding the need of sophisticated high-cost equipment and highly trained analysts. The utilization of quantum dots (QDs) and molecularly imprinted polymers (MIPs) stands out amongst these methodologies.

In the introduction of this Thesis, several extraction techniques available for Hg and As have been explained, and the advantages and disadvantages of all of them briefly commented. In addition, the literature about new adsorbents based on imprinted polymers and nanocomposites for Hg and As screening and speciation has been also reviewed. The state of the art includes molecularly or ionic imprinted polymer (MIP/IIP) based solid-phase extraction (SPE) and QDs applications for total determination and speciation of Hg and As.

The first part of the Thesis (Chapters 1, 2, and 3) deals with several developments for assessing inorganic arsenic (iAs) in foodstuff. In **Chapter 1**, a method based on a composite consisting of an IIP on silica-coated Mn-doped ZnS QDs was developed as a sensor probe for room temperature phosphorescence (RTP) determination of iAs in fish as a screening technique. In **Chapter 2**, results from a selective IIP-SPE pre-concentration procedure for iAs speciation before high performance liquid chromatography – inductively coupled plasma mass spectrometry (HPLC-ICP-MS) determination were discussed. Finally, **Chapter 3** deals with a vortex-assisted dispersive micro-solid phase extraction (VA-D-μ-SPE) method using an IIP as an absorbent before HPLC-ICP-MS that was optimized for iAs speciation in rice.

Developments of several analytical strategies for Hg determination/speciation in seafood are given in the second part of the current Thesis (Chapters 4 and 5). The synthesis and application of a phenobarbital containing polymer/silica-coated QD composite as a sensor probe for the selective screening of mercury (inorganic mercury and methylmercury) in fish by a RTP quenching assay is explained in **Chapter 4**; whereas, **Chapter 5** is devoted to an MIP-SPE method coupled to HPLC-ICP-MS for Hg speciation in seaweed.

The versatility of QDs and IIPs has been highlighted for the determination of As and Hg, and for coupling with several analytical instrumentation for developing screening and confirmative methods. IIP-SPE and IIP-QDs prove to be useful to increase the selectivity and sensitivity of As and Hg determinations in complex samples such as foodstuff.

USC
UNIVERSIDADE
DE SANTIAGO
DE COMPOSTELA

USC
UNIVERSIDADE
DE SANTIAGO
DE COMPOSTELA

I. INTRODUCTION

USC
UNIVERSIDADE
DE SANTIAGO
DE COMPOSTELA

1. ARSENIC AND MERCURY EXTRACTION AND DETECTION IN FOODSTUFF

USC
UNIVERSIDADE
DE SANTIAGO
DE COMPOSTELA

1.1. INTRODUCTION

There are around thirty chemical elements that are called essential trace elements and that play a crucial function in various biochemical and physiological mechanisms in living organisms. In fact, as for many food components, the intake of metal ions can be a double-edged sword. The majority of the known metals and metalloids are very toxic to living organisms and even those considered as essential can be toxic if they are present in excess [1]. Several hazardous trace metals and metalloids such as arsenic (As), mercury (Hg), lead (Pb) and cadmium (Cd) are classified as non-essential to metabolism and they have no known biological functions. Those metals are deleterious in various respects for the environment and human beings [2]. Concentrations of several toxic metal and metalloids in the environment have been largely increased as a result of several natural and anthropogenic activities. Although the toxic metal concentration is comparatively low in the natural environment, it increases in the human body through the food chain and causes humans to get ill under long-term exposure [3]. As a safeguard for human health, guidelines and regulations stipulating maximum permissible concentrations (MPCs) of metals in foods have been set to limit our dietary exposure to toxic metals. However, the situation for toxic metals is more complex because toxicity depends on several aspects such as the concentration, chemical form, route of exposure, and the characteristic factors of the exposed individuals (age, gender, genetics, and nutritional status) [4].

Traditional detection methods for non-essential trace metals include atomic absorption spectrometry (AAS), atomic fluorescence spectrometry (AFS), spectrophotometry, inductively coupled plasma mass spectrometry (ICP-MS), inductively coupled plasma optical emission spectrometry (ICP-OES), neutron activation analysis (NAA), d.c. argon plasma multielement atomic emission spectrometry (DCP-MAES), X-ray absorption spectroscopy (XAS), and X-ray fluorescence (XRF) [5-7]. A combination of chromatographic separation techniques with spectrometric detection is the most commonly used procedures for allowing speciation analysis in food samples. These developments include high-performance liquid

chromatography coupled with inductively coupled plasma mass spectrometry (HPLC-ICP-MS), gas chromatography coupled with inductively coupled plasma mass spectrometry (GC-ICP-MS), ion chromatography coupled with inductively coupled plasma mass spectrometry (IC-ICP-MS), capillary electrophoresis coupled with inductively coupled plasma mass spectrometry (CE-ICP-MS), and HPLC coupled with electron spray ionization tandem mass spectrometry (HPLC-ESI-MS-MS) [8, 9]. Almost all these techniques have the potential of relatively rapid elemental speciation with low detection limits. Most of these methods involve the use of high cost and high technical equipment, and that is a major disadvantage. Moreover, those methods have interference problems, matrix effect, and they use toxic solvents throughout the analysis. To overcome these problems, it is necessary to develop highly efficient and cost-effective methods as selective green alternatives for sample preparation and detection of those elements in food matrices [10, 11]. The current study is mainly focused on developing screening and confirmation methods for Hg and As speciation analysis in food.

1.2. MERCURY

Mercury (Hg) is registered as one of the top ten chemicals of public health concern by the World Health Organization (WHO). There are several forms of Hg in the environment as elemental Hg (Hg^0), inorganic Hg species (such as mercurous Hg_2^{2+} ion, and mercuric Hg^{2+} ion), and organic Hg species [12]. Mercury can be released to the environment through several natural processes, e.g. weathering of rocks, degassing of the earth's crust, and volcanism. Besides, anthropogenic activities as a consequence of rapid urbanization and industrialization, such as coal combustion, the mining industry and by-products, production and use of agriculture fertilizers, and waste incineration, are also important sources of Hg [13]. Mercury travels long distances through the environment as gaseous elemental Hg (Hg^0), and deposits into the aquatic and terrestrial compartments of environment as oxidised Hg (Hg^{2+}). Afterwards, it is subjected to microbial methylation and converted to highly toxic organic species such as methylmercury (MeHg) or dimethylmercury (Me_2Hg). The

MeHg produced can enter and be bioaccumulated and biomagnified through the aquatic food chain. Humans are primarily exposed to MeHg via fisheries or other sea product consumption [14]. Nondietary sources for human exposure to Hg are associated with inhalation of Hg vapours, dermal exposure through the skin using lightening creams, dental amalgamation, use of thiomersal as a preservative in pharmaceuticals, including vaccines, and cosmetics, and ophthalmic products [15].

Awareness of Hg toxicity increased after the "mad hatter syndrome" among the hat makers in England, and the "Minamata" incident in 1956 in Kyushu Island (Japan) where the public consumed MeHg-contaminated seafood [16-18]. To date, numerous studies have examined worldwide Hg exposure and impacts on human health [19]. Recent researches have shown that the aquatic path is not the only source of MeHg contamination; for example, rice is another major source of MeHg, especially in China [20, 21]. Some studies have reported that total Hg (tHg) in fish was totally in the form of MeHg [22], whereas other studies have assumed that the MeHg levels are ~ 90% of the tHg concentration in fish [23, 24]. Since Hg species have a high affinity for thiol groups, it has been assumed that Hg distribution in the body is mediated by the complex formation of Hg species with thiol-containing compounds like cysteine and glutathione [25, 26].

About 90-95% of MeHg from the diet is absorbed in the gastrointestinal tract, while more than 90% of MeHg is presently bound to the haemoglobin of erythrocytes in the blood, being able to cross the central nervous system (CNS) and placenta [27]. Furthermore, MeHg can cross the mammary gland and accumulate in breast milk [28]; subsequently, MeHg can produce a delay of foetus brain development leading to learning incapacities and social problems [29]. MeHg is mainly excreted via faeces while urinary removal is insignificant, and it is also excreted via the biliary system as inorganic forms at a very low rate (1% body burden/day) [30].

Although there are enough data available about the effects of MeHg on the CNS, only a few data are presented on its carcinogenicity [31, 32]. Gaudet *et al.* [33] have reported the effects of MeHg in advocating breast cancer. Moreover, the carcinogenic

potential of Hg depends on its speciation. According to the United States Environmental Protection Agency (USEPA) and the International Agency for Research on Cancer (IARC), Hg^0 is classified under group D and group 3, respectively. This classification would suggest that Hg^0 is not a potential human carcinogen. However, the USEPA has classified inorganic Hg and MeHg under group C, while IARC classified inorganic Hg in group 3 and MeHg in group 2B; thus, it is possible for inorganic Hg and MeHg to act as human carcinogens [34]. The differences in the toxicity and the target organs of Hg compounds are species-specific. Speciation analysis is of important relevance to understand the kinetics and toxic mechanisms [35].

The harmonization of trade and food safety codes becomes a necessary requirement as the demand of international trades grows. To fulfil this requirement, many national, regional and international standards and regulations have been introduced. The WHO estimated a guideline value of 1 μg L^{-1} of tHg in drinking water. According to European Union/European Commission (EU/EC) regulations, the maximum level of Hg allowed in fish and fisheries products is 0.5 mg kg^{-1} wet weight, excluding those fish species listed in section 3.3.2 in the EU/EC regulation. That section mainly consider fish species included in the higher trophic level such as yellowfin tuna, swordfish, shark, marlin, eel, etc. with a maximum level allowed of 1 mg kg^{-1} [36]. Two international organizations, the Joint Expert Committee on Food Additives (JECFA) and the European Food Safety Authority (EFSA) established a recommended provisional tolerable weekly intake (PTWI), and a tolerable weekly intake (TWI) value for Hg. According to the contaminants in the food chain (CONTAM) panel of EFSA, a TWI for Hg of 1.3 μg kg^{-1} body weight was suggested. Concerning Hg, the JECFA established two recommended values, one for MeHg (1.6 μg kg^{-1} body weight), and the other for inorganic Hg (4 μg kg^{-1} body weight) [28, 37].

1.3. ARSENIC

Arsenic (As) is a trace element widely distributed in the environment and one of the most significant toxic hazards because it threatens human life and health [38, 39]. Arsenic is present naturally at trace levels in the air, water, soil, animal and plants [40]. However, natural concentrations of As can be elevated by natural phenomena such as geological events, and mainly by human activities (ore mining and smelting, use of As-containing fertilizers and pesticides, and fossil fuel burning) which can pose serious health issues [41, 42]. Arsenic was categorized as number one in their substances priority list of 2017 by the Agency for Toxic Substances and Disease Registry (ATSDR) of the United States; additionally, it has also been classified as a human carcinogen by the IARC [43, 44].

The toxicological effect and bioavailability of an element depends on its concentration and the chemical form [45]. Arsenic can be present in food and in the environment in several forms. In general, inorganic As (iAs), mainly the As (III) and As (V), is more toxic than organic As. Furthermore, As (III) is more toxic than As (V) [46]. Arsenobetaine (AsB) and arsenosugar compounds (AsS) are nontoxic and are commonly found in marine animals and seaweeds, respectively. Arsenobetaine generally contributes to approximately 80% of total As in fish and seafood. Hence, the determination of As species in food is an important factor to consider in human health and food risk assessment studies [46, 47].

Health risk associated with the exposure to As is a significant global health issue and affects millions people. The symptoms of acute exposure to arsenic include vomiting, abdominal pain, and diarrhoea. Arsenic chronic exposure is associated with cancer, skin diseases, developmental and morphological alterations, cardiovascular disease, neurotoxicity, epigenetic changes (DNA methylation), increased risk of diabetes mellitus, adverse pregnancy outcomes, and a variety of complications in body organ systems [48-50]. Numerous factors may affect As toxicity in humans such as age, gender, race, lifestyle, inherited genetic characteristics, socio-economic status, exposure route, As species, and dietary factors [48, 51]. Once contaminated food or drink is consumed, around 70% of the As is

excreted in the urine, and a small amount is excreted through skin, hair, nail, and faeces [49, 52].

Because of the importance of the consumption of contaminated drinking water the WHO and USEPA set the maximum contaminant level (MCL) for As in drinking water as 10 µg L^{-1} [53]. Moreover, a similar MCL value for As in drinking water was introduced in Japan [54]. Different As regulatory limits are established for a few food types by different standardization organizations. For monitoring purposes, the EU/EC has set the limits for iAs at 0.20 mg kg^{-1} for non-parboiled milled rice (i.e. polished or white rice), 0.25 mg kg^{-1} for parboiled rice and husked rice, 0.30 mg kg^{-1} for rice waffles, wafers, crackers and cakes, and 0.10 mg kg^{-1} for rice destined for the production of food for infants and young children [55]. As another example of regulatory differences for food, the maximum limit for As (w/w) in fish is 0.5 mg kg^{-1} in China, 1.1 mg kg^{-1} in India, 2.0 mg kg^{-1} in Australia and New Zealand, while it is 3.5 µg kg^{-1} for fish protein in Canada [56, 57]. The JECFA also introduced a MCL for As at 0.1 mg kg^{-1} for edible fats and oils, fat spreads and blended spreads, and 0.5 mg kg^{-1} for food grade salt [58].

The 'tolerable intake' limit is widely used to describe 'safe' levels of intake. The JECFA published a PTWI while the EFSA panel on CONTAM has discussed using a TWI. Though JECFA has set its PTWI for As at 15 µg kg^{-1} body weight, the EFSA has stated that this value is no longer appropriate, as the JECFA limit had not taken into account the presence of iAs which causes cancer, mainly in the lung and urinary bladder [59].

1.4. FOOD SAMPLE PREPARATION FOR Hg AND As ANALYSIS

Sample pre-treatments methods are constantly developing and are especially important for Hg and As analysis in food samples because the ratio between the different chemical forms must be guaranteed during this step. However, direct analysis of food samples can suffer from both matrix interferences, and the low concentrations of chemical species. Therefore, there is a need for developing sample pre-treatment methods that can be used to remove or reduce the matrix, and pre-concentrate the species of interest prior analysis [60].

Regarding fish and seafood, inedible parts such as shells, husks, skin, byssus are removed, and the edible part is homogenized by a mechanical blender. In some cases, samples are pulverized or freeze-dried. The sample preparation step depends on the aim of the study (element speciation or element determination). Moreover, there are several pre-concentration methods (based on solid or liquid sorptive based) that have been used for the extraction of Hg and As species from food samples [61, 62].

1.4.1. Sample preparation for total mercury determination

Acid digestion is the most commonly used sample pre-treatment method for tHg determination in many types of food samples. Wet digestion methods can be carried out in an open flask, in a pressurized, sealed container, or using a microwave-assisted decomposition. Moreover, the solvent or acid combination (H_2O, H_2O_2, HNO_3, H_2SO_4, HCl, HF etc.), and volumes employed are different [60]. Mohammed*, et al.* [63] proposed an open flask digestion method for fish muscle samples and concentrated HNO_3 acid was the most efficient digestion solvent for all metal (Hg, As, Sb, Pb and Cd). The efficient extraction of Hg was achieved at a digestion temperature of 85 °C for 120 min. The drawback of this simple and cost-effective method was that it was time-consuming, and it was difficult to simultaneously extract As and Hg in the same sample (Hg was found to be lost due to volatilization at higher temperatures). To overcome problem, Chen*, et al.* [64] proposed a method based on reflux to successfully recover tHg and Hg^{2+} at high temperatures (110 °C) [64]. Microwave heating enables a rapid decomposition of samples due to control over time and heating power. Microwave digestion can be performed in open, closed, and flow systems. Open microwave systems have the risk of the escape of volatile components, which may influence greatly the results [65]. Different digestion conditions, acids and solvents combinations were used by different researchers, and some examples are summarized in Table 1.

Table 1. Some recent examples of food sample preparation for tHg determination

Sample matrix	Digestion mode	Digestion solvent	Temp (°C)	Time (min)	Ref.
Fish	Hot plate	1 mL H_2O, 1 mL HNO_3, 1 mL HF, 5 mL H_2SO_4	320	30	[66]
,,	_	HNO_3: H_2SO_4 (7:3 v/v)	95	180	[67]
,,	Water bath	HCl: HNO_3 (3:1)	80	300	[68]
,,	Digestion block	1 mL H_2O_2, 2 mL HNO_3, 2 mL H_2SO_4	70	30	[69]
,,	Microwave	5 mL HNO_3, 5 mL H_2O_2	_	_	[70]
,,	,,	2 mL HNO_3, 0.5 mL H_2O_2	_	37	[71]
Seafood	,,	1 mL HNO_3	_	45	[29]
Rice	_	4 mL HNO_3, 1 mL H_2SO_4	95	180	[72]
,,	Water bath	4 mL HNO_3, 1 mL H_2SO_4	95	180	[73]
Seaweed	Reflux digestion	6 mL HNO_3, 2 mL H_2O	95	120	[74]
,,	Microwave	2.5 mL HNO_3, 2.5 mL H_2SO_4	_	31	[75]
Breast milk	Pressure digestion	1 mL HNO_3	140	360	[76]
,,	Microwave	2 mL HNO_3	_	_	[77]
Infant formula	,,	3.8 mL HNO_3, 0.1 mL HF	_	20	[78]
Infant cereals	,,	7 mL HNO_3, 2 mL H_2O_2	_	46.5	[79]
Vegetable	Water bath	HNO_3: H_2SO_4 (4:1 v/v)	95	150	[80]
,,	_	15 mL of HNO_3: H_2SO_4, $HClO_4$ (5:1:1)	80	_	[81]
Mushroom	Microwave	3 mL HNO_3	_	_	[82]
,,	,,	3 mL HNO_3, 0.5 mL H_2O_2	_	_	[83]

1.4.2. Extraction methods for mercury speciation

Extraction of Hg for speciation analysis of food is usually facilitated by acidic (such as HCl) or alkaline (such as tetramethylammonium hydroxide, TMAH) digestion or leaching. Extractions were usually performed with the assistance of microwave or ultrasound. However, soft extraction conditions are required for avoiding Hg degradation and loss [84]. As an example, Kutscher, *et al.* [85] have compared four extraction methods for the identification of MeHg-binding proteins in fish muscle and found that a combination of tris(hydroxymethyl)aminomethane (Tris) buffer with sodium dodecyl sulphate (SDS) as denaturing agent results in nearly 100% recovery [85]. Some other examples are summarized in Table 2. Even though many analytical methods have been developed for Hg extraction, most of them suffer significant loss and/or cross-species transformations during sample preparation. Hence, isotope dilution mass spectrometry (IDMS) methods have been developed, and have been found to provide significant added value for analytical quality assurance and quality control [86].

Table 2. Some recent examples of sample extraction methods for Hg speciation

Sample matrix	Extraction mode	Extraction solvent	Temp (°C)	Time (min)	Ref
Fish	Open air	10 mL of 0.6% L-Cysteine	20	1440	[87]
,,	Ultrasonication	5 M HCl	RT	5	[88]
,,	,,	10 mL of 0.1% HCl + 0.05% L-Cysteine	40	15	[89]
,,	Water bath	5 mL of 3.6 M HNO_3	55	960	[90]
,,	Microwave	TMAH	_	15	[91]
,,	,,	100 µL of 25% TMAH	_	7	[92]
Seafood	,,	10 mL of 4 M HCl	100	10	[93]
Cooked seafood	Ultrasonication	20 mL of 2 M HCl	_	60	[94]
Fish oil	Microwave	10 mL of 0.6% 2-ME, 3% Methanol, 1% Lipase, 2% Triton X-100, 1% HNO_3	60	7	[95]
Fish, kelp	Ultrasonication	5 mL 5M HCl	_	10	[96]
Rice	Water bath	Trypsin, Acetate buffer	_	20	[97]
Lotus seed	Ultrasonication	10 mL solution (EDTA, Methanol, HNO_3)	40	60	[98]
Lotus root	,,	10 mL of 5M HNO_3	40	60	[99]

EDTA: Ethylenediaminetetraacetic acid, **ME**: Mercaptoethanol, **TMAH**: Tetramethylammonium hydroxide

1.4.3. Sample preparation methods for total arsenic determination

Acid digestion is commonly used as a sample pre-treatment for total arsenic (tAs) determination in a foodstuff. Several acids combinations have been used and each method has some advantages and disadvantages. As an example, a $HNO_3/HClO_4/H_2SO_4$ mixture under reflux extraction has been used for tAs determination in fish by Storelli and Marcotrigiano [100]. The main drawback of this method is that it is time-consuming (6 h), and it is difficult to apply the same digestion conditions for the determination of other metals such as lead (Pb). To avoid long digestion times, microwave-assisted digestion with several acid combinations (such as HNO_3 [101], HNO_3 and H_2O_2 mixture [102], HNO_3, HCl, H_2O_2 and HF mixtures [103], etc) has been proposed. Some other examples and alternatives (hot plate, ultrasounds water bath, etc.) are summarized in Table 3.

Table 3. Some recent examples of food sample preparation for tAs determination

Sample matrix	Digestion mode	Digestion solvent	Temp (°C)	Time (min)	Ref
Fish	Microwave	2 mL H_2O_2, 10 mL HNO_3	180	60	[102]
,,	Hot plate	2.5 mL $HClO_4$, 7.5 HNO_3	80	120	[104]
,,	Oven	10 mL HNO_3, 5 mL $HClO_4$, 5 mL H_2O	150	120	[105]
,,	Microwave	2 mL HNO_3, 10 mL H_2O	180	20	[106]
,,	,,	5 mL HNO_3, 3 mL H_2O_2, 3.5 mL HCl, 0.1 mL HF	_	50	[103]
Rice milk	,,	4 mL HNO_3	230	30	[107]
Rice products	Water bath	1 mL 10% HNO_3, 2 mL 10% $K_2S_2O_8$	80-90	180	[108]
Rice	Hot plate	8 mL HNO_3	110	180	[109]
,,	Water bath	10 mL 0.28 M HNO_3	95	90	[110]
,,	Heating block	5 mL HNO_3, 3 mL H_2O_2	60, 130	180-240	[111]
Mushrooms	Microwave	2 mL HNO_3, 1 mL H_2O_2	200	45	[112]
Mushrooms	,,	10 mL HNO_3	180	38	[113]
Vegetable	,,	9 mL HNO_3, 2 mL H_2O_2	190	60	[114]
Strawberry	Hot plate	2 mL HNO_3, 2 mL H_2O_2	180	_	[115]
Tea	Microwave	5 mL HNO_3, 3 mL H_2O	170	32	[116]

1.4.4. Extraction methods for arsenic speciation

The sample extraction method is very important in As speciation analysis due to the complexity of the matrices. Several analytical methods and extraction solvents have been used for As speciation analysis in food (Table 4). Distillation methods have been proposed for the extraction of As species from fish samples using HBr and 6.0 M HCl under refluxed for 15 min [100]. The disadvantages of these methods are that they are slow and consume high amounts of acids. Kalantzi, *et al.* [117] have proposed a vortex and ultrasound-assisted method for extracting inorganic As (As(III) and As(V)), and organic As species (AB, MMA, DMA) from fish. Freeze-dried fish powder sample was mixed with $(NH_4)_2HPO_4$ (10 mM, pH 7.9) and vortexed for 1 min prior to ultrasonication (3 min, 40 °C). These two steps were repeated 10 times. In another study, Sanz, *et al.* [118] have proposed ultrasounds assisted enzymatic hydrolysis procedures for the extraction of As species from rice samples. Other examples of food sample preparation for the extraction of As species are given in Table 4.

Table 4. Some examples of extraction methods for As speciation

Sample matrix	Targets	Extraction mode	Extraction solvent	Temp (°C)	Time (min)	Ref.
Fish	As (III), As (V)	Microwave	1% HNO_3	100	90	[102]
Fish	iAs, AB, MMA, DMA	Ultrasound water-bath	10 mL (1% HNO_3, 1% H_2O_2)	55	120	[119]
Fish	iAs, AB, MMA, DMA	Vortex, ultrasound water-bath	1.2 mL $(NH_4)_2HPO_4$	40	50	[117]
Fish	iAs, DMA, MMA	Microwave	10 mL 2% HNO_3, 5 mL 1% H_2O_2	95	30	[120]
Fish, shellfish	As (III), As (V), DMA, MMA	Microwave	6 mL H_2O	80	_	[121]
Shrimp	iAs, AB, AC, DMA, MMA, TMAO, Tetra	Microwave	Methanol	55	15	[122]
Chicken	As (III), As (V), DMA, ASA, ROX	Microwave	5 mL mixture (22% Methanol, 90 mol/L $(NH_4)_2HPO_4$, 0.7% TFA	71	21	[123]
Rice	As (III), As (V), DMA, MMA	Microwave	7 mL 0.25 M HNO_3	95	90	[124]
Rice	As (III), As (V), DMA, MMA	Microwave	10 mL of 1% HNO_3	95	40	[125]
Rice	As (III), As (V), DMA, MMA	Hot plate	20 mL 0.15 M HNO_3	90	150	[109]
Rice	As (III), As (V), AB, MMA, DMA	Ultrasonic probe	10 mg α Amylase, 30 mg Protease, 3 mL H_2O		3	[118]
Rice products	As (III), As (V)	Water bath	5 mL 0.28 M HNO_3	95	90	[108]
Mushrooms	AB, As (III), As (V), DMA, MMA	Microwave	8 mL H_2O	80	45	[112]

Table 4. Some examples of extraction methods for As speciation (Continued)

Sample matrix	Targets	Extraction mode	Extraction solvent	Temp (°C)	Time (min)	Ref.
Mushrooms	AB, As (III), As (V), DMA, MMA, AC	Ultrasound water-bath	30 mL 0.3 M Acetic acid	60	10	[113]
Vegetable	As (III), As (V), DMA	Microwave	20 mL 1% HNO_3	90	90	[114]
Strawberry	As (III), As (V), DMA, MMA	Microwave	10 mL H_2O	_	4	[115]
Tea	As (III), As (V), DMA, MMA	Microwave	10 mL 0.05% HNO_3, 10 mL H_2O	90	30	[116]

AB: Arsenobetaine, **AC**: Arsenocholine, **ASA**: p-arsanilic acid, **DMA**: Dimethyl arsenic, **MMA**: Monomethyl arsenic, **ROX**: Roxarsone **TFA**: Tri-fluoroacetic acid

1.5. REFERENCES

[1] V. Mudgal, N. Madaan, A. Mudgal, R. Singh, S. Mishra, Effect of toxic metals on human health, The Open Nutraceuticals Journal, 3 (2010).

[2] P.K. Rai, S.S. Lee, M. Zhang, Y.F. Tsang, K.-H. Kim, Heavy metals in food crops: Health risks, fate, mechanisms, and management, Environment International, 125 (2019) 365-385.

[3] L. Wang, X. Peng, H. Fu, C. Huang, Y. Li, Z. Liu, Recent advances in the development of electrochemical aptasensors for detection of heavy metals in food, Biosensors and Bioelectronics, 147 (2020) 111777.

[4] P.B. Tchounwou, C.G. Yedjou, A.K. Patlolla, D.J. Sutton, Heavy Metal Toxicity and the Environment, in: A. Luch (Ed.) Molecular, Clinical and Environmental Toxicology: Volume 3: Environmental Toxicology, Springer Basel, Basel, (2012) 133-164.

[5] S. Mounicou, J. Szpunar, R. Lobinski, Metallomics: the concept and methodology, Chemical Society Reviews, 38 (2009) 1119-1138.

[6] R.K. Soodan, Y.B. Pakade, A. Nagpal, J.K. Katnoria, Analytical techniques for estimation of heavy metals in soil ecosystem: A tabulated review, Talanta, 125 (2014) 405-410.

[7] H. Hu, J. Zhao, L. Wang, L. Shang, L. Cui, Y. Gao, B. Li, Y.-F. Li, Synchrotron-based techniques for studying the environmental health effects of heavy metals: Current status and future perspectives, TrAC Trends in Analytical Chemistry, 122 (2020) 115721.

[8] H. Yu, C. Li, Y. Tian, X. Jiang, Recent developments in determination and speciation of arsenic in environmental and biological samples by atomic spectrometry, Microchemical Journal, 152 (2020) 104312.

[9] S. Gutiérrez Sama, C. Barrère-Mangote, B. Bouyssière, P. Giusti, R. Lobinski, Recent trends in element speciation analysis of crude oils and heavy petroleum fractions, TrAC Trends in Analytical Chemistry, 104 (2018) 69-76.

[10] J.W. Olesik, J.A. Kinzer, E.J. Grunwald, K.K. Thaxton, S.V. Olesik, The potential and challenges of elemental speciation by capillary electrophoresis-inductively coupled plasma mass spectrometry and electrospray or ion spray mass spectrometry, Spectrochimica Acta Part B: Atomic Spectroscopy, 53 (1998) 239-251.

[11] L.B. Escudero, M.Á. Maniero, E. Agostini, P.N. Smichowski, Biological substrates: Green alternatives in trace elemental preconcentration and speciation analysis, TrAC Trends in Analytical Chemistry, 80 (2016) 531-546.

[12] WHO, Ten chemicals of major public health concern, World Health Organization, (2010) 1-4.

[13] B.K.K.K. Jinadasa, S.W. Fowler, Critical review of mercury contamination in Sri Lankan fish and aquatic products, Marine Pollution Bulletin, 149 (2019) 110526.

[14] S.Y. Kwon, J.D. Blum, R. Yin, M.T.-K. Tsui, Y.H. Yang, J.W. Choi, Mercury stable isotopes for monitoring the effectiveness of the Minamata Convention on Mercury, Earth-Science Reviews, 203 (2020) 103111.

[15] J.F. Risher, H.E. Murray, G.R. Prince, Organic mercury compounds: human exposure and its relevance to public health, Toxicology and Industrial Health, 18 (2002) 109-160.

[16] M. Harada, Minamata disease: methylmercury poisoning in Japan caused by environmental pollution, Critical reviews in toxicology, 25 (1995) 1-24.

[17] M. Akito, Y. Shinichiro, H. Akihiro, K. Michiaki, S. Ikuko, T. Akihide, A. Hirokatsu, Reevaluation of Minamata Bay, 25 years after the dredging of mercury-polluted sediments, Marine Pollution Bulletin, 89 (2014) 112-120.

[18] G.J. Myers, P.W. Davidson, M. Weitzman, B.P. Lanphear, Contribution of heavy metals to developmental disabilities in children, Mental Retardation and Developmental Disabilities Research Reviews, 3 (1997) 239-245.

[19] B.M. Sharma, O. Sáňka, J. Kalina, M. Scheringer, An overview of worldwide and regional time trends in total mercury levels in human blood and breast milk from 1966 to 2015 and their associations with health effects, Environment International, 125 (2019) 300-319.

[20] X. Feng, P. Li, G. Qiu, S. Wang, G. Li, L. Shang, B. Meng, H. Jiang, W. Bai, Z. Li, X. Fu, Human Exposure To Methylmercury through Rice Intake in Mercury Mining Areas, Guizhou Province, China, Environmental Science & Technology, 42 (2008) 326-332.

[21] G. Qiu, X. Feng, P. Li, S. Wang, G. Li, L. Shang, X. Fu, Methylmercury Accumulation in Rice (Oryza sativa L.) Grown at Abandoned Mercury Mines in Guizhou, China, Journal of Agricultural and Food Chemistry, 56 (2008) 2465-2468.

[22] J.S. Sevillano-Morales, M. Cejudo-Gómez, A.M. Ramírez-Ojeda, F. Cámara Martos, R. Moreno-Rojas, Risk profile of methylmercury in seafood, Current Opinion in Food Science, 6 (2015) 53-60.

[23] N.R. Razavi, M.T. Arts, M. Qu, B. Jin, W. Ren, Y. Wang, L.M. Campbell, Effect of eutrophication on mercury, selenium, and essential fatty acids in Bighead Carp (*Hypophthalmichthys nobilis*) from reservoirs of eastern China, Science of the Total Environment, 499 (2014) 36-46.

[24] U. Strandberg, M. Palviainen, A. Eronen, S. Piirainen, A. Laurén, J. Akkanen, P. Kankaala, Spatial variability of mercury and

polyunsaturated fatty acids in the European perch (*Perca fluviatilis*) – Implications for risk-benefit analyses of fish consumption, Environmental Pollution, 219 (2016) 305-314.

[25] Z. Yin, H. Jiang, T. Syversen, J.B. Rocha, M. Farina, M. Aschner, The methylmercury-L-cysteine conjugate is a substrate for the L-type large neutral amino acid transporter, Journal of Neurochemistry, 107 (2008) 1083-1090.

[26] W.T.A. Simmons, T.W. Clarkson, N. Ballatori, Transport of a neurotoxicant by molecular mimicry: the methylmercury–L-cysteine complex is a substrate for human L-type large neutral amino acid transporter (LAT) 1 and LAT2, Biochemical Journal, 367 (2002) 239-246.

[27] R.A. Bernhoft, Mercury toxicity and treatment: a review of the literature, Journal of Environmental and Public Health, 2012 (2012).

[28] EFSA, EFSA provides risk assessment on mercury in fish: precautionary advice given to vulnerable groups. https://www.efsa.europa.eu/fr/press/news/contam040318, (2014). Accessed 10 March 2020.

[29] Z.F. Anual, W. Maher, F. Krikowa, L. Hakim, N.I. Ahmad, S. Foster, Mercury and risk assessment from consumption of crustaceans, cephalopods and fish from West Peninsular Malaysia, Microchemical Journal, 140 (2018) 214-221.

[30] K.M. Rice, E.M. Walker, Jr., M. Wu, C. Gillette, E.R. Blough, Environmental mercury and its toxic effects, Journal of Preventive Medicine and Public Health 47 (2014) 74-83.

[31] P. Boffetta, E. Merler, H. Vainio, Carcinogenicity of mercury and mercury compounds, Scandinavian journal of work, environment & health, 19 (1993) 1-7.

[32] R. Zefferino, C. Piccoli, N. Ricciardi, R. Scrima, N. Capitanio, Possible mechanisms of mercury toxicity and cancer promotion:

Involvement of gap junction intercellular communications and inflammatory cytokines, Oxidative medicine and cellular longevity, 2017 (2017) 1-6.

[33] H.M. Gaudet, E. Christensen, B. Conn, S. Morrow, L. Cressey, J. Benoit, Methylmercury promotes breast cancer cell proliferation, Toxicology Reports, 5 (2018) 579-584.

[34] IARC, International Agency for Research on Cancer (IARC) - Summaries & Evaluations of mercury and mercury compounds http://www.inchem.org/documents/iarc/vol58/mono58-3.html, 1993. Accessed 10 March 2020.

[35] H. Lohren, L. Blagojevic, R. Fitkau, F. Ebert, S. Schildknecht, M. Leist, T. Schwerdtle, Toxicity of organic and inorganic mercury species in differentiated human neurons and human astrocytes, Journal of Trace Elements in Medicine and Biology, 32 (2015) 200-208.

[36] EU/EC-1881, Setting maximum levels for certain contaminants in foodstuffs. Official Journal of the European Union, 2006.

[37] A.R. Popovic, J.M. Djinovic-Stojanovic, D.S. Djordjevic, D.J. Relic, D.V. Vranic, M.P. Milijasevic, L.L. Pezo, Levels of toxic elements in canned fish from the Serbian markets and their health risks assessment, Journal of Food Composition and Analysis, 67 (2018) 70-76.

[38] K. Sureshkumar, A. Deep, K.-H. Kim, S.K. Kailasa, H.-O. Yoon, Nanomaterial-based electrochemical sensors for arsenic-A review, Biosensors and Bioelectronics, 95 (2017) 106-116.

[39] S. Antonova, E. Zakharova, Inorganic arsenic speciation by electroanalysis. From laboratory to field conditions: A mini-review, Electrochemistry Communications, 70 (2016) 33-38.

[40] A. Balouch, M.S. Jagirani, A., F.A. Mustafai, A. Tunio, S. Sabir, A.M. Mahar, K. Rajar, M.T. Shah, M.K. Samoon, Review:

Arsenic remediation by synthetic and natural adsorbents, 2017, 18 (2017) 19.

[41] J.A. Baig, T.G. Kazi, A.Q. Shah, H.I. Afridi, G.A. Kandhro, S. Khan, N.F. Kolachi, S.K. Wadhwa, F. Shah, M.B. Arain, M.K. Jamali, Evaluation of arsenic levels in grain crops samples, irrigated by tube well and canal water, Food and Chemical Toxicology, 49 (2011) 265-270.

[42] P. Wang, G. Sun, Y. Jia, A.A. Meharg, Y. Zhu, A review on completing arsenic biogeochemical cycle: Microbial volatilization of arsines in environment, Journal of Environmental Sciences, 26 (2014) 371-381.

[43] ATSDR, ATSDR's Substance Priority List, Agency for Toxic Substances and Disease Registry (https://www.atsdr.cdc.gov/SPL/), Accessed 10 March 2020.

[44] IARC, IARC monographs on the evaluation of carcinogenic risk to human, (Volume 1-123) https://monographs.iarc.fr/list-of-classifications-volumes/, 2018.

[45] A.A. Meharg, E. Lombi, P.N. Williams, K.G. Scheckel, J. Feldmann, A. Raab, Y. Zhu, R. Islam, Speciation and localization of arsenic in white and brown rice grains, Environmental Science & Technology, 42 (2008) 1051-1057.

[46] M.S. Rahman, A.H. Molla, N. Saha, A. Rahman, Study on heavy metals levels and its risk assessment in some edible fishes from Bangshi River, Savar, Dhaka, Bangladesh, Food Chemistry, 134 (2012) 1847-1854.

[47] J.M. Durand, P.E. Lippens, J. Olivier-Fourcade, J.C. Jumas, M. Womes, Sulfur K-edge XAS study of As_2S_3-Sb_2S_3-Tl_2S glasses, Journal of Non-Crystalline Solids, 208 (1996) 36-48.

[48] Y.M. Hsueh, W.J. Chen, C.Y. Lee, S.N. Chien, H.S. Shiue, S.R. Huang, M.I. Lin, S.-C. Mu, R.L. Hsieh, Association of arsenic

methylation capacity with developmental delays and health status in children: A prospective case–control trial, Scientific Reports, 6 (2016) 37287.

[49] A.K.S. Mohammed, S.S. Jayasinghe, E.P.S. Chandana, C. Jayasumana, P.M.C.S. De Silva, Arsenic and human health effects: A review, Environmental Toxicology and Pharmacology, 40 (2015) 828-846.

[50] M.K. Upadhyay, A. Shukla, P. Yadav, S. Srivastava, A review of arsenic in crops, vegetables, animals and food products, Food Chemistry, 276 (2018) 608–618.

[51] T. Joseph, B. Dubey, E.A. McBean, Human health risk assessment from arsenic exposures in Bangladesh, Science of the Total Environment, 527-528 (2015) 552-560.

[52] A. Ghosh, S. Majumder, M.A. Awal, D.R. Rao, Arsenic exposure to dairy cows in Bangladesh, Archives of Environmental Contamination and Toxicology, 64 (2013) 151-159.

[53] K.S. Almberg, M.E. Turyk, R.M. Jones, K. Rankin, S. Freels, J.M. Graber, L.T. Stayner, Arsenic in drinking water and adverse birth outcomes in Ohio, Environmental Research, 157 (2017) 52-59.

[54] MHLWJP, Drinking Water Quality Standards in Japan, https://www.mhlw.go.jp/english/policy/health/water_supply/4.html, 2015. Accessed 12 March 2020.

[55] EU/EC, Commission Regulation (EC), No 2015/1006 of amending Regulation (EC) No 1881/2006 as regards maximum levels of inorganic arsenic in foodstuffs Official journal of European Union, L161 (1006/2015) 14-16.

[56] K. Bhupander, D. Mukherjee, Assessment of human health risk for arsenic, copper, nickel, mercury and zinc in fish collected from tropical wetlands in India, Advances in Life Science and Technology, 2 (2011) 13-24.

[57] G. Chiocchetti, C. Jadán-Piedra, D. Vélez, V. Devesa, Metal (loid) contamination in seafood products, Critical Reviews in Food Science and Nutrition, 57 (2017) 3715-3728.

[58] JECFA, Working document for information and use in discussions related to contaminants and toxins in the gsctff, FAO/ WHO, Rome, Italy, (2017).

[59] EFSA, Scientific Opinion on Arsenic in Food, EFSA Journal, 7 (2009) 1351.

[60] B.B. Kebbekus, Preparation of samples for metals analysis, in: S. Mitra (Ed.) Sample Preparation Techniques in Analytical Chemistry, Wiley-Interscience, (2003) 227-270.

[61] M. Asensio-Ramos, L.M. Ravelo-Pérez, M.Á. González-Curbelo, J. Hernández-Borges, Liquid phase microextraction applications in food analysis, Journal of Chromatography A, 1218 (2011) 7415-7437.

[62] J. Werner, T. Grześkowiak, A. Zgoła-Grześkowiak, E. Stanisz, Recent trends in microextraction techniques used in determination of arsenic species, Trends in Analytical Chemistry, (2018) 121-136.

[63] E. Mohammed, T. Mohammed, A. Mohammed, Optimization of an acid digestion procedure for the determination of Hg, As, Sb, Pb and Cd in fish muscle tissue, MethodsX, 4 (2017) 513-523.

[64] G. Chen, B. Lai, X. Mao, Reflux open-vessel digestion system can overcome volatilization loss in mercury speciation analysis, Talanta, 191 (2019) 209-215.

[65] S.L.C. Ferreira, V.A. Lemos, L.O.B. Silva, A.F.S. Queiroz, A.S. Souza, E.G.P. da Silva, W.N.L. dos Santos, C.F. das Virgens, Analytical strategies of sample preparation for the determination of mercury in food matrices — A review, Microchemical Journal, 121 (2015) 227-236.

[66] Y. Kenji, M. Keisuke, K. Gen, K. Shigeaki, H. Yasuhisa, M. Akito, Y. Megumi, Food sources are more important than biomagnification on mercury bioaccumulation in marine fishes, Environmental Pollution, (2020) 113982.

[67] M. Jing, D. Lin, P. Wu, M.J. Kainz, K. Bishop, H. Yan, R. Wang, Q. Wang, Q. Li, Effect of aquaculture on mercury and polyunsaturated fatty acids in fishes from reservoirs in Southwest China, Environmental Pollution, 257 (2020) 113543.

[68] M. Kainz, K. Telmer, A. Mazumder, Bioaccumulation patterns of methyl mercury and essential fatty acids in lacustrine planktonic food webs and fish, Science of The Total Environment, 368 (2006) 271-282.

[69] L.S. Azevedo, I.A. Pestana, A.F. da Costa Nery, W.R. Bastos, C.M.M. Souza, Mercury concentration in six fish guilds from a floodplain lake in western Amazonia: Interaction between seasonality and feeding habits, Ecological Indicators, 111 (2020) 106056.

[70] T. Filippini, M. Malavolti, S. Cilloni, L.A. Wise, F. Violi, C. Malagoli, L. Vescovi, M. Vinceti, Intake of arsenic and mercury from fish and seafood in a Northern Italy community, Food and Chemical Toxicology, 116 (2018) 20-26.

[71] V. Zupo, G. Graber, S. Kamel, V. Plichta, S. Granitzer, C. Gundacker, K.J. Wittmann, Mercury accumulation in freshwater and marine fish from the wild and from aquaculture ponds, Environmental Pollution, 255 (2019) 112975.

[72] X. Xu, J. Han, J. Pang, X. Wang, Y. Lin, Y. Wang, G. Qiu, Methylmercury and inorganic mercury in Chinese commercial rice: Implications for overestimated human exposure and health risk, Environmental Pollution, 258 (2020) 113706.

[73] M. Ao, X. Xu, Y. Wu, C. Zhang, B. Meng, L. Shang, L. Liang, R. Qiu, S. Wang, X. Qian, L. Zhao, G. Qiu, Newly deposited

atmospheric mercury in a simulated rice ecosystem in an active mercury mining region: High loading, accumulation, and availability, Chemosphere, 238 (2020) 124630.

[74] R. Fernández-Martínez, I. Rucandio, I. Gómez-Pinilla, F. Borlaf, F. García, M.T. Larrea, Evaluation of different digestion systems for determination of trace mercury in seaweeds by cold vapour atomic fluorescence spectrometry, Journal of Food Composition and Analysis, 38 (2015) 7-12.

[75] S. Paz, C. Rubio, I. Frías, Á.J. Gutiérrez, D. González-Weller, V. Martín, C. Revert, A. Hardisson, Toxic metals (Al, Cd, Pb and Hg) in the most consumed edible seaweeds in Europe, Chemosphere, 218 (2019) 879-884.

[76] S. Bose-O'Reilly, B. Lettmeier, D. Shoko, G. Roider, G. Drasch, U. Siebert, Infants and mothers levels of mercury in breast milk, urine and hair, data from an artisanal and small-scale gold mining area in Kadoma / Zimbabwe, Environmental Research, 184 (2020) 109266.

[77] L.R. da Cunha, T.H.M. da Costa, E.D. Caldas, Mercury Concentration in Breast Milk and Infant Exposure Assessment During the First 90 Days of Lactation in a Midwestern Region of Brazil, Biological Trace Element Research, 151 (2013) 30-37.

[78] M. Sager, C.R. McCulloch, D. Schoder, Heavy metal content and element analysis of infant formula and milk powder samples purchased on the Tanzanian market: International branded versus black market products, Food Chemistry, 255 (2018) 365-371.

[79] R. Hernández-Martínez, I. Navarro-Blasco, Survey of total mercury and arsenic content in infant cereals marketed in Spain and estimated dietary intake, Food Control, 30 (2013) 423-432.

[80] Q. Jia, X. Zhu, Y. Hao, Z. Yang, Q. Wang, H. Fu, H. Yu, Mercury in soil, vegetable and human hair in a typical mining area in

China: Implication for human exposure, Journal of Environmental Sciences, 68 (2018) 73-82.

[81] P.R. Shakya, N.M. Khwaounjoo, Heavy metal contamination in green leafy vegetables collected from different market sites of Kathmandu and their associated health risks, Scientific World, 11 (2013) 37-42.

[82] A. Kavčič, K. Mikuš, M. Debeljak, J. Teun van Elteren, I. Arčon, A. Kodre, P. Kump, A.G. Karydas, A. Migliori, M. Czyzycki, K. Vogel-Mikuš, Localization, ligand environment, bioavailability and toxicity of mercury in Boletus spp. and Scutiger pes-caprae mushrooms, Ecotoxicology and Environmental Safety, 184 (2019) 109623.

[83] C. Ostos, F. Pérez-Rodríguez, B.M. Arroyo, R. Moreno-Rojas, Study of mercury content in wild edible mushrooms and its contribution to the Provisional Tolerable Weekly Intake in Spain, Journal of Food Composition and Analysis, 37 (2015) 136-142.

[84] Y. Gao, Z. Shi, Z. Long, P. Wu, C. Zheng, X. Hou, Determination and speciation of mercury in environmental and biological samples by analytical atomic spectrometry, Microchemical Journal, 103 (2012) 1-14.

[85] D.J. Kutscher, A. Sanz-Medel, J. Bettmer, Metallomics investigations on potential binding partners of methylmercury in tuna fish muscle tissue using complementary mass spectrometric techniques, Metallomics, 4 (2012) 807-813.

[86] S. Clémens, M. Monperrus, O.F.X. Donard, D. Amouroux, T. Guérin, Mercury speciation in seafood using isotope dilution analysis: A review, Talanta, 89 (2012) 12-20.

[87] L. Schmidt, C.A. Bizzi, F.A. Duarte, V.L. Dressler, E.M.M. Flores, Evaluation of drying conditions of fish tissues for inorganic

mercury and methylmercury speciation analysis, Microchemical Journal, 108 (2013) 53-59.

[88] M.V. Balarama Krishna, K. Chandrasekaran, D. Karunasagar, On-line speciation of inorganic and methyl mercury in waters and fish tissues using polyaniline micro-column and flow injection-chemical vapour generation-inductively coupled plasma mass spectrometry (FI-CVG-ICPMS), Talanta, 81 (2010) 462-472.

[89] X. Chen, C. Han, H. Cheng, Y. Wang, J. Liu, Z. Xu, L. Hu, Rapid speciation analysis of mercury in seawater and marine fish by cation exchange chromatography hyphenated with inductively coupled plasma mass spectrometry, Journal of Chromatography A, 1314 (2013) 86-93.

[90] U. Arroyo-Abad, M. Pfeifer, S. Mothes, H.-J. Stärk, C. Piechotta, J. Mattusch, T. Reemtsma, Determination of moderately polar arsenolipids and mercury speciation in freshwater fish of the River Elbe (Saxony, Germany), Environmental Pollution, 208 (2016) 458-466.

[91] A. Sakanupongkul, R. Sananmuang, Y. Udnan, R.J. Ampiah-Bonney, W.C. Chaiyasith, Speciation of mercury in water and freshwater fish samples by a two-step solidified floating organic drop microextraction with electrothermal atomic absorption spectrometry, Food Chemistry, 277 (2019) 496-503.

[92] A. Thongsaw, R. Sananmuang, Y. Udnan, G.M. Ross, W.C. Chaiyasith, Dual-cloud point extraction for speciation of mercury in water and fish samples by electrothermal atomic absorption spectrometry, Spectrochimica Acta Part B: Atomic Spectroscopy, 160 (2019) 105685.

[93] A.V. Zmozinski, S. Carneado, C. Ibáñez-Palomino, À. Sahuquillo, J.F. López-Sánchez, M.M. da Silva, Method development for the simultaneous determination of methylmercury and inorganic mercury in seafood, Food Control, 46 (2014) 351-359.

[94] W. Liao, G. Wang, W. Zhao, M. Zhang, Y. Wu, X. Liu, K. Li, Change in mercury speciation in seafood after cooking and gastrointestinal digestion, Journal of Hazardous Materials, 375 (2019) 130-137.

[95] C.-H. Yao, S.-J. Jiang, A.C. Sahayam, Y.-L. Huang, Speciation of mercury in fish oils using liquid chromatography inductively coupled plasma mass spectrometry, Microchemical Journal, 133 (2017) 556-560.

[96] S. Wang, X. Song, J. Hu, R. Zhang, L. Men, M. Wei, T. Xie, J. Cao, Direct speciation analysis of organic mercury in fish and kelp by on-line complexation and stacking using capillary electrophoresis, Food Chemistry, 281 (2019) 41-48.

[97] L. Li, F. Wang, B. Meng, M. Lemes, X. Feng, G. Jiang, Speciation of methylmercury in rice grown from a mercury mining area, Environmental Pollution, 158 (2010) 3103-3107.

[98] D. Zhang, S. Yang, Q. Ma, J. Sun, H. Cheng, Y. Wang, J. Liu, Simultaneous multi-elemental speciation of As, Hg and Pb by inductively coupled plasma mass spectrometry interfaced with high-performance liquid chromatography, Food Chemistry, 313 (2020) 126119.

[99] D. Zhang, S. Yang, H. Cheng, Y. Wang, J. Liu, Speciation of inorganic and organic species of mercury and arsenic in lotus root using high performance liquid chromatography with inductively coupled plasma mass spectrometric detection in one run, Talanta, 199 (2019) 620-627.

[100] M.M. Storelli, G.O. Marcotrigiano, Organic and inorganic arsenic and lead in fish from the South Adriatic Sea, Italy, Food Additives & Contaminants, 17 (2000) 763-768.

[101] B.K.K.K. Jinadasa, G.S. Chathurika, C.D. Jayaweera, G.D.T.M. Jayasinghe, Mercury and cadmium in swordfish and yellowfin tuna

and health risk assessment for Sri Lankan consumers, Food Additives & Contaminants: Part B, (2018) 75-80.

[102] D. Cui, P. Zhang, H. Li, Z. Zhang, W. Luo, Z. Yang, Biotransformation of dietary inorganic arsenic in a freshwater fish Carassius auratus and the unique association between arsenic dimethylation and oxidative damage, Journal of Hazardous Materials, 391 (2020) 122153.

[103] A. Shakeri, M. Sharifi Fard, B. Mehrabi, M. Rastegari Mehr, Occurrence, origin and health risk of arsenic and potentially toxic elements (PTEs) in sediments and fish tissues from the geothermal area of the Khiav River, Ardebil Province (NW Iran), Journal of Geochemical Exploration, 208 (2020) 106347.

[104] X. Xiong, K. Zhang, Y. Chen, C. Qu, C. Wu, Arsenic in water, sediment, and fish of lakes from the Central Tibetan Plateau, Journal of Geochemical Exploration, 210 (2020) 106454.

[105] A.A. Ouattara, K.M. Yao, K.C. Kinimo, A. Trokourey, Assessment and bioaccumulation of arsenic and trace metals in two commercial fish species collected from three rivers of Côte d'Ivoire and health risks, Microchemical Journal, 154 (2020) 104604.

[106] G.L. Lescord, T.A. Johnston, M.J. Heerschap, W. Keller, F.M. Southee, C.M. O'Connor, R.D. Dyer, B.A. Branfireun, J.M. Gunn, Arsenic, chromium, and other elements of concern in fish from remote boreal lakes and rivers: Drivers of variation and implications for subsistence consumption, Environmental Pollution, 259 (2020) 113878.

[107] F.C. da Rosa, M.A.G. Nunes, F.A. Duarte, É.M.D.M. Flores, F.B. Hanzel, A.S. Vaz, D. Pozebon, V.L. Dressler, Arsenic speciation analysis in rice milk using LC-ICP-MS, Food Chemistry: X, 2 (2019) 100028.

[108] G.M. dos Santos, D. Pozebon, C. Cerveira, D.P. de Moraes, Inorganic arsenic speciation in rice products using selective hydride generation and atomic absorption spectrometry (AAS), Microchemical Journal, 133 (2017) 265-271.

[109] F. Zhang, F. Gu, H. Yan, Z. He, B. Wang, H. Liu, T. Yang, F. Wang, Effects of soaking process on arsenic and other mineral elements in brown rice, Food Science and Human Wellness, (2020).

[110] G. Carracelas, J. Hornbuckle, M. Verger, R. Huertas, S. Riccetto, F. Campos, A. Roel, Irrigation management and variety effects on rice grain arsenic levels in Uruguay, Journal of Agriculture and Food Research, 1 (2019) 100008.

[111] U. Mandal, P. Singh, A.K. Kundu, D. Chatterjee, J. Nriagu, S. Bhowmick, Arsenic retention in cooked rice: Effects of rice type, cooking water, and indigenous cooking methods in West Bengal, India, Science of The Total Environment, 648 (2019) 720-727.

[112] I. Komorowicz, A. Hanć, W. Lorenc, D. Barałkiewicz, J. Falandysz, Y. Wang, Arsenic speciation in mushrooms using dimensional chromatography coupled to ICP-MS detector, Chemosphere, 233 (2019) 223-233.

[113] S. Chen, B. Yuan, J. Xu, G. Chen, Q. Hu, L. Zhao, Simultaneous separation and determination of six arsenic species in Shiitake (Lentinus edodes) mushrooms: Method development and applications, Food Chemistry, 262 (2018) 134-141.

[114] L. Ma, Z. Yang, Q. Kong, L. Wang, Extraction and determination of arsenic species in leafy vegetables: Method development and application, Food Chemistry, 217 (2017) 524-530.

[115] A.I. González de las Torres, I. Giráldez, F. Martínez, P. Palencia, W.T. Corns, D. Sánchez-Rodas, Arsenic accumulation and speciation in strawberry plants exposed to inorganic arsenic enriched irrigation, Food Chemistry, 315 (2020) 126215.

[116] R.F. Milani, E. Lima de Paiva, L.I. Peron, M.A. Morgano, S. Cadore, Arsenic species in herbal tea leaves and infusions determination by HPLC-ICP-MS, LWT, 98 (2018) 606-612.

[117] I. Kalantzi, K. Mylona, K. Sofoulaki, M. Tsapakis, S.A. Pergantis, Arsenic speciation in fish from Greek coastal areas, Journal of Environmental Sciences, 56 (2017) 300-312.

[118] E. Sanz, R. Muñoz-Olivas, C. Cámara, M.K. Sengupta, S. Ahamed, Arsenic speciation in rice, straw, soil, hair and nails samples from the arsenic-affected areas of Middle and Lower Ganga plain, Journal of Environmental Science and Health, Part A, 42 (2007) 1695-1705.

[119] R. Juncos, M. Arcagni, S. Squadrone, A. Rizzo, M. Arribére, J.P. Barriga, M.A. Battini, L.M. Campbell, P. Brizio, M.C. Abete, S. Ribeiro Guevara, Interspecific differences in the bioaccumulation of arsenic of three Patagonian top predator fish: Organ distribution and arsenic speciation, Ecotoxicology and Environmental Safety, 168 (2019) 431-442.

[120] E. Avigliano, J. Schlotthauer, B.M. de Carvalho, M. Sigrist, A.V. Volpedo, Inter-and intra-stock bioaccumulation of anionic arsenic species in an endangered catfish from South American estuaries: Risk assessment through consumption, Journal of Food Composition and Analysis, 87 (2020) 103404.

[121] Y. Gao, P. Baisch, N. Mirlean, F.M. Rodrigues da Silva Júnior, N. Van Larebeke, W. Baeyens, M. Leermakers, Arsenic speciation in fish and shellfish from the North Sea (Southern bight) and Açu Port area (Brazil) and health risks related to seafood consumption, Chemosphere, 191 (2018) 89-96.

[122] M.E. Josende, S.M. Nunes, R. de Oliveira Lobato, M. González-Durruthy, L.W. Kist, M.R. Bogo, W. Wasielesky, S. Sahoo, J.P. Nascimento, C.A. Furtado, D. Fattorini, F. Regoli, K. Machado, A.V. Werhli, J.M. Monserrat, J. Ventura-Lima, Graphene oxide and GST-

omega enzyme: An interaction that affects arsenic metabolism in the shrimp Litopenaeus vannamei, Science of The Total Environment, 716 (2020) 136893.

[123] D. Zhao, J. Wang, D. Yin, M. Li, X. Chen, A.L. Juhasz, J. Luo, A. Navas-Acien, H. Li, L.Q. Ma, Arsanilic acid contributes more to total arsenic than roxarsone in chicken meat from Chinese markets, Journal of Hazardous Materials, 383 (2020) 121178.

[124] I. Herath, P. Kumarathilaka, J. Bundschuh, A. Marchuk, J. Rinklebe, A fast analytical protocol for simultaneous speciation of arsenic by Ultra-High Performance Liquid Chromatography (UHPLC) hyphenated to Inductively Coupled Plasma Mass Spectrometry (ICP-MS) as a modern advancement in liquid chromatography approaches, Talanta, 208 (2020) 120457.

[125] T.-L. Wu, X.-D. Cui, P.-X. Cui, S.T. Ata-Ul-Karim, Q. Sun, C. Liu, T.-T. Fan, H. Gong, D.-M. Zhou, Y.-J. Wang, Speciation and location of arsenic and antimony in rice samples around antimony mining area, Environmental Pollution, 252 (2019) 1439-1447.

2. NEW ADSORBENTS BASED ON IMPRINTED POLYMERS AND COMPOSITE NANOMATERIALS FOR ARSENIC AND MERCURY SCREENING/SPECIATION: A REVIEW

KAMAL K. JINADASA, ELENA PEÑA-VÁZQUEZ, PILAR BERMEJO-BARRERA, ANTONIO MOREDA-PIÑEIRO

MICROCHEMICAL JOURNAL 156 (2020) 104886

https://doi.org/10.1016/j.microc.2020.104886

USC
UNIVERSIDADE
DE SANTIAGO
DE COMPOSTELA

New adsorbents based on imprinted polymers and composite nanomaterials for arsenic and mercury screening/speciation: A review

Kamal K. Jinadasa, Elena Peña-Vázquez, Pilar Bermejo-Barrera, Antonio Moreda-Piñeiro

Trace Element, Spectroscopy and Speciation Group (GETEE), Strategic Grouping in Materials (AEMAT), Department of Analytical Chemistry, Nutrition and Bromatology, Faculty of Chemistry, Universidade de Santiago de Compostela. Avenida das Ciencias, s/n. 15782, Santiago de Compostela, Spain

Abstract

Non-essential trace elements, especially mercury (Hg) and arsenic (As), and their speciation analysis in fish and fishery products have gained increasing attention regarding human exposure, risk assessment and toxicological endpoints. Reliable, robust and sophisticated hyphenated laboratory instrumentation is available today, providing very low quantification limits for total element contents and single element species. Not only the instrumentation but also fast and reliable novel sample pre-treatment methods are important, and challenges in speciation analysis are focused on developing new low cost and fast screening methods. This review includes the developments on molecularly/ionic imprinted polymers (MIPs/IIPs) based solid phase extraction and quantum dots (QDs) for Hg and As determination/speciation.

Keywords: Mercury, arsenic, molecularly/ionic imprinted polymers, nanoparticles, carbon dots, quantum dots

2.1. INTRODUCTION

Food and environment monitoring of mercury (Hg) and arsenic (As) have received ample scientific attention in recent years due to the hazard to human health posed by the contamination of fish. The level of Hg and As in the environment depends on the number of natural

(weathering and meteorization of rocks, degasification of the earth's crust, terrestrial, and volcanism) and anthropogenic (coal combustion, mining industry by-product, agriculture fertilizer, and waste incineration) activities [1-3]. There are several Hg and As chemical forms found in environmental samples and foodstuffs. The Agency for Toxic Substances and Disease Registry (ATSDR) noted that As and Hg were ranked number one and three, respectively, in the hazardous substances list in 2017 [4]. These metals are toxic to humans even at very low concentrations and do not play any known biological role.

After the Minamata tragedy due to methylmercury (MeHg) poisoning in humans who ingested fish and shellfish in Japan in 1956, the world became concerned about Hg poisoning and its toxicity effects [5]. Other mercury poisoning cases have occurred due to contaminated foods in Sweden, Iraq, Ghana and China [6-8]. These incidents forced the international community to curtail the emission of mercury after the "Minamata Convention on Mercury" was signed on October 10, 2013.

Mercury can occur as several chemical forms such as elemental mercury (Hg^0), divalent inorganic mercury (Hg^{2+}), monomethylmercury (CH_3Hg^+), dimethylmercury ($(CH_3)_2Hg$), ethyl mercury ($EtHg^+$) and phenyl mercury ($PhHg^+$) [9-11]. MeHg represents approximately 90% of total Hg (tHg) in fish, and together with inorganic mercury (Hg^{2+}) represents the main concern from a toxicological point of view [12,13].

Arsenic is the twentieth most abundant element in the earth's crust, and it has influenced human history more than other toxic compounds [14]. Arsenic species are mainly classified as inorganic (arsenite (As(III)) and arsenate (As(V) being the most toxic species), and organic species (mainly monomethyl arsenic acid (MMA), and dimethyl arsinic acid (DMA), also considered to be a toxic As compound). As (III) and As (V) are the dominant species in environmental samples; whereas, MMA and DMA can be considered products of biotransformation in a detoxification mechanism [15, 16]. The biomethylation of iAs species has been considered as a potential detoxification pathway in marine and freshwater microorganisms [17]. However, the intermediate products (such as trivalent methyl and

dimethyl As, MMA^{III} and DMA^{III}) of iAs biomethylation to pentavalent methyl As (MMA^{V} and DMA^{V}) are more toxic than iAs [18]. Arsenobetaine (AsB) is a common and nontoxic As species present in most seafood, especially fish and shellfish. Arsenosugars (AsS) and arsenolipids (AsL) are other complex arsenic compounds commonly found in certain seafood [19,20]. AsS, mainly ribose derivatives, are the major As compounds in algae, representing 80% of total As [21]. There is little information about AsL (arseno fatty acids, AsFA; arseno hydrocarbons, AsHC; arseno glycophospholipids, AsPL, etc.) in seafood. These species can be associated with oily fish and fish oil [21]. Arsenocoline (AsC) is rarely found in seafood because it is metabolized to AsB. However, AsC is the main As compound in sea anemones and jellyfish [22,23]. Some authors have mentioned an unidentified or unclear fraction as a residual As, mostly thiol As compounds [24,25]. The total As content is higher in marine fish than in freshwater fish [26]. The content of inorganic As (iAs) in fish is usually lower than in rice, grains and flour. Hence, researchers do not show much concern about iAs in fish and seafood; however, biotransformation of non-toxic As to potentially toxic inorganic intermediates has been reported [27-29].

The intake of Hg and As through the diet is a high concern for the food regulatory agencies, and foodstuffs such as fish require regular monitoring. Maximum levels (ML) of inorganic As have been reported in several guidelines by many countries as mg kg^{-1} in crustaceans and fish, and 1 mg kg^{-1} in molluscs and edible seaweed (Australia New Zealand (ANZFA)); 3.5 mg kg^{-1} for fish protein (Canadian Food Inspection Agency (CFIA)); 0.1 mg kg^{-1} in fish, fish products and fish seasonings (Ministry of Health of the People's Republic of China); 3 mg/kg for algal condiments (Centre d'Etude et de Valorisation des Algues, France (CEVA)), etc. The European Food Safety Authority (EFSA) and the Food and Drug Administration of the United States (USFDA) have reported MLs for certain foodstuffs (e.g., rice, rice-based products and infant cereals) but not for seafood. Concerning health risk assessment, the Joint FAO-WHO Expert Committee on Food Additives (JECFA) has established a Provisional Tolerable Weekly Intake (PTWI) value of 15 μg kg^{-1} of body weight

(equivalent to 2.1 μg kg^{-1} of body weight per day), but this was withdrawn in 2010. The EFSA established a Tolerable Weekly Intake (TWI) value, for example, the suggestion of TWI for Hg of 1.3 μg kg of body weight [30,31]. Hence, the Panel on Contaminants in the Food Chain (CONTAM) has suggested a range of values for the 95% lower confidence limit of the benchmark dose of 1% extra risk (0.3-8 mg kg^{-1} body weight), which would be more appropriate than a single reference point in the risk characterization for inorganic As [32,33].

Public health scientists and regulators are generally in agreement regarding the tHg and MeHg dietary exposure guidance for adults, but there is a lack of agreement about the dietary exposure of the most sensitive groups such as pregnant women, nursing mothers and children [34]. For total Hg in fish, a ML of 0.5 mg kg^{-1} w/w (wet weight) has been established in the European Union (EU), with the exception of large predatory fish such as swordfish, tuna and sharks (ML of 1.0 mg kg^{-1} w/w) [35]. The PTWI established by the JECFA for methylmercury is 1.6 μg kg^{-1} body weight, and 4 μg kg^{-1} body weight for inorganic mercury; whereas, a TWI of 1.3 μg kg^{-1} body weight for methylmercury was established by the EFSA [36]. Health Canada has recommended a Provisional Tolerable Daily Intake (PTDI) for sensitive groups (women in reproductive status and infants) of $2x10^{-4}$ mg kg^{-1} body weight, and $5x10^{-4}$ mg kg^{-1} body weight for adults. Moreover, Canada also uses 0.2 mg kg^{-1} as a guideline ML for frequently consumed fish, and 0.5 mg kg^{-1} as a guideline in fish for commercial use [37]. The USFDA recommends 1 mg kg^{-1} action level for MeHg in fish for commercial sale. However, the United States Environmental Protection Agency (USEPA) has established a more conformist reference dose (RfD) of $1x10^{-4}$ mg kg^{-1} body weight per day for MeHg in edible fish, and 0.3 mg kg^{-1} as tissue residue criteria for fish for human consumption [34].

2.2. MOLECULARLY/IONIC IMPRINTING TECHNOLOGY

There are several stages when performing total element (Hg and As) determinations, as well as when applying speciation strategies [(1) extraction and preconcentration, (2) separation, and (3) determination/quantification] [38]. Each step requires the careful

optimization of those variables affecting the procedure. Acid digestion is commonly used for total (or partial) decomposing biological samples, such as fish, for the assessment of total metal concentrations. This sample pre-treatment technique, although quite efficient for total sample decomposition, does not guarantee the integrity/stability of element species. Many different approaches, such as solid phase extraction (SPE), solid phase microextraction (SPME), cloud point extraction (CPE), liquid phase microextraction (LPME), and magnetic solid phase extraction (MSPE), have been adopted for speciation of Hg and As [39,40]. However, some of these techniques can suffer from low selectivity, which implies additional clean-up stages for removing co-extracted concomitants before analysis. Improvements on selectivity and extract clean-up stages are an area of intense research and Molecularly Imprinted Polymers (MIPs) are one of the most versatile and appealing options for sample preparation [41]. MIPs are synthetic materials with artificially generated recognition sites capable of specifically rebinding a target molecule in preference to other closely related compounds [42]. These polymers are obtained by the reaction of a template, monomers and cross linkers with the support of a radical initiator in a proper solvent. It is necessary to solubilize the template, monomers and crosslinkers into a porogenic solvent that plays a major role as a dispersing media and pore forming agent in the mixture [41-43]. Porogenic solvent polarity affects the formation of the template-monomer complex. In general, such a solvent should be of low polarity, and it helps to increase MIP selectivity.

Nowadays, free radical polymerization is very popular. Azo N-N'-bis isobutyronitrile (AIBN) is common and widely used as a polymerization initiator for MIPs/IIPs synthesis [44]. Normally, the initiator is used in very low amounts compared with the template (approximately 1% weight or molar % with total number of moles), and its activity (rate and mode of decomposition to radicals) is controlled in several ways such as heat, light and chemical or electrochemical reactions [45].

The preparation of an MIP consists of three steps: 1) formation of a pre-polymerization complex; 2) polymerization of the complex

monomer; (3) removal of the template to produce the imprinted polymer. Three different approaches (namely, covalent, non-covalent and semi-covalent) have been involved in MIP preparation [43], and several synthetic methods (co-precipitation, reverse micelles, sol-gel synthesis, hydrothermal reaction, thermolysis of precursor, flow injection synthesis and electrospray synthesis) have been used [46]. Some authors have classified MIP preparation methods as bulk polymerization, suspension polymerization, multistep swelling polymerization, precipitation polymerization, surface polymerization and *in-situ* polymerization [45]. Other researchers have classified the polymerization methods available to prepare monodisperse particles (use of water-based emulsions, seeded suspension polymerizations, non-aqueous dispersion polymerizations, and precipitation polymerization) [47]. Each method has characteristic advantages and limitations. Most researchers follow the precipitation polymerization method instead of the bulk polymerization method because the latter requires a grinding step which destroys some recognition cavities. The main advantages of precipitation polymerization include the absence of stabilizers and suspension agents, complete freedom to utilize water soluble or water insoluble monomers, higher binding capacity, and obtaining particles of uniform micro spherical size [47].

2.2.1. Ionic imprinted polymers

Ionic Imprinted Polymers (IIPs) are prepared using an ion as a template instead of a molecule, ion which reacts with a suitable monomer (vinylated reagent) and then polymerizes in the presence of a cross-linker and an initiator. Oxyanions, such as arsenite and arsenate, can react/interact with conventional monomers and can therefore form stable complexes with vinyl groups for polymerization. In these cases, the complexing ligand (monomer) is chemically immobilized in the polymeric matrix. However, simple ions such as Hg(II) and MeHg(I) are not able to react with conventional monomers, and the strategy is based on using binary/ternary mixed ligand complexes involving a non-vinylated reagent showing affinity to the ion and which is able to interact with the vinylated monomer. The latter approach is commonly referred as trapping technique

[48,49] since the non-vinylated reagent is not chemically bonded to the polymer chains, but it is trapped inside the polymeric matrix. Non-vinylated reagent residues are therefore not totally fixed in the polymeric chain, and selectivity can worsen because similar ions in size and/or exhibiting affinity to the ligand can also interact to the recognition cavities generated in the polymer. The right selection of the monomer is therefore important and depends on the ion and the ability to interact with the functional groups of the template/template-non-vinylated reagent complex [48-50].

2.2.1.1. Vinylated and non-vinylated monomers for mercury ions

IIPs for mercury ions (Hg(II) and MeHg(I) as templates) required the use of the trapping technique using a pre-polymerization mixture based on a binary non-vinylated/vinylated system. Vinylated monomers are mainly methacrylic acid (MAA) [51-56], although MAA derivates such as 2-hydroxyethyl methacrylate (HEMA) [57], and other typical vinylated monomers [2-vinylpyridine (2-VP) [58], 4-vinylpyridine (4-VP) [59], and 3-aminopropyltriethoxysilane (APTES) [60]] have been also used. Because of mercury ions have a specific affinity to sulphur, functional monomers (non-vinylated monomers) containing sulfhydryl groups form stable pre-polymerization complexes with mercury, and ligands such as N-methacryloyl-2-mercaptoethylamine (MMEA) [51], 1-pyrrolidinedithiocarboxylic acid ammonium (PDC) [52], 4-(2-thiazolylazo) resorcinol (TAR) [54], and dithizone [60] have been found to be suitable to form binary complexes with mercury ions. Moreover, reagents also containing N-based functional groups have been found to interact easily with Hg through N–Hg(II)–N bonds. Ligands reported to selectively react with Hg ions such as phenobarbital and thymine (allyl thymine, AT) have been also used, and the prepared IIPs have been found to offer high selectivity for Hg ions [53,56,61]. Diazoaminobenzene (DAAB) [59] and 2,2′-dipyrydyl amine (PA) [55], and non-commercially available monomers (synthesized ligands) such as N-methacryloyl-(l)-cysteine (MAC) [57] and AT [61], have been also used.

Vinylpyridine monomers contain a N moiety which guarantee Hg ions-monomer interactions, and IIPs based on using the conventional 2-VP monomer have been synthesized for a selective recognition of Hg(II) ions [58]. Hg(II) ions anchorage into the polymeric chains was weaker than when using S- and N-based selective ligands for Hg since template (Hg(II)) removal after IIP synthesis was possible under moderate (pH and temperature) conditions [58]. A bifunctional monomer, N-(pyridin-2-ylmethyl)ethenamine (V-Pic), exhibiting two N moieties and a vinyl group was synthesized and used as a monomer for preparing a magnetic IIP by mixing the $Hg(V\text{-}Pic)_2 \cdot 2NO_3$ complex with vinyl functionalized Fe_3O_4 nanoparticles synthesized via triethoxy silane reaction with an adequate cross-linker and initiator [62]. Synthesis based on using a template-bifunctional monomer system leads to a weak template anchorage which allows template removal under soft conditions, guaranteeing the integrity of the IIP layer over the nanoparticle core.

Most of reported IIPs for mercury were synthesized by using inorganic mercury (Hg(II)) as a template [51,52,54-60,62] and selectivity of the sorbents was high for Hg(II) ions independently of the non-vinylated reagent used for synthesis. Competitive adsorption of other metallic ions, mainly Cd(II) and Zn(II) ions with similar ionic radii, was found to be negligible, demonstrating good recognition capabilities/selectivity. However, some studies showed that selectivity for organic mercury, mainly MeHg(I), was poor probably because the large size of MeHg(I) hinders the ion diffusion and further interaction with functional groups [51,52,59,60]. The prepared IIPs are therefore unsuitable for speciation studies and for analysing fishery products since MeHg(I) is the major species in these materials. However, the use of MeHg(I) instead of Hg(II) as a template [53,56] generates a bigger recognition cavity than that formed when using Hg(II) as a template, and the interaction of both inorganic and organic mercury species leads to suitable speciation studies [56].

Table 1 summarizes the information about publications of Hg determination which use IIPs for sample pre-treatment. Similarly, Table 2 summarizes the analytes, adsorption capacities, mode (batch

or column), instrumental techniques, and pre-concentration factors reported when using the proposed IIPs.

2.2.1.2. Vinylated and non-vinylated monomers for inorganic arsenic ions

Regarding As based-IIPs, O atoms in arsenite and arsenate oxyanions interact properly with reagents containing hydroxyl groups. In addition, hydroxyl groups in these oxyanions also allow effective interaction with N moieties in vinylpyridine monomers. Therefore, polymerization schemes based on using typical vinylated monomers such as MAA [63,64] and 4-VP [65] have been developed using arsenite (As(III)) as a template. Other monomers without hydroxyl moieties such as styrene have been also used [65,66] but selectivity and sorption capacity of styrene-based IIPs for As(III) have been reported to be poorer than those offered by IIPs prepared from vinylpyridine monomers (2-VP) and mainly from the bifunctional 1-vinylimidazole, monomer which showed enhanced imprinting effect and arsenate-binding functionalities [65]. In addition to 1-vinylimidazole [65, 67], a cyclic functional monomer (CFM) containing a positively charged imidazolium moiety was used to develop an As(III) based-IIP (the synthesis of the CFM was achieved by using 1-(1H-imidazol-1-ylmethyl)-1H-imidazole and 4,5-bis(bromomethyl) acridine as reagents) [68]. The prepared IIP demonstrated to offer high selectivity for As(III) and high adsorption capacity which are attributed to the macrocyclic effect of CFM (strong affinity to oxyanion by size matching and electrostatic-dual effects derived from its positively charged imidazole ring and appropriate ring size) [68].

Although the oxyanions structures of As(III) and As(V) allow adequate interaction with conventional and bifunctional vinylated monomers, the binary non-vinylated/vinylated scheme was also proposed by Önnby *et al*. [69] using 4-hydroxybiphenyl as an auxiliary non-vinylated reagent.

Both arsenite [63,64,67-69] and arsenate [65, 66] oxyanions have been used as templates for IIP synthesis. Despite selectivity of most prepared IIPs was reported to be high for the arsenic (arsenite or

arsenate) species used as a template, the imprinting properties/capacities for the other inorganic arsenic species was not established, except for 1-vinylimidazole-based IIP which was reported to be selective for both arsenite and arsenate forms [67]. Therefore, possibilities of most of developed IIPs for inorganic arsenic speciation can not be attained, and most of them are suitable for assessing a specific inorganic arsenic form.

Revised literature suggests that the use of styrene as a functional monomer does not lead to selective adsorbents, and distribution ratios and selectivity coefficients are better for 4-VP- and, mainly, for 1-vinylimidazole-based IIPs than those calculated for styrene-based IIP [65]. In addition, results by Mafu *et al*. [66] for a styrene-based IIP have revealed low imprinting capacities (distribution ratios quite similar for IIP and non-imprinted polymers (NIP) adsorbents) and lack of selectivity for arsenate ions (other ions such as Cd(II), Pb(II), and Hg(II) are quantitatively retained in the prepared polymer). Selectivity of prepared IIPs based on other monomers has been found to be similar, although the use of 1-vinylimidazole (bifunctional monomer) offers the highest selectivity [65,67] and possibilities for pre-concentrating both inorganic arsenic species [67].

Table 1 and Table 2 summarize details regarding IIPs for arsenic ions as well as analytical features of the developed methods.

Table 1. Features regarding IIPs synthesis for mercury and arsenic ions

Template ion	Monomer(s)	Cross-linker	Polymerization procedure	Leaching solution for template removal	Ref.
Hg(II)	MAA plus MMEA	EGDMA	bulk	5.0 % thiourea in 2.0 M HCl	[51]
Hg(II)	MAA plus PDC	TMPTMA	dispersion copolymerization	4.0 M HNO_3 followed by 0.5 M thiourea in 0.5 M HCl	[52]
MeHg(I)	MAA plus phenobarbital	EGDMA	precipitation	1.0 M thiourea in 1.0 M HCl	[53]
Hg(II)	MAA plus TAR	EGDMA	bulk	1.0 M thiourea in 0.5 M HCl	[54]
Hg (II)	MAA plus 2, 2′-di pyridyl amine	EGDMA	precipitation	6.0 M HCl	[55]
MeHg(I)	MAA plus phenobarbital	EGDMA	precipitation	1.0 M thiourea in 1.0 M HCl	[56]
Hg(II)	HEMA plus MAC	EGDMA	precipitation	0.5 % thiourea in 0.05 M HCl	[57]
Hg (II)	2-VP	EGDMA	precipitation	1.0 M EDTA	[58]
Hg(II)	4-VP plus DAAB	EGDMA	bulk	0.5 M thiourea in 0.1 M HCl	[59]
Hg (II)	APTES plus dithizone	TEOS	sol-gel process	0.5 M HCl	[60]
Hg(II)	AT	EDGMA	emulsion	---[a]	[61]
Hg (II)	V-Pic	EGDMA	co-precipitation	0.1 M HCl followed by 0.1 M EDTA	[62]
As(III)	MAA	EGDMA	precipitation	1.0 M HCl	[63]
As(III)	MAA	EGDMA	precipitation	1.0 M HCl	[64]
As(V)	4-VP, styrene, 1-vinylimidazole	EGDMA	bulk	2.0 M HNO_3	[65]
As(V)	Styrene	EGDMA	bulk	3.0 M HNO_3	[66]

Table 1. Features regarding IIPs synthesis for mercury and arsenic ions (Continued)

Template ion	Monomer(s)	Cross-linker	Polymerization procedure	Leaching solution for template removal	Ref.
As(III)	1-vinylimidazole	DVB	precipitation	2.0 M HNO_3	[67]
As(III)	CFM	EGDMA	precipitation	0.5 M NaOH	[68]
As(III)	2-VP plus 4-hydroxybiphenil	EGDMA	bulk	4.0 M HCl	[69]

1-pyrrolidinedithiocarboxylic acid ammonium salt (PDC), 2-Hydroxyethyl methacrylate (HEMA), 2-vynilpiridine (2-VP), 3-Aminopropyl)triethoxysilane (APTES), 4-vynilpiridine (4-VP), 4-(2-thiazolylazo) resorcinol (TAR), allyl thymine (AT), cyclic functional monomer based on 1-(1H-imidazol-1-ylmethyl)-1H-imidazole and 4,5-bis(bromomethyl) acridine (CFM), diazoaminobenzene (DAAB), ethylenediaminetetraacetic acid (EDTA), ethylene glycol dimethylacrylate (EGDMA), methacrylic acid (MAA), N-methacryloyl-(l)-cysteine (MAC), N-methacryloyl-2-mercaptoethylamine (MMEA), tetraethoxysilane (TEOS), trimethylolpropane trimethacrylate (TMPTMA), N-(pyridin-2-ylmethyl)ethenamine (V-Pic)
(a) not given

Table 2. Some analytical features for mercury and arsenic ions assessment by using IIP-SPE as a sample pre-treatment

	Analyte	Mode	Sample	Instrumental technique	Adsorption capacity (mg g^{-1})	Enrichment factor	Ref.
MAA/MMEA based IIP	Hg(II)	batch	seawater	ICP-MS	28	---[a]	[51]
MAA/PDC based IIP	Hg(II)	batch	estuarine/river water	CVAAS	64[b]	---[a]	[52]
MAA/phenobarbital based IIP	MeHg(I)	column	fish	HRCSAAS	0.02	---[a]	[53]
MAA/TAR based IIP	Hg (II)	batch	tap and river water	CVAAS	125[b]	---[a]	[54]
MAA/2, 2′-di pyrydyl amine based IIP	Hg (II)	batch	water and fish	CVAAS	28	120	[55]
MAA/phenobarbital based IIP	Hg(II), MeHg(I), EtHg(I)	column	seawater	HPLC-ICP-MS	---[a]	50	[56]
HEMA/MAC based IIP	Hg(II)	batch	human serum	CVAAS	0.45	---[a]	[57]
2-VP based IIP	Hg(II)	column	water and fish	CVAAS	25	---[a]	[58]
4-VP/DAAB based IIP	Hg(II)	batch	water	CVAAS	205[b]	---[a]	[59]
APTES/dithizone based IIP	Hg (II)	batch/ column	water, human hair, fish	AFS and ICP-MS	3.7[b]	---[a]	[60]

Table 2. Some analytical features for mercury and arsenic ions assessment by using IIP-SPE as a sample pre-treatment (Continued)

	Analyte	Mode	Sample	Instrumental technique	Adsorption capacity (mg g^{-1})	Enrichment factor	Ref.
AT based IIP	Hg(II)	batch	tap water	ICP-OES	200	---[a]	[61]
V-Pic based IIP	Hg(II)	batch (magnetic IIP)	fish	ICP-OES	147	---[a]	[62]
MAA based IIP	As(III)	---		Potentiometry	---	---	[63]
MAA based IIP	As(III)	---		Potentiometry	---	---	[64]
1-vinylimidazole-based IIP	As(V)	Column		ICP-MS	3.6 10^{-3}	25	[65]
Styrene based IIP	As(V)	Batch/column		ICP-OES	0.48 (batch), 0.57 (column)	---	[66]
1-vinylimidazole-based IIP	As(III) and As(V)	Column	fish	HPLC-ICP-MS	---	59 (As(III)) and 58 (As(V))	[67]
CFM based IIP	As(III)	Batch/column		AFS	55	---	[68]
4-hydroxybiphenyl /2-VP based IIP	As(V)	Batch		ETAAS	7.9	---	[69]

1-pyrrolidinedithiocarboxylic acid ammonium salt (PDC), 2-Hydroxyethyl methacrylate (HEMA), 2-vinylpiridine (2-VP), 3-Aminopropyl)triethoxysilane (APTES), 4-(2-thiazolylazo) resorcinol (TAR), 4-vynilpiridine (4-VP), allyl thymine (AT), atomic fluorescence spectrometry (AFS), cold vapor atomic absorption spectrometry (CVAAS), cyclic functional monomer based on 1-(1H-imidazol-1-ylmethyl)-1H-imidazole and 4,5-bis(bromomethyl) acridine (CFM), diazoaminobenzene (DAAB), electrothermal atomic absorption spectrometry (ETAAS), high performance liquid chromatography (HPLC), high resolution continuum source atomic absorption spectrometry (HRCSAAS), inductively coupled plasma – optical emission spectrometry (ICP-OES), inductively coupled plasma – mass spectrometry (ICP-MS), ionic imprinted polymer (IIP), methacrylic acid (MAA), N-methacryloyl-(l)-cysteine (MAC), tetraethoxysilane (TEOS), N-(pyridin-2-ylmethyl)ethenamine (V-Pic)

(a) not given; (b) μmol g^{-1}

2.2.1.3. Template removal procedures

Template removal is a critical stage when preparing MIPs/IIPs since the treatment for template removal must guarantee an efficient template leaching (available recognition cavities) and must not damage the polymer structure. Treatments for mercury based-IIP, however, require the use of strong leaching conditions involving the use of thiourea dissolved in hydrochloric acid (from 0.05 to 1.0 M) solutions [53,54,56,57,59]. Other reported procedures have been based on sequential elution steps using nitric acid (4.0 M) and thiourea (0.5 M) dissolved in 0.5 M hydrochloric acid [52], or more drastic conditions such as thiourea (5 %(w/v)) in 2.0 M hydrochloric acid by heating at 60˚C 1C for 48 h [51].

As previously mentioned, the use of bifunctional monomers appears to lead to a weak template vinylated monomer interaction which allows a template removal under moderate conditions. Therefore, ethylenediaminetetraacetic acid (EDTA) solutions (1.0 M) [58] and EDTA (0.1 M) and hydrochloric acid (0.1 M) mixtures [62] have been found suitable for an efficient template removal. Soft conditions for template removal are mainly needed for nanocomposite materials since strong acid conditions can damage the bond between the IIP layer and the modified surface of the nanoparticle.

Reported procedures for template (arsenite/arsenate) removal also require strong leaching conditions, and treatments consists of using acidic solutions, mainly nitric acid (2.0 to 3.0 M) [65-67] and hydrochloric acid (1.0 and 4.0) [63,64,69], although template removal has been also performed with alkaline solutions (0.5 M sodium hydroxide) [68].

2.3. NANOMATERIALS FOR Hg AND As DETERMINATION

In addition to well-established methodologies based on spectrometry hyphenated or not with chromatographic techniques, an intense research area for metallic ions assessment using simple and low-cost instrumentation is of current interest. Colorimetric, and mainly luminescent properties, of various nanomaterials such as gold and silver nanoparticles (Au/Ag NPs), carbon dots (CDs) and semiconductor quantum dots (QDs) have led to the development of

nanomaterial-based optical sensors with several applications for inorganic and organic targets as well as for biocompounds [70-74].

2.3.1. Silver and gold nanoparticles

Noble metal nanomaterials such as Au NPs and Ag NPs, exhibit high molar extinction coefficients in the visible region attributed to their unique localized surface plasmon resonance (LSPR) [75]. The LSPR is dependent on the interparticle distance which implies colour changes when the NPs are dispersed or aggregated. Therefore, sensing colorimetric methods can be developed for targets that induce changes of the interparticle distance (NPs aggregation). Colour change attributed to NPs aggregation can be selective to a certain target if NPs are surface modified with functional groups which allows an effective interaction with the target, and enhances aggregation. For Hg ions sensing, surface' NPs modification is usually carried out with compounds containing sulfydryl groups due to the strong Au–S and Ag–S bond.

As reviewed by Ding *et al*. [70], the functional ligands used to detect Hg ions (mainly Hg(II)) are small organic molecules, such as N-1-(2-mercaptoethyl)thymine, and 3-mercaptopropionate acid (MPA) alone or combined with adenosine monophosphate (AMP). In addition, compounds that generate quaternary ammonium (QA) group terminated thiols from the surfaces of Au NPs have found to be useful since Hg(II) ions induce the abstraction of QA ligands from the NPs surfaces and leads to aggregation. Finally, oligonucleotides containing thymine (T) are also functional ligands which induce aggregation as consequence of T–Hg(II)–T coordination chemistry.

Raw Au/Ag NPs (also referred as label-free Au/Ag NPs) have been also used for developing colorimetric assays for Hg detection, and mechanisms are based on Hg(II)-induced ligand exchange, Hg^0 deposition, and T–Hg(II)–T coordination chemistry [70]. Hg(II)-induced ligand exchange can lead to NPs aggregation (Au NPs in the presence of Cu(II) diethyldithiocarbamate (DDTC) complex since Hg-DDTC complex is more stable that Cu-DDTC) [76]), or anti-aggregation (Ag NPs and 6-thioguanine due to the stronger affinity between 6-thioguanine and Hg(II) than that with Ag NPs [77]).

Deposition of Hg^0 on the NPs' surfaces occurs in the presence of reducing agents (citrate ions and ascorbic acid) which induced NPs aggregation; whereas, T–Hg(II)–T coordination chemistry mechanisms implies oligonucleotides containing T [70]. This nucleobase induces Au NPs aggregation (Au–N bonds) which is hampered in the presence of Hg(II) ions [70].

2.3.2. Quantum dots and carbon dots

Semiconducting colloidal nanocrystals known as quantum dots (QDs) are being extensively used as fluorescence probes because require simple instrumentation (fluorimeters) and offer a number of advantages such as convenience, low cost, ultra-sensitivity, and rapid analysis [70-72,74]. QDs have attracted great interest because of their unique optical properties (large stokes shift, broad absorption spectra, narrow emission spectra), high photoluminescence (PL) efficiency, and long-term photostability [72]. QDs based on elements from groups II-VI and III-V (CdSe, CdS, CdTe, and ZnS) have been widely used, although applicability of Cd based QDs are less appealing because of Cd toxicity. Therefore, QDs based on ZnSe, ZnS and Mn and Cu doped ZnS QDs, as well as carbon dots (CDs), have been developed. QDs/CDs sensor probes are mainly based on the luminescent (fluorescence and phosphorescence) quenching when certain compounds (targets) are present, being the magnitude of the luminescence reduction proportional to the target concentration.

Most of QDs and CDs synthesis requires heating at high temperatures (solvothermal method), procedure which is typically assisted by microwave or ultrasound when preparing CDs. However, doped-ZnS QDs synthesis can be performed at room temperature which is a clear advantage over other QDs/CDs since the preparation is more straightforward [74]. Details regarding QDs/CDs chemosensors for assessing Hg(II), MeHg(I), As(III), and As(V) ions are summarized in Table 3.

Table 3. Features regarding mercury and arsenic ions sensing by QD/CD-based chemosensors

Nanomaterial	Analyte	Sample	Sensing technique	Ref.
ZnS QDs and ZnS QD impregnated chitosan film	Hg(II)	---	Fluorescence enhancement (new fluorescence wavelength)	[78]
Mn-doped ZnSe QD	Hg(II)	Water	Fluorescence enhancement (new fluorescence wavelength)	[79]
CdTe QDs	Hg(II)	Water and drinks (tea infusions, soda water, orange juice and red wine)	Fluorescence quenching	[80]
TGA-capped CdTe QDs and dBSA-TGA-capped CdTe QDs	Hg(II)	Water	Fluorescence quenching	[81]
MPA-capped CdTe QDs	Hg(II)	Water	Fluorescence quenching	[82]
L-cysteine-capped Mn-doped ZnS QDs	Hg (II)	Water	Room temperature phosphorescence quenching	[83]
pQDs	Hg (II)	---	Fluorescence quenching	[84]
Fe_3O_4@SiO_2/dendrimers/ CdTe QDs	Hg(II)	Water and fish	Electrochemiluminescence quenching	[85]
Tb(III)GMP-CdSe/ZnS QDs	As(V)	Water and fish	Fluorescence enhancement	[86]
Fe_3O_4GQDs	As(III)	---	Fluorescence enhancement	[87]
CDs	Hg(II)	Water and canned fish	Fluorescence quenching	[88]
CNQDs	Hg(II)	Water	Fluorescence quenching	[89]
CNQDs	Hg (II)	Water, fish and black tea	Chemiluminescence quenching	[90]
PVAm-CNQDs	Hg(II)	Water	Fluorescence quenching	[91]

Table 3. Features regarding mercury and arsenic ions sensing by QD/CD-based chemosensors (Continued)

Nanomaterial	Analyte	Sample	Sensing technique	Ref.
In situ CDs	MeHg(I)	Water and fish	Fluorescence quenching	[92]
1-vinylimidazole-IIP-Mn-doped ZnS QDs	As(III), As(V)	Fish	Room temperature phosphorescence quenching	[93]
Phenobarbital/MAA-MIP-Mn-doped ZnS QDs	Hg(II), MeHg(I)	Fish	Room temperature phosphorescence quenching	[94]

Denatured bovine serum albumin (dBSA), carbon dots (CDs), carbon nitride quantum dots (CNQDs), guanosine monophosphate (GMP), graphene oxide quantum dots (GQDs), ionic imprinted polymer (IIP), methacrylic acid (MAA), molecularly imprinted polymer (MIP), mercaptopropionic acid (MPA), fluorescent semiconducting polymer quantum dots (pQDs), polyvinylamine (PVAm), quantum dots (QDs), thioglycolic acid (TGA)

2.3.2.1. Nanoprobes based on quantum dots

Possibilities of cation exchange reactions between Hg(II) ions and raw QDs have been tested for developing simple nanoprobes [78,79]. Direct Hg(II) ions fluorescence sensing with raw ZnS QDs has been proposed on the basis of a cation exchange reaction between Hg(II) ions and ZnS QDs and Zn(II) ions in excess [78]. Treatment with Hg(II) ions led to a different absorption edge and fluorescence peak of the QD, but other ions such as Ag(I) and Pb(II) produce similar cation exchange reactions with similar fluorescence bands than those observed for Hg(II) ions exchange. A similar behaviour of Hg(II) and interfering Ag(I) and Pb(II) ions was also observed by using the biopolymer chitosan as a stabilizing agent (ZnS QD impregnated chitosan film) which leads lack of selectivity during Hg(II) sensing [78]. A similar mechanisms (cation exchange reaction between Hg(II) ions and Mn-doped ZnSe QDs) is the basis of other nanoprobe with raw QDs [79]. The doping amount of Mn(II) in doped ZnSe QD was estimated to be 1.8%, which is reduced to 1.1% when increasing concentrations of Hg(II) ions (1.1% of Mn(II) is the residual Mn(II) concentration which could not be replaced by Hg(II)) [79]. Mn(II) replacement by Hg(II) ions promotes the appearance of new fluorescence peak at 600 nm, and significant enhancement of fluorescence intensity at 600 nm was observed only when Hg(II) ions are present (fluorescence which is directly related to the Hg(II) ions concentration) [79]. Selectivity for Hg(II) ions is therefore obtained when measuring at the 600 nm fluorescence wavelength.

Raw CdTe QDs have been also used for preparing a nanoprobe based on the fluorescence quenching when the nanomaterial is mixed with L-cysteine and Hg(II) ions [80]. The presence of L-cysteine promote 1.3-fold fluorescence increases of CdTe QDs because of the strong affinity of the thiol group towards Cd(II) on the surface of CdTe QDs (the bonded Cd-S can improve the recombination fluorescence of CdTe QDs by creating more radiative centers at the CdTe/Cd-SR complex and stimulation blocking of nonradiative electron-hole recombination defect sites on the surface of CdTe) [80]. When Hg(II) ions are present, a significant fluorescence quenching is produced, moreover the fluorescence peak shifts to higher

wavelengths (red), which implies mechanisms of competition of ligands and also electron transfer [80]. However, the same effect was also obtained for other ions such as Ag(I) and Cu(II), and a specific nanoprobe for Hg(II) is only possible after using masking agents such as DDTC for Ag(I) and Cu(II) interferences removal [80].

Selectivity improvements can be achieved by modifying the surface of the raw QDs (capped QDs) [74]. Because of the strong affinity of Hg(II) ions to sulfidryl groups, reagents such as thioglycolic acid (TGA) [81], mercaptopropionic acid (MPA) [82], and L-cysteine [83] have been used for developing selective QD probes for Hg(II) ions. Quenching mechanisms of Hg(II) ions and TGA capped-CdTe QDs and L-cysteine capped-Mn-doped ZnS QDs was explained by both electron transfer and ion-binding, but the former effect may play a leading role [81,83]. However, Li *et al*. [82] suggest that quenching mechanisms in MPA capped-CdTe QDs is attributed to nanoparticles agglomeration due to changes of surface chemical properties when Hg(II) ions are present.

Regarding selectivity, TGA capped-CdTe QDs sensing has been reported to be interfered by Cu(II) and Ag(I) ions, and a further QD coating with denatured bovine serum albumin (dBSA) was needed to diminish interferences since dBSA provides enhanced coordinated interactions between CdTe QD surface and sulfur atoms through the formation of a shell-like $CdTe_x(dBSA)_{1-x}$ complex [81]. However, nanoprobes based on MPA capped-CdTe QDs [82] and L-cysteine capped-Mn-doped ZnS QDs [83] have been reported to be quite selective to Hg(II) ions.

Other composites such as a QD derived from fluorescent semiconducting polymer (pQDs) prepared from poly (3,4-ethylenedioxythiophene) (PEDOT) [84] and Fe_3O_4@SiO_2/dendrimers/CdTe-QD system [85], have been also developed for selective Hg(II) ions sensing. The reagent 3,4-ethylenedioxythiophene (EDOT) dissolved in 1-n-butyl-3-methylimidazolium tetrafluoroborate ($BMIMBF_4$) was polymerized on an indium tin oxide (ITO) working electrode, and the generated pQDs exfoliated from the fibrous electropolymerized PEDOT film were found to be selective for Hg(II) ions [84]. The sensing mechanisms was explained on the basis of pQDs

aggregation induced by Hg(II) ions which diminishes fluorescence. Hg(II) ions act as coordinating centers to bridge several pQDs together, by interacting with thiophene groups from PEDOT and imidazole groups from BMIM associated with pQD via π-π interaction [84].

Finally, the formation of strong and stable T-Hg(II)-T complexes (coordination chemistry mechanisms) by using oligonucleotides containing thymine has been also used for developing a selective aptasensor for Hg(II) ions detection consisting of adsorbed Fe_3O_4@SiO_2/dendrimers/CdTe@CdS QDs-DNA composite (polyamidoamine dendrimer, PAMAM) and conjugated Au NPs-ssDNA onto an ITO working electrode [85]. Fe_3O_4@SiO_2/dendrimers/QDs exhibited amplified electrochemiluminescence (ECL) emissions (switch "on" state) and with the hybridization between T-rich ssDNA immobilized on the Fe_3O_4@SiO_2/dendrimers/QDs and AuNPs modified with complementary aptamer (AuNPs-ssDNA) the ECL of QDs nanocomposites was efficiently quenched (switch "off" state). In the presence of Hg(II) ions, formation of strong and stable T-Hg(II)-T complexes led to the release of the AuNPs-ssDNA from double-stranded DNA(dsDNA) and the recovery of the ECL signal of QDs (second signal switch "on" state) [85].

Regarding arsenic, a nanoprobe consisting of CdSe/ZnS QDs coated with the Tb(III)-guanosine monophosphate complex (Tb-GMP) has been developed for the selective determination of As(V) ions [86]. The material exhibits two emission fluorescence bands, one attributed to the Tb-GMP system and another to the CdSe/ZnS QDs, the former is selectively quenched in presence of acid phosphatase (ACP) because of GMP hydrolysis. The presence of As(V) inhibits the activity of ACP, resulting an increase of fluorescence attributed to Tb-GMP which is proportional to the As(V) ions concentration [86].

Fe_3O_4 NPs functionalized graphene oxide quantum dots (GQDs), formally magnetic graphene oxide quantum dots (m-GQDs, Fe-GQDs) have been also used as a sensor for "turn on" sensing of As(III) ions [87]. The fluorescence emission of the composite is attributed to the transfer of electrons from the N atom of amide bond

with Fe_3O_4 NPs to the π-conjugation system of GQDs. The presence of As(III) ions causes large fluorescence enhancement because of aggregation due to complex formation, and intramolecular and extra-molecular interactions between As(III) ions and m-GQDs. The coordination between As(III) ions and Fe_3O_4 NPs through the hydroxyl groups leads to a physical and chemical adsorption process, which occurs at all pHs. Other metallic ions promote aggregation and hence fluorescence enhancement depending on the pH, and the As(III) sensing procedure has been found to be interfered when working at alkaline pHs [87].

2.3.2.2. Nanoprobes based on carbon dots

CDs synthesis is performed by heating compounds rich in C under controlled conditions, and microwave assistance is typically used to speed up the process [88-91], although ultrasound have been also applied for *in situ* CDs synthesis [92]. The recognition mechanism for CDs for Hg(II) ions detection involves the electrostatic interaction between Hg(II) ions and certain functional groups in the CDs. The use of thiourea, in combination with citric acid and urea, during CDs synthesis promotes the presence of S atoms in the nanostructures, which allows the strong binding between Hg(II) ions and the surface of the CDs [88]. The binding facilitates the electron/hole recombination annihilation through an alternate and efficient electron transfer process, and hence CDs fluorescence quenching [88]. Selectivity, however, was moderate, and I^- as well as some amino acids (glutamic acid, glutamine, cysteine, and histidine) have been found to be serious interferences when assessing Hg(II) ions.

Carbon nitride quantum dots (CNQDs) are synthesized using a nitrogen containing reagent (urea) together with the carbon source (citric acid or sodium citrate) [89,90]. Cao *et al*. explain the fluorescence quenching on the basis of two possible mechanisms, the ability of Hg(II) ions to form a stable non-fluorescent complex with the CNQDs, and an aggregate-induced quenching as a consequence of Hg(II) ions simultaneous binding to multiple N atoms of the CNQDs and O-contained groups (CNQDs was synthesised in the presence of

oleic acid) which induces aggregation [89]. High selectivity has been reported since the greater affinity of Hg(II) ions towards N, and the larger radius of Hg(II) ions than other metallic ions. High selectivity for Hg(II) ions has been also observed in a chemiluminescence (CL) system formed by CNQDs and the oxidant potassium ferricyanide which induces CL [90]. The presence of Hg(II) ions inhibits the CL reaction and the luminescence quenching is easily related to the Hg(II) ions concentration.

CNQDs synthesized from citric acid and N-(2-hydroxyethyl)ethylenediamine as a N source have been also used for preparing fluorescent hydrogel films after reaction with polyvinylamine (PVAm) and polymerization with acrylamide (AM) [91]. The PVAm-g-N-CDs/PAM hydrogel film responds to Hg(II) ions due to the formation of a stable non-fluorescent N-CDs-Hg(II) complex which facilitate non-radiative electron/hole recombination annihilation, and hence fluorescence quenching [91]. Although the highest fluorescence quenching was observed with the addition of Hg(II) ions, other metallic ions showed a moderate effect.

Finally, ultrasonication (ultrasound probe) has been used for *in situ* CDs synthesis from D-fructose and polyethylene glycol (PEG), procedure which is completed after only 60 s [92]. When the sonochemical CDs synthesis is performed in the presence of MeHg(I), a significant fluorescence quenching occurs, phenomena attributed to the hydrophobicity of MeHg(I) and its ultrasound-assisted permeation through the PEG coating. Other metallic ions, Hg(II) included, do not quench the CDs fluorescence, which implies a high selectivity for MeHg(I).

2.3.3. Molecularly/ionic imprinted polymer - quantum dots composites

Selectivity of the chemosensor systems is quite important to ensure a specific target assessment. As previously commented, IIPs are excellent materials for providing selectivity for the ion used as a template during the polymerization process, and improved selectivity of QD-based chemosensors can be achieved by coating the QDs' surface with MIPs and IIPs [74]. Despite there are several MIP-QD-

based chemosensors for organic targets [73,74], IIP-QDs-based systems for metallic ions are scarce. One of the drawbacks for preparing IIP-QDs is the template removal stage, which usually required concentrated mineral acids such as nitric acid and hydrochloric acid, compared to organic solvents used for treating MIP-QDs. IIP anchorage on the QDs' surface can be altered after the template removal process, and the luminescence properties of the QDs could also diminish.

An IIP-QDs chemosensor consisting of Mn doped ZnS QDs coated with an IIP based on the bifunctional 1-vinylimidazole monomer and As(III) ion as template has been prepared and applied for assessing inorganic arsenic (iAs) [93]. The presence of two N atoms in the 1-vinylimidazole structure allows the specific interaction with As(III) and As(V) ions, which promotes room temperature phosphorescence (RTP) quenching. The distribution ratio for both inorganic arsenic species were similar (151 for As(III) and 91 for As(V)) which implies that the chemosensor is adequate for assessing both inorganic forms. Distribution ratios for other metallic ions and for organoarsenic compounds were found to be quite small, and the selectivity factors for these ions and organoarsenic compounds were high, which proved the high selectivity of the prepared material for iAs [93]. Template removal based on nitric acid solutions, commonly used for template (As(III)) removal in 1-vinylimidazole-based IIPs [65,67] led to IIP coating leak as well as low RTP, and the use of ionic liquids as extractants (1% (m/v) 1-hexyl-3-methylimidazolium acetate) was found to give a successful template removal without damage of the IIP-QD composite [93].

A strategy based on covering the QDs with an MIP containing a specific ligand for recognizing an ion, instead of using the IIP synthesized with the ion template, could help to overcome problems derived from IIP-QDs damage during the template removal process. This is the case of a phenobarbital-based MIP-QD composite synthesized with MAA as a vinylated monomer and phenobarbital as a non-vinylated ligand over functionalized Mn-doped ZnS QDs [94]. Phenobarbital is a ligand that shows high and selective affinity for mercury ions [53,56], and phenobarbital trapped into the polymeric

matrix ensures specificity towards both Hg(II) and MeHg(I) ions by interaction through the N functionalities [94].

2.4. CONCLUSIONS

Current trends in the development of new techniques in elemental analysis must take economic and environmental aspects into consideration. Many nanomaterials-based trace element sample pre-treatment techniques have been developed in the past for simplifying operations and increasing the analytical performance of the methods. Solid phase extraction, especially those using MIPs/IIPs, have provided a significant contribution to element pre-concentration and speciation analysis in biological, food and environmental analysis. QDs have gained attention over other techniques as detection platforms, and a progressive growth in their analytical applications has taken place. However, when it comes to elemental analysis, especially in Hg and As, MIP and QDs applications are limited, even though they have shown to be powerful and versatile tools in the field of environmental analysis.

2.5. ACKNOWLEDGMENTS

This work was supported by the *Dirección Xeral de I+D – Xunta de Galicia Grupos de Referencia Competitiva* (project number ED431C2018/19), and Development of a Strategic Grouping in Materials - AEMAT (grant ED431E2018/08).

2.6. REFERENCES

[1] S.C.T. Nicklisch, L.T. Bonito, S. Sandin, A. Hamdoun, Mercury levels of yellowfin tuna (*Thunnus albacares*) are associated with capture location, Environmental Pollution, 229 (2017) 87-93.

[2] F.A. Ordiano, M.F. Galván, M.R. Rosiles, Bioaccumulation of mercury in muscle tissue of yellowfin tuna, *Thunnus albacares*, of the Eastern Pacific Ocean, Biological Trace Element Research, 144 (2011) 606-620.

[3] P. Li, X. Feng, G. Qiu, L. Shang, Z. Li, Mercury pollution in Asia: a review of the contaminated sites, Journal of Hazardous Materials, 168 (2009) 591-601.

[4] ATSDR, ATSDR's Substance Priority List, Agency for Toxic Substances and Disease Registry (https://www.atsdr.cdc.gov/SPL/), Access date: 2018-12-20.

[5] M. Harada, Minamata disease: methylmercury poisoning in Japan caused by environmental pollution, Critical Reviews in Toxicology, 25 (1995) 1-24.

[6] L. Amin-Zaki, M. Majeed, M.R. Greenwood, S.B. Elhassani, T.W. Clarkson, R.A. Doherty, Methylmercury poisoning in the Iraqi suckling infant: a longitudinal study over five years, Journal of Applied Toxicology, 1 (1981) 210-214.

[7] L.R. Goldman, M.W. Shannon, C.O.E. Health, Technical report: mercury in the environment: implications for pediatricians, Pediatrics, 108 (2001) 197-205.

[8] P.B. Tchounwou, W.K. Ayensu, N. Ninashvili, D. Sutton, Environmental exposure to mercury and its toxicopathologic implications for public health, Environmental Toxicology: An International Journal, 18 (2003) 149-175.

[9] S.L. Ferreira, V.A. Lemos, L.O. Silva, A.F. Queiroz, A.S. Souza, E.G. da Silva, W.N. dos Santos, C.F. das Virgens, Analytical strategies of sample preparation for the determination of mercury in food matrices—a review, Microchemical Journal, 121 (2015) 227-236.

[10] N.T. Loux, An assessment of mercury-species-dependent binding with natural organic carbon, Chemical Speciation and Bioavailability, 10 (1998) 127-136.

[11] Y. Gao, Z. Shi, Z. Long, P. Wu, C. Zheng, X. Hou, Determination and speciation of mercury in environmental and biological samples by analytical atomic spectrometry, Microchemical Journal, 103 (2012) 1-14.

[12] N.R. Razavi, M.T. Arts, M. Qu, B. Jin, W. Ren, Y. Wang, L.M. Campbell, Effect of eutrophication on mercury, selenium, and essential fatty acids in Bighead Carp (*Hypophthalmichthys nobilis*) from reservoirs of eastern China, Science of the Total Environment, 499 (2014) 36-46.

[13] U. Strandberg, M. Palviainen, A. Eronen, S. Piirainen, A. Laurén, J. Akkanen, P. Kankaala, Spatial variability of mercury and polyunsaturated fatty acids in the European perch (*Perca fluviatilis*) – Implications for risk-benefit analyses of fish consumption, Environmental Pollution, 219 (2016) 305-314.

[14] Z. Gong, X. Lu, M. Ma, C. Watt, X.C. Le, Arsenic speciation analysis, Talanta, 58 (2002) 77-96.

[15] J. Ma, M.K. Sengupta, D. Yuan, P.K. Dasgupta, Speciation and detection of arsenic in aqueous samples: a review of recent progress in non-atomic spectrometric methods, Analytica Chimica Acta, 831 (2014) 1-23.

[16] Y. Gao, P. Baisch, N. Mirlean, d.S.J.F.M. Rodrigues, L.N. Van, W. Baeyens, M. Leermakers, Arsenic speciation in fish and shellfish

from the North Sea (Southern bight) and Açu Port area (Brazil) and health risks related to seafood consumption, Chemosphere, 191 (2018) 89-96.

[17] J.L. Levy, J.L. Stauber, M.S. Adams, W.A. Maher, J.K. Kirby, D.F. Jolley, Toxicity, biotransformation, and mode of action of arsenic in two freshwater microalgae (*Chlorella sp.* and *Monoraphidium arcuatum*), Environmental Toxicology and Chemistry, 24 (2005) 2630-2639.

[18] M.A. Rahman, C. Hassler, Is arsenic biotransformation a detoxification mechanism for microorganisms?, Aquatic Toxicology, 146 (2014) 212-219.

[19] M.A. Rahman, H. Hasegawa, R.P. Lim, Bioaccumulation, biotransformation and trophic transfer of arsenic in the aquatic food chain, Environmental Research, 116 (2012) 118-135.

[20] V. Taylor, B. Goodale, A. Raab, T. Schwerdtle, K. Reimer, S. Conklin, M.R. Karagas, K.A. Francesconi, Human exposure to organic arsenic species from seafood, Science of The Total Environment, 580 (2017) 266-282.

[21] S. García-Salgado, G. Raber, R. Raml, C. Magnes, K.A. Francesconi, Arsenosugar phospholipids and arsenic hydrocarbons in two species of brown macroalgae, Environmental Chemistry, 9 (2012) 63-66.

[22] T.D. Ninh, Y. Nagashima, K. Shiomi, Unusual arsenic speciation in sea anemones, Chemosphere, 70 (2008) 1168-1174.

[23] K.i. Hanaoka, H. Ohno, N. Wada, S. Ueno, W. Goessler, D. Kuehnelt, C. Schlagenhaufen, T. Kaise, K.J. Irgolic, Occurrence of organo-arsenicals in jellyfishes and their mucus, Chemosphere, 44 (2001) 743-749.

[24] M.E. Bergés-Tiznado, F. Páez-Osuna, A. Notti, F. Regoli, Biomonitoring of arsenic through mangrove oyster (*Crassostrea*

corteziensis Hertlein, 1951) from coastal lagoons (SE Gulf of California): occurrence of arsenobetaine and other arseno-compounds, Environmental Monitoring and Assessment, 185 (2013) 7459-7468.

[25] A.H. Petursdottir, J.J. Sloth, J. Feldmann, Introduction of regulations for arsenic in feed and food with emphasis on inorganic arsenic, and implications for analytical chemistry, Analytical and Bioanalytical Chemistry, 407 (2015) 8385-8396.

[26] U. Arroyo-Abad, M. Pfeifer, S. Mothes, H.J. Stärk, C. Piechotta, J. Mattusch, T. Reemtsma, Determination of moderately polar arsenolipids and mercury speciation in freshwater fish of the River Elbe (Saxony, Germany), Environmental Pollution, 208 (2016) 458-466.

[27] K.O. Amayo, A. Raab, E.M. Krupp, T. Marschall, M. Horsfall Jr, J. Feldmann, Arsenolipids show different profiles in muscle tissues of four commercial fish species, Journal of Trace Elements in Medicine and Biology, 28 (2014) 131-137.

[28] J. Borak, H.D. Hosgood, Seafood arsenic: implications for human risk assessment, Regulatory Toxicology and Pharmacology, 47 (2007) 204-212.

[29] K.J. Whaley-Martin, I. Koch, K.J. Reimer, Arsenic species extraction of biological marine samples (Periwinkles, *Littorina littorea*) from a highly contaminated site, Talanta, 88 (2012) 187-192.

[30] JECFA, Summary of conclusion of the 72 of the Joint FAO/WHO Expert Committee on Food Additives, FAO/WHO, Rome, Italy, 2010.

[31] EFSA, Scientific Opinion on Arsenic in Food, EFSA Journal, 7 (2009) 1351.

[32] P. Liu, C.-N. Wang, X.Y. Song, Y.F. Yu, Y.N. Wu, Dietary intake of arsenic by children and adults from Jinhu area of China, Food Additives and Contaminants, 27 (2010) 1128-1135.

[33] T. Llorente-Mirandes, R. Rubio, J.F. López-Sánchez, Inorganic arsenic determination in food: a review of analytical proposals and quality assessment over the last six years, Applied Spectroscopy, 71 (2017) 25-69.

[34] S.C. Jewett, L.K. Duffy, Mercury in fishes of Alaska, with emphasis on subsistence species, Science of The Total Environment, 387 (2007) 3-27.

[35] EU/EC-1881, Commission Regulation (EC), No 1881/06 of setting maximum levels for certain contaminants in foodstuffs, Official Journal of European Union, L364 (2006) 5-24.

[36] A.R. Popovic, J.M. Djinovic-Stojanovic, D.S. Djordjevic, D.J. Relic, D.V. Vranic, M.P. Milijasevic, L.L. Pezo, Levels of toxic elements in canned fish from the Serbian markets and their health risks assessment, Journal of Food Composition and Analysis, 67 (2018) 70-76.

[37] M.S. Evans, D. Muir, W.L. Lockhart, G. Stern, M. Ryan, P. Roach, Persistent organic pollutants and metals in the freshwater biota of the Canadian Subarctic and Arctic: An overview, Science of The Total Environment, 351-352 (2005) 94-147.

[38] W. Maher, F. Krikowa, M. Ellwood, S. Foster, R. Jagtap, G. Raber, Overview of hyphenated techniques using an ICP-MS detector with an emphasis on extraction techniques for measurement of metalloids by HPLC–ICPMS, Microchemical Journal, 105 (2012) 15-31.

[39] W.C. Tseng, K.C. Hsu, C.S. Shiea, Y.L. Huang, Recent trends in nanomaterial-based microanalytical systems for the speciation of trace elements: A critical review, Analytica Chimica Acta, 884 (2015) 1-18.

[40] Z. Mester, R. Sturgeon, J. Pawliszyn, Solid phase microextraction as a tool for trace element speciation, Spectrochimica Acta Part B: Atomic Spectroscopy, 56 (2001) 233-260.

[41] A. Martín-Esteban, Molecularly-imprinted polymers as a versatile, highly selective tool in sample preparation, Trends in Analytical Chemistry, 45 (2013) 169-181.

[42] E. Turiel, A. Martín-Esteban, Molecularly imprinted polymers for sample preparation: a review, Analytica Chimica Acta, 668 (2010) 87-99.

[43] A. Speltini, A. Scalabrini, F. Maraschi, M. Sturini, A. Profumo, Newest applications of molecularly imprinted polymers for extraction of contaminants from environmental and food matrices: A review, Analytica Chimica Acta, 974 (2017) 1-26.

[44] G. Vasapollo, R.D. Sole, L. Mergola, M.R. Lazzoi, A. Scardino, S. Scorrano, G. Mele, Molecularly imprinted polymers: present and future prospective, International Journal of Molecular Sciences, 12 (2011) 5908-5945.

[45] H. Yan, K.H. Row, Characteristic and synthetic approach of molecularly imprinted polymer, International Journal of Molecular Sciences, 7 (2006) 155-178.

[46] W. Wu, Q. He, C. Jiang, Magnetic Iron Oxide Nanoparticles: Synthesis and Surface Functionalization Strategies, Nanoscale Research Letters, 3 (2008) 397.

[47] S. Chaitidou, O. Kotrotsiou, K. Kotti, O. Kammona, M. Bukhari, C. Kiparissides, Precipitation polymerization for the synthesis of nanostructured particles, Materials Science and Engineering: B, 152 (2008) 55-59.

[48] T.P. Rao, S. Daniel, J.M. Gladis, Tailored materials for preconcentration or separation of metals by ion-imprinted polymers for solid-phase extraction (IIP-SPE), Trends Anal. Chem. 23 (2004) 28–35.

[49] T.P. Rao, R. Kala, S. Daniel, Metal ion-imprinted polymers--novel materials for selective recognition of inorganics, Anal. Chim. Acta 578 (2006) 105-116.

[50] F. Shakerian, K.-H. Kim, E. Kwon, J.E. Szulejko, P. Kumar, S. Dadfarnia, A.M. Haji Shabani, Advanced polymeric materials: Synthesis and analytical application of ion imprinted polymers as selective sorbents for solid phase extraction of metal ions, Trends in Analytical Chemistry, 83 (2016) 55-69.

[51] M. Firouzzare, Q. Wang, Synthesis and characterization of a high selective mercury (II)-imprinted polymer using novel aminothiol monomer, Talanta, 101 (2012) 261-266.

[52] T. Yordanova, I. Dakova, K. Balashev, I. Karadjova, Polymeric ion-imprinted nanoparticles for mercury speciation in surface waters, Microchemical Journal, 113 (2014) 42-47.

[53] R. Rodríguez-Fernández, E. Peña-Vázquez, P. Bermejo-Barrera, Synthesis of an imprinted polymer for the determination of methyl-mercury in marine products, Talanta 144 (2015) 636–641.

[54] D.K. Singh, S. Mishra, Synthesis and characterization of Hg(II)-ion-imprinted polymer: Kinetic and isotherm studies, Desalination 257 (2010) 177–183.

[55] M. Roushani, S. Abbasi, H. Khani, Synthesis and application of ion-imprinted polymer nanoparticles for the extraction and preconcentration of mercury in water and food samples employing cold vapor atomic absorption spectrometry, Environmental Monitoring Assessment 187 (2015) 601.

[56] M.P. Rodríguez-Reino, R. Rodríguez-Fernández, E. Peña-Vázquez, R. Domínguez-González, P. Bermejo-Barrera, A. Moreda-Piñeiro, Mercury speciation in seawater by liquid chromatography-inductively coupled plasma-mass spectrometry following solid phase extractionpre-concentration by using an ionic imprinted polymer

based on methyl-mercury–phenobarbital interaction, Journal of Chromatography A 1391 (2015) 9–17.

[57] M. Andaç¸ S. Mirel, S. Şenel, R. Say, A. Ersöz, A. Denizli, Ion-imprinted beads for molecular recognition based mercury removal from human serum, International Journal of Biological Macromolecules 40 (2007) 159–166.

[58] M. Soleimani, M.G. Afshar, Highly selective solid phase extraction of mercury ion based on novel ion imprinted polymer and its application to water and fish samples, Journal of Analytical Chemistry 70 (2015) 5–12.

[59] Y. Liu, X. Chang, D. Yang, Y. Guo, S. Meng, Highly selective determination of inorganic mercury(II) after preconcentration with Hg(II)-imprinted diazoaminobenzene–vinylpyridine copolymers, Analytica Chimica Acta 538 (2005) 85–91.

[60] Z. Zhang, J. Li, X. Song, J. Mac, L. Chen, Hg^{2+} ion-imprinted polymers sorbents based on dithizone–Hg^{2}+ chelation for mercury speciation analysis in environmental and biological samples, RSC Advances 4 (2014) 46444.

[61] X. Liu, C. Qi, T. Bing, X. Cheng, D. Shangguan, Specific mercury(II) adsorption by thymine-based sorbent, Talanta 78 (2009) 253–258.

[62] E. Najafi, F. Aboufazeli, H.R.L.Z. Zhad, O. Sadeghi, V. Amani, A novel magnetic ion imprinted nano-polymer for selective separation and determination of low levels of mercury(II) ions in fish samples, Food Chemistry 141 (2013) 4040–4045.

[63] T. Alizadeh, M. Rashedi, Synthesis of nano-sized arsenic-imprinted polymer and its use as As^{3+} selective ionophore in a potentiometric membrane electrode: Part 1, Analytica Chimica Acta, 843 (2014) 7-17.

[64] T. Alizadeh, M. Rashedi, Y. Hanifehpour, S.W. Joo, Improvement of durability and analytical characteristics of arsenic-imprinted polymer-based PVC membrane electrode via surface modification of nano-sized imprinted polymer particles: Part 2, Electrochimica Acta, 178 (2015) 877-885.

[65] Y.K. Tsoi, Y.M. Ho, K.S.Y. Leung, Selective recognition of arsenic by tailoring ion-imprinted polymer for ICP-MS quantification, Talanta, 89 (2012) 162-168.

[66] L.D. Mafu, B.B. Mamba, T.A. Msagati, Synthesis and characterization of ion imprinted polymeric adsorbents for the selective recognition and removal of arsenic and selenium in wastewater samples, Journal of Saudi Chemical Society, 20 (2016) 594-605.

[67] K.K. Jinadasa, E. Peña-Vázquez, P. Bermejo-Barrera, A. Moreda-Piñeiro, Ionic imprinted polymer solid-phase extraction for inorganic arsenic selective pre-concentration in fishery products before high-performance liquid chromatography –inductively coupled plasma-mass spectrometry speciation, Journal of Chromatography A 1619 (2020) 460973.

[68] L. Fang, X. Min, R. Kang, H. Yu, S.G. Pavlostathis, X. Luo, Development of an anion imprinted polymer for high and selective removal of arsenite from wastewater, Science of the Total Environment, 639 (2018) 110-117.

[69] L. Önnby, V. Pakade, B. Mattiasson, H. Kirsebom, Polymer composite adsorbents using particles of molecularly imprinted polymers or aluminium oxide nanoparticles for treatment of arsenic contaminated waters, Water Research, 46 (2012) 4111-4120.

[70] Y. Ding, S. Wang, J. Li, L. Chen, Nanomaterial-based optical sensors for mercury ions, Trends in Analytical Chemistry, 82 (2016) 175-190.

[71] H. Kuang, Y. Zhao, W. Ma, L. Xu, L. Wang, C. Xu, Recent developments in analytical applications of quantum dots, Trends in Analytical Chemistry, 30 (2011) 1620-1636.

[72] C. Frigerio, D.S. Ribeiro, S.S.M. Rodrigues, V.L. Abreu, J.A. Barbosa, J.A. Prior, K.L. Marques, J.L. Santos, Application of quantum dots as analytical tools in automated chemical analysis: A review, Analytica Chimica Acta, 735 (2012) 9-22.

[73] R. Li, Y. Feng, G. Pan, L. Liu, Advances in molecularly imprinting technology for bioanalytical applications, Sensors, 19 (2019) 177.

[74] A. Moreda-Piñeiro, J. Sánchez-González, M.P. Chantada-Vázquez, A.M. Bermejo, P. Bermejo-Barrera, MIPs as a versatile tool for micro-solid-phase extraction and probe sensing, Current Chemical Biology 12 (2018) 114–134.

[75] K.A. Willets, R.P. Van Duyne, Localized surface plasmon resonance spectroscopy and sensing, Annual Review Physical Chemistry 58 (2007) 267–297.

[76] J. Duan, H. Yin, R.Wei, W.Wang, Facile colorimetric detection of Hg^{2+} based on anti-aggregation of silver nanoparticles, Biosensors and Bioelectronics 57 (2014) 139–142.

[77] L. Chen, J. Li, L. Chen, Colorimetric detection of mercury species based on functionalized gold nanoparticles, ACS Applied Materials and Interfaces 6 (2014) 15897–15904.

[78] A. Jaiswal, S.S. Ghsoh, A. Chattopadhyay, Quantum dot impregnated-chitosan film for heavy metal ion sensing and removal, Langmuir 28 (2012) 15687–15696.

[79] Z.Q. Zhou, R. Yan, J. Zhao, L.Y. Yang, J.L. Chen, Y.J. Hu, F.L. Jiang, Y. Liu, Highly selective and sensitive detection of Hg^{2+} based on fluorescence enhancement of Mn-doped ZnSe QDs by Hg^{2+}-Mn^{2+} replacement, Sensors and Actuators B 254 (2018) 8–15.

[80] T. Gong, J. Liu, X. Liu, J. Liu, J. Xiang, Y. Wu, A sensitive and selective sensing platform based on CdTe QDs in the presence of L-cysteine for detection of silver, mercury and copper ions in water and various drinks, Food Chemistry 213 (2016) 306–312.

[81] Y.S. Xia, C.Q. Zhu, Use of surface-modified CdTe quantum dots as fluorescent probes in sensing mercury (II), Talanta 75 (2008) 215–221.

[82] J. Ke, X. Li, Q. Zhao, Y. Hou, J. Chen, Ultrasensitive quantum dot fluorescence quenching assay for selective detection of mercury ions in drinking water. Scientific Reports 4 (2014) 5624.

[83] L. Tan, Y. Li, Y. Tang, C. Kang, Z. Yu, S. Xu, Room temperature phosphorescence sensor for Hg^{2+} based on Mn-doped ZnS quantum dots, Journal of Nanoscience and Nanotechnology 12 (2012) 7788–7795.

[84] K.P. Prasad, Y. Chen, M.A. Sk, A. Than, Y. Wang, H. Sun, K.-H. Lim, X. Dong, P. Chen, Fluorescent quantum dots derived from PEDOT and their applications in optical imaging and sensing, Materials Horizons 1 (2014) 529–534.

[85] B. Babamiri, A. Salimi, R. Hallaj, Switchable electrochemiluminescence aptasensor coupled with resonance energy transfer for selective attomolar detection of Hg^{2+} via CdTe@CdS/dendrimer probe and Au nanoparticle quencher, Biosensensor and Bioelectronics 102 (2018) 328–335.

[86] S.H. Wen, R.P. Liang, H.H. Zeng, L. Zhang, J.D. Qiu, CdSe/ZnS quantum dots coated with carboxy-PEG and modified with the terbium(III) complex of guanosine 5′-monophosphate as a fluorescent nanoprobe for ratiometric determination of arsenate via its inhibition of acid phosphatase activity, Microchimica Acta 186 (2019) 45.

[87] S. Pathan, M. Jalal, S. Prasad, S. Bose, Aggregation-induced enhanced photoluminescence in magnetic graphene oxide quantum dots as a fluorescence probe for As(III) sensing, Journal of Materials Chemistry A, 7 (2019) 8510-8520.

[88] R. Tabaraki, N. Sadeghinejad, Microwave assisted synthesis of doped carbon dots and their application as green and simple turn off–on fluorescent sensor for mercury (II) and iodide in environmental samples, Ecotoxicology and Environmental Safety 153 (2018) 101–106.

[89] X. Cao, J. Ma, Y. Lin, B. Yao, F. Li, W. Weng, X. Lin, A facile microwave-assisted fabrication of fluorescent carbon nitride quantum dots and their application in the detection of mercury ions, Spectrochim. Acta A 151 (2015) 875–880.

[90] H. Abdolmohammad-Zadeh, E. Rahimpour, A novel chemosensor based on graphitic carbon nitride quantum dots and potassium ferricyanide chemiluminescence system for Hg(II) ion detection, Sensor. Actuat. B Chem. 225 (2016) 258–266.

[91] S. Yu, K. Chen, F. Wang, Y. Zhu, X. Zhang, Polymer composite fluorescent hydrogel film based on nitrogen-doped carbon dots and their application in the detection of Hg^{2+} ions, Luminescence 32 (2017) 970–977.

[92] I. Costas-Mora, V. Romero, I. Lavilla, C. Bendicho, In situ building of a nanoprobe based on fluorescent carbon dots for methylmercury detection, Anal. Chem. 86 (2014) 4536–4543.

[93] K.K Jinadasa, E. Peña-Vázquez, P. Bermejo-Barrera, A. Moreda-Piñeiro, Synthesis and application of a surface ionic imprinting polymer on silica-coated Mn-doped ZnS quantum dots as a chemosensor for the selective quantification of inorganic arsenic in fish, Analytical and Bioanalytical Chemistry 412 (2020) 1663–1673.

[94] K.K Jinadasa, E. Peña-Vázquez, P. Bermejo-Barrera, A. Moreda-Piñeiro, A phenobarbital containing polymer/silica coated quantum dot composite for the selective recognition of mercury species in fish samples using a room temperature phosphorescence quenching assay, Talanta 216 (2020) 120959.

II. OBJECTIVES

USC
UNIVERSIDADE
DE SANTIAGO
DE COMPOSTELA

II. Objectives

The aim of this Thesis is the development of rapid analysis methods to assess the levels of mercury and arsenic, as well as mercury (inorganic mercury and methylmercury) and inorganic arsenic species, in foodstuff (fish, seaweed and rice).

The specific objectives are as follows:

- Synthesis of nanoparticles with selective response to total mercury, and inorganic arsenic based on molecularly/ionic imprinted polymer and luminescent quantum dots (MIP/IIP-QDs), and characterization of the prepared nanomaterials using TEM-EDX, FT-IR and XRF.
- Development of room temperature phosphorescent screening methods based on IIP-QDs for a fast and low-cost determination of inorganic arsenic [As(III) and As(V)] in fish.
- Synthesis of molecularly and ionic imprinted polymers as new selective absorbents to develop solid-phase and micro-solid phase extraction procedures for the isolation/pre-concentration of inorganic mercury and methylmercury, and inorganic arsenic species [As(III) and As(V)] from foodstuff.
- Development of IIP based-solid phase extraction (on-column) procedures combined with HPLC-ICP-MS for inorganic arsenic [As(III) and As(V)] speciation in fish. The developed methods will be compared with screening procedures based on selective luminescent IIP-QDs for total inorganic arsenic.
- Development of micro-solid phase extraction procedures (ionic imprinted polymer vortex-assisted dispersive micro-solid phase extraction) combined with HPLC-ICP-MS for inorganic arsenic speciation in rice.
- Development of room temperature phosphorescent screening methods based on phenobarbital containing polymer/ silica coated QDs composites for a fast and low-cost determination of total mercury (inorganic mercury and methylmercury) in fish.
- Development of MIP based-solid phase extraction (on-column) procedures combined with HPLC-ICP-MS for inorganic mercury and methylmercury speciation in seaweed.

USC
UNIVERSIDADE
DE SANTIAGO
DE COMPOSTELA

III. RESULTS AND DISCUSSION

USC
UNIVERSIDADE
DE SANTIAGO
DE COMPOSTELA

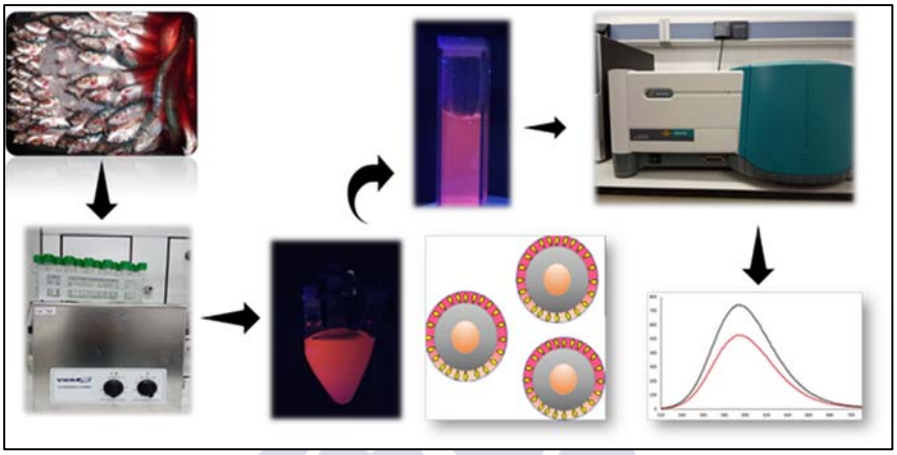

CHAPTER 1

SYNTHESIS AND APPLICATION OF A SURFACE IONIC IMPRINTING POLYMER ON SILICA-COATED Mn-DOPED ZnS QUANTUM DOTS AS A CHEMOSENSOR FOR THE SELECTIVE QUANTIFICATION OF INORGANIC ARSENIC IN FISH

KAMAL K JINADASA, ELENA PEÑA-VÁZQUEZ, PILAR BERMEJO-BARRERA, ANTONIO MOREDA-PIÑEIRO

ANALYTICAL AND BIOANALYTICAL CHEMISTRY

VOLUME 412 (2020) 1663–1673

https://doi.org/10.1007/s00216-020-02405-1

USC
UNIVERSIDADE
DE SANTIAGO
DE COMPOSTELA

Synthesis and application of a surface ionic imprinting polymer on silica-coated Mn-doped ZnS quantum dots as a chemosensor for the selective quantification of inorganic arsenic in fish

Kamal K Jinadasa, Elena Peña-Vázquez, Pilar Bermejo-Barrera, Antonio Moreda-Piñeiro

Trace Element, Spectroscopy and Speciation Group (GETEE), Strategic Grouping in Materials (AEMAT), Department of Analytical Chemistry, Nutrition and Bromatology, Faculty of Chemistry, Universidade de Santiago de Compostela. Avenida das Ciencias, s/n. 15782, Santiago de Compostela, Spain

Abstract

A novel room temperature phosphorescence chemosensor probe has been successfully developed and applied to the selective detection and quantification of inorganic arsenic (As(III) plus As(V)) in fish samples. The prepared material (IIP@ZnS:Mn QDs) was based on Mn-doped ZnS quantum dots coated with (3-aminopropyl) triethoxysilane and an As(III) ionic imprinted polymer. The novel use of vinyl imidazole as a complexing reagent when synthesizing the ionic imprinted polymer guarantees that both inorganic arsenic species (As(III) and As(V)) can interact with the recognition cavities in the ionic imprinted polymer. After characterization, several studies were performed to enhance the interaction between the targets (As(III) and As(V) ions) and the IIP@ZnS:Mn QDs nanoparticles. The optimization and validation process showed that the composite material offers high selectivity (high imprinting factor) for inorganic arsenic species. The limit of quantification for total inorganic As was 29.6 μg kg^{-1}, value lower than the EU/EC regulation limits proposed for other foodstuffs than fish, such as rice. The proposed method is therefore simple, requires short analysis times and offers good sensitivity, precision (inter-day relative standard deviations lower than 10%), and quantitative analytical recoveries. The method has been successfully applied to assess total inorganic arsenic in several fishery products, showing good agreement with the total inorganic arsenic

concentration (As(III) plus As(V)) found after applying other advanced and expensive methods such those based on high performance liquid chromatography hyphenated to inductively coupled plasma – mass spectrometry.

Keywords: Silica-coated Mn-doped ZnS quantum dots, ionic imprinted polymer, room temperature phosphorescence, inorganic arsenic, fish, chemosensor probe

1.1. INTRODUCTION

Arsenic (As) is one of the major global environmental pollutants and it is a naturally occurring element at trace levels in the air, water, soil, and in animals and plants [1]. The Agency for Toxic Substances and Disease Registry (ATSDR) of the United States ranked arsenic as number one in their Substance Priority List in 2017, while the International Agency for Research on Cancer (IARC) has classified arsenic as a class one carcinogen due to the existence of sufficient evidence of human carcinogenetic effect [2,3]. Food and water are the main pathways for As exposure in human population. Moreover, seafood and fish are one of the major contributors to As in the diet [4]. The toxicity and bioavailability of As depends on its concentration and chemical form; hence, speciation data is essential to define the toxicological endpoint [5]. Arsenobetaine (AsB) is considered a non-toxic form and it has been identified to be the major arsenical in seafood, while other organic toxic As species such as monomethyl arsenic (MMA), dimethyl arsenic (DMA), and most toxic inorganic As species such as arsenite [As(III)] and arsenate [As(V)] have been also found in seafood and fish [6].

Semiconductor nanocrystals or quantum dots (QDs) have been widely used as probes for recognizing and sensing molecules [7,8] because of their unique optical and electronic properties such as large surface-to-volume ratios, high luminescence efficiency, narrow symmetric emission and excellent photostability and quantum-size effects [9,10]. Inherent luminescent properties of QDs make them to be appealing materials for chemosensors development as reviewed by Costa-Mora et al. [11]. Most of applications, however, have exploited

the QDs' fluorescent properties, and little attention has been paid to room temperature phosphorescence (RTP). The main advantage of RTP is the longer luminescence (RTP) lifetime, which helps to avoid interferences from auto-fluorescence and scattering light, and increases detection reliability [8]. Therefore, some doped (functionalized) semiconductor systems based on RTP have been developed for the detection of several molecules and metal ions such as acetone in water and urine [12], thiram residues in fresh fruit peels [13], and 2,4,6-trinitrotoluene [8], sulfide [14], Hg(II) [15], Pb(II) [16], and Mn(VII) [17] in water samples.

However, selectivity of QDs-based chemosensors has been reported to be poor and the methods are not straightforward for complex samples. Selectivity improvement can be easily reached when combining Molecular Imprinting Technology (MIT) with QDs. MIT is an appealing technique to design tailor-made materials with high selectivity for a target molecule (Molecularly Imprinted Polymers, MIPs) [18], or for a target ion (Ionic Imprinted Polymers, IIPs) [19]. The synthesis of MIP/IIP-QD composites becomes therefore a hot spot in analytical science because allows overcoming the problems related to the lack of selectivity of QD measurements, and offers sensitive determinations based on the inherent QDs' luminescent properties. Recent reviews on this issue show an increasing number of MIP-QDs-based fluorescence methods for the selective detection of organic compounds [20].

Despite IIPs have been used for selective adsorbents in solid phase extraction (SPE) procedures [19], there are few developments for IIP-QD composites for metal ions sensing. To the best of our knowledge, there are only two recent developments combining IIP and QDs for fluorescence sensing of Cu(II) and Hg(II) in water [22] and Cr(VI) in aqueous solutions [23]. The approach performed by Qi *et al.* [22] consists of grafted IIP-CdTe QDs for a fluorescence multiplexed detection of Cu(II)and Hg(II) ions; whereas, Cr(IV) detection was carried out by Mn-doped ZnS QDs [23]. Sensitive and selectivity RTP chemosensors based on IIP-QDs have still not been developed, and our studies are the first RTP probe for metal ions and also the first for inorganic arsenic (As(III) and As(V)). The use of a bifunctional

monomer such as 1-vinyl imidazole allows selective recognition cavities for the template ion (As(III)) and also for As(V), structurally similar ions, which generate a selective chemosensor for inorganic As species (both inorganic As species are highly toxic species). The chemosensor system proposed is therefore less expensive than methodologies based on high performance liquid chromatography (HPLC) and atomic spectrometric techniques (mainly inductively coupled plasma – mass spectrometry, ICP-MS), and requires a simple sample pre-treatment. The development of new methods for detecting inorganic As in fish with convenience, low cost, high sensitivity, and fast analysis is a great challenge. To the best of the authors' knowledge, the current research is the first attempt to develop a phosphorescent IIP-QDs composite for the detection and quantification of total inorganic As. High sensitive and selective total inorganic As can be attained using low-cost instrumentation such as those based on phosphorescence measurements.

1.2. MATERIALS AND METHODS

1.2.1. Reagents

All chemicals and reagents used were of analytical grade or better, and they were used as received in the lab, except 2,2'-azobisisobutyronitrile (AIBN) and divinylbenzene (DVB), both reagents from Sigma Aldrich (Steinheim, Germany), which were subjected to a further purification procedure (polymerization inhibitor removal according to Chantada-Vázquez *et al.* [24]. Briefly, AIBN was purified by crystallization at -20 °C after dissolving the reagent in Chromasolv methanol (Merck, Darmstadt, Germany) at 50-60 °C. DVB reagent was passed throughout a mini column containing 0.50 g of neutral alumina (Merck). All aqueous solutions were prepared with ultrapure water with a resistivity of 18.2 MΩ cm^{-1} (Milli Q-A10, Millipore, Bedford, MA, USA). Mn-doped ZnS QDs were synthesized using zinc sulphate heptahydrate (Panreac, Barcelona, Spain), manganese dichloride (Merck) and sodium sulfide hydrate from Fluka (Buchs, Switzerland). APTES (3-aminopropyl)-triethoxysilane, powdered sodium(meta)arsenite, and 1-vinyl imidazole were from

Sigma Aldrich. Arsenite and arsenate stock standard solutions, 1000 mg L^{-1}, were from Panreac. Standard solutions of monomethyl arsenic (MMA), dimethyl arsenic (DMA), arsenobetaine (AsB) and arsenocholine (AsC) (1000 mg L^{-1}) were prepared by dissolving the appropriate amounts of MMA (Carlo Erba, Milan, Italy), DMA (Merck), and AsB and AsC (Tri Chemical Laboratory Inc, Yamanashi, Japan).

Nitric acid (Hyperpur, 69%), 33% hydrogen peroxide, acetic acid, and ethanol were supplied by Panreac; whereas, ammonium dihydrogen phosphate was from BDH (Poole, United Kingdom). NexIon Setup Solution (10 µg L^{-1} of Be, Ce, Fe, In, Li, Mg, Pb, and U in 1% HNO_3) was purchased by Perkin Elmer (Shelton, CT, USA). Multi-element standard solutions (cross-reactivity studies) were prepared by combining single Ca, Co and Mg stock standard solutions (1000 mg L^{-1}) from Merck, single Cr, Hg, K, P, Pb and Zn, stock standard solutions (1000 mg L^{-1}) from Scharlab (Barcelona, Spain), and single Cd, Cu, Fe and Na stock standard solutions (1000 mg L^{-1}) from Perkin Elmer. Internal standard (Ge) for ICP-MS measurements were prepared from a single-element standard (1000 mg L^{-1}) purchased from Perkin Elmer. 1-hexyl-3-methylimidazolium was purchased from IoLiTec Ionic Liquids Technologies, (Heilbronn, Germany). The BCR-668 (mussel tissue) certified reference material (CRM) was from the European Commission Joint Research Centre, Institute for Reference Materials and Measurements (Geel, Belgium).
Other consumables were Durapore 0.20 µm membrane filters (Millipore), disposable syringes (sterile, 5 mL) (Dispomed, Gelnhausen, Germany), replacement polytetrafluorethylene frits (20 µm porosity for use with 6 mL glass SPE tubes) from Supelco (Bellefonte, USA), and cellulose acetate 0.45 µm syringe filters (Labbox Labware S.L., Barcelona, Spain).

1.2.2. Instrumentation

Morphology of synthesized IIP-QDs was assessed by transmission electron microscopy – energy-dispersive spectroscopy (TEM-EDS) using a JEM-2010F (JEOL, (Tokyo, Japan) equipped with an IncaEnergy TEM detector (Oxford Instruments, High Wycombe,

United Kingdom) operating as high-angle annular dark-field scanning transmission electron microscopy (HAADF-STEM). Microstructure of the prepared material was assessed by X-ray diffraction spectrometry (XRD) using an EMPYREAM instrument from PaNalytical (Almelo, Netherlands). A Spectrum-Two FT-IR spectrometer from Perkin Elmer (Waltham, MA, USA) operating at the attenuated total reflectance (ATR) mode was also used for characterizing the synthesized material.

A Cary Eclipse fluorescence spectrophotometer from Varian (Victoria, Australia) equipped with a xenon discharge lamp and 10 mm quartz cells and operating in phosphorescence mode was used for RTP measurements. Single determination of inorganic As species (III and V) by HPLC-ICP-MS were performed with a Flexar high-performance liquid chromatograph hyphenated to a NexION 300 inductively coupled plasma mass spectrometer (Perkin Elmer, Waltham, USA). The As species were separated using a PRP×100 column (10 μm, 4.1×100 mm) from Hamilton (Reno, NV, USA). The same ICP-MS instrument connected to a SeaFast SC2DX autosampler (Elemental Scientific, Omaha, NB, USA) was also used for total As determination after microwave assisted acid digestion of fish samples using a Milestone Ethos Plus high-performance lab station (Sorisole, BG, Italy).

An ASE150 accelerated solvent extractor (Dionex Corporation, Sunnyvale, CA, USA) was used for template removal from IIP-QDs nanoparticles. An USC60TH ultrasonic cleaner bath (45 kHz, 120 W) from VWR (Leuven, Belgium), an ultracentrifuge (Sigma 2K15, Osterode, Germany), a Basic 20 pH meter with glass combined electrode (Crison, Barcelona, Spain), a domestic Taurus blade grinder (Taurus, Barcelona, Spain), an oven model 207 from Selecta (Barcelona, Spain), and a Classic ML analytical balance (Mettler Toledo, Columbus, OH, USA) were used throughout this research.

1.2.3. Synthesis of IIP@ZnS:Mn QDs

Water-soluble IIP coated Mn-doped ZnS QDs (IIPs@ZnS:Mn QDs =IIP-QDs) were synthesized via the procedure explained by Ren and

Chen [25] with some modifications. The procedure includes four steps:

(1) Briefly, 12.5 mmol $ZnSO_4 \cdot 7H_2O$, 1 mmol of $MnCl_2$ and 40 mL of ultrapure water were placed into a three-neck flask under ultrasonication and N_2 stream. After 10 min, 10 mL of 1.25 mmol of Na_2S was added dropwise using an addition funnel. The ultrasonication continued for 30 min, and then 2.5 mL of APTES was added. Afterwards, ultrasonication was kept for 4.5 h under the N_2 stream. The synthesized Mn-doped ZnS QDs were isolated by centrifugation at 3000 rpm for 20 min. The centrifugation step was repeated 3 times, washing with 5 mL ethanol between each step. Synthesized nanoparticles were dried inside a desiccator in the dark, and finally stored at 4 °C.

(2) A pre-polymerization mixture was prepared by dissolving 1.5 mmol of $NaAsO_2$ and 6.5 mmol of vinyl imidazole in 10 mL of acetic acid in methanol (25 % v/v), sparging with N_2. The mixture was stored in the dark for 12 h to facilitate template and monomer assembly. The template was not used in this step for the synthesis of the non-imprinted polymer (NIP).

(3) The third step of the synthesis consists of mixing approximately 0.5 g of ZnS:Mn doped QDs with the pre-polymerization mixture (10 mL of 25%(v/v) acetic acid in methanol containing $NaAsO_2$ and 1-vinyl imidazole), 32 mmol of DVB, 25 mL ultrapure water, and 40 mg of AIBN. The polymerization was carried out for 5 h under ultrasounds. Finally, the IIP-QDs were cleaned with 60 mL of ethanol, dried and stored in the dark at 4 °C.

(4) Template removal is a critical procedure in the IIP-QDs synthesis process. Three different procedures were tested to remove the template ($NaAsO_2$) by using an aqueous solution of ionic liquid (IL) 1-hexyl-3-methylimidazolium acetate at 1% (m/v) as an extractant. In the first procedure, 0.5 g of IIP-QDs were packed into 5 mL syringes (polymer material between polytetrafluorethylene frits), and a volume of 750 mL of the IL solution was passed at a 0.5 mL min^{-1} flow rate. In the second procedure, a mass of 0.5 g of IIP-QDs was placed into a beaker and stirred with 50 mL of IL solution for 6 h (the process was repeated 10 times with fresh extractant solution). In

the third method, a mass 0.5 g of IIP-QDs was introduced into the ASE cell and the extraction was carried out during 7 cycles (temperature 80 °C, pressure 1500 psi, extraction time 10 min, extraction volume 20 mL). Negligible $NaAsO_2$ amounts (As(III) concentrations by ICP-MS) were found in the final washing solution after the application of any of the procedures. The ASE procedure is a quick and easy-to-use method; however, the resulted IIP-QDs were less stable when suspended in the aqueous solution than those IIP-QDs after template removal by using the other two methods. This may be due to high pressure of the ASE. Therefore, on-column and stirring procedures were finally selected for template removal.

1.2.4. Phosphorescence measurements

Measurements were carried out in phosphorescence scan mode at room temperature (20-25 °C). The excitation and emission slit widths were 10 nm and 20 nm, respectively. The photomultiplier voltage was set as a medium, while excitation wavelength (289 nm) and emission wavelength (595 nm; scan started at 520 nm and ended up at 720 nm) were selected. Moreover, the acquisition parameters in phosphorescence mode (total decay time, number of flashes, delay time and gate time) were 0.006 s, 1, 0.1 ms and 3.0 ms, respectively. All the measurements were carried out with the appropriate quantity of IIP-QDs or NIP@ZnS:Mn QDs (NIP-QDs) dispersed in a constant volume of 0.1M/0.1M KH_2PO_4-NaOH solution. The determination of inorganic As (III and V) was based on the decrease on the phosphorescence intensity (quenching effect) when these ions are present and interact with the recognition cavities of the IIP layer over the luminescent QDs.

1.2.5. Analysis of samples

Fish samples were obtained from local markets in Santiago de Compostela, and the following species were studied: yellowfin tuna (*Thunnus albacares)*, swordfish (*Xiphias gladius)*, blue shark (*Prionace glauca)* and cod (*Gadus morhua).* Inorganic arsenic extraction was performed using the following procedure: Approximately, 1.0 g of homogenate fish sample (0.2 g of CRM) was

mixed with 5 mL of ultra-pure water under ultrasounds for 30 min. The mixture was then centrifuged (3000 rpm, 10 min), and the supernatant was decanted. The above procedure was repeated twice, and supernatants were combined and filtered before RTP and HPLC-ICP-MS (method used for comparison purposes, details in Table S1, electronic supplementary information ESI) measurements.

For total As assessment in fish, samples were acid digested by using microwave assistance. Briefly, 1.0 g of fish sample (0.2 g of CRM) was placed in the microwave reactors and pre-digested with 3.0 mL of 69 % (v/v) HNO_3, 4.0 mL of ultrapure water and 1.0 mL of H_2O_2 for 15 min at room temperature. Pre-digested samples were then subjected to microwave by increasing the temperature from room temperature to 180 °C for 15 min, followed by a treatment at this temperature for 10 min. Acid digests were then made up to 25 mL with ultrapure water, and they were stored in polyethylene bottles at room temperature before ICP-MS analysis (operating conditions in Table S2, ESI).

1.3. RESULTS AND DISCUSSION

1.3.1. Preparation and characterization of IIP/NIP@ZnS:Mn QDs

Silica coating core-shell rational design has been developed for synthesis nanomaterials with versatile advantages [8]. Silica is considered as 'generally recognized as a safe' (GRAS) by the United States Food and Drug Administrator (US-FDA) due to low toxicity [26]. APTES (3-aminopropyl) triethoxysilane) and TEOS (tetraethoxysilane) are the most common used silica-based compounds and they are applied to enhance the mechanical stability of colloidal particles [27]. These reagents also offer good biocompatibility, non-swelling properties, and low cost [27]. Moreover, silica-coated nanomaterials improve wettability, and also surfaces can easily be modified with bio-conjugators [28]. Additionally, silica is facilitated to increase in size by 'seed-growth' process, chemically inert, and optically transparent [29], and APTES could also act as functional monomer for further IIP and MIP synthesis.

The synthesis of IIP-QDs and NIP-QDs (Figure 1) requires the use of APTES coated ZnS:Mn QDs synthesis before the formation of

ionic imprinted polymer films onto the surface of QDs using $NaAsO_2$ as a template ion and 1-vinyl imidazole as a bifunctional monomer. The use of bifunctional vinylated compounds guarantees the presence of vinyl groups for further polymerization, and also the presence of functional groups for interaction (complexation) with the ion (template). In the case of 1-vinyl imidazole, the presence of two nitrogen atoms in the structure allows the interaction with As(III) ions and also with As(V) ions, as will be demonstrated when studying the imprinting and selectivity factors (section 1.3.3). As reported by Tsoi *et al.* [32], 1-vinyl imidazole based As-IIPs have superior selectivity and analyte recognition than those IIPs obtained when using other monomers such as styrene and vinylated pyridine.

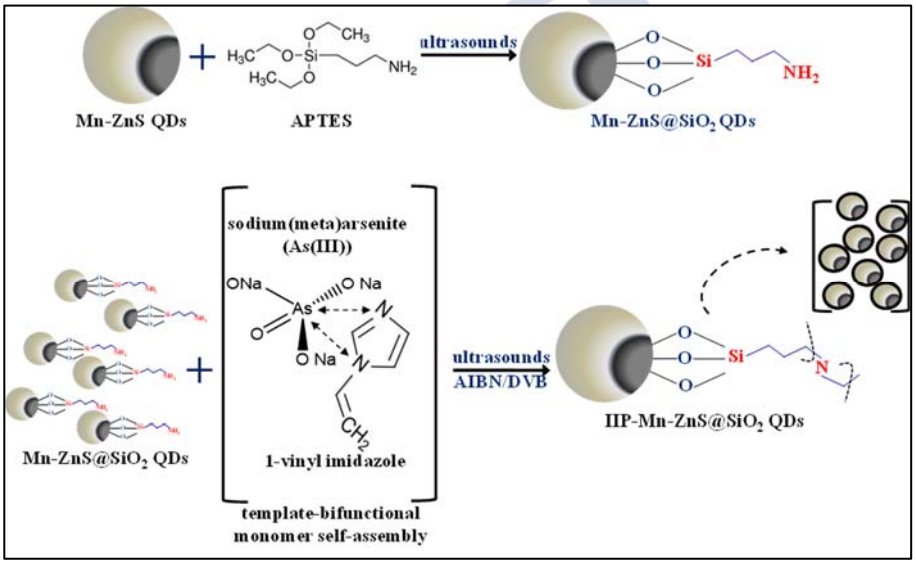

Figure 1. Schematic procedure for the synthesis of Mn-ZnS@SiO_2 QDs and IIP-Mn-ZnS@SiO_2 QDs

FTIR spectra (400-4000 cm^{-1}) of IIP-QDs (before and after removing template) and NIP-QDs are shown in Figure 2. The bands from 1000-1150 cm^{-1}, 790-795 cm^{-1}, and 470 cm^{-1} are attributed to the asymmetric and symmetric stretching vibration of Si-O-Si, and Si-O of SiO_2. The peaks at 2923 cm^{-1} and 2853 cm^{-1} are due to C-H

stretching vibration of the propyl group [30,31]. In addition, the characteristics peak at 610 cm^{-1} is assigned to the ZnS band [24]. Moreover, the weak absorption peaks at 1638 and 1456 cm^{-1} are assigned to the C=C and C≡N structure of the aromatic imidazole ring [32]. These findings prove that IIP and NIP layer was efficiently anchored onto the surface of the APTES-ZnS:Mn QDs.

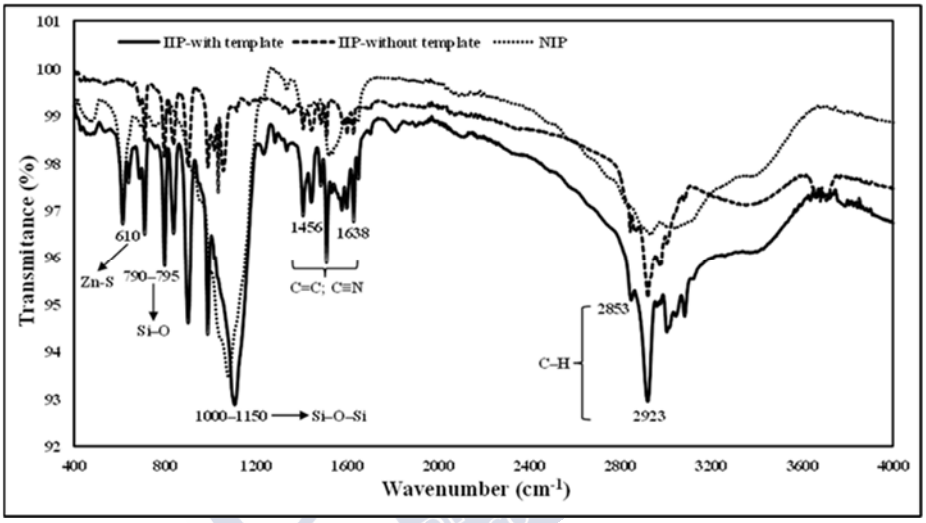

Figure 2. Fourier transform infra-red spectra for IIP-QDs (with and without template), and NIP-QDs

XRD was used to study the purity and crystalline structure of the nanoparticles. Figure S1 (ESI section) showed the X-ray diffraction pattern of the IIP-QDs (before and after template removal), and NIP-QDs. The XRD pattern of ZnS QD showed broad diffraction β-ZnS peaks at 2θ values of 28.74°, 47.7° and 56.5° which correspond to the cubic structure with peaks assigned to 111, 220 and 311. These figures agree with those reported by Mohagheghpour *et al.* [33] regarding $Zn_{1-x}Mn_xS$ QDs. The mean crystallite size after using the Debye–Scherrer equation [34] was estimated to be 17.2±1.5 (1.7±0.02 nm) for IIP-QD before template removal and 19.3±2.3 (1.9±0.02 nm) for IIP-QD after template removal. These findings show that the template removal process did not affect the crystalline structure.

The structure of the QDs was examined by TEM, and IIP/NIP-QDs particles were found to be agglomerated spheres covered with the polymer (NIP and IIP) as shown in Figure 3A-C. EDS analysis (Figure S2A-C, ESI section) confirms the presence of Zn, S, Mn, and Si in the prepared composites, and also the presence of As in IIP-QDs before template (As(III)) removal (Figure S2B, ESI section).

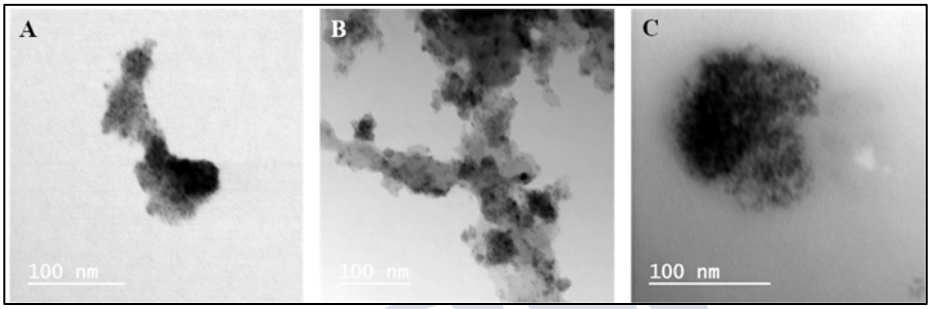

Figure 3. TEM analysis for NIP-QDs (A), IIP-QDs before template removal (B), and IIP-QDs after template removal (C)

1.3.2. Variables affecting the RTP quenching by inorganic arsenic species

1.3.2.1. Effect of the interaction time between inorganic As and IIP-QDs

In order to investigate the influence of the interaction time between As(III) ions and IIP-QDs on RTP intensity, an aqueous IIP-QDs (50 mg L^{-1}) solution was prepared in 0.1 M KH_2PO_4/0.1 M NaOH (pH 8.0), and then 1.5 mL aliquots of the prepared IIP-QDs solution were mixed with 40 µL of aqueous As (III) at 500 µg L^{-1} prepared in 0.1 M KH_2PO_4/0.1 M NaOH (pH 8.0) and 460 µL prepared in 0.1 M KH_2PO_4/0.1 M NaOH (pH 8.0) which yields to an As(III) concentration of 10 µg L^{-1} after dilution in the screw-capped vials (40 µL to 2.0 mL). The RTP intensity was measured until 30 min in 2 min intervals and RTP intensity was found to be stable after 15 min. Therefore, 15 min was selected as interaction time for further experiments.

1.3.2.2. Effect of the pH

The effect of the pH on RTP intensity was studied within the 5.0-8.0 pH range by preparing IIP-QDs (50 mg L^{-1}) solutions in 0.1 M KH_2PO_4/0.1 M NaOH at each pH. In accordance to Smedley and Kinniburgh [35], As(III) species prevails at pH between 7 and 10, and a better chemosensor response for As(III) is expected at a neutral pH and/or at slight alkaline pHs. The required amount of As (III) standard solution (final As(III) concentration between 0 and 50 µg L^{-1}) was also prepared in 0.1 M KH_2PO_4/0.1 M NaOH at the selected pH. Experiments involved the use of 1.5 mL of IIP-QDs solution, and variable volumes of As(III) solutions to obtain As(III) within the 0-50 µg L^{-1} after dilution to 2.0 mL (0.1 M KH_2PO_4/0.1 M NaOH at the selected pH was used as diluent). RTP intensities were measured after 15 min and results in triplicate are plotted on Figure 4A. Good linearity was observed between 0-20 µg L^{-1}, and the highest RTP quenching (highest slope) was observed at pH 7.0, that was chosen for further experiments.

1.3.2.3. Effect of the IIP-QDs concentration

Several IIP-QDs concentrations (20, 50, 100, 200 and 500 mg L^{-1}) prepared in 0.1M KH_2PO_4/0.1 M NaOH at pH 7.0 were used to investigate the effect of the IIP-QDs concentration on the As (III) RTP quenching system (As concentrations ranging from 0-20 µg L^{-1}). Results are given in Figure 4B, and the highest slope (highest RTP quenching) was obtained when using an IIP-QDs concentration of 20 mg L^{-1}. Additional experiments were further performed with higher As(III) concentrations (50 and 100 µg L^{-1}) and higher IIP-QDs concentrations. However, RTP quenching did not increase probably due to nanoparticles aggregation and cloudiness [36]. Therefore, IIP-QDs concentration was fixed at 20 mg L^{-1}.

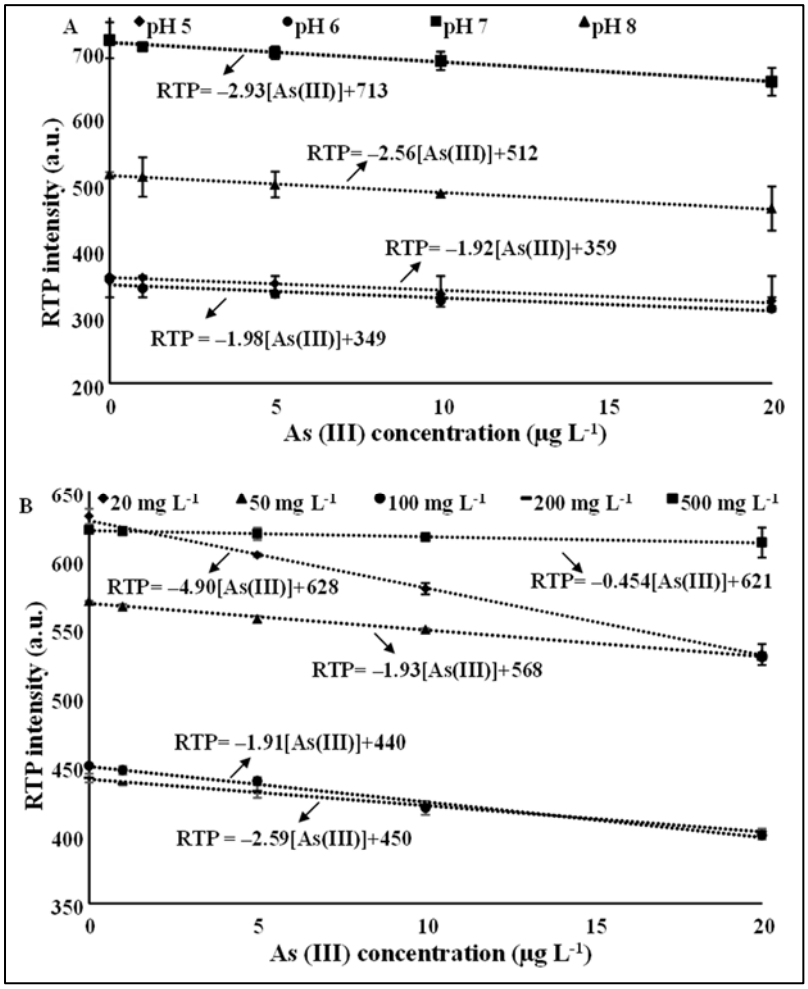

Figure 4. Effect of the pH (A) and IIP-QDs concentration (B) on the RTP quenching by As (III) concentration

1.3.2.4. Interaction between IIP-QDs and As (III) and As (V) species

Although the template used for IIP synthesis (As(III)) was used for optimizing the best conditions for RTP quenching, the effect of both inorganic As species (As(III) and As(V)) were evaluated since a screening RTP probe is expected for total inorganic As (As(III) plus

As(V)). The quenching effect of As (III) and As (V) at concentrations within the 0-20 μg L^{-1} range was tested using 20 mg L^{-1} IIP-QDs under optimum conditions (use of 0.1M KH_2PO_4/0.1M NaOH, pH 7.0 as a diluent and RTP measurement after 15 min). Experiments in triplicate showed slopes of -4.90±0.29 and -4.38±0.65 for As (III) and As (V), respectively. The slightly experimental difference obtained may be due to the quenching effect depending on the recognition cavity generated by the template molecule ($NaAsO_2$), although the prepared material shows good recognition properties also for As(V). The quenching effect on IIP-QDs caused by the interaction with As(III) and As(V) within the 0-20 μg L^{-1} range is graphically shown in Figure 5A,B.

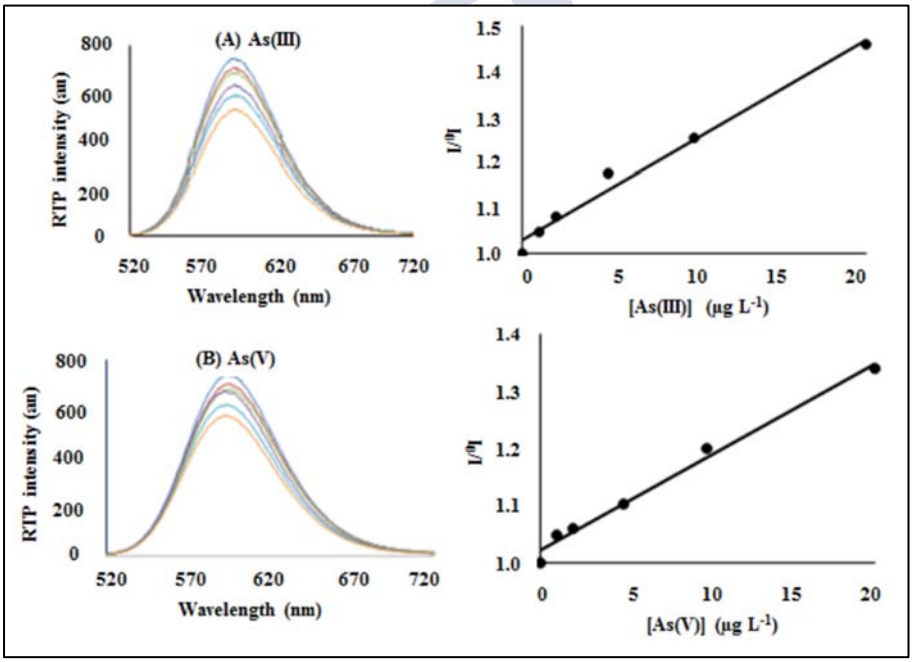

Figure 5. RTP quenching of IIP-QDs concentration in presence of increasing concentrations of As(III) (A) and As(V) (B)

1.3.3. Imprinting effect and selectivity

Several experiments were performed with IIP-QDs and NIP-QDs in the optimum conditions to compare the template (As(III)) responses and responses from other As species [As (V), AsC, AsB, MMA and DMA], and other elements which are present in fish such as microelements (Pb, Cd, Hg) and macro elements (P, K, Na, K, Ca, Mg, Zn, Fe, Co and Cu). The RTP quenching was measured by following Stern–Volmer equation [37].

$$\frac{P_0}{P} = 1 + K_{SV}[C] \quad (1)$$

where P_0 and P are the RTP intensity of the IIP-QDs or NIP-QDs in the absence and presence of the template (As(III)) or other tested elements, [C] is the concentration of As(III) or other tested As species and elements, and K_{SV} is the Stern-Volmer constant.

The effect of the template (As(III)), other As species and microelements was studied up to 20 μg L^{-1}; whereas, the quenching effect of macro elements was studied at concentrations up to 100 μg L^{-1}. Results are listed in Table 1 and K_{SV} values of 0.0106 for As (III) and 0.0073 for As (V) when using IIP-QDs were calculated. Similar experiments performed by using NIP-QDs have showed negligible interaction between As(III) and As(V) with NIP-QDs (absence of quenching) which prove that RTP quenching occurs only when there are recognition cavities in the IIP layer over the QD nanoparticles.

Recognition properties of the prepared composite through As(V) is attributed to the presence of 1-vinyl imidazole, a bifunctional vinylated compound (acting as monomer and interactive agent) which allows interaction with As(III) and As(V). In the study of Tsoi *et al.* [33], the authors investigated the selectivity and interaction mechanism of As-IIPs polymers based on the polymerization of styrene and the heterocyclic analogues vinylated pyridine and 1-vinyl imidazole (containing one and two nitrogen atoms, respectively). They concluded that 1-vinyl imidazole based As-IIP has superior selectivity and analyte recognition due to the higher density of arsenic-binding N-functionalities of the monomer. Fontanals *et al.* [38] also found that vinyl imidazole-DVB resins with a high nitrogen content (higher polarity) retained a bigger amount of polar compounds (phenols, oxamyl, methomyl). Therefore, it seems that the synthesized polymer

can retain the template (As(III)) and also might recognize other ions of similar characteristics such as As(V) in the case of the present study. The strength of these interactions with the nitrogen ions would be pH-dependent.

Experiments performed with IIP-QDs and NIP-QDs for other As species (organic As species) as well as for other elements (Table 1) have led to very small K_{SV} constants which implies that the prepared material is quite selective for inorganic As.

Table 1 also lists values regarding imprinting effect (IE as the ratio between K_{SV} for IIP-QDs and K_{SV} for NIP-QDs for each target), and selectivity (SF as the ratio between K_{SV} for IIP-QDs for the template and K_{SV} for IIP-QDs for the element/specie under study), which were calculated in accordance to

$$IE = \frac{K_{SV(IIP)}}{K_{SV(NIP)}} \quad (2)$$

where $K_{SV(IIP)}$ and $K_{SV(NIP)}$ are the Stern–Volmer constants for template and for each element/As specie under study when using IIP-QDs and NIP-QDs, respectively; and the selectivity factor

$$SF = \frac{K_{SV(IIP,As(III))}}{K_{SV(IIP,Q)}} \quad (3)$$

where $K_{SV(IIP,\ As(III))}$ is the Stern–Volmer constant for template using IIP-QDs, and $K_{SV(IIP,\ Q)}$ is the Stern–Volmer constant for each element/As specie under study when using IIP-QDs. Similarly, selectivity factors were calculated comparing $K_{SV(IIP,As(III))}$ and the Stern–Volmer constants for each element/As specie under study when using NIP-QDs

$$SF_{NIP} = \frac{K_{SV(IIP,As(III))}}{K_{SV(NIP,Q)}} \quad (4)$$

The calculated IE was 153.4 for As (III) and 91.3 for As(V); whereas IE values were very small (lower than 1.5) for organic As species and other ions (Table 1). These results agree with calculated SF values, which are small for inorganic As, and high for organic As species and other ions. These findings imply that the material's response is quite similar and selective for both inorganic As species, and that the RTP quenching (variable used for quantitative determinations) is only attributed to the presence of As(III) and

As(V). In addition, the high IF values for inorganic As species means that RTP quenching is consequence of the presence of specific recognition cavities for As(III) and As(V) in the IIP layer.

Table 1. Stern-Volmer constants, imprinting effect and selectivity factors (IIP-QDs and NIP-QDs) for As(III), As(V), organic As species, and other ions

	$K_{SV(IIP)}$[a]	$K_{SV(NIP)}$[a]	Imprinting effect ($K_{SV\ (IIP)}/K_{SV(NIP)}$)	Selectivity factor, SF, ($K_{SV\ (IIP,\ As(III))}/K_{SV(\ IIP,Q)}$)	Selectivity factor SF_{NIP} ($K_{SV\ (IIP,\ As(III))}/K_{SV\ (NIP,Q)}$)
As(III)	0.0106	0.00007	151.4	_	21.2
As(V)	0.0073	0.00008	91.3	1.45	132
AsB	0.00005	0.002	0.025	212.	5.3
AsC	0.0004	0.0018	0.22	26.5	5.9
MMA	0.0008	0.0012	0.67	13.3	8.8
DMA	0.0016	0.0018	0.89	6.6	5.9
Hg	0.0008	0.0026	0.31	13.2	4.1
Pb	0.0009	0.0009	1.00	11.8	11.8
Cd	0.001	0.001	1.00	10.6	10.6
P	0.0003	0.0002	1.50	35.3	53.0
K	0.00005	0.0003	0.17	212	35.3
Ca	0.0001	0.0006	0.17	106	17.7
Mg	0.0005	0.0004	1.25	21.2	26.5
Na	0.0022	0.0009	2.44	4.8	11.8
Zn	0.0011	0.0019	0.58	9.6	5.6
Fe	0.0007	0.0004	1.75	15.1	26.5
Co	0.0002	0.0003	0.67	53.0	35.3
Cu	0.0006	0.001	0.60	17.7	10.6

(a) $K_{SV(IIP)}$ and $K_{SV(NIP)}$: Stern–Volmer constants for the template and for each element/As specie under study when using IIP-QDs and NIP-QDs, respectively

1.3.4. Analytical performances

1.3.4.1. Calibration and matrix effect

The matrix effect was evaluated by comparing RTP quenching attributed to As(III) in aqueous 0.1M KH_2PO_4/0.1M NaOH, pH 7.0 (external aqueous calibration) and also when mixing fish extracts (standard addition calibration) at several dilution factors (1:10, 1:20 and 1:40, which implies the use of 200, 100 and 50 µL of a fish extract with IIP-QDs under optimum conditions). The standard addition and external calibration were prepared in three different days and each concentration level was also performed in triplicate. The slopes of the standard addition calibration graphs obtained for several sample dilution ratios were -3.64±0.30, -2.77±0.11 and -5.59±0.34 for 1:10, 1:20 and 1:40 dilution factors, respectively. The higher slope was observed when using the higher dilution factor (1:40), slope quite similar to that obtained when using external aqueous calibration (-4.90±0.29). There was no significant difference (p>0.05) between external calibration and 1:40 standard addition matrix dilution calibration curve. Hence 1:40 dilution was selected in real sample analysis and this dilution has been found to be adequate for assessing low concentrations of As (III) plus As(V) in fish samples. However, improvements on sensitivity could be obtained by using small dilution factors and the standard addition technique as a calibration method.

1.3.4.2. Limit of detection and limit of quantification

The limit of detection (LOD) and the limit of quantification (LOQ) were calculated based on EURACHEM guideline as 3σ (σ is a standard deviation of 11 blank readings) for LOD, and as 10 σ for LOQ [39]. The RTP intensity of a solution of 1.5 mL of 20 mg L^{-1} IIP-QDs in 0.1M KH_2PO_4/0.1M NaOH, pH 7.0 plus 0.5 mL of 0.1 M KH_2PO_4/0.1 M NaOH was measured under the previously optimized conditions. Then the standard deviation was divided by the slope of the calibration graph (As(III) as a calibrant), and the calculated LOD and LOQ values were 8.9 and 29.6 µg kg^{-1}, respectively. There was no published guideline for inorganic As levels in fish species; however, there is a published guidance for inorganic As in rice products [40]: 0.20 mg kg^{-1} for non-parboiled milled rice, 0.25 mg kg^{-1} for parboiled

rice and husked rice, 0.30 mg kg^{-1} for rice waffles, rice wafers, rice crackers and rice cakes, and 0.10 mg kg^{-1} for rice destined for the production of food for infants and young children. The calculated LOD and LOQ values are lower than the established maximum values by the EU/EC regulations.

1.3.4.3. Precision and accuracy

Inter-day and intraday precision was assessed by using an aqueous calibration method (1:40 dilution which implies absence of matrix effect). Three As(III) concentration levels (1.0, 5.0 and 20 µg L^{-1}) were measured seven times in three different days for inter-day assays, and all concentration levels (1.0, 2.0, 5.0, 10 and 20 µg L^{-1}) were measured in triplicate on seven consecutive days for intraday assays. Results (Table 2) show relative standard deviations (RSD) lower than 11% for inter-day precision, and lower than 7% for intraday assays. RSD for all the levels was below 10%. According to published method validation guidance [41], good precision is attained when RSD values are lower than 20%, which means that the proposed method shows good inter-day and intraday precision.

Table 2. Intra-day and inter-day precision (RSD %) and analytical recovery (AR %) of the method

Parameter	Concentration (µg L^{-1})	As(III)	
		AR (%)	RSD (%)
Inter-day (n=7)	1	107±1	5
	5	105±1	11
	20	107±2	10
Intraday (n=7)	1	101±10	4
	2	103±11	5
	5	102±5	6
	10	98±7	7
	20	101±3	5

Regarding analytical recovery, inter-day assays show values within the 105-107% range, whereas, intraday analytical recovery varied from 98 to103%. All values are close to 100% which also implies good analytical recovery for inter-day and intraday assays.

A CRM (BCR-668) showing certified total As concentration was analysed for total As assessment (microwave assisted acid digestion and ICP-MS measurement). Results are given in Table 3, and good accuracy has been observed for total As determination (found total As concentration within the certified total As concentration range). However, the BCR-668 has not been certified for total inorganic As neither for single As(III) and As(V) species. Therefore, this CRM was subjected to the proposed RTP method for assessing total inorganic As (As(III) plus As(V)) and also to HPLC-ICP-MS (single As(III) and As(V) concentrations), and results (total inorganic As) have been found quite similar when applying both determination techniques (Table 3).

1.3.5. Applications

The developed method was applied to five fish samples to assess total inorganic As (As(III) plus As(V)). In addition, the same fish samples were analysed by HPLC-ICP-MS for assessing single As(III) and As(V) concentrations, and total As concentration was also determined by ICP-MS after a microwave assisted acid digestion procedure. Each sample was analysed in triplicate, and results are tabulated in Table 3. A paired sample t-test (95% confidence interval) was applied to compare total inorganic As by the proposed RTP method and by HPLC-ICP-MS (sum of single As(III) and As(V) concentrations. There was no significant differences between the results obtained using both methods since the calculated t (t_{cal}=0.647) was lower than the tabulated t (t_{tab}=2.78) at a 95% confidence level (P>0.05), four degrees of freedom.

Table 3. Total As and total inorganic As (mean ± SD, n=3) in BCR-668 and fish samples

Sample	Total As (mg kg^{-1})[a]	Inorganic As (mg kg^{-1})[b]	Inorganic As (mg kg^{-1})[c]
BCR-668 (certified value)	7.1±0.5	_	_
BCR-668 (found value)	6.8±0.1	0.54±0.05	0.58±0.02
Swordfish-1	0.60±0.02	0.37±0.06	0.37±0.01
Swordfish-2	1.79±0.09	0.34±0.03	0.35±0.04
Yellowfin tuna	1.98±0.02	0.29±0.02	0.28±0.02
Blue shark	4.94±0.30	0.99±0.09	0.95±0.02
Cod	0.34±0.02	0.02±0.01	0.03±0.01

[a] Microwave assisted acid digestion followed by ICP-MS determination
[b] Inorganic As: Sum of As(III) and As(V) measured by HPLC-ICP-MS
[c] Inorganic As: As(III) plus As(V) measured by IIP-QDs based RTP

1.4. CONCLUSIONS

The developed RTP method based on IIP-QDs has been found to be highly sensitive, allowing the selective assessment of toxic arsenic (inorganic arsenic) in fish by using low-cost laboratory instrumentation. The use of vinyl imidazole as a complexing agent has been useful so that the IIP can recognize both As (III) and As (V) ions, allowing a simultaneously determination of both toxic arsenic species. Other arsenic species (organoarsenic compounds) as well other ions do not interact with the prepared composite material, and RTP quenching is only attributed to the inorganic As species (As(III) plus As(V)). Under the optimum conditions, the composite RTP-based chemosensor allowed the accurate determination of total inorganic arsenic in several fish samples and in the BCR-668 CRM (values statistically comparable with those obtained after applying a high expensive instrumentation such as HPLC-ICP-MS). The current method has therefore several advantages such as being a simple procedure with high selectivity and stability, low cost, short analysis time and sensitive (low LOD/LOQ), and may offer a new approach to the development of low-cost and sensitive methods for trace As level monitoring in other foodstuff and biological materials.

1.5. ACKNOWLEDGMENTS

This work was supported by the *Dirección Xeral de I+D – Xunta de Galicia Grupos de Referencia Competitiva* (project number 6RC2014/2016 and ED431C2018/19), and Development of a Strategic Grouping in Materials - AEMAT (grant ED431E2018/08). Authors thanks to Dr. Bruno Dacuña-Mariño (*Unidade de Raios X*) at *Rede de Infraestruturas de Apoio á Investigación e ao Desenvolvemento Tecnolóxico* – University of Santiago de Compostela) for XRD technical support, to Eugenio Solla (*Servicio de Microscopía Electrónica*) at CACTI–University of Vigo for TEM/EDS technical support, and to Dr. María Celeiro (LIDSA, Department of Analytical Chemistry, Nutrition and Bromatology – University of Santiago de Compostela) for ASE technical assistance.

Disclosure Statement

The authors declare no conflicts of interest

1.6. REFERENCES

[1] C.W. Liu, C.P. Liang, CP, F.M. Huang, Y.M. Hsueh. Assessing the human health risks from exposure of inorganic arsenic through oyster (*Crassostrea gigas*) consumption in Taiwan. Sci. Total Environ. 361 (2006) 57-66.

[2] ATSDR (2017) ATSDR's Substance Priority List. Agency for Toxic Substances and Disease Registry. https://www.atsdr.cdc.gov/SPL/. Accessed 20 December 2018.

[3] IARC (2018) IARC monographs on the evaluation of carcinogenic risk to human. https://monographs.iarc.fr/list-of-classifications-volumes/. Accessed 29 December 2018.

[4] J.H. Tidwell, G.H. Allan. Fish as a food: Aquaculture's contribution. EMBO reports 2 (2001) 958-963

[5] A.A. Meharg, E. Lombi, P.N. Williams, K.G. Scheckel, J. Feldmann, A. Raab, Y. Zhu, R. Islam. Speciation and localization of arsenic in white and brown rice grains. Environ. Sci. Tech. 42 (2008) 1051-1057.

[6] Y. Gao, P. Baisch, N. Mirlean, J.F.M.Rodrigues da Silva, N.L. Van, W. Baeyens, M. Leermakers. Arsenic speciation in fish and shellfish from the North Sea (Southern bight) and Açu Port area (Brazil) and health risks related to seafood consumption. Chemosphere 191 (2018) 89-96.

[7] X. Wei, Z. Zhou, J. Dai, T. Hao, H. Li, Y. Xu, L. Gao, J. Pan, C. Li, Y. Yan. Composites of surface imprinting polymer capped Mn-doped ZnS quantum dots for room-temperature phosphorescence probing of 2,4,5-trichlorophenol. J. Lumin. 155 (2014) 298-304.

[8] Y.Q. Wang, W.S. Zou. 3-Aminopropyltriethoxysilane-functionalized manganese doped ZnS quantum dots for room-temperature phosphorescence sensing ultratrace 2,4,6-trinitrotoluene in aqueous solution. Talanta 85 (2011) 469-475.

[9] X. Peng, L. Manna, W. Yang, J. Wickham, E. Scher, A. Kadavanich, A.P. Alivisatos. Shape control of CdSe nanocrystals. Nature 404 (2000) 59-61.

[10] A. Valizadeh, H. Mikaeili, M. Samiei, S.M. Farkhani, N. Zarghami, M. Kouhi, A. Akbarzadeh, S. Davaran. Quantum dots: synthesis, bioapplications, and toxicity. Nanoscale Research Letters 7 (2012) 480; http://www.nanoscalereslett.com/content/7/1/480.

[11] I. Costas-Mora, V. Romero, I. Lavilla, C. Bendicho. An overview of recent advances in the application of quantum dots as luminescent probes to inorganic-trace analysis. Trends Anal. Chem. 57 (2014) 64-72.

[12] E. Sotelo-Gonzalez, M.T. Fernandez-Argüelles, J.M. Costa-Fernandez, A. Sanz-Medel. Mn-doped ZnS quantum dots for the determination of acetone by phosphorescence attenuation. Anal. Chim. Acta 712 (2012) 120-126.

[13] C. Zhang, K. Zhang, T. Zhao, B. Liu, Z. Wang, Z. Zhang. Selective phosphorescence sensing of pesticide based on the inhibition of silver(I) quenched ZnS:Mn^{2+} quantum dots. Sensor Actuat. B-Chem. 252 (2017) 1083-1088.

[14] T. Gan, N. Zhao, G. Yin, J. Liu, W. Liu. Mercaptopropionic acid-capped Mn-doped ZnS quantum dots and Pb^{2+} as sensing system for rapid and sensitive room-temperature phosphorescence detection of sulfide in water. J. Photoch. Photobio. A 364 (2018) 88-96.

[15] L. Tan, Y. Li, Y. Tang, C. Kang, Z. Yu, S. Xu. Room temperature phosphorescence sensor for Hg^{2+} based on Mn-doped ZnS quantum dots. J. Nanosci. Nanotechnol. 12 (2012) 7788-7795.

[16] J. Chen, Y. Zhu, Y. Zhang. Glutathione-capped Mn-doped ZnS quantum dots as a room-temperature phosphorescence sensor for the detection of Pb^{2+} ions. Spectrochim. Acta A 164 (2016) 98-102.

[17] P. Deng, L.Q. Lu, W.C. Cao, X.K. Tian. Phosphorescence detection of manganese (VII) based on Mn-doped ZnS quantum dots. Spectrochim. Acta A 173 (2017) 578-583.

[18] L. Chen, X. Wang, W. Lu, X. Wu, J. Li. Molecular imprinting: Perspectives and applications. Chem. Soc. Rev. 45 (2016) 2137-2211

[19] J. Fu, L. Chen, J. Li, Z. Zhang. Current status and challenges of ion imprinting, J. Mater. Chem. A 3 (2015) 13598-13627.

[20] M. Niu, C. Pham-Huy, H. He. Core-shell nanoparticles coated with molecularly imprinted polymers: a review. Microchim. Acta 183 (2016) 2677–2695.

[21] A. Moreda-Piñeiro, J. Sánchez-González, M.P. Chantada-Vázquez, A.M. Bermejo, P. Bermejo-Barrera. MIPs as a versatile tool for micro-solid-phase extraction and probe sensing. Curr. Chem. Biol. 12 (2018) 114-134.

[22] J. Qi, B. Li, X. Wang, Z. Zhang, Z. Wang, J. Han, Chen L. Three-dimensional paper-based microfluidic chip device for multiplexed fluorescence detection of $Cu^{2+}$and Hg^{2+} ions based on ion imprinting technology. Sensor. Actuat. B-Chem. 251 (2017) 224-233.

[23] M.Y. Zhang, R.F. Huang, X.G. Ma, L.H. Guo, Y. Wang, Y.M. Fan. Selective fluorescence sensor based on ion-imprinted polymer-modified quantum dots for trace detection of Cr(VI) in aqueous solution. Anal. Bioanal. Chem. 411 (2019) 7165-7175.

[24] M.P. Chantada-Vázquez, J. Sánchez-González, E. Peña-Vázquez, M.J. Tabernero, A.M. Bermejo, P. Bermejo-Barrera, .A. Moreda-Piñeiro. Synthesis and characterization of novel molecularly imprinted polymer – coated Mn-doped ZnS quantum dots for specific fluorescent recognition of cocaine. Biosen. Bioelectron. 75 (2016) 213-221.

[25] X. Ren, L. Chen. Quantum dots coated with molecularly imprinted polymer as fluorescence probe for detection of cyphenothrin. Biosen. Bioelectron. 64 (2015) 182-188.

[26] Y. Piao, A. Burns, J. Kim, U. Wiesner, T. Hyeon. Designed fabrication of silica-based nanostructured particle systems for nanomedicine applications. Adv. Funct. Mater. 18 (2008) 3745-3758.

[27] K Zhi, L Wang, Y Zhang, Y Jiang, L Zhang, A Yasin. Influence of size and shape of silica supports on the sol–gel surface molecularly imprinted polymers for selective adsorption of gossypol. Materials (2018), https://doi.org/10.3390/ma11050777.

[28] D.K. Yi, S.T. Selvan, S.S. Lee, G.C. Papaefthymiou, D. Kundaliya, J.Y. Ying. Silica-coated nanocomposites of magnetic nanoparticles and quantum dots. J. Am. Chem. Soc. 127 (2005) 4990-4991.

[29] M. Darbandi, R. Thomann, T. Nann. Single quantum dots in silica spheres by microemulsion synthesis. Chem. Mater. 17 (2005) 5720-5725.

[30] X. Wei, Z. Zhou, T. Hao, H. Li, Y. Xu, K. Lu, Y. Wu, J. Dai, J. Pan, Y. Yan. Highly-controllable imprinted polymer nanoshell at the surface of silica nanoparticles based room-temperature phosphorescence probe for detection of 2,4-dichlorophenol. Anal. Chim. Acta 870 (2015) 83-91

[31] B. Babamiri, A. Salimi, R. Hallaj. Switchable electro chemiluminescence aptasensor coupled with resonance energy transfer for selective attomolar detection of Hg^{2+} via CdTe@ CdS/dendrimer probe and Au nanoparticle quencher. Biosen. Bioelectron. 102 (2018) 328-335.

[32] Y.K. Tsoi, Y.M. Ho, K.S.Y. Leung. Selective recognition of arsenic by tailoring ion-imprinted polymer for ICP-MS quantification. Talanta 89 (2012) 162-168.

[33] E. Mohagheghpour, F. Moztarzadeh, M. Rabiee, M. Tahriri, M. Ashuri, H. Sameie, R. Salimi, S. Moghadas. Micro-emulsion synthesis, surface modification, and photophysical properties of nanocrystals for biomolecular recognition. IEEE Nanobiosci. 11 (2012) 317-323.

[34] R.J. Uzuriaga-Sánchez, A. Wong, S. Khan, M.I. Pividori, G. Picasso, M.D.P.T. Sotomayor, Synthesis of a new magnetic-MIP for the selective

detection of 1-chloro-2,4-dinitrobenzene, a highly allergenic compound. Mater. Sci. Eng. C 74 (2017) 365-373.

[35] P.L. Smedley, D.G. Kinniburgh, A review of the source, behaviour and distribution of arsenic in natural waters. Appl.Geochem. 17 (2002) 517-568.

[36] N. Verma, A.K. Singh, N. Saini. Synthesis and characterization of ZnS quantum dots and application for development of arginine biosensor. Sens. Biosensing Res. 15 (2017) 41-45.

[37] H. Li, Y. Li, J. Cheng. Molecularly imprinted silica nanospheres embedded CdSe quantum dots for highly selective and sensitive optosensing of pyrethroids. Chem. Mater. 22 (2010) 2451-2457.

[38] N. Fontanals, R.M. Marcé, M. Galià, F. Borrull. Synthesis of hydrophilic sorbents from *N*-vinylimidazole/divinylbenzene and the evaluation of their sorption properties in the solid-phase extraction of polar compounds. J. Polym. Sci. Pol. Chem. 42 (2004) 2019–2025.

[39] EURACHEM (2014) The Fitness for purpose of Analytical methods. 2 ed.: EURACHEM

[40] EU/EC 1006/2015. Commission Regulation (EC), No 2015/1006 of amending Regulation (EC) No 1881/2006 as regards maximum levels of inorganic arsenic in foodstuffs Official Journal of European Union, L 161, 14-16.

[41] SANTE 2017. (11813) Guidance document on analytical quality control and method validation procedures for pesticide residues and analysis in food and feed: European Commission.

1.7. ELECTRONIC SUPPLEMENTARY INFORMATION (ESI)

Table S1. HPLC-ICP-MS operating conditions

ICP-MS	
Radio frequency power (W)	1600
Ar flow rate (plasma/auxiliary/nebulizer) (L/min)	16/1.2/0.92
KED mode, He flow rate (mL/min)	4
Integration time (ms)	250
Dwell time (ms)	443000
Mass monitored	^{75}As
HPLC	
Column	Hamilton PRP×100, 10 µm, 4.1×100 mm
Mobile phase	$(NH_4)H_2PO_4$, 15 mmol, pH 6.0
Flow rate	1 mL min^{-1}, 8.5 min
Injection volume	20 µL

Table S2. Operating ICP-MS conditions for total As determination in acid digests from fish samples.

Operating ICP-MS conditions		
Radiofrequency power		1600 W
Gas flows	Nebulization	0.92 mL min^{-1}
	Auxiliary	1.2 mL min^{-1}
	Plasma	16 mL min^{-1}
KED mode He flow rate		4.0 mL min^{-1}
Analytes		^{75}As,
Internal standards		^{74}Ge

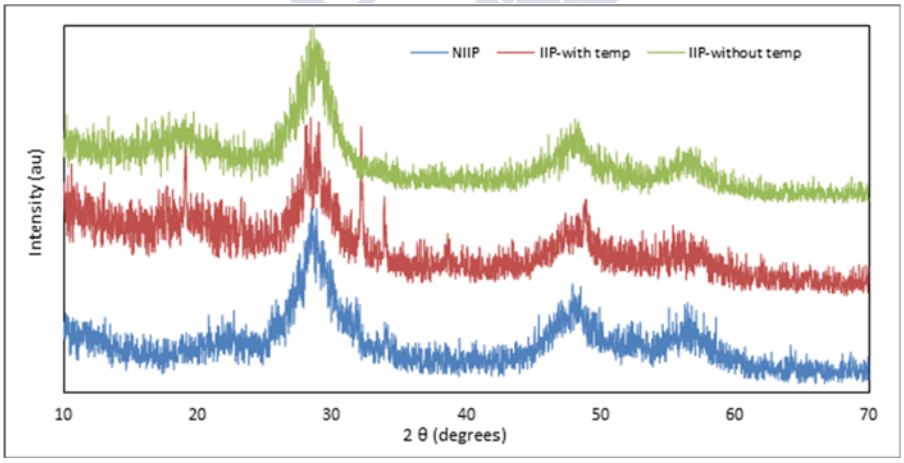

Figure S1. XRD spectra for IIP-QDs (with and without template), and NIP-QDs

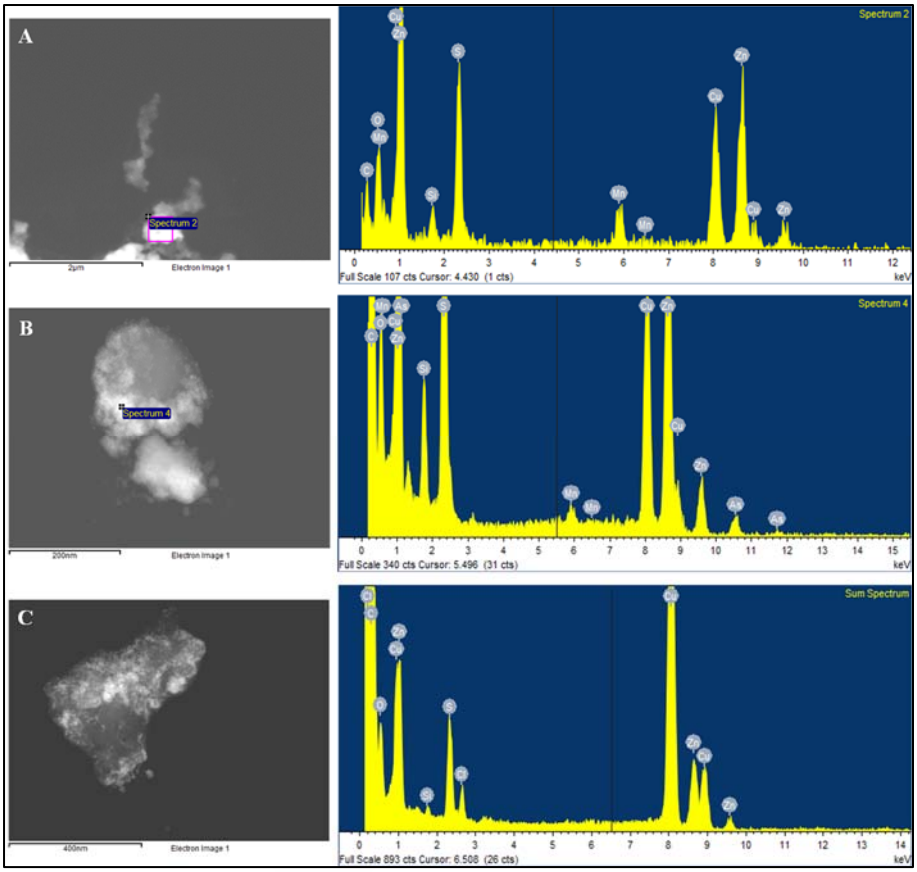

Figure S2. TEM-EDS analysis for NIP-QDs (A), IIP-QDs before template removal (B), and IIP-QDs after template removal (C)

USC
UNIVERSIDADE
DE SANTIAGO
DE COMPOSTELA

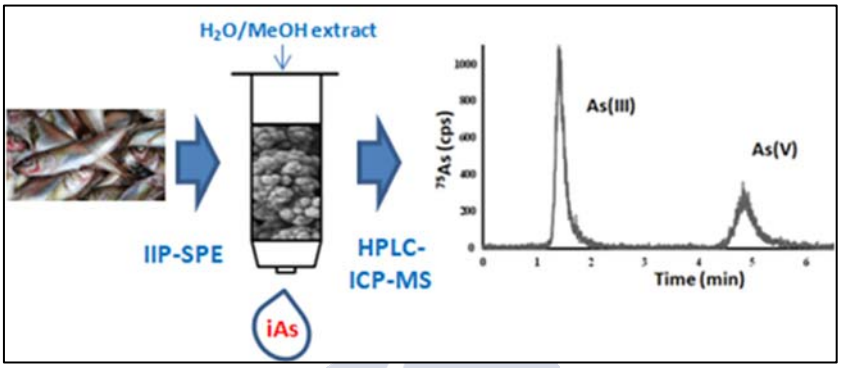

CHAPTER 2

IONIC IMPRINTED POLYMER SOLID-PHASE EXTRACTION FOR INORGANIC ARSENIC SELECTIVE PRE-CONCENTRATION IN FISHERY PRODUCTS BEFORE HIGH-PERFORMANCE LIQUID CHROMATOGRAPHY-INDUCTIVELY COUPLED PLASMA-MASS SPECTROMETRY SPECIATION

KAMAL K. JINADASA, ELENA PEÑA-VÁZQUEZ, PILAR BERMEJO-BARRERA, ANTONIO MOREDA-PIÑEIRO

JOURNAL OF CHROMATOGRAPHY A

VOLUME 1619 (2020), 460973

https://doi.org/10.1016/j.chroma.2020.460973

USC
UNIVERSIDADE
DE SANTIAGO
DE COMPOSTELA

Ionic imprinted polymer solid-phase extraction for inorganic arsenic selective pre-concentration in fishery products before high-performance liquid chromatography – inductively coupled plasma-mass spectrometry speciation

Kamal K. Jinadasa, Elena Peña-Vázquez, Pilar Bermejo-Barrera, Antonio Moreda-Piñeiro

Trace Element, Spectroscopy and Speciation Group (GETEE), Strategic Grouping in Materials (AEMAT), Department of Analytical Chemistry, Nutrition and Bromatology. Faculty of Chemistry. Universidade de Santiago de Compostela. Avenida das Ciencias, s/n. 15782, Santiago de Compostela. Spain

Abstract

Low levels of inorganic arsenic [As(III) and As(V)] in fishery products have been selectively isolated from fish extracts (1.0 g of wet fish samples pre-treated with 10 mL of 1:1 methanol/water under sonication at 25 °C for 30 min) by ionic imprinted polymer (IIPs) based solid phase extraction procedure (on-column mode). The selective adsorbent was synthesized using sodium (meta) arsenite as a template, 1-vinyl imidazole as a functional monomer, divinylbenzene as a cross-linker, and 2,2'-azobisisobutyronitrile as an initiator. Optimized pre-concentration conditions imply fish extract (10 mL) pH adjustment at 8.5 before loading (flow rate of 0.25 mL min^{-1}), and elution with ultrapure water (2 mL) at 0.50 mL min^{-1}. A pre-concentration factor of 50 was finally obtained after evaporation to dryness (N_2 stream) and re-dissolution in 0.2 mL of ultrapure water before HPLC-ICP-MS. Synthesized material was found to pre-concentrate inorganic arsenic species; whereas organic arsenic compounds, mainly arsenobetaine (the major organoarsenic compound in fish/seafood products), were not found to interact with the adsorbent. The developed selective method gave limits of quantification of 1.05 and 1.31 μg kg^{-1} for As (III) and As (V), respectively, and good precision [relative standard deviations lower than 12% in fish extracts spiked at several As (III) and As (V) levels].

The proposed method was finally applied to the selective determination of As (III) and As (V) species in several fishery products.

Keywords: Inorganic arsenic speciation, fish, ionic imprinted polymer, HPLC-ICP-MS

2.1. INTRODUCTION

Fish and shellfish tend to bio-accumulate pollutants from seawater and have been identified as the major As exposure pathway to humans [1-3]. Several organoarsenic species are generated when inorganic arsenic is metabolized by marine biota and, in addition to un-metabolized inorganic As (III & V), organoarsenic species such as monomethylarsonic acid (MA), dimethylarsinic acid (DMA), arsenobetaine (AB), arsenocholine (AC), trimethylarsine oxide (TMAO) and tetramethylammonium ion (TETRA) are found in marine organisms [4]. Moreover, arsenosugars, as well as arsenolipids, have also been reported as organoarsenic species in seafood products such as seaweed [5]. Among all these As species, inorganic As [arsenite, As (III); and arsenate, As (V)] are the most toxic As forms (10 to 60 times more toxic than other As species) and have been classified as Group I carcinogens [6]. MA and DMA are considered to be moderately toxic and cancer promoters; whereas, AB and AC are innocuous [6]. The maximum lethal dose (MLD-50) for As (III), As (V), MA, DMA, AC, and AB have been established at 14, 20, 700-1800, 700-2600, 6500, and >10,000 mg kg^{-1} body weight, respectively [2,7].

Arsenic speciation is therefore necessary since toxicity depends on the As form, while AB (the non-toxic species) is the most abundant As species in fish and shellfish [8]. The European Commission (Regulation 2015/1006) has set maximum levels only for inorganic arsenic in rice and rice-based products [9]. New sample preparation techniques to allow inorganic As pre-concentration, to decrease interferences and to exclude co-elution are therefore needed [10]. In addition, high-performance liquid chromatography (HPLC) is the separation/determination technique of choice for As speciation

because of its operational simplicity [11]. The assessment of low levels of inorganic As species in the presence of high concentrations of organoarsenic forms, mainly AB, is troublesome. Small dilution factors and/or the application of a pre-concentration stage are therefore required to assess inorganic As forms. However, these methodologies increase the analytical signals from organic As species, which can overlap the inorganic As responses, as usually occurs when performing As speciation with chromatographic methodologies based on anion-exchange conditions. Several sample pre-treatments have been developed to assess inorganic As. Recent proposals are based on using liquid-based microextraction techniques [12,13], but most of the developments use solid-phase extraction (SPE) and micro-solid phase extraction (μ-SPE) processes as sample pre-treatments [14-17]. SPE (and also more recently μ-SPE) is one of the most common and popular techniques for target pre-concentration due to its flexibility, speed, simplicity, high degree of safety, and low-cost. In addition, SPE is a well-known environmentally friendly methodology that is easy to automate [17,18]. Advances on SPE imply the use/development of new adsorbents which allow effective target pre-concentration with a small amount of adsorbent and guarantee selectivity. In addition to commercial silica-based strong anion exchange cartridges [14], new nano-based adsorbents have been also proposed [15-17].

The molecular imprinting technique (MIT) has offered an appealing way to prepare highly selective materials. Adsorbents for SPE based on MIT are currently being developed for several organic and inorganic targets, including large biomolecules. Materials prepared using MIT are usually referred to as an ionic imprinted polymer (IIP) when the target (the template used for generating the recognition cavities) is an ion. Difficulties can occur when using ions as templates because these simple structures lack functional groups that can interact with the monomer (vinylated reagent). A basic strategy consists of trapping a chelating ligand (a non-vinylated reagent) via imprinting of binary/ternary mixed ligand complexes of ions with a non-vinylated chelating agent and a vinyl ligand (monomer) [19]. After polymerization, the non-vinylated ligand is not

chemically bound to the polymer chains, but instead is trapped inside the polymeric matrix and allows the polymer-ion interactions. The selectivity of the prepared IIPs can be enhanced when using bifunctional reagents (a reagent exhibiting chelating properties through the ion, and also containing vinyl groups for polymerization) [19].

The trapping technique using methacrylic acid as a vinylated reagent (monomer) and hydroquinone as a non-vinylated reagent (chelating agent) has been used by Alizadeh and Rashedi for preparing (bulk polymerization), an IIP-based membrane electrode sensitive and selective to As (III) species [20]. Bifunctional reagents such as 1-vinyl imidazole and 4-vinyl pyridine have been proposed by Tsoi *et al*. for preparing a selective adsorbent for As (V) by bulk polymerization [21]. These two developments, however, are focused on assessing only one inorganic As form, and selectivity through the other inorganic As species (and also organoarsenic species) was not performed/reported. In addition, as is the case with other speciation procedures for inorganic As by SPE/μ-SPE and liquid-based microextraction, oxidation or a reduction stage was required to assess total inorganic As by atomic spectrometry-based techniques [12-17], and potentiometry [20]. The aim of the current proposal has been the development of a highly sensitive and selective method for assessing inorganic As species [As(III & V)] in samples containing high concentrations of organoarsenic species such as fishery products. A SPE method based on a new IIP as an adsorbent combined with HPLC hyphenated with inductively coupled plasma mass spectrometry (ICP-MS) has been developed. The IIP adsorbent was prepared by using the precipitation polymerization method, As (III) as a template, and 1-vinyl imidazole as a bifunctional monomer. IIP-SPE optimization was performed to allow a simultaneous pre-concentration of As (III) and As (V) species for a further determination by HPLC-ICP-MS.

2.2. MATERIAL AND METHODS

2.2.1. Instrumentation

Arsenic speciation was performed with a Flexar LC HPLC (LC pump, column oven, and LC autosampler) from Perkin Elmer (Waltham, MA, USA) hyphenated to a Perkin Elmer Nex-Ion 300X ICP–MS. A PRP×100 column (10 µm, 100 × 4.1 mm) connected to a PRP×100 guard column (10 µm, 25 × 2.3 mm) from Hamilton (Reno, NV, USA) was used for inorganic As separation. The same ICP-MS instrument connected to a SeaFast SC2 DX autosampler (Elemental Scientific, Omaha, NB, USA) was used for total As determinations. Synthesized IIP and NIP were characterized by Fourier transform infrared spectrometry with ATR correction using a Spectrum-Two FT-IR from Perkin Elmer, and by scanning electron microscopy (SEM) with a ZEISS EVO LS 15 (Carl Zeiss, Oberkochen, Germany). A low-profile roller (Stovall, Greensboro, NC, USA), placed inside a Boxcult temperature-controlled chamber (Stuart Scientific, Surrey, UK), was used for IIP synthesis. Samples were digested (total As determination) using an Ethos Plus microwave accelerated system (Milestone, Sorisole, Italy) with 100-mL closed Teflon vessels. SPE was performed by using an 8-channel Minipuls 3 peristaltic pump (Gilson, Middleton, WI, USA), and PVC 2-stop tubing (1.52 mm i.d.) from SCP Sciences (Baie-D'Urfe, Quebec, Canada). Other equipment included an USC60TH ultrasonic cleaner bath (45 kHz, 120 W) from VWR (Leuven, Belgium), an ultracentrifuge (Sigma 2K15, Osterode, Germany), a pH meter with glass combined electrode (Crison Basic 20, Barcelona, Spain), a domestic Taurus blade grinder (Taurus, Barcelona, Spain), an oven model 207 from Selecta (Barcelona, Spain), and a Classic ML analytical balance (Mettler Toledo, Columbus, OH, USA).

2.2.2. Reagents

All aqueous solutions were prepared with ultrapure water with a resistivity of 18.2 MΩ cm obtained from a Milli Q-A10 system from Millipore Co. (Billerica, MA, USA). Sodium (meta) arsenite ($NaAsO_2$), used as a template for IIP synthesis, was obtained from Sigma-Aldrich (St. Louis, MO, USA). Arsenite and arsenate stock

standard solutions, 1000 mg L^{-1}, were from Panreac (Barcelona, Spain). Standard solutions of MA, DMA, AB and AC (1000 mg L^{-1}) were prepared by dissolving the appropriate amounts of MA ($CH_3AsO(ONa)_2 \cdot 6H_2O$) purchased from Carlo Erba (Milan, Italy); DMA ($C_2H_6AsNaO_2 \cdot 3H_2O$), purchased from Merck (Darmstadt, Germany); and AB ($AsC_5H_{11}O_2$) and AC ($AsC_5H_{14}O$), both from Tri Chemical Laboratory Inc. (Yamanashi, Japan). Bifunctional monomer 1-vinyl imidazole (≥99.0% purity) and initiator 2,2'-azobisisobutyronitrile (AIBN) were obtained from Fluka (Buchs, Switzerland); whereas, divinylbenzene (DVB) was from Sigma-Aldrich. 1-vinyl imidazole was used directly without a purification stage; whereas, AIBN and DVB were subjected to a purification process before use. AIBN was dissolved in methanol (50–60 °C) and was then re-crystallized at –20 °C (AIBN). Regarding DVB, the reagent was passed through a mini-column containing a 0.50 g of neutral alumina (Merck) for removal of impurities. Nitric acid (Hyper pure, 69%), and 33% of hydrogen peroxide were supplied by Panreac (Barcelona, Spain). NexIon Setup Solution (10 µg L^{-1} of Be, Ce, Fe, In, Li, Mg, Pb, and U in 1% HNO_3) was purchased from Perkin Elmer (Shelton, CT, USA). Ammonium chloride, ammonium hydroxide and methanol (Chromasolv) were from Merck; whereas, ammonium hydrogen carbonate and acetic acid (glacial) were from Panreac and ammonium dihydrogen phosphate was from BDH (Poole, United Kingdom). Multi-element standard solutions (cross-reactivity study) were prepared by combining single Ca, Co and Mg stock standard solutions (1000 mg L^{-1}) from Merck, single Cr, Hg, K, P, Pb and Zn stock standard solutions (1000 mg L^{-1}) from Scharlab (Barcelona, Spain), and single Cd, Cu, Fe and Na stock standard solutions (1000 mg L^{-1}) from Perkin Elmer. Internal standard solutions (Ge, Sc, and Rh) were prepared from single-element standards (1000 mg L^{-1}) purchased from Perkin Elmer. DORM–2 (dogfish muscle) and DOLT-3 (dogfish liver) were from National Research Council of Canada (Ottawa, Canada), and BCR 278 (mussel tissue) was from Community Bureau of Reference – Commission of the European Communities (Brussels, Belgium). Other consumables were Durapore 0.22 µm membrane filters (Millipore), replacement Teflon frits (Supelco,

Bellefonte, PA, USA), and disposable syringes (sterile, 5 mL) from Dispomed (Gelnhausen, Germany).

2.2.3. Sample pre-treatments

The following fish samples were used: yellowfin tuna (*Thunnus albacares*) and swordfish (*Xiphias gladius*) obtained from Tropic Frozen Foods (Pvt) Ltd (Sri Lanka), bluefin tuna (*Thunnus thynnus*) and blue shark (*Prionace glauca*) also as frozen products, and fresh cod (*Gadus morhua*) bought in local supermarkets in Santiago de Compostela. Approximately 0.2 kg of flesh was blended, homogenized and stored in pre-cleaned polyethylene bottles with hermetic seals at -20 °C before use.

Fish samples, as well as CRMs were subjected to microwave-assisted acid digestion in triplicate for further total As determination by ICP-MS (electronic supplementary information, ESI)**.** Approximately 1.0 g of homogenized fresh fish samples (0.2 g of dried CRMs) were placed in the microwave reactors and pre-digested with 3.0 mL of 69% (v/v) HNO_3 plus 4.0 mL of ultrapure water and 1.0 mL of H_2O_2 for 15 min at room temperature. Pre-digested samples were then subjected to microwave-assisted acid digestion (1^{st} step: from room temperature to 180 °C for 15 min; 2^{nd} step: 180 °C for 10 min). Acid digests were made up to 25 mL with ultrapure water and stored in polyethylene bottles at room temperature before measurements. Two reagent blanks were prepared in each sample pre-treatment set.

For As species isolation, homogenized fish samples (1.0 g for wet samples and 0.20 g for dried CRMs) were weighted in 50 mL centrifuge tubes and subjected to an ultrasound-water bath extraction process using 10 mL of 1:1 methanol/ultrapure water as an extractant and 30 min sonication at 45 kHz (120 W) and room temperature. This extracting solution was selected from the available literature [10, 22-25]. The suspensions were then centrifuged at 3000 rpm for 10 min, and the supernatants were kept in polyethylene bottles and stored at –20 °C.

2.2.4. Synthesis of As-ion imprinted polymer

As IIP was synthesized in accordance with procedures described in the literature [21], although some modifications were implemented. Briefly, 1.6 mmol of $NaAsO_2$ (template) and 6.5 mmol of 1-vinyl imidazole (bi-functional monomer used directly without purification) dissolved in 20 mL of 1:3 acetic acid/methanol (porogen) were sonicated for 5 min. Afterward, 32 mmol of DVB (cross-linker) and 40 mg of AIBN (initiator) were added and sonication followed for 5 min. Based on the amounts of reagents, the template/bifunctional monomer/cross-linker molar ratio was 1:4:20 in the polymerization mixture. After stirring, the mixture was purged with N_2 for 10 min, and the test tubes were immediately sealed and placed in a low-profile roller (33 rpm along its long axis) inside a temperature-controllable chamber at 60 °C for 12 h. The synthesized material was vacuum filtered, washed three times with methanol, and oven-dried overnight at 40 ºC.

Non-imprinted polymers (NIPs) were also prepared in the same way as IIPs, using the same masses and volumes as for IIP synthesis, but without adding the template ($NaAsO_2$). The NIPs were then subjected to the same washing pre-treatment described above.

For the removal of the template (arsenite), IIP portions of 200 mg were packed into 5 mL syringes between two Teflon frits, and approximately 200 mL of 2.0 M HNO_3 was pumped at a flow rate of 1 mL min^{-1} until As was not detected in the filtrate by ICP-MS (measurement conditions in ESI). Afterwards, the packed syringes were extensively washed by pumping ultrapure water.

2.2.5. Extraction (SPE) and quantification (HPLC-ICP-MS) of As species

IIP-SPE syringes (200 mg of IIP each one) were conditioned by passing 10 mL of 0.1M/0.1 M NH_3/NH_4Cl buffer solutions (pH 8.5). Afterward, 10 mL of sample (water/methanol extract) or arsenite/arsenate standard solutions, both adjusted at pH 8.5 (use of 0.1M/0.1 M NH_3/NH_4Cl buffer solutions), were passed through the syringe at a flow rate of 0.25 mL min^{-1}. After loading, elution was performed by pumping four cycles of 0.5 mL ultrapure water (flow rate of 0.5 mL min^{-1}). The eluted solution (2.0 mL) was collected in a centrifuge tube, evaporated to dryness under N_2 stream, an d re-

dissolved with 0.2 mL of ultrapure water for subsequent HPLC-ICP-MS analysis. Each experiment was performed in triplicate**,** and at least two reagent blanks were prepared/analyzed.

Table 1. HPLC-ICP-MS operating conditions

ICP-MS	
Radio frequency power (W)	1600
Ar flow rate (plasma/auxiliary/nebulizer) (L min^{-1})	16/1.2/0.92
KED mode, He flow rate (mL min^{-1})	4
Integration time (ms)	250
Dwell time (ms)	443000
Mass monitored	^{75}As
HPLC	
Column	Hamilton PRP×100, 10 µm, 4.1×100 mm
Mobile phase	$(NH_4)H_2PO_4$, 15 mmol, pH 6.0
Flow rate	1 mL min^{-1}, 8.5 min
Injection volume	20 µL

Anion exchange HPLC conditions were optimized to obtain the separation of six arsenic species [AC, AB, As (III), DMA, MA and As (V)] in a single chromatographic run. A phosphate buffer was selected for working with an anion exchange column such as PRP×100 column because of the excellent As (V) recoveries and fast As (V) elution [26]. Since only the inorganic arsenic species were pre-concentrated by IIP-SPE, AB and AC co-elution using the PRP×100 column under isocratic conditions was negligible. Therefore, isocratic elution ($(NH_4)H_2PO_4$, 15 mmol L^{-1}, pH 6.0, 1.0 mL min^{-1}) as shown in Table 1 was used for measurements.

Inorganic arsenic [As(III)) and As(V)] determination in the extracts after IIP-SPE was performed using the standard addition technique covering As species concentrations within the 0-0.4 µg L^{-1} range (0-20 µg L^{-1} range after pre-concentration). Chromatograms of a pre-concentrated water/methanol extract from fish after IIP-SPE

conditions and for pre-concentrated 0.02-0.4 µg L^{-1} standard solutions of As(III)) and As(V) are shown in Figure 1.

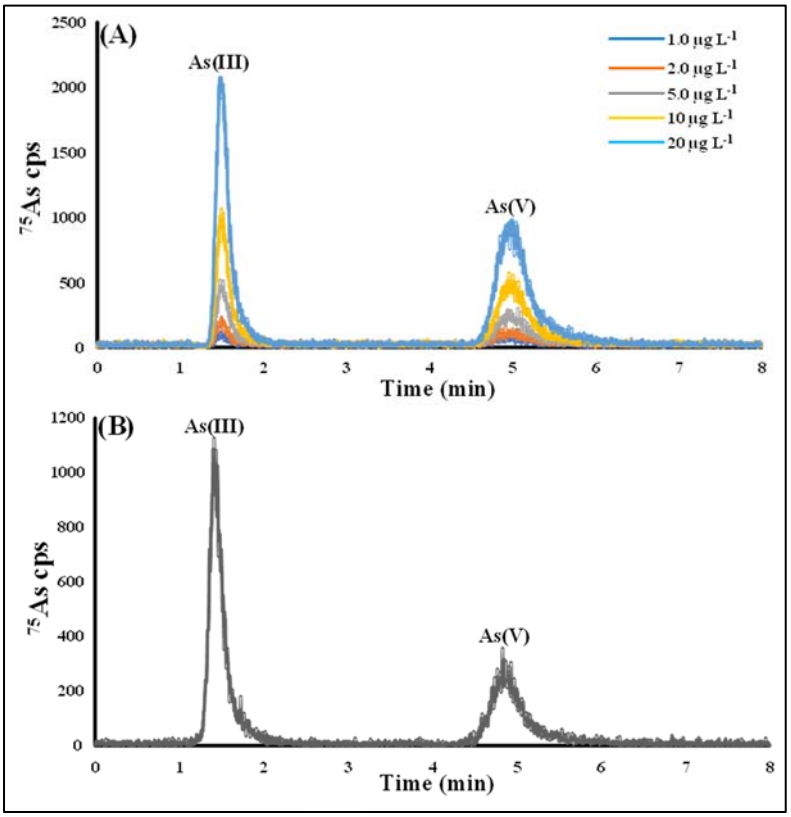

Figure 1. HPLC-ICP-MS chromatograms for pre-concentrated As(III) and As(V) standards within the 0-20 µg L^{-1} range (A), and for a pre-concentrated extract from a cod fish sample (B).

2.3. RESULTS AND DISCUSSION

2.3.1. IIP synthesis and characterization

The use of vinylated compounds when preparing IIPs simultaneously allows metal ion chelation and further polymerization through the vinyl groups in the presence of the cross-linker and the initiator [21,27]. Tsoi *et al*. [21] have studied the density of ion binding N-

functionalities of three potential monomers (1-vinyl imidazole, 4-vinyl pyridine, and styrene), and 1-vinyl imidazole was found to offer the best performance. However, they synthesized As-IIP in the most common bulk polymerization procedure. According to the literature, this procedure has a number of drawbacks that are related to the crushing, grounding and sieving steps [19]. In addition, the bulk polymerization procedure is tedious and time-consuming, and generates polymer beads which are irregular in size and shape, leading to polymer bead losses after sieving, as well as a diminished loading capacity [28]. The current IIP has been synthesized by fixing a template/monomer/cross-linker molar ratio of 1:4:20, a ratio which requires 120 mL of porogen for performing a precipitation polymerization approach. Early attempts when using large porogen volumes were not successful, and polymerization did not occur. Further experiments showed that polymerization occurred when using low porogen volumes (volumes within the 20-30 mL range), and the obtained polymer consisted of discrete small particles, such as those observed when using the precipitation polymerization approach. The use of porogen volumes lower than 20 mL led to bulk polymerization. These results are in good agreement with those reported by Tsoi *et al.* [21]. Therefore, the synthesized polymer was not prepared strictly following the conditions of the precipitation polymerization; however, the discrete particles obtained indicate that the polymerization process is closer to the precipitation polymerization than to the bulk polymerization approach. After IIP synthesis, the polymer mass was 1.78 g, which means a synthesis performance close to 37% (amounts of monomer, template and cross-linker were fixed/used for achieving a theoretical MIP amount of 4.8 g).

FT-IR spectrometry with ATR correction (Figure 2A) shows C-H ring mode (725-880 cm^{-1}) and -CN groups (1525-1575 cm^{-1}) characteristic bands. The absorption peak at 2924 cm^{-1} is attributed to C-H stretches, and the weak absorption bands at 1602 and 1456 cm^{-1} are assigned to the C=C and C=N structure of aromatic imidazole ring. Finally, the band at 1510 cm^{-1} is associated with -NH bending. These findings show that the bifunctional monomer (1-vinyl imidazole) is integrated into the polymeric chain. SEM images (Figure 2B-D) show

agglomerated spherical porous beads for IIPs (before and after template removal) and for NIP. Despite the high degree of agglomeration and at the same 50.00 kx magnification, particle sizes are lower in MIP (before and after template removal) beads (SEM images in Figure 1B and 1C) than for NIP particles (SEM image in Figure 1D).

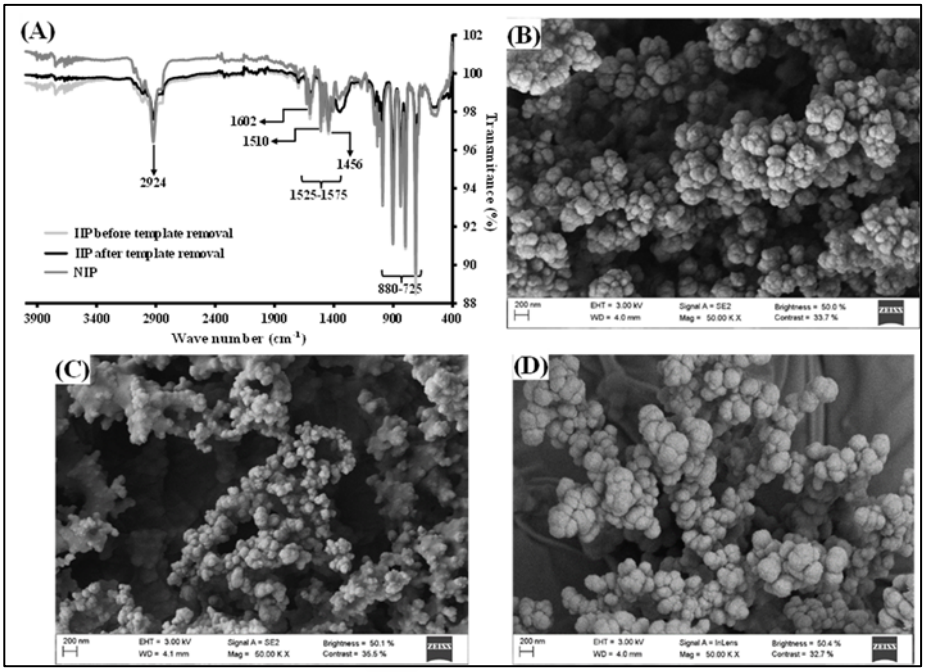

Figure 2. FT-IR spectra (A) of synthesized IIP, synthesized IIP after template removal, and NIP, and SEM images of synthesized IIP (B), synthesized IIP after template removal (C), and NIP (D).

2.3.2. Optimization of IIP-SPE parameters

IIP-SPE operating conditions have been optimized by using un-spiked and spiked (1.0 μg L^{-1} of As(III)) fish extracts which were obtained by subjecting fish (cod) samples to ultrasound-assisted extraction (UAE) as stated in section 2.2.5. Un-spiked samples were always analysed in order to subtract As(III)/As(V) naturally occurring in fish samples. In

addition, eluate evaporation to dryness and re-dissolution in 1.0 mL of water was not performed during the SPE optimization stages. Each tested loading/eluting condition was performed in triplicate and at least one reagent blank was obtained for each set of operating conditions. An aqueous calibration (As(III) and As(V) concentrations ranging from 0 to 20 μg L^{-1}) was used for assessing recovered As(III) and As(V) concentrations.

IIP-based SPE was performed without a washing stage before elution. Preliminary experiments showed that a washing stage, typically used in most of SPE procedures, led to a partial elution of analytes (mainly As(V)). Since IIP was prepared using As(III) as a template, As(V) interaction with the IIP recognition cavities are less intense, and analyte losses occur during the washing stage. Several washing solutions such as the buffer used for sorbent conditioning (0.1M/0.1 M NH_3/NH_4Cl, pH 8.5) and organic solvents such as methanol and acetonitrile were found unsuitable as washing solutions. Despite the fact that a washing stage was omitted, As(III) and As(V) sorption was proved to be specific (through the generated recognition/imprinted cavities) because negligible sorption was observed when using NIP as a sorbent under the same operating conditions (absence of a washing step). IIP-As(III)/As(V) interaction occurs via N-functionalized moieties (1-vinyl imidazole integrated into the polymeric chain), which should be moderate for As(III), and weak for As(V) because partial losses are obtained in the washing stage.

2.3.2.1. Loading conditions

Un-optimized eluting conditions (water as an extractant, 0.5 mL min^{-1} elution flow rate) were used when optimizing loading parameters (fish extract pH and loading flow rate). The selection of the optimum fish extract pH for IIP-SPE loading was performed using fish extracts (10 mL) spiked with 1 μg L^{-1} As (III) and adjusting the pH from 7.0 to 9.0 with NH_3/NH_4Cl buffer solutions at the tested pHs. The analytical recovery for As (III) as well as As (V) concentrations (mean of three replicates in Figure 3A) was found to be higher when using fish extracts at the higher pH levels. As reported by Smedley

and Kinniburgh [29], the distribution of As (III) species is dependent on pH and is highlighted over pH ranges of 7.0 to 10.0. Our findings are in good agreement with reported As(III)-pH dependence. The highest As(III) recovery (and the highest As(V) concentration) was obtained at pH 8.5.

The loading flow rate (IIP-SPE column mode) was studied by pumping the fish extract (pH 8.5) at 0.25, 0.50, 0.75, and 1.00 mL min^{-1}. As shown in Figure 3B, retention is slightly decreased when using high loading flow rates because of an inefficient interaction between analytes and the sorbent. Therefore, sample loading was finally set at 0.25 mL min^{-1}.

2.3.2.2. Elution conditions

As previously mentioned, ultrapure water, as well as diluted nitric acid solutions, were found to be useful for desorbing retained As(III) and As(V) from IIP beads. In addition, elution efficiency was also found to be higher when passing the elution solution discontinuously. Water was therefore selected as an eluting solution, and 2.0 mL of the eluting solution was pumped in four cycles of 0.5 mL each at flow rates within the 0.25 – 1.0 mL min^{-1} range. As typically reported for on-column SPE methods, higher elution efficiencies were observed when using small eluting flow rates (Figure 3C), and an eluting flow rate of 0.50 mL min^{-1} was selected.

Finally, the volume of the eluting solution (ultrapure water) was studied. As previously commented, the eluting volume was also pumped in short cycles to increase eluting efficiency. As shown in Figure 3D, As(III) and As(V) elution is efficiently obtained when using volumes within the 2.0–5.0 mL range. Therefore, the minimum eluting volume (2 mL of ultrapure water) was finally selected.

2.3.2.3. Breakthrough volume and sample (fish extract) volume

In order to obtain a higher enrichment factor, large sample volumes (and/or small eluting solution volumes) are required. Several volumes (10, 25, 37.5, 50 and 100 mL) of aqueous As (III) and As (V) standard solutions (1.0 μg L^{-1} each one) were pre-concentrated in triplicate

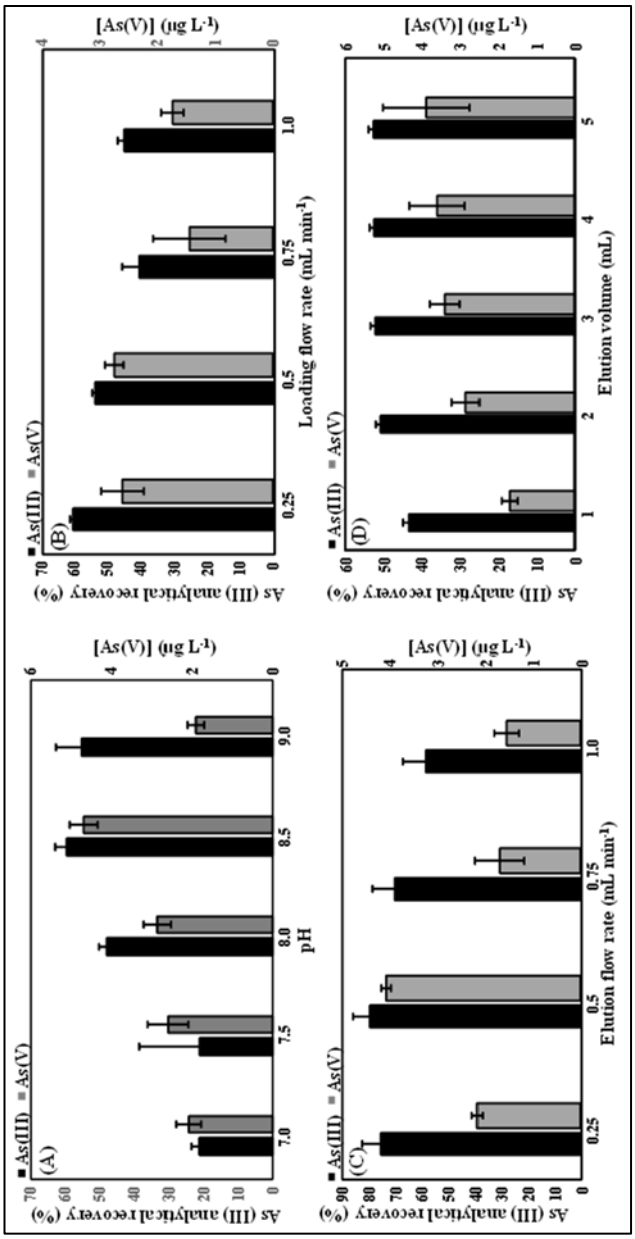

Figure 3. Effect of the extract pH (A), loading flow rate (B), elution flow rate (C), and elution volume (D) on the As(III) analytical recovery and on the extracted As(V) concentration.

under optimized IIP-SPE conditions. Preliminary results when using 200 mg IIP syringes showed that the breakthrough volume was 25 mL (both As (III) and As (V) recoveries decreased 70% when using higher volumes). Experiments were further performed by loading fish extracts spiked with As (III) and As (V) (1.0 µg L^{-1} each). Similar As(III) recoveries were obtained when loading 10 and 25 mL; whereas, As(V) recoveries were diminished when using 25 mL fish extract (Figure 4). These findings imply that the breakthrough volume is at least 25 mL for As(III), but it is 10 mL for As(V). The different breakthrough volume for As(III) and As(V) ions is attributed to the fact that IIP's recognition cavities should fit better with As(III) ions than with As(V) ions because IIP has been synthesized using As(III) as a template. Therefore, As(V) desorption (losses) are observed when loading high sample volumes (although As(V) ions interact and are adsorbed on the IIP particles, a fraction of adsorbed As(V) ions is eluted when passing an excess of sample volume). Therefore, the fish extract volume was fixed at 10 mL. Taking into account the fish extract (10 mL) and eluting solution (2.0 mL) volumes, and also the fact that the eluate is evaporated to dryness and re-dissolved in 0.200 mL of water, the proposed IIP-SPE procedure shows a pre-concentration factor of 50.

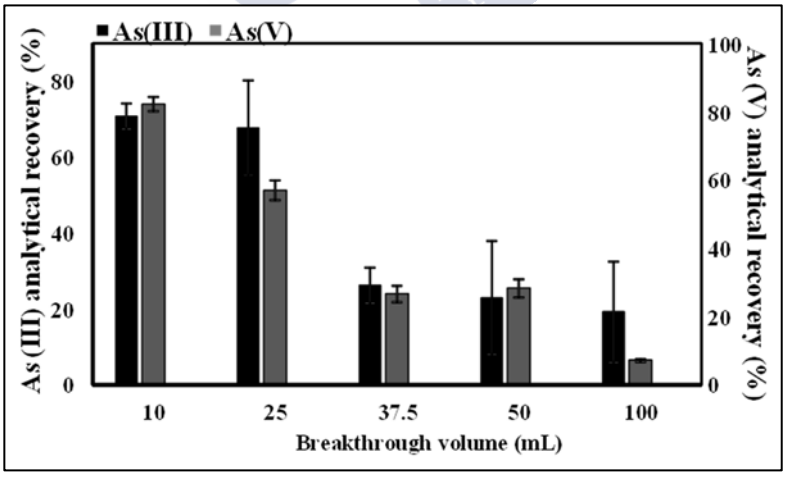

Figure 4. Effect of the fish extract volume (breakthrough volume) on the As(III) and As(V) analytical recovery.

2.3.3. Imprinting effect and selectivity

Different experiments were conducted in order to evaluate the imprinted effect of IIP over NIP, and also the selectivity of the synthesized IIP (cross-reactivity studies). Interactions (retention) of organoarsenic species (AB, AC, MA, and DMA), as well as other metallic ions (Hg(II), Cd(II), Pb(II), K(I), Ca(II), Mg(II), Na(I), Zn(II), Co(II), Fe(III), Cr(III), and Cu(II)), were studied using aqueous standards at 4.0 μg L^{-1} each. They were subjected to the optimized IIP/NIP-SPE procedure in triplicate. After HPLC-ICP-MS (inorganic arsenic and organoarsenic species) and ICP-MS (metallic ions) determination (measurement conditions in ESI), parameters such as extraction efficiency, distribution ratio (D) and selectivity coefficient ($S_{As(III)/X}$), defined as shown in Table 2, were calculated. As expected, the polymeric material (IIP) discriminates As(III) and As(V) species (extraction efficiencies of 92% and 90%, respectively) from organoarsenic forms (extraction efficiencies within the 0-17% range) and also other metallic ions (extraction efficiencies lower than 10%). In addition, extraction efficiencies were lower than 50% for As(III) and As(V) when using NIP (Table 2), highlighting the imprinted recognition capacities of the synthesized IIP. According to Table 2, high distribution ratios and low selectivity coefficients were observed for As (III) and As (V); whereas, other ions and organoarsenic species showed low distribution ratios and high selectivity coefficients. These findings demonstrate that IIP offers selective recognition properties for inorganic As (As(III) and As(V)).

Table 2. Extraction efficiency, distribution ratio and selectivity coefficient of IIP and NIP

	IIP		
	Extraction efficiency (%)[a]	Distribution ratio[b]	Selectivity coefficient[c]
As (III)	92	19.2	---[d]
As(V)	89	19.7	0.98
AB	9	0.1	198
AC	0	0	---[d]
MA	17	0.2	92
DMA	0	0.1	555
P	0	0	---[d]
K	10	0.1	169
Ca	1	0	1744
Mg	0	0	58565
Na	2	0	1221
Zn	0	0	6924
Co	4	0	432
Fe	10	0.1	174
Cr	2	0	1007
Pb	0	0	---[d]
Hg	0	0	---[d]
Cd	0	0	---[d]
Cu	0	0	---[d]
	NIP		
As (III)	36	0.57	---[d]
As(V)	46	0.86	22
AB	13	0.15	129
AC	0	0	---[d]
MA	15	0.19	103
DMA	2	0.31	63
P	0	0	---[d]
K	10	0.11	179
Ca	1	0.01	1957

Table 2. Extraction efficiency, distribution ratio and selectivity coefficient of IIP and NIP (Continued)

	NIP		
	Extraction efficiency (%)[a]	Distribution ratio[b]	Selectivity coefficient[c]
Mg	0	0	15421
Na	2	0.02	1227
Zn	0	0	6567
Co	4	0.05	432
Fe	11	0.13	150
Cr	2	0.02	1002
Pb	0	0	---[d]
Hg	0	0	---[d]
Cd	0	0	---[d]
Cu	0	0	---[d]

A_1 = Analyte concentration in aqueous solution at equilibrium
A_2 = Analyte concentration enriched by IIP/NIP at equilibrium
A_T = Total analyte concentration used in extraction
$D_{As(III)}$= Distribution ratio of As(III) (template)
D_X=Distribution ratio of other compounds
(a) % =$(A_2/A_T) \times 100$; (b) D =(A_2/A_1); (c) $S_{As(III)/X}=D_{As(III)}/D_X$; (d) not calculated

2.3.4. Analytical performances

2.3.4.1. Calibration

In addition to aqueous As(III) and As(V) calibrations (concentrations within the 0 – 20 μg L^{-1} range), several standard addition graphs were performed by spiking fish extracts with increasing As(III) and As(V) concentration up to 0.4 μg L^{-1} before IIP-SPE (concentrations within the 0 - 20 μg L^{-1} after IIP-SPE). Since mean slopes for aqueous calibration and standard addition (Table 3) are different, a calibration based on standard additions throughout the IIP-SPE on-column procedure is needed for achieving accurate results.

Table 3. Mean slopes of calibration and standard addition, and LOD and LOQ values

	Slope (mean±Sd)			
	Calibration[a]	Standard addition[a]	LOD (µg kg^{-1})[b]	LOQ (µg kg^{-1})[b]
As(III)	1154±138	2666±318	0.32	1.05
As(V)	1095±158	6465±1136	0.39	1.31

[a] n=10, [b] pre-concentration factor 50

2.3.4.2. Limit of detection and limit of quantification

The pre-concentration factor (PF) of the method, defined as the ratio of sample extract to eluate [29,30], was found to be 50 for both As(III) and As(V) species. In addition, experiments in triplicate were performed to establish the enhancement factor (EF), which is defined as the ratio of the slope of calibration curves with and without pre-concentration [29,30]. EFs of 59 and 58 were obtained for As(II) and As(V). Similar EF and PF values indicate quantitative recovery for the pre-concentration procedure in absence of matrix effect. As previously commented, the existence of the matrix effect is exceeded/compensated by using the standard addition technique.

The limit of detection (LOD) and the limit of quantification (LOQ) were calculated according to the Eurachem guideline as three (LOD) and ten (LOQ) times the standard deviation of an analytical blank [31]. Analytical responses were then expressed as concentrations dividing by the mean slope of the standard addition graph. Table 3 lists the LOD and LOQ values after taking into account the pre-concentration factor of 50 and referring to sample mass. These values are quite lower than the maximum levels for inorganic As in rice and rice-based products (0.3 mg kg^{-1} for total inorganic As) established by the EU [9].

2.3.4.3. Precision and accuracy

Precision and analytical recovery have been established through intraday and inter-day assays which implied several fish extracts spiked with As(III) and As(V) at concentration levels of 0.04, 0.20, and 0.40 µg L^{-1} (concentrations of 2.0, 10, and 20 µg L^{-1} after pre-concentration). Intraday assays were performed by preparing three

standard additions in three different days, replicating seven times one of the tested concentration levels each day (0.2, 2.0, or 5.0 µg L^{-1}); whereas, the other concentration levels were replicated twice. Inter-day assays were assessed by preparing six standard additions in seven different days but replicating each concentration level twice. Both intraday and inter-day precision, as well as intraday and inter-day analytical recoveries (Table 4), were found to be good.

Table 4. Inter-day and intraday analytical recovery (AR) and precision (RSD)

Parameter	Concentration (µg L^{-1})	As(III)		As(V)	
		AR (%)	RSD (%)	AR (%)	RSD (%)
Inter-day (n=7)	0.2	93±1	12	83±11	15
	1.0	100±5	5	101±8	8
	2.0	92±6	5	98±5	6
Intraday (n=7)	0.2	94±8	1	87±7	1
	1.0	98±5	2	92±6	2
	2.0	97±4	2	85±5	2

Inter-day and intraday assays were performed with the same set of 6 IIP-packed syringes, which implies 25 adsorption-desorption cycles each one. As shown in Figure 5, the analytical relative recovery for As(III) and As(V) solutions at 0.2 µg L^{-1} (10 µg L^{-1} after pre-concentration) was found to be within the 80-100% range. These relative recovery values were calculated as reported in Equation 1:

Equation 1 $$RR(\%) = \frac{C_{measured} - C_{sample}}{C_{added}} \times 100$$

where $C_{measured}$ is the total concentration of the target analyte measured after the addition of a certain concentration of analyte (C_{added}) to a fish extract sample. All these findings imply that the same IIP syringe can be re-used at least 25 times without losing recognition/sorption properties.

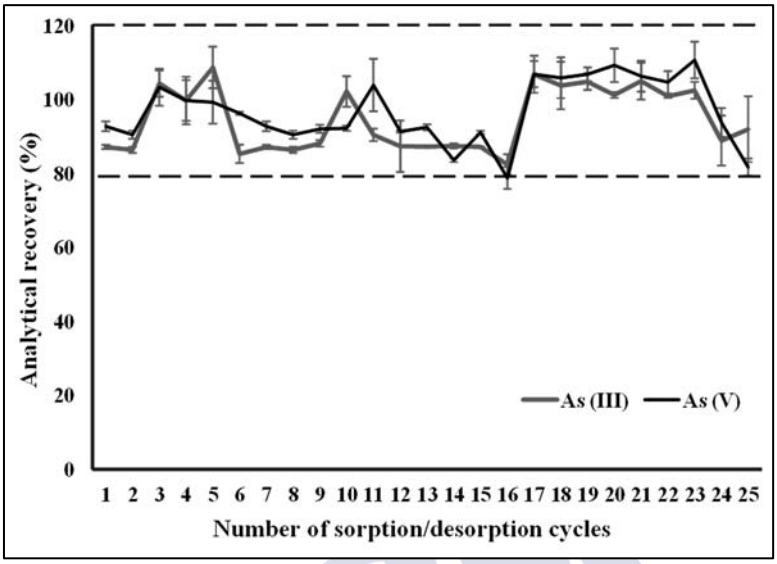

Figure 5. Analytical recovery for As(III) and As(V) standards at 0.2 µg L^{-1} using the same IIP syringe over two weeks (25 sorption/desorption cycles).

Three CRMs showing certified total As contents were analysed for total As (microwave-assisted acid digestion and ICP-MS) and also for As(III) and As(V) (UAE, IIP-SPE and HPLC-ICP-MS). Table 5 lists the found total As concentrations in the three CRMs, which are in good agreement with the certified total As concentrations after applying a *t*-test at a 95% confidence range. Although As(III) and As(V) concentrations are not certified in the analysed CRMs, found As(III) and As(V) concentrations after applying the proposed method (data listed in Table S2, ESI section) were quite similar to some reported data for inorganic As species in these CRMs [3]. Differences between the amounts of reported As(III)/As(V) concentrations in these CRMs suggest the need for improving As speciation methods for inorganic (As(III) and As(V)) assessment, and also the preparation of new CRMs with certified/indicative As(III)/As(V) concentrations.

Table 5. Total As (mean ± SD, n=3) in several CRMs after microwave assisted acid digestion and ICP-MS measurement

	DOLT-3	DORM-2	BCR278
Certified concentration (mg kg^{-1})	10.2±0.5	17.2±0.4	5.9±0.2
Found concentration (mg kg^{-1})	9.8±0.2	17.0±0.7	5.9±0.3

2.3.5. Application

The developed and validated method was applied to fish samples commercially available in markets in Sri Lanka and Spain. Results in Table 6 shows that the percentage of inorganic As was found to be within the 8-20 % range, although inorganic As in one swordfish sample (coded as Swordfish 1) was 61%, mainly due to the high As(V) concentration found in this sample (0.28±0.01mg kg^{-1}).

Table 6. Total As and As(III) and As(V) concentrations (mean ± SD, n=3) in several fish samples

	Total As (mg kg^{-1})[a]	As (III) (mg kg^{-1})[b]	As (V) (mg kg^{-1})[b]	Inorganic As (mg kg^{-1})[b,c]	Inorganic As percentage (%)
Swordfish-1	0.60±0.02	86.3±2.8[d]	0.28±0.01	0.37±0.01	61±3
Swordfish-2	1.8±0.1	0.33±0.05	13.9±2.9[d]	0.35±0.05	19±5
Yellowfin tuna	2.0±0.1	0.27±0.03	24.5±3.4[d]	0.29±0.03	15±3
Tuna sp.	0.31±0.01	39.3±1.3[d]	7.3±0.3[d]	0.047±0.001	15±1
Blue shark	4.9±0.3	0.98±0.17	9.7±5.9[d]	0.99±0.17	20±13
Cod	0.34±0.02	15.0±4.7[d]	12.1±5.6[d]	0.027±0.007	8±4

(a) Microwave assisted acid digestion and ICP-MS measurement;
(b) Ionic imprinted polymer based solid phase extraction and HPLC-ICP-MS measurement;
(c) Sum of As(III) and As(V) concentration;
(d) Concentration expressed in µg kg^{-1}

2.4. CONCLUSIONS

The synthesized IIP has been shown to offer high selectivity for inorganic As (As(III) and As(V)). The development of an IIP-SPE procedure has allowed the quantification of very low concentrations (lower than 0.02 mg kg^{-1} for As (V)) of these two toxic As species in commercially available fish. The high selectivity of the material offers the possibility of inorganic As speciation by HPLC methods because organoarsenic compounds (mainly AB) are not retained/pre-concentrated, which implies the avoidance of co-elution and allows for the accurate determination of low concentrations of As(III) and As(V). The prepared material could also be useful for pre-concentrating inorganic As in other complex samples exhibiting low inorganic As levels, or for samples with moderately low concentrations of inorganic As that are analysed by less sensitive hyphenated techniques.

2.5. ACKNOWLEDMENTS

This work was supported by the *Dirección Xeral de I+D – Xunta de Galicia Grupos de Referencia Competitiva* (project number 6RC2014/2016 and ED431C2018/19), and Development of a Strategic Grouping in Materials - AEMAT (grant ED431E2018/08). The authors also wish to thank Dr. M. José Pazos-Guldrís (*Unidade de Microscopía)* at *Rede de Infraestruturas de Apoio á Investigación e ao Desenvolvemento Tecnolóxico – Universidade de Santiago de Compostela)* SEM technical support.

2.6. REFERENCES

[1] Z. Šlejkovec, Z. Bajc, D.Z. Doganoc, Arsenic speciation patterns in freshwater fish, Talanta, 62 (2004) 931-936.

[2] S. McSheehy, J. Szpunar, R. Morabito, P. Quevauviller, The speciation of arsenic in biological tissues and the certification of reference materials for quality control, TrAC Trends Anal. Chem. 22 (2003) 191-209.

[3] T. Llorente-Mirandes, R. Rubio, J. F. López-Sánchez, Inorganic arsenic determination in food: A review of analytical proposals and quality assessment over the last six years, Appl. Spectrosc. 71 (2017) 25–69.

[4] A. Leufroy, L. Noël, V. Dufailly, D. Beauchemin, T. Guérin, Determination of seven arsenic species in seafood by ion exchange chromatography coupled to inductively coupled plasma-mass spectrometry following microwave assisted extraction: Method validation and occurrence data, Talanta, 83 (2011) 770-779.

[5] European Food Safety Authority, Scientific opinion on arsenic in food, EFSA J. 7 (10):1351 (2009) 1-199.

[6] WHO, Technical Report Series 959, Evaluation of Certain Food Additives and Contaminants, 72nd Report of the Joint FAO/WHO Expert Committee on Food Additives. Geneva, Switzerland, 2010.

[7] M. Contreras-Acuña, T. García-Barrera, M.A. García-Sevillano, J.L. Gómez-Ariza, Arsenic metabolites in human serum and urine after seafood (*Anemonia sulcata*) consumption and bioaccessibility assessment using liquid chromatography coupled to inorganic and organic mass spectrometry, Microchem. J. 112 (2014) 56-64.

[8] J. Moreda–Piñeiro, E. Alonso-Rodríguez, V. Romarís-Hortas, A. Moreda-Piñeiro, P. López-Mahía, S. Muniategui-Lorenzo, D. Prada-Rodríguez, P. Bermejo-Barrera, Assessment of the bioavailability of

toxic and non-toxic arsenic species in seafood samples, Food Chem., 130 (2012) 552-560.

[9] COMMISSION REGULATION (EU) 2015/1006 of 25 June 2015 amending Regulation (EC) No 1881/2006 as regards maximum levels of inorganic arsenic in foodstuffs. Official Journal of the European Union L161 (2015) 14-16.

[10] Á.H. Pétursdóttir, H. Gunnlaugsdóttir, Selective and fast screening method for inorganic arsenic in seaweed using hydride generation inductively coupled plasma mass spectrometry (HG-ICPMS), Microchem. J. 144 (2019) 45-50.

[11] H. Rekhi, S. Rani, N. Sharma, A, K, Malik, A review on recent applications of high-performance liquid chromatography in metal determination and speciation analysis, Crit. Rev. Anal. Chem. 47 (2017) 524-537.

[12] J.M.R Castor, L. Portugal, L. Ferrer, L. Hinojosa-Reyes, J.L. Guzmán-Mar, A. Hernández-Ramírez, V. Cerdà, An evaluation of the bioaccessibility of arsenic in corn and rice samples based on cloud point extraction and hydride generation coupled to atomic fluorescence spectrometry, Food Chem. 204 (2016) 475-482.

[13] H. Shirkhanloo, A. Rouhollahi, H.Z. Mousavi, Ultra-trace arsenic determination in urine and whole blood samples by flow injection-hydride generation atomic absorption spectrometry after preconcentration and speciation based on dispersive liquid-liquid microextraction, Bull. Korean Chem. Soc. 32 **(**2011) 3923-3927.

[14] G. Chen, T. Chen, SPE speciation of inorganic arsenic in rice followed by hydride-generation atomic fluorescence spectrometric quantification, Talanta 119 (2014) 202-206.

[15] C. Magoda, P.N. Nomngongo, N. Mabuba, Magnetic iron–cobalt/silica nanocomposite as adsorbent in micro solid-phase

extraction for preconcentration of arsenic in environmental samples. Microchem. J. 128 **(**2016) 242-247.

[16] S.A. Jabasingh, T. Ravi, A. Yimam, Magnetic hetero-structures as prospective sorbents to aid arsenic elimination from life water streams. Water Sci. 32 **(**2018) 151-170.

[17] N. Tavakkoli, S. Habibollahi, S.A. Tehrani, Separation and preconcentration of Arsenic (III) ions from aqueous media by adsorption on MWCNTs, Arab. J. Chem. 10 (2017) S3682-S3686.

[18] E. Najafi, F. Aboufazeli, H.R. Lotfi Zadeh Zhad, O. Sadeghi, V. Amani, A novel magnetic ion imprinted nano-polymer for selective separation and determination of low levels of mercury(II) ions in fish samples, Food Chem. 141 (2013) 4040-4045.

[19] T. Prasada Rao, R. Kala, S. Daniel, Metal ion-imprinted polymers—Novel materials for selective recognition of inorganics, Anal. Chim. Acta 578 (2006) 105–116.

[20] T. Alizadeh, M. Rashedi, Synthesis of nano-sized arsenic-imprinted polymer and its use as As3+ selective ionophore in a potentiometric membrane electrode: Part 1. Anal. Chim. Acta, 843 (2014) 7-17.

[21] Y.K. Tsoi, Y.M. Ho, K.S.Y. Leung, Selective recognition of arsenic by tailoring ion-imprinted polymer for ICP-MS quantification, Talanta, 89 (2012) 162-168.

[22] J.J. Sloth, E.H. Larsen, K. Julshamn, Determination of organoarsenic species in marine samples using gradient elution cation exchange HPLC-ICP-MS, J Anal. At. Spectrom. 18 (2003) 452-459.

[23] A. Moreda-Piñeiro, E. Peña-Vázquez, P. Hermelo-Herbello, P. Bermejo-Barrera, J. Moreda-Piñeiro, E. Alonso-Rodríguez, S. Muniategui-Lorenzo, P. López-Mahía, D. Prada-Rodríguez, Matrix

solid-phase dispersion as a sample pretreatment for the speciation of arsenic in seafood products, Anal. Chem. 80 (2008) 9272-9278.

[24] B. Batista, L. Nacano, S. De Souza, F. Barbosa Jr, Rapid sample preparation procedure for As speciation in food samples by LC-ICP-MS, Food Addit. Contam. Part A 29 (2012) 780-788.

[25] C.M.M. Santos, M.A.G. Nunes, I.S. Barbosa, G.L. Santos, M.C. Peso-Aguiar, M.G.A. Korn, E.M.M. Flores, V.L. Dressler, Evaluation of microwave and ultrasound extraction procedures for arsenic speciation in bivalve mollusks by liquid chromatography–inductively coupled plasma-mass spectrometry, Spectrochim. Acta Part B: At. Spectr. 86 **(**2013) 108-114

[26] A.A. Ammann, Arsenic speciation analysis by ion chromatography - A critical review of principles and applications, Am. J. Anal. Chem. 2 (2011) 27-45.

[27] Y. Zhai, Y. Liu, X. Chang, X. Ruan, J. Liu, Metal ion-small molecule complex imprinted polymer membranes: Preparation and separation characteristics, React. Funct. Polym. 68 (2008) 284-291.

[28] J. Otero Romaní, A. Moreda Piñeiro, P. Bermejo Barrera, A. Martin Esteban, Synthesis, characterization and evaluation of ionic-imprinted polymers for solid-phase extraction of nickel from seawater, Anal. Chim. Acta 630 (2008) 1-9.

[29] R. Saxena, K. Madaan, S. Bansal, M. Saxena, N. Sharma, A Review on nanomaterials as solid phase extractants for determination of lead in environmental samples, J. Appl. Chem. 11 (2018) 27-38.

[30] R. M. Toudeshki, S. Dadfarnia, A.M.H. Shabani, Surface molecularly imprinted polymer on magnetic multi-walled carbon nanotubes for selective recognition and preconcentration of metformin in biological fluids prior to its sensitive chemiluminescence

determination: Central composite design optimization, Anal. Chim. Acta 1089 (2019) 78-89.

[31] EURACHEM guide, The fitness for purpose of analytical methods, LGC, Teddington, UK, 1998.

[32] A.Q. Shah, T.G. Kazi, J.A. Baig, M.B. Arain, H.I. Afridi, G.A. Kandhro, S.K. Wadhwa, N.F. Kolachi, Determination of inorganic arsenic species (As3+ and As5+) in muscle tissues of fish species by electrothermal atomic absorption spectrometry (ETAAS), Food Chem. 119 (2010) 840–844.

[33] J. Moreda-Piñeiro, E. Alonso-Rodríguez, A. Moreda-Piñeiro, C. Moscoso-Pérez, S. Muniategui-Lorenzo, P. López-Mahía, D. Prada-Rodríguez, P. Bermejo-Barrera, Simultaneous pressurized enzymatic hydrolysis extraction and clean up for arsenic speciation in seafood samples before high performance liquid chromatography-inductively coupled plasma-mass spectrometry determination, Anal. Chim. Acta. 679 (2010) 63–73.

[34] J.P. Jesus, C.A. Suárez, J.R. Ferreira, M.F. Giné, Sequential injection analysis implementing multiple standard additions for As speciation by liquid chromatography and atomic fluorescence spectrometry (SIA-HPLC-AFS), Talanta 85 (2011) 1364–1368.

2.7. ELECTRONIC SUPPLEMENTARY INFORMATION (ESI)

ICP-MS measurements

Total As in acid digests from fish, as well as other trace elements such as Ca, Cd, Co, Cr, Cu, Fe, Hg, K, Mg, Na, P, Pb, and Zn in cross-reactivity studies, were determined by ICP–MS under operating conditions given in Table S1. Total As determination implied 1:10 dilution of acid digests with ultrapure water, the use of ^{74}Ge (10 µg L^{-1}) as an internal standard, and kinetic energy discrimination (KED) by using He (4.0 mL min^{-1}) as a collision gas for selectively polyatomic interferences attenuation. Nitric acid (1.0% (v/v)) matched calibration within the 0 - 100 µg L^{-1} range was performed for assessing total As contents. The determination of other elements (cross-reactivity studies, Table S1) was carried out using ^{54}Sc (10 µg L^{-1}) as an internal standard for Ca, K, Mg, Na, and P under standard conditions, and ^{74}Ge (10 µg L^{-1}) as an internal standard for Cu (standard conditions) and for Co, Cr, Fe and Zn (KED mode, He 4.0 mL min^{-1}). Finally, ^{103}Rh (10 µg L^{-1}) was used as an internal standard for Cd, Hg and Pb determinations (standard conditions measurements). Determinations were performed using 1.0% (v/v) nitric acid matched calibration within the 0 - 100 µg L^{-1} range for all elements.

Table S1. Operating ICP-MS conditions for total As determination in acid digests from fish samples, and for P, K, Ca, Mg, Na, Zn, Co, Fe, Cr, Pb, Hg, Cd, and Cu determination in cross reactivity studies.

Operating ICP-MS conditions		
Radiofrequency power		1600 W
Gas flows	Nebulization	0.92 mL min^{-1}
	Auxiliary	1.2 mL min^{-1}
	Plasma	16 mL min^{-1}
Standard mode		Ca, Cu, K, Mg, Na, P
KED mode: He flow rate/ 4.0 mL min^{-1}		As, Cd, Co, Cr, Fe, Hg, Pb, Zn
Analytes		^{75}As, ^{43}Ca, ^{111}Cd, ^{59}Co, ^{53}Cr, ^{63}Cu, ^{57}Fe, ^{39}K, ^{202}Hg, ^{26}Mg, ^{23}Na, ^{31}P, ^{208}Pb, ^{66}Zn
Internal standards		^{74}Ge (As, Co, Cr, Fe, and Zn) ^{54}Sc (Ca, K, Mg, Na, and P) ^{103}Rh (Cd, Hg, and Pb)

Table S2. As(III) and As(V) concentrations (mean ± SD, n=3) in several CRMs

	[As(III)] (mg kg^{-1})		[As(V)] (mg kg^{-1})	
Concentration	Reported	Found	Reported	Found
DOLT-3	0.3±0.1[a]; 0.074–0.136[b]	0.34±0.16	0.073±0.007[c]; 0.4–0.2[d]	0.16±0.05
DORM-2	0.61±0.04[e]; 0.03–0.081[f]	0.63±0.01	0.029±0.018; 0.026±0.002[c]	0.08±0.01
BCR-278	----[g]	0.84±0.09	----[g]	0.92±0.01

(a) As(III) concentration reported by Batista *et al.* [24]; (b) As(III) concentration reported by Leufroy *et al.* [4]; (c) As(V) concentration reported by *Leufroy et al.* [4]; (d) As(V) concentration reported by Batista *et al.* [24]; (e) As(III) concentration reported by Santos *et al.* [25]; (f) As(III) concentration reported by Leufroy *et al.* [4], Shah *et al.* [32], Moreda-Piñeiro *et al.* [33], and Jesus *et al.* [34]; (g) not given

USC
UNIVERSIDADE
DE SANTIAGO
DE COMPOSTELA

CHAPTER 3

IONIC IMPRINTED POLYMER - VORTEX-ASSISTED DISPERSIVE MICRO-SOLID PHASE EXTRACTION FOR INORGANIC ARSENIC SPECIATION IN RICE BY HPLC-ICP-MS

B.K.K. KAMAL JINADASA, ELENA PEÑA-VÁZQUEZ, PILAR BERMEJO-BARRERA, ANTONIO MOREDA-PIÑEIRO

USC
UNIVERSIDADE
DE SANTIAGO
DE COMPOSTELA

Ionic imprinted polymer - vortex-assisted dispersive micro-solid phase extraction for inorganic arsenic speciation in rice by HPLC-ICP-MS

B.K.K. Kamal Jinadasa, Elena Peña-Vázquez, Pilar Bermejo-Barrera, Antonio Moreda-Piñeiro

Trace Element, Spectroscopy and Speciation Group (GETEE), Strategic Grouping in Materials (AEMAT), Department of Analytical Chemistry, Nutrition and Bromatology. Faculty of Chemistry. Universidade de Santiago de Compostela. Avenida das Ciencias, s/n. 15782, Santiago de Compostela. Spain

Abstract

This study combines ultrasound-assisted extraction and vortex-assisted dispersive micro-solid phase extraction using an ionic imprinted polymer as a selective sorbent for rapid isolation and pre-concentration of inorganic arsenic species (As(III) and As(V)) in extracts from rice samples prior to their determination by high performance liquid chromatography coupled to inductively coupled plasma mass spectrometry. All factors affecting the ultrasound assisted extraction of the species from rice (ultrasound amplitude, sonication time and sonication mode) and their selective pre-concentration by ionic imprinted polymer-based vortex-assisted dispersive micro-solid phase extraction (sorbent amount, extract pH, vortex extraction time and speed, eluting solution and vortex elution time and speed) were optimized. The analytical performance of the procedure was studied at optimum conditions: ultrasound continuous sonication at 40% amplitude for 1.0 min using 1:1 methanol/ultrapure as an extractant, 50 mg of sorbent, extract pH at 8.0, vortex loading at 1000 rpm for 1.0 min, and elution with ultrapure water by vortexing at 1000 rpm for 1.0 min, pre-concentration procedure which leads to a pre-concentration factor of 10. The limits of detection obtained for As (III) and As (V) were 0.20 and 0.41 μg kg^{-1}, respectively, and were well below the maximum levels established by the European Union in rice and rice containing products. The method was found to be precise

(intraday and interday relative standard deviations ≤ 11%) and selective. The accuracy was confirmed by analysing the ERM-BC211 (rice, As species) certified reference material, and the method was successfully applied to commercial rice samples.

Keywords: Dispersive micro-solid phase extraction, inorganic arsenic, ionic imprinted polymer, rice

3.1. INTRODUCTION

Consumption of contaminated water and food is one of the major sources of exposure to toxic contaminants such as arsenic (As) for humans [1]. Arsenic toxicity depends on its chemical form, solubility and many other intrinsic and extrinsic factors, and the most toxic forms of arsenic are the inorganic arsenic species (iAs) [trivalent arsenite As(III), which is 2-10 times more toxic than pentavalent arsenate As(V)] [2].

Rice is one of the major staple foods for about 50% of the world population, mainly from the Asian and African countries [3]. Approximately 50% of total arsenic in rice is inorganic arsenic, ranging from 0.4 to 100%. Therefore, the development of simple, sensitive, rapid and reliable methods for the determination and speciation of iAs in rice is of great relevance.

The determination of iAs species in rice requires close attention to sample preparation strategies [4], and there are several sample preparation methods that have been used for As extraction from rice with different heating devices [5-8], or by speeding up the extraction with ultrasound [9,10] or microwave energy [11-13] assistance.

Conventional solid-phase extraction (SPE) is one of the most common and popular sample pre-treatment techniques, and drawbacks of conventional cartridges-based SPE can be overcome by dispersing the sorbent into the liquid sample/extract. The technique, referred to as dispersive solid phase extraction (DSPE) [14], and as dispersive micro solid-SPE (D-μ-SPE) when using a small amount (μg or mg range) of micro- or nanosorbents in the sample [15]. D-μ-SPE is an environmentally friendly and miniaturized extraction technique that

speeds up mass transference, reduces the extraction and desorption times, and can be used for extract clean-up and targets pre-concentration [16, 17]. A wide range of materials can be used as sorbents for D-μ-SPE, such as silica nanoparticles, carbon nanotubes, graphene, graphene oxide, metal organic and zeolite imidazolate frameworks, immunosorbents, and molecularly or ionic-imprinted polymer (MIP/IIP), the latter proposed for selectivity improvement [16].

Dispersion can be enhanced by applying ultrasound (ultrasound-assisted dispersive micro-solid phase extraction, UA-D-μ-SPE), air (air-assisted dispersive micro-solid phase extraction, AA-D-μ-SPE), and vortex stirring (vortex-assisted dispersive micro-solid phase extraction, VA-D-μ-SPE) [15,18]. Most applications have been described for organic target pre-concentration [15-17]. Regarding metals, pure nanosilica and nanosilica-ionic liquid hybrid material, and carbon nanotubes have been used for D-μ-SPE of Se(IV) [19,20] and As(V) [21] before electrothermal atomic absorption spectrometry (ETAAS).

The high selectivity offered by MIP as sorbents for D-μ-SPE and the simplicity and speed of the technique can be an appealing combination for efficient and fast clean-up and pre-concentration purposes. Some examples can be found in the literature such as those that use magnetic MIPs and VA-D-μ-SPE for screening of dicofol in tea samples [22] and ciprofloxacin in human serum, plasma, urine and pharmaceutical samples [23]. The benefits of imprinted polymer combined with D-μ-SPE for metallic species have been yet not explored, and the aim of the current study has been the development and application of an IIP selective to iAs (As(III) and As(V)) as a sorbent for VA-D-μ-SPE. Arsenic species (As(III) and As(V) included) have been isolated from rice by ultrasound-assisted extraction (UAE) before the selective pre-concentration of iAs by the proposed IIP-VA-D-μ-SPE. Pre-concentrated iAs species were then separated and determined by high-performance liquid chromatography-inductively coupled plasma mass spectrometry (HPLC-ICP-MS).

3.2. MATERIALS AND METHODS

3.2.1. Instrumentation

The ICP-MS was a NexIon 300X (Perkin Elmer, Waltham, MA, USA) with a SeaFast SC2 DX autosampler (Elemental Scientific, Omaha, NB, USA). The chromatographic system consisted of a Flexar LC HPLC instrument (LC pump, column oven, and LC autosampler) from Perkin Elmer, equipped with a PRP×100 column (10 µm, 100 × 4.1 mm) and a PRP×100 guard column (10 µm, 25 × 2.3 mm) from Hamilton (Reno, NV, USA). A low-profile roller (Stovall, Greensboro, NC, USA), placed inside a Boxcult temperature-controlled chamber (Stuart Scientific, Surrey, UK), was used for IIP synthesis. Fourier transform infrared spectrometry (FT-IR) with ATR correction (instrument Spectrum-Two, Perkin Elmer) (Figure S 1), and scanning electron microscopy (SEM) with a ZEISS EVO LS 15 instrument (Carl Zeiss, Oberkochen, Germany) were used for IIP characterization (Figure S 2). Other devices were: a VibraCell VCx 130 ultrasonic processor (Sonics, Newtown, CT, USA), an USC60TH ultrasonic cleaner bath (45 kHz, 120 W) from VWR (Leuven, Belgium), a Reax top vortex mixer (Heidolph, Schwabach, Germany), a 2K15 ultracentrifuge (Sigma, Osterode, Germany), a Basic 20 pH meter (Crison, Barcelona, Spain), an oven model 207 from Selecta (Barcelona, Spain), a Taurus 850 domestic blender (Taurus, Barcelona, Spain), a Minipuls 3 peristaltic pump (8 channels) from Gilson (Middleton, WI, USA), and a Classic ML analytical balance (Mettler Toledo, Columbus, OH, USA).

3.2.2. Reagents

Ultrapure water (resistivity of 18.2 MΩ cm) obtained from a Milli Q-A10 system (Millipore Co., Billerica, MA, USA) was used throughout the study. Sodium (meta)arsenite ($NaAsO_2$) was from Sigma-Aldrich (St. Louis, MO, USA). Ammonium chloride, ammonium hydroxide and methanol (Chromasolv) were from Merck (Darmstadt, Germany); ammonium hydrogen carbonate and acetic acid (glacial) were from Panreac (Barcelona, Spain); and ammonium dihydrogen phosphate from BDH (Poole, United Kingdom). Chemicals used in IIP synthesis were 1-vinyl imidazole (≥99.0% purity) and 2,2'-azobisisobutyronitrile

(AIBN) from Fluka (Buchs, Switzerland), and divinylbenzene (DVB) from Sigma-Aldrich (AIBN and DVB were subjected to a purification process before use [24]). As(III) and As(V) metal stock solutions (1000 mg L^{-1}) were from Panreac, while monomethyl arsenic (MMA) and dimethyl arsenic (DMA) standard solutions (1000 mg L^{-1}) were prepared by dissolving appropriate amounts of $CH_3AsO(ONa)_2 \cdot 6H_2O$ (Carlo Erba, Milan, Italy) and $C_2H_6AsNaO_2 \cdot 3H_2O$ (Merck), respectively. Multi-element standard solutions (for cross-reactivity studies) were prepared by combining single Ca, Co and Mg stock standard solutions (1000 mg L^{-1}) from Merck, single Cr, Hg, K, P, Pb and Zn stock standard solutions (1000 mg L^{-1}) from Scharlab (Barcelona, Spain), and single Cd, Cu, and Fe stock standard solutions (1000 mg L^{-1}) from Perkin Elmer (Shelton, CT, USA). NexIon Setup Solution (10 μg L^{-1} of Be, Ce, Fe, In, Li, Mg, Pb, and U in 1% HNO_3) and internal standard solutions (1000 mg L^{-1}, Ge, Sc, and Rh) were from Perkin Elmer. The certified reference material (CRM) ERM-BC211 (rice, As species) was from the Institute for Reference Materials and Measurements (Geel, Belgium). Other consumables were Durapore 0.22 μm membrane filters (Millipore), 2.0 mL polypropylene microtubes tubes (Labbox, Barcelona, Spain), PVC 2-stop tubing (1.52 mm i.d.) from SCP Sciences (Baie-D'Urfe, Quebec, Canada), replacement Teflon frits (Supelco, Bellefonte, PA, USA), and 5.0 mL disposable syringes (Dispomed, Gelnhausen, Germany).

3.2.3. Synthesis of the ionic imprinted polymer

Details regarding As (III)-based IIP synthesis can be found elsewhere [25] and consisted of a template/bifunctional monomer/cross-linker molar ratio fixed at 1:4:20 [1.6 mmol of $NaAsO_2$ (template), 6.5 mmol of 1-vinylimidazole (bi-functional monomer), and 32 mmol of DVB (cross-linker)] and 20 mL 1:3 acetic acid/methanol porogen. The presence of N moieties in the bifunctional monomer 1-vinylimidazole allows the interaction with the hydroxyl groups in oxyanions such as As(III) and As(V) [26]. After adding the initiator (AIBN, 40 mg) and purging (N_2 for 10 min), polymerization was performed in a low-profile roller (rotation of the tubes at 33 rpm around the long axis) placed inside a temperature-controllable chamber at 60°C for 12 h.

The resulting polymer was washed with 5.0 mL methanol three times, and oven-dried at 40ºC overnight. Template removal was performed by packaging approximately 200 mg of IIP into 5.0 mL syringes between two Teflon frits, and by passing 200 mL of 2.0 M HNO_3 at a flow rate of 1.0 mL min^{-1} until the last leachate solution was free of As (ICP-MS analysis). The polymer particles were washed with ultrapure water and dried in a desiccator. Non-imprinted polymers (NIPs) were synthesized using the same procedure but in the absence of the As(III). Details regarding IIP characterization is given in Electronic Supplementary Information (ESI).

3.2.4. Rice samples

Rice samples were purchased in local supermarkets at Santiago de Compostela. Portions of 100 g were first ground to fine powders using a domestic blender, and powdered samples were then stored in pre-cleaned polyethylene bottles with hermetic seals at 4°C before use.

3.2.5. Microwave assisted acid digestion

Portions of 0.500 g of rice samples and CRM (three replicates each one and at least two reagent blanks in each microwave acid digestion set) were directly weighted in the Teflon reactors and were mixed with 3.0 mL of 69 % (w/v) nitric acid, 1.0 mL of 33 % (w/v) hydrogen peroxide, and 4.0 mL of ultrapure water. After closing the reactors they were subjected to microwave energy (800 W power) in a four-stage heating program involving a first heating ramp from room temperature to 90°C in 4.0 min, followed by a second heating ramp from 90°C to 150°C in 7.0 min, and a third heating ramp from 150°C to 200°C in 8.0 min. Finally, the reactors were heated at 200°C for 20 min, and were then allowed to cool down for 1.0 h. The acid digests were finally made up to 25 mL with ultrapure water and stored in polyethylene flasks.

3.2.6. Ultrasound assisted extraction (UAE)

Approximately 1.000 g of powdered rice sample was weighed into a 15 mL centrifuge tube, and 10 mL of the extracting solution (1:1 methanol/water [27]) were added. The ultrasound probe operating in

continuous mode (frequency of 20 kHz with a power of 68 W, and amplitude at 40% of the maximum range) was immersed into the solution that was irradiated by ultrasonic waves for 1.0 min (the test tubes were immersed in an ice-bath to avoid temperature increases). Then, the extract was isolated from the solid residues by ultracentrifugation (4°C, 3000 rpm, 10 min) before further VA-D-μ-SPE pre-concentration.

3.2.7. Vortex-assisted dispersive micro-solid phase extraction (VA-D-μ-SPE)

For VA-D-μ-SPE, portions of 50 mg of IIP (or NIP in some experiments) in 2 mL microtubes were conditioned by adding 1.5 mL of ultrapure water (pH 8.0, adjusted using 0.1M/0.1 M NH_3/NH_4Cl buffer solution), and subjecting the mixture to vortex stirring (1000 rpm, 1 min) and ultracentrifugation (4 °C, 12000 rpm, 10 min) to discard the liquid supernatant. A volume of 1.5 mL of rice extract (pH fixed at 8.0) was added, and the mixture was vortexed (1000 rpm, 1 min) and ultracentrifuged (4 °C, 12000 rpm, 10 min). After discarding the liquid phase, elution was performed using 150 μL of ultrapure water and vortexing (1000 rpm, 1 min) and centrifugation (4 °C, 12000 rpm, 10 min). The supernatants were isolated and direct measured by HPLC-ICP-MS. The experiments were performed in triplicate and at least two reagent blanks were prepared for each experiment set.

3.2.8. ICP-MS and HPLC-ICP-MS measurements

The determination of total As in acid digests from rice, and the multi-element determinations when studying the imprinting effect and cross-reactivity were performed by ICP-MS (operating conditions listed in Table S1 (ESI) by using 1.0 %(v/v) nitric acid matched calibrations covering the 0-100 $\mu g\ L^{-1}$ concentrations range.

As(III) and As(V) in the extracts from rice were determined by HPLC-ICP-MS under operating conditions listed in Table 1. Quantification was performed using the standard addition technique by spiking rice extracts with As(III) and As(V) concentrations within the 0.1 – 2.0 $\mu g\ L^{-1}$, and subjecting the spiked extracts to the VA-D-μ-SPE process (standard addition calibration covering As(III) and As(V)

concentrations from 1.0 to 20 µg L^{-1}, taking into account a pre-concentration factor of 10). Chromatograms for an aqueous standard (1.0 µg L^{-1}), an extract from the CRM and two rice samples (basmati and wild rice) are given in Figure 1(a-d).

Table 1. Operating HPLC-ICP-MS parameters

ICP-MS	
Radio frequency power (W)	1600
Ar flow rate (L min^{-1}) (plasma/auxiliary/nebulizer)	16/1.2/0.92
KED mode, He flow rate (mL min^{-1})	4
Integration time (ms)	250
Mass monitored	^{75}As
HPLC	
Column	Hamilton PRP×100, 10 µm, 4.1×100 mm
Mobile phase	$(NH_4)H_2PO_4$, 15 mmol, pH 6.0
Flow rate	1 mL min^{-1}, 8.5 min
Injection volume	20 µL

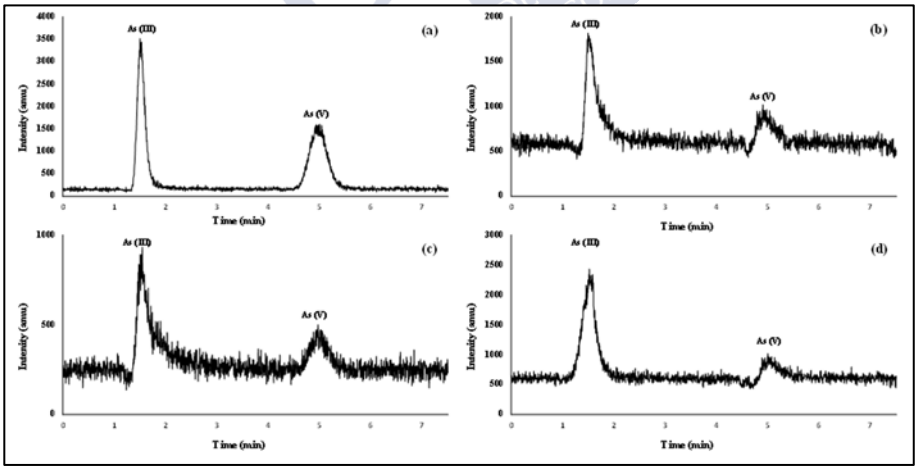

Figure 1. HPLC-ICP-MS chromatograms for a 20 µg L^{-1} As(III) and As(V) aqueous standard (a), and a pre-concentrated extract from ERM-BC211 CRM (b), wild rice (c), and basmati rice (d)

3.3. RESULTS AND DISCUSSION

3.3.1. Optimization of VA-D-μ-SPE

The VA-D-μ-SPE procedure was optimized using rice extracts aliquots (1.5 mL each one) spiked with iAs (2.0 μg L^{-1} for As(III) and As(V)). For As(III) and As(V) analytical recovery assessment, un-spiked rice extracts were also analysed in each set of conditions. Extracts from rice (Jasmin) were obtained by applying non-optimised UAE conditions (continuous sonication at 60% amplitude for 5.0 min). Several parameters affecting the VA-D-μ-SPE process (rice extract pH, loading vortex stirring time and speed, eluting vortex time and speed, and IIP amount)were fully evaluated (experiments performed in triplicate and at least two blanks prepared for each set of tested conditions). As(III) and As(V) concentrations (analytical recoveries) were assessed using aqueous calibrations and after subtracting the As(III) and As(V) contents in the un-spiked rice extracts.

3.3.1.1. Rice extract pH and loading vortex stirring time and speed

Variables affecting the loading stage were studied using un-optimized eluting conditions (water as extractant, and elution vortex stirring speed at 2000 rpm for 2.0 min). The pH of the rice extract plays an important role for favouring the interactions between dissolved analytes (As(III) and As(V)) and IIP particles during dispersion. The influence of the extract pH was tested by varying the pH from 6.0 (extract pH after UAE) to 10.0 (pHs higher than 6.0 were obtained by adding a few drops of ammonia to the 10 mL extract obtained after UAE). The spiked 1.5 mL aliquots of rice extracts after pH adjustment were mixed with 50 mg of IIP, and the loading step was carried out by vortexing at 2000 rpm for 3.0 min (non-optimized elution conditions as explained above). Figure 2(a) shows that As (V) analytical recovery is high (approximately 40%) when fixing the pH within the 6.0-8.0 range, and decreases at the highest tested pHs (9.0 and 10.0). However, As (III) analytical recovery is highest (approximately 40%) when loading rice extracts at pH 8.0. These findings agree with As(III)/As(V)-pH dependence [28], which implies As(V) and As(III) species prevalent at neutral pH and/or at slightly alkaline pHs. The

highest iAs analytical recoveries were observed at pH 8.0, and this pH was selected.

The role of the vortex agitator is to disperse the IIP into the sample solution to improve the extraction efficiency. By fixing the extract pH at 8.0 and the loading vortex time at 2.0 min, several loading vortex speeds (from 500 to 2500 rpm, 500 rpm intervals) were tested. Analytical recoveries for As(III) and As(V) were found to be dependent of the vortex speed (Figure 2(b)). Low vortex speed (500 rpm) and vortex speeds higher than 1000 rpm led to poor extraction yields. The low analytical recoveries when vortexing at the lowest speed is attributed to an inefficient contact between As ions and the dispersed IIP particles. In addition, analyte-sorbent desorption (back diffusion), reported for several microextraction techniques [29-31], are responsible for the low extraction yields when using high vortex speeds. Taking into account these findings, the loading vortex speed was fixed at 1000 rpm.

Finally, the vortex rotational speed was fixed at 1000 rpm, and loading experiments (rice extract at pH 8.0) were performed by varying the vortex stirring time from 1.0 to 5.0 min. Calculated iAs analytical recoveries (Figure 2(c)) show that the effect of the vortexing time during the loading stage is not significant, and the loading vortex time was set at 1.0 min.

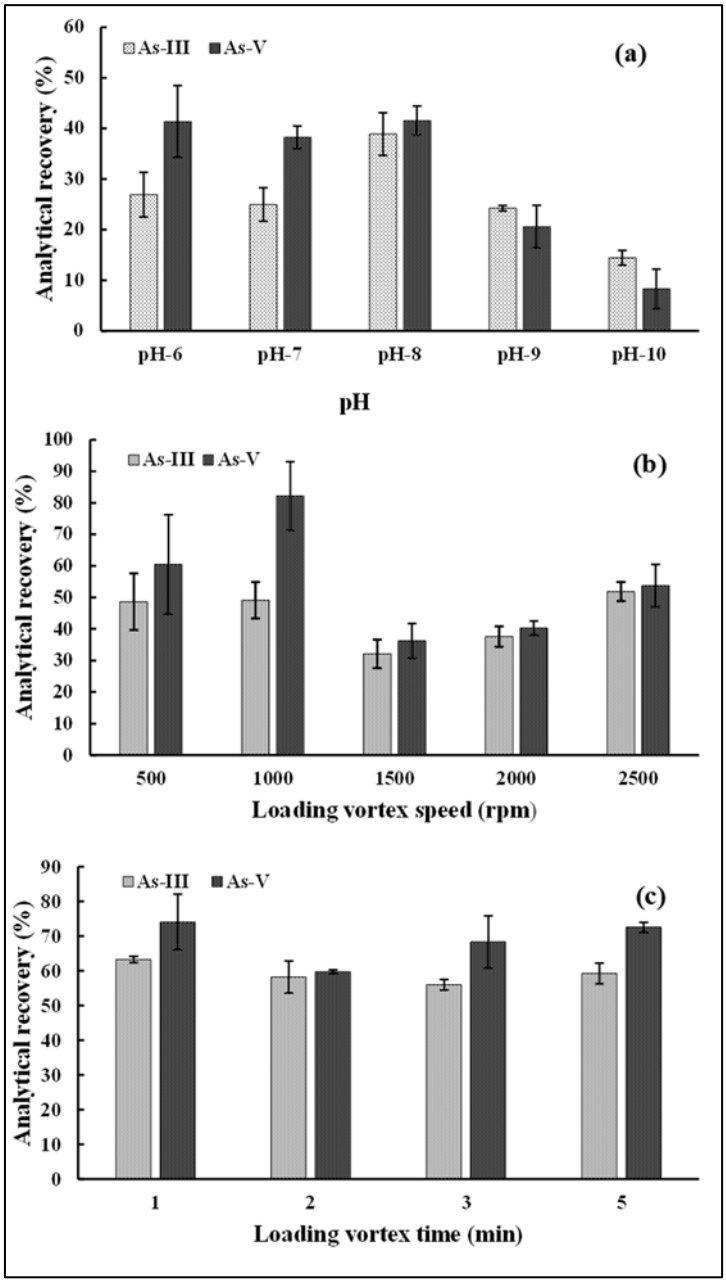

Figure 2. Effect of the extract pH (a), loading vortex speed (b), and loading vortex time (c) on the analytical recovery of As(III) and As(V)

3.3.1.2. Eluting vortex stirring time and speed

In the current experiments, 150 µL of ultrapure water were used for iAs species elution. Several elution times (within the 1.0-5.0 min range) and elution speeds (from 500 to 2500 rpm) were tested under optimized loading vortex conditions. As shown in Figure 3(a,b), iAs analytical recoveries were not significantly different within the time/speed range studied, and elution vortex conditions were finally fixed at 1000 rpm for 1.0 min.

3.3.1.3. Effect of the IIP sorbent amount

It is well known that the use of appropriate amounts of the IIP sorbent affects the extraction efficiency of the VA-D-µ-SPE procedure [16]. Therefore, several amounts of IIP (10, 20, 50 and 100 mg) were used to evaluate the recovery of As(III) and As(V) using the above optimized conditions. Experiments in triplicate (Figure 3(c)) showed that iAs species recoveries were gradually increased up till 50 mg of IIP sorbent, and there were no statistically significant differences between the recoveries of As(V) when using 50 or 100 mg of IIP. Hence, 50 mg of IIP was found to be adequate to quantitatively retain iAs. This mass of polymer was thus selected for further studies.

3.3.2. Optimization of ultrasound-assisted extraction (UAE)

Methanol/water mixtures (typically 1:1 ratio) have been found to be effective for extracting As species from biological matrices, rice included, and the extractive process is usually assisted by ultrasounds (ultrasounds water-bath) and by microwaves [27,32]. Three factors affecting the extractive process (use of ultrasound probe for assisting the extraction), ultrasounds amplitude (20, 30, 40, 50, 60, 70 and 80%), sonication time (2, 5, 7, 10, 15 min), and sonication mode (continuous and non-continuous), have been fully evaluated using 10 mL of 1:1 methanol/ultrapure water as an extractant. Experiments were performed in triplicate with 1.0000 g subsamples spiked with As (III) and As (V) at 5.0 µg L^{-1}, and the obtained extracts were further subjected to the optimized VA-D-µ-SPE. Un-spiked rice subsamples were also subjected to the tested conditions in order to properly assess

the analytical recovery of the spiked As(III) and As(V) concentrations after HPLC-ICP-MS (use of an aqueous calibration).

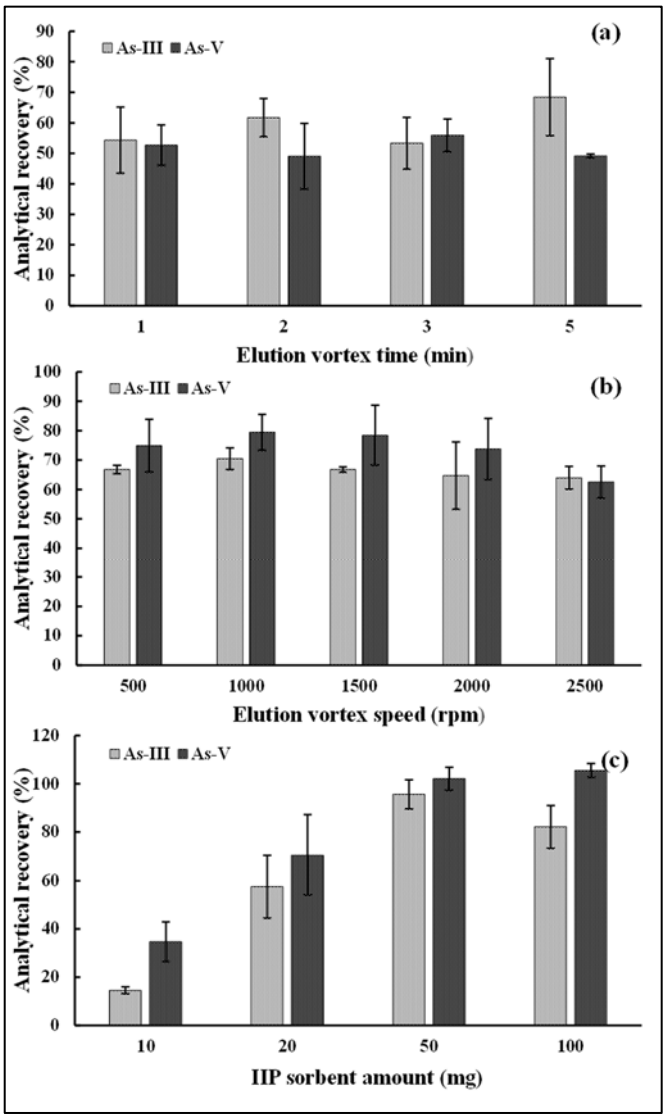

Figure 3. Effect of the elution vortex time (a), elution vortex speed (b), and IIP amount (c) on the analytical recovery of As(III) and As(V)

Results (As(III) and As(V) analytical recoveries for each set of conditions) show that ultrasounds amplitude (Figure S3(a), ESI) and continuous and non-continuous sonication (Figure S3(c), ESI) do not affect iAs extraction from rice. A continuous sonication at 40% ultrasound amplitude was chosen. Regarding the sonication time, Figure S3(b)(ESI) shows similar As(III) and As(V) analytical recoveries within the 2.0–10 min range; whereas the extraction efficiency of both species is impaired at high sonication times (15 min). The optimum sonication (extraction) time was therefore fixed at 2.0 min.

3.3.3. Imprinting effect and cross-reactivity (IIP selectivity) studies

The imprinting effect (iAs adsorption onto IIP particles through the imprinted recognition cavities) and the selectivity (avoidance of adsorption of other elements and/or arsenic species through the imprinted recognition cavities) were evaluated by subjecting aqueous standards of As(III) and As(V) at 5 μg L^{-1}, aqueous standards containing microelements (Cd, Co, Cr, Cu, Mn, Ni, Pb, Hg, and the As species DMA and MMA) at concentrations of 2.0 μg L^{-1}, and aqueous standards containing macro-elements (Al, Ca, Fe, K, Mg, and Zn) at concentrations of 5.0 μg L^{-1}, to the optimized VA-D-μ-SPE procedure using IIP and NIP as sorbents (experiments in triplicate for MMA and DMA experiments, and experiments replicated six times for other elements). Extracts regarding MMA and DMA experiments were directly analysed by HPLC-ICP-MS (conditions in Table 1); whereas, extracts when testing other elements were analysed by ICP-MS (conditions listed in Table S1, electronic supplementary information, ESI). In the latter case, two eluates (150 μL each one) were combined and diluted up to 2.0 mL with 1.0 %(v/v) nitric acid before ICP-MS analysis.

Imprinting effect and selectivity were assessed by calculating the extraction efficiency (EF), the distribution ratio ($D_{(M)}$), and the selectivity coefficient ($S_{(M)}$) according to

$$EF\ (\%) = \frac{A_2}{A_T} \times 100 \qquad \text{Equation 1}$$

$$D_{(M)} = \frac{A_2}{A_1} \qquad \text{Equation 2}$$

$$S_{(M)}=\frac{D_{(As(III))}}{D_{(M)}} \qquad \text{Equation 3}$$

where, A_1 is the amount of metal ion in aqueous solution at equilibrium, A_2 is the amount of metal ion extracted by the IIP/NIP at equilibrium, A_T is the total amount of metallic ion used in the extraction, $D_{As(III)}$ is the distribution ratio for As(III) (template), and D_M is the distribution ratio for other elements/DMA and MMA species.

As expected (Table 2), As(III) and As(V) showed the highest EFs (100% when using IIP as a sorbent); whereas, EFs fall to 31 and 41% for As(III) and As(V), respectively, when using NIP as a sorbent. These finding imply that the interactions between the IIP particles and As(III) (template) and also As(V) are mainly through the imprinted recognition cavities generated in IIP, and the non-specific interactions (adsorption) are a minority. In addition, the IIP sorbent offers high selectivity against other arsenic species present in rice, such as MMA and DMA, which are not retained in the IIP (EFs lower than 10%) and against other elements, with EFs range from 0 to 20% (Table 2). The low $D_{(M)}$ ratios and high $S_{(M)}$ factors assessed for As(III) and As(V), and the high $D_{(M)}$ ratios and low $S_{(M)}$ factors for MMA and DMA, and other elements (Table 2) confirm that the prepared IIP sorbent is highly selective to iAs.

3.3.4. Analytical performances of the UAE-VA-D-µ-SPE method

3.3.4.1. Calibration and matrix effect

Aqueous calibrations (pH 8.0 by adding small volumes of 0.1 M NH_3 solution) with As(III) and As(V) concentrations ranging from 1.0 to 20 µg L^{-1} were prepared across several days. Similarly, several standard addition calibrations were prepared by subjecting rice extracts (10 mL) spiked with As(III) and As(V) within the 0.1 – 2.0 µg L^{-1} range to the proposed VA-D-µ-SPE procedure in triplicate. Taking into account that the pre-concentration factor of the VA-D-µ-SPE process is 10, the concentration levels of the standard addition calibrations varied from 1.0 to 20 µg L^{-1}. Good linearity (correlation coefficient from 0.995 to 1.00) was observed for both aqueous and standard addition curves for both arsenic species. The mean slopes

obtained for aqueous standards (three calibrations) were 865±35 and 812±36 for As(III) and As(V), respectively; whereas, slopes for the standard addition calibration were smaller than for aqueous calibration, 627±71 for As(III) and 718±63 for As(V). These differences are attributed to the matrix effect and suggest that a calibration based on standard additions throughout the VA-D-µ-SPE procedure is needed for achieving accurate results.

Table 2. Values of extraction efficiencies (%), distribution ratios and selectivity coefficients of IIP and NIP after the VA-D-µ-SPE procedure

	Extraction Efficiency (%)		Distribution ratio (D_M)		Selectivity Coefficient ($D_{As(III)}/D_M$)	
	IIP	**NIP**	**IIP**	**NIP**	**IIP**	**NIP**
As (III)	100	31	∞	0.46	-	-
As(V)	100	41	∞	0.70	1	98
MMA	11	2	0.12	0.03	564	2675
DMA	0	2	0	0.03	∞	2684
Al	0	0	0	0	∞	∞
Ca	0	0	0	0	∞	∞
Fe	0	1	0	0.01	∞	6278
K	0	0	0	0	∞	∞
Mg	13	0	0.16	0	441	∞
Zn	18	0	0.22	0	306	∞
Cd	0	0	0	0	∞	∞
Co	0	0	0	0	∞	∞
Cr	0	0	0	0	∞	∞
Cu	0	0	0	0	∞	∞
Mn	5	0	0.05	0	1403	∞
Ni	0	0	0	0	∞	∞
Pb	0	0	0	0	∞	∞
Hg	0	20	0	0.25	∞	280

3.3.4.2. Limit of detection (LOD) and limit of quantification (LOQ)

The limit of detection (LOD) and the limit of quantification (LOQ) were determined after the analysis of eleven blank samples. The concentration corresponding to three times the standard deviation of the blank was defined as LOD, while the concentration corresponding to 10 times the standard deviation of the blank was considered as LOQ. Instrumental LOD/LOQ were 0.20 μg L^{-1} and 0.67 μg L^{-1} for As(III), and 0.41 μg L^{-1} and 1.38 μg L^{-1} for As(V). LOD/LOQ values after considering the pre-concentration factor of 10 (VA-D-μ-SPE) and the whole UAE process were 0.20 μg kg^{-1} and 0.67 μg kg^{-1} for As(III), and 0.41 μg kg^{-1} and 1.38 μg kg^{-1} for As(V). The assessed LODs are similar to those obtained by Vu *et al.* when using HPLC-ICP-MS with a dynamic reaction cell (oxygen as a reaction gas) to minimize interferences [8]. The values obtained are well below the EU regulation limits for iAs in rice, i.e., 200 μg kg^{-1} for white rice, 250 μg kg^{-1} for husked rice, 300 μg kg^{-1} for rice waffles, wafers, crackers and cakes, and 100 μg kg^{-1} for rice destined for the production of food for infants and young children [33]. The obtained LODs are also lower than maximum values proposed by the government of Canada (200 μg kg^{-1} and 300 μg kg^{-1} for polished and husked rice, respectively) [34], and by the U.S. Food and Drug Administration (FDA) (100 μg kg^{-1} of iAs in rice cereals for infants) [35].

3.3.4.3. Precision and accuracy

Inter-day and intraday assays were performed for assessing precision of the VA-D-μ-SPE and HPLC-ICP-MS procedure. Inter-day precision was evaluated after the analysis of rice extracts spiked with both iAs species at three concentration levels (0.1, 0.5 and 2.0 μg L^{-1}), and was expressed as the relative standard deviation (RSD) of seven spiking VA-D-μ-SPE experiments for each concentration tested. Similarly, intraday precision was performed by preparing seven standard addition calibrations through the VA-D-μ-SPE procedure in consecutive days, and by replicating three times each concentration level (0.1, 0.2, 0.5, 1.0 and 2.0 μg L^{-1}). RSD values are listed in Table 3. Good inter-day and intraday precision have been attained (RSDs lower than 11% for As(III) and lower than 7% for As(V)).

Inter-day and intraday analytical recovery were also obtained from the same experiments performed for inter-day and intraday precision assessment, and as shown in Table 3, analytical recoveries within the 89-103% range were obtained for all cases. Because RSDs values lower than 20% for inter-day/intraday precision assays, and analytical recoveries within the 80-120% range for inter-day/intraday analytical recovery assays were obtained, precision and analytical recovery of the proposed method is acceptable.

Table 3. Inter-day and intraday precision and analytical recovery

		As(III)		As(V)	
	Concentration (μg L^{-1})	Analytical recovery (%)	RSD (%)	Analytical recovery (%)	RSD (%)
Interday	0.1	89	11	103	7
	0.5	94	11	97	7
	2.0	93	10	96	7
Intraday	0.1	91	8	99	7
	0.2	99	9	98	5
	0.5	95	8	95	7
	1.0	99	4	97	6
	2.0	89	9	97	7

Accuracy was also evaluated by analysing a certified reference material ERM-BC211 with a certified value of iAs of 124±11 μg kg^{-1}. Three subsamples of ERM-BC211 were subjected to the optimised UAE, VA-D-μ-SPE and HPLC-ICP-MS procedure, and the found iAs concentration was 120±5 μg kg^{-1} (concentration calculated by summing the As(III) and As(V) concentrations, 107±5 and 13±1 μg kg^{-1}, respectively, and taking into account the propagation of error for assessing the standard deviation). Results show that there are no statistically significant differences between the certified and the experimental value ($P > 0.05$, t-test, 95% confidence level). As an example, Figure 1(c) shows a chromatogram for an extract obtained from the ERM-BC211. In addition, as listed in Table 4, total As concentration (252±2 μg kg^{-1}) is not statistically different ($P > 0.05$,

t-test, 95% confidence level) to the certified total As content in the CRM (260±13 μg kg^{-1}).

Despite the fact that ERM-BC211 is not certified for single As(III) and As(V) concentrations, the As(III) and As(V) concentrations found in the current research are in good agreement with those reported by Maher *et al.* (106 ±18 μg kg^{-1} of As(III) and 16 ±6 μg kg^{-1} of As(V)) after a microwave-assisted extraction with 2%(v/v) nitric acid and HPLC-ICP-MS analysis [13]. These authors confirmed the validity of their results using X-ray absorption near edge spectroscopy (XANES) [13]. However, our results are quite different from those reported by Vu *et al.* (< LOD for As(III) and 134.79 ±10.93 μg kg^{-1} for As(V)) [8]. The high concentration of As(V) found by these authors could possibly be due to the fast oxidation of As(III) to As(V) during the sample preparation and analysis steps [4, 36].

3.3.4.4. IIP reusability

Reusability of the IIP sorbent was tested by using three single IIP portions (50 mg each) which were used in successive days at the same time that inter-day and intraday assays were performed. In this experiment, rice extracts spiked with 1.0 μg L^{-1} As(III) were subjected to the proposed VA-D-μ-SPE procedure for over 10 days, implying 23 sorption-desorption cycles each. As shown in Figure S3 (ESI), analytical recoveries for As(III) were found to be within the 80-100% range during at least 20 sorption-desorption cycles. Therefore, the same IIP portion can be reused 20 times with quantitative results.

3.3.5. Application

The UAE-VA-D-μ-SPE procedure was used for the determination of As (III) and As (V) ions in three rice samples (Basmati, Jasmin, and wild rice). As(III), As(V), and iAs, and also total As concentrations (microwave assisted acid digestion and ICP-MS) are listed in Table 4. In general, As(III) concentrations were higher than As(V) levels in the three rice samples. The iAs concentrations ranged from 30±5 to 213±16 μg kg^{-1}, and are in agreement with the iAs concentrations found in the literature [4]. These results show that the iAs levels in

some of the studied commercial rice samples is quite close to the EU/EC regulated values (200 μg kg^{-1} for white rice, 250 μg kg^{-1} for husked rice [33]). Basmati rice surpasses the EU limit for rice destined for the production of food for infants and young children, and the recommended action level guidance by FDA (100 μg kg^{-1} of iAs) [35]. In addition, iAs level in wild rice is also close to the limit proposed by FDA.

Table 4. Concentration of total As, iAs, As(III) and As(V) in ERM-BC211 certified reference material and commercial rice samples

Rice type	Total As (μg kg^{-1})	iAs percentage (%)	As(III) (μg kg^{-1})	As(V) (μg kg^{-1})	iAs (μg kg^{-1})[a]
ERM-BC211[b]	252±2	48±2	107±5	13±1	120±5
Wild rice	92±11	101±15	76±17	17+3	93±17
Basmati rice	139±6	92±9	120±13	7±1[c]	127±13
Jasmin rice	51±2	59±10	30±11	< LOD[d]	30±11

(a) Concentration obtained as a sum of As(III) and As(V) concentrations; (b) Certified total As concentration of 260±13 μg kg^{-1}; (c) Concentration between the LOD and the LOQ of the method; (d) Lower than 2.2 μg kg^{-1}

3.4. CONCLUSIONS

The proposed VA-D-μ-SPE procedure based on IIPs as sorbents has demonstrated to offer excellent selectivity for both As(III) and As(V) ions. It can be implemented for the selective assessment (pre-concentration) of iAs without the need for pre-oxidation and/or pre-reduction steps to ensure a quantitative iAs pre-concentration/isolation. Although HPLC-ICP-MS was used as a hyphenated analytical technique for assessing As(III) and As(V) in the current research, the proposed selective pre-concentration method can be used as a previous step for selective and direct iAs quantification by atomic spectrometry techniques such as ICP-MS, inductively coupled plasma – optical emission spectrometry (ICP-OES), electrothermal atomization atomic spectrometry (ETAAS), and

hydride generation based atomic spectrometry techniques. VA-D-μ-SPE is a low cost procedure because it does not require sophisticated laboratory devices. In addition, IIP synthesis is not expensive and each 50 mg subsample can be reused at least 20 times. Regarding the proposed UAE procedure for isolating As species from rice, the selected conditions and extractants have proved to avoid As(III) oxidation during the sample pre-treatment (UAE) and pre-concentration step (VA-D-μ-SPE). Finally, the developed sample pre-treatment procedure and HPLC-ICP-MS provided quantitative iAs recoveries and showed good accuracy when analysing the ERM-BC211 certified reference material, and LOD/LOQ values lower than the maximum iAs levels established by several international regulations in rice and rice-based products.

3.5. ACKNOWLEDGEMENTS

The authors thank *Xunta de Galicia* for financial support (*Grupo de Referencia Competitiva* project number ED431C2018/19, and Program for the Development of the Strategic Grouping in Materials - AEMAT project number ED431E2018/08). These programs are co-funded by FEDER (UE).

Conflict of interest

The authors have declared no conflict of interest.

3.6. REFERENCES

[1] S. Hensawang, P. Chanpiwat, Health impact assessment of arsenic and cadmium intake via rice consumption in Bangkok, Thailand. Environ. Monit. Assess. 189 (2017) 599.

[2] P.B. Tchounwou, C.G. Yedjou, A.K. Patlolla, D.J. Sutton, Heavy metal toxicity and the environment, in: A. Luch (Ed.), Molecular, clinical and environmental toxicology, Experientia Supplementum, vol 101, Springer, Basel, (2012) 133-164.

[3] T.N. Maraseni, R.C. Deo, J. Qu, P. Gentle, P.R. Neupane, An international comparison of rice consumption behaviours and greenhouse gas emissions from rice production. J. Clean. Prod. 172 (2018) 2288-2300.

[4] M. Welna, A. Szymczycha-Madeja, P. Pohl, Comparison of strategies for sample preparation prior to spectrometric measurements for determination and speciation of arsenic in rice, Trends Anal. Chem. 65 (2015) 122-136.

[5] T. Narukawa, A. Hioki, K. Chiba. Speciation and monitoring test for inorganic arsenic in white rice flour, J. Agric. Food Chem. 60 (2012) 1122-1127.

[6] S.C. Sofuoglu, H. Güzelkaya, Ö. Akgül, P. Kavcar, F. Kurucaovalı, A. Sofuoglu, Speciated arsenic concentrations, exposure, and associated health risks for rice and bulgur, Food Chem.Toxicol. 64 (2014) 184-191.

[7] K. Baba, T. Arao, Y. Maejima, E. Watanabe, H. Eun, M. Ishizaka, Arsenic speciation in rice and soil containing related compounds of chemical warfare agents, Anal. Chem. 80 (2008) 5768-5775.

[8] H.A. Vu, M.H. Nguyen, H.A. Vu-Thi, Q. Do-Hong, X.H. Dang, T.N.B. Nguyen, H.Q. Trinh, T. L. Bich, T.T. Nguyen, D. Le-Van,

M.B. Tu, D.B. Chu, Speciation analysis of arsenic compounds by high-performance liquid chromatography in combination with inductively coupled plasma dynamic reaction cell quadrupole mass spectrometry: application for Vietnamese rice samples, J. Anal. Meth. Chem., (2019) 5924942.

[9] E. Yilmaz, Use of hydrolytic enzymes as green and effective extraction agents for ultrasound assisted-enzyme based hydrolytic water phase microextraction of arsenic in food samples, Talanta. 189 (2018) 302-307.

[10] E. Sanz, R. Muñoz-Olivas, C. Cámara, A rapid and novel alternative to conventional sample treatment for arsenic speciation in rice using enzymatic ultrasonic probe, Anal. Chim. Acta. 535 (2005) 227-235.

[11] T. Narukawa, K. Inagaki, T. Kuroiwa, K. Chiba, The extraction and speciation of arsenic in rice flour by HPLC–ICP-MS, Talanta 77 (2008) 427–432.

[12] G. Raber, N. Stock, P. Hanel, M. Murko, J. Navratilova, K.A. Francesconi, An improved HPLC–ICPMS method for determining inorganic arsenic in food: Application to rice, wheat and tuna fish, Food Chem. 134 (2012) 524-532.

[13] W. Maher, S. Foster, F. Krikowa, Measurement of inorganic arsenic species in rice after nitric acid extraction by HPLC-ICPMS: verification using XANES, Environ. Sci. Technol. 47 (2013) 5821−5827.

[14] M. Anastassiades, S.J. Lehotay, D. Štajnbaher, F.J. Schenck, Fast and easy multiresidue method employing acetonitrile extraction/partitioning and “dispersive solid-phase extraction” for the determination of pesticide residues in produce, J. AOAC Int. 86 (2003) 412-431.

[15] A. Chisvert, S. Cárdenas, R. Lucena, Dispersive micro-solid phase extraction, Trends Anal. Chem. 112 (2019) 226-233.

[16] T. Khezeli, A.Daneshfar, Development of dispersive micro-solid phase extraction based on micro and nano sorbents, Trends Anal.Chem.89 (2017) 99-118.

[17] M. Ghorbani, M. Aghamohammadhassan, M. Chamsaz, H. Akhlaghi, T. Pedramrad, (2019). Dispersive solid phase microextraction, Trends Anal. Chem. 118 (2019) 793-809.

[18] M. Rutkowska, K. Owczarek, M. Guardia, J. Płotka-Wasylka, J. Namieśnik, Application of additional factors supporting the microextraction process, Trends Anal. Chem. 97 (2017) 104-119.

[19] M. Llaver, R.G. Wuilloud, Separation and preconcentration of inorganic Se species in tap and natural waters using unfunctionalized nanosilica as sorption material in dispersive micro-solid phase extraction, Microchem. J.146 (2019) 763–770.

[20] M. Llaver, E.A. Coronado, R.G. Wuilloud, High performance preconcentration of inorganic Se species by dispersive micro-solid phase extraction with a nanosilica-ionic liquid hybrid material, Spectrochim. Acta Part B 138 (2017) 23–30.

[21] A.C. Grijalba, L.B. Escudero, R.G. Wuilloud, Ionic liquid-assisted multiwalled carbon nanotube-dispersive micro-solid phase extraction for sensitive determination of inorganic As species in garlic samples by electrothermal atomic absorption spectrometry, Spectrochim. Acta Part B 110 (2015) 118–123.

[22] X. Cheng, H.Yan, X. Wang, N. Sun, X. Qiao, Vortex-assisted magnetic dispersive solid-phase microextraction for rapid screening and recognition of dicofol residues in tea products, Food Chem. 162 (2014) 104–109.

[23] R. Mirzajani, A. Keshavarz, The core–shell nanosized magnetic molecularly imprinted polymers for selective preconcentration and determination of ciprofloxacin in human fluid samples using a vortex-assisted dispersive micro-solid-phase extraction and high-performance liquid chromatography. J. Iran. Chem. Soc. 16 (2019), 2291-2306.

[24] M.P. Chantada-Vázquez, J. Sánchez-González, E. Peña-Vázquez, M.J. Tabernero, A.M. Bermejo, P. Bermejo-Barrera, A. Moreda-Piñeiro, Synthesis and characterization of novel molecularly imprinted polymer – coated Mn-doped ZnS quantum dots for specific fluorescent recognition of cocaine, Biosens. Bioelectron. 75 (2016) 213-221.

[25] K.K. Jinadasa, E. Peña-Vázquez, P. Bermejo-Barrera, A. Moreda-Piñeiro, Ionic imprinted polymer solid-phase extraction for inorganic arsenic selective pre-concentration in fishery products before high-performance liquid chromatography –inductively coupled plasma-mass spectrometry speciation, J. Chromatogr. A (2020). doi.org/10.1016/j.chroma.2020.460973 (in the press).

[26] Y.K. Tsoi, Y.M. Ho, K.S.Y. Leung, Selective recognition of arsenic by tailoring ion-imprinted polymer for ICP-MS quantification, Talanta, 89 (2012) 162-168.

[27] A. Moreda-Piñeiro , E. Peña-Vázquez , P. Hermelo-Herbello , P. Bermejo-Barrera , J. Moreda-Piñeiro , E. Alonso-Rodríguez , S. Muniategui-Lorenzo , P. López-Mahía, D. Prada-Rodríguez , Matrix solid-phase dispersion as a sample pretreatment for the speciation of arsenic in seafood products, Anal. Chem. 80 (2008) 9272–9278.

[28] P.L. Smedley, D.G. Kinniburgh, A review of the source, behaviour and distribution of arsenic in natural waters. Appl. Geochem. 17 (2002) 517–568.

[29] C. Basheer, J. Lee, S. Pedersen-Bjergaard, K.E. Rasmussen, H.K. Lee, Simultaneous extraction of acidic and basic drugs at neutral sample pH: A novel electro-mediated microextraction approach, J. Chromatogr. A 1217 (2010) 6661–6667.

[30] J. Sánchez-González, S. García-Carballal, P. Cabarcos, M.J. Tabernero, P. Bermejo-Barrera, A. Moreda-Piñeiro, Determination of cocaine and its metabolites in plasma by porous membrane-protected molecularly imprinted polymer micro-solid-phase extraction and liquid chromatography—tandem mass spectrometry, J. Chromatogr. A 1451 (2016) 15–22.

[31] J. Sánchez-González, S. Odoardi, A.M. Bermejo, P. Bermejo-Barrera, F.S. Romolo, A. Moreda-Piñeiro, S. Strano-Rossi, Development of a micro-solid-phase extraction molecularly imprinted polymer technique for synthetic cannabinoids assessment in urine followed by liquid chromatography–tandem mass spectrometry, J. Chromatogr. A 1550 (2018) 8–20.

[32] I. Pizarro, M. Gómez, C. Cámara, M.A. Palacios, Arsenic speciation in environmental and biological samples: Extraction and stability studies, Anal. Chim. Acta, 495 (2003) 85-98.

[33] EU/EC, Commission Regulation (EU) 2015/1006 of 25 June 2015 amending Regulation (EC) No 1881/2006 as regards maximum levels of inorganic arsenic in foodstuffs, Off. J. European Union, L161 (2015) 14-16.

[34] Government of Canada, Health Canada's proposal to add maximum levels for inorganic arsenic in polished (white) and husked (brown) rice to the List of contaminants and other adulterating substances in foods, https://www.canada.ca/en/health-canada/services/food-nutrition/public-involvement-partnerships/proposal-add-maximum-levels-inorganic-arsenic-white-

and-brown-rice-list-of-contaminants-other-adulterating-substances/document.html, Accessed: 17/01/2020.

[35] Food and Drug Administration (FDA), Draft guidance for industry: Action level for inorganic arsenic in rice cereals for infants, https://www.fda.gov/regulatory-information/search-fda-guidance-documents/draft-guidance-industry-action-level-inorganic-arsenic-rice-cereals-infants, Accessed: 17/01/2020.

[36] U. Araujo-Barbosa, E. Peña-Vazquez, M.C. Barciela-Alonso, S.L. Costa Ferreira, A.M. Pinto dos Santos, P. Bermejo-Barrera, Simultaneous determination and speciation analysis of arsenic and chromium in iron supplements used for iron-deficiency anemia treatment by HPLC-ICP-MS, Talanta 170 (2017) 523-529.

3.7. ELECTRONIC SUPPLEMENTARY INFORMATION (ESI)

ICP-MS measurements

Total As in acid digests from fish, as well as other trace elements such as Ca, Cd, Co, Cr, Cu, Fe, Hg, K, Mg, Na, P, Pb, and Zn in cross-reactivity studies, were determined by ICP–MS under operating conditions given in Table S1. Total As determination implied 1:10 dilution of acid digests with ultrapure water, the use of ^{74}Ge (10 µg L^{-1}) as an internal standard, and kinetic energy discrimination (KED) by using He (4.0 mL min^{-1}) as a collision gas for selectively polyatomic interferences attenuation. Nitric acid (1.0% (v/v)) matched calibration within the 0-100 µg L^{-1} range was performed for assessing total As contents. The determination of other elements (cross-reactivity studies, Table S1) was carried out using ^{54}Sc (10 µg L^{-1}) as an internal standard for Ca, K, Mg, Na, and P under standard conditions, and ^{74}Ge (10 µg L^{-1}) as an internal standard for Cu (standard conditions) and for Co, Cr, Fe and Zn (KED mode, He 4.0 mL min^{-1}). Finally, ^{103}Rh (10 µg L^{-1}) was used as an internal standard for Cd, Hg and Pb determinations (standard conditions measurements). Determinations were performed using 1.0% (v/v) nitric acid matched calibration within the 0-100 µg L^{-1} range for all elements.

Table S1. Operating ICP-MS conditions for total As determination in acid digests from fish samples, and for P, K, Ca, Mg, Na, Zn, Co, Fe, Cr, Pb, Hg, Cd, and Cu determination in cross reactivity studies.

Operating ICP-MS conditions		
Radiofrequency power		1600 W
Gas flows	Nebulization	0.92 mL min^{-1}
	Auxiliary	1.2 mL min^{-1}
	Plasma	16 mL min^{-1}
Standard mode		Ca, Cu, K, Mg, Na, P
KED mode: He flow rate/ 4.0 mL min^{-1}		As, Cd, Co, Cr, Fe, Hg, Pb, Zn
Analytes		^{75}As, ^{43}Ca, ^{111}Cd, ^{59}Co, ^{53}Cr, ^{63}Cu, ^{57}Fe, ^{39}K, ^{202}Hg, ^{26}Mg, ^{23}Na, ^{31}P, ^{208}Pb, ^{66}Zn
Internal standards		^{74}Ge (As, Co, Cr, Fe, and Zn) ^{54}Sc (Ca, K, Mg, Na, and P) ^{103}Rh (Cd, Hg, and Pb)

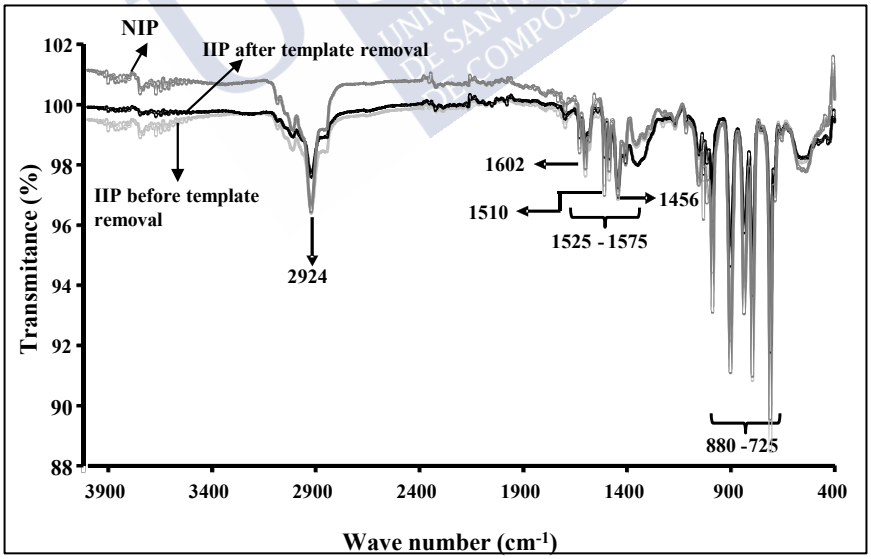

Figure S1. FT-IR spectra of IIP (before and after template removal) and NIP

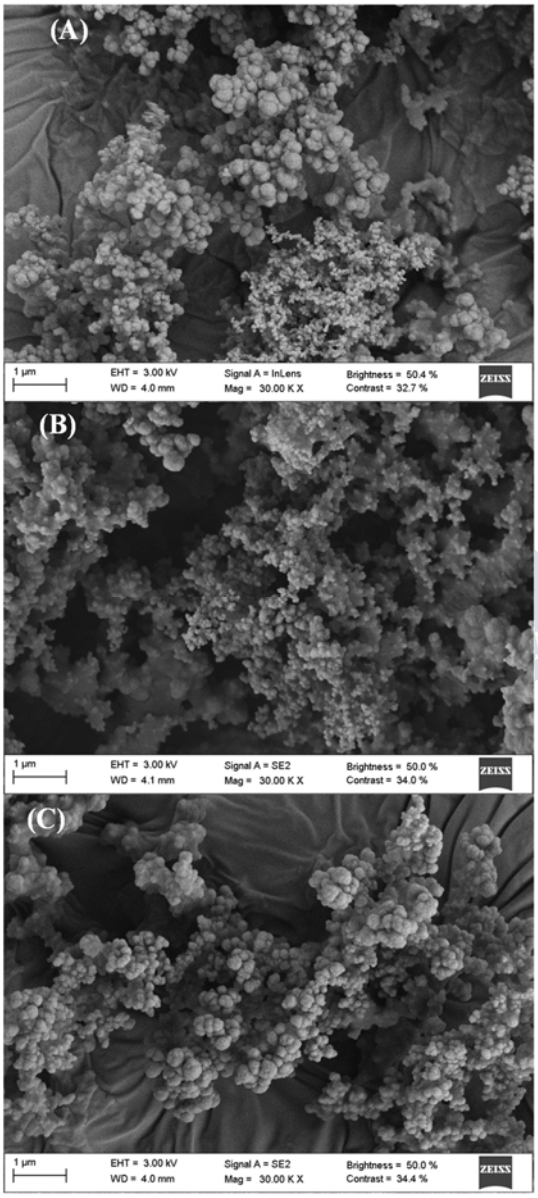

Figure S2. (A) SEM images of synthesized IIP (B) synthesized IIP after template removal (C), and NIP

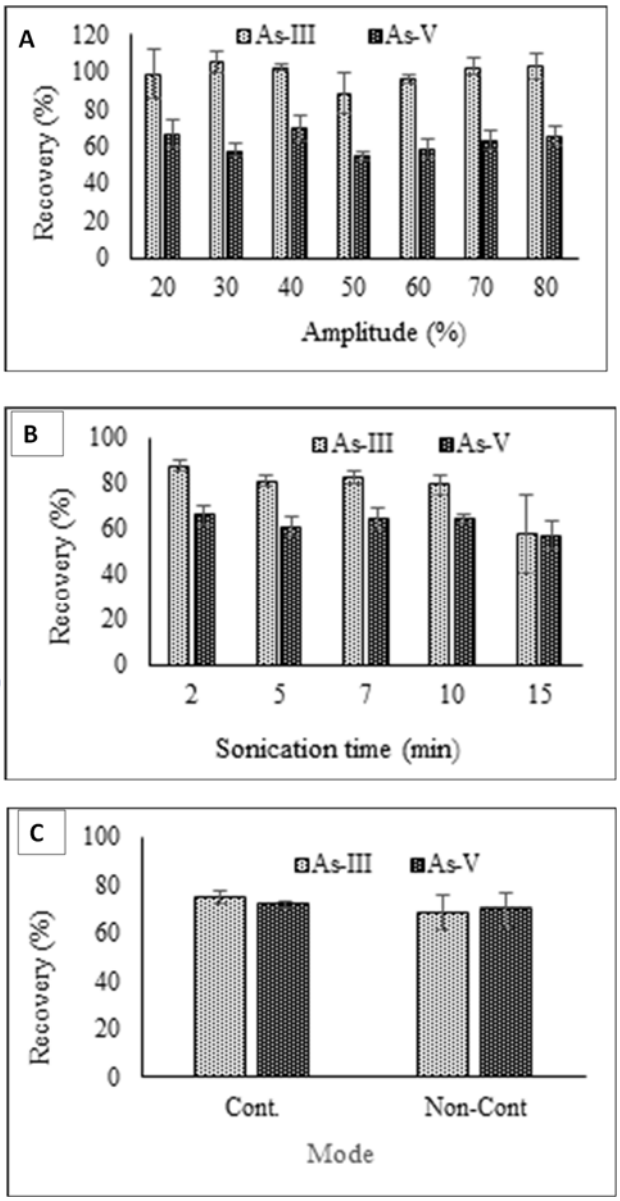

Figure S3. (A) Optimization of percentage of amplitude, (B) Sonication time, (C) Sonication mode

USC
UNIVERSIDADE
DE SANTIAGO
DE COMPOSTELA

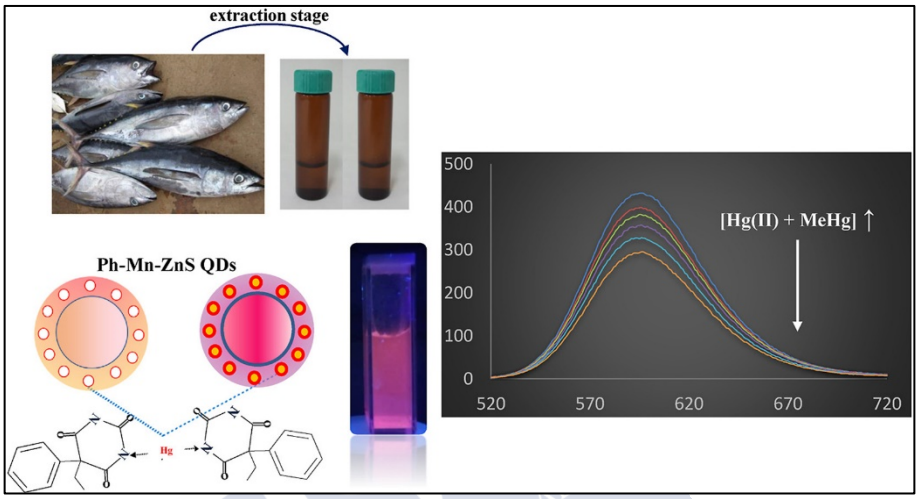

CHAPTER 4

A PHENOBARBITAL CONTAINING POLYMER/ SILICA COATED QUANTUM DOT COMPOSITE FOR THE SELECTIVE RECOGNITION OF MERCURY SPECIES IN FISH SAMPLES USING A ROOM TEMPERATURE PHOSPHORESCENCE QUENCHING ASSAY

KAMAL K. JINADASA, ELENA PEÑA-VÁZQUEZ, PILAR BERMEJO-BARRERA, ANTONIO MOREDA-PIÑEIRO

TALANTA 216 (2020) 120959

https://doi.org/10.1016/j.talanta.2020.120959

USC
UNIVERSIDADE
DE SANTIAGO
DE COMPOSTELA

A phenobarbital containing polymer/ silica coated quantum dot composite for the selective recognition of mercury species in fish samples using a room temperature phosphorescence quenching assay

Kamal K. Jinadasa, Elena Peña-Vázquez, Pilar Bermejo-Barrera, Antonio Moreda-Piñeiro

Trace Element, Spectroscopy and Speciation Group (GETEE), Strategic Grouping in Materials (AEMAT), Department of Analytical Chemistry, Nutrition and Bromatology, Faculty of Chemistry, Universidade de Santiago de Compostela. Avenida das Ciencias, s/n. 15782, Santiago de Compostela, Spain

Abstract

An analytical procedure using low-cost instrumentation (fluorescence/phosphorescence spectrophotometer) has been developed to assess total mercury in fishery products. Determinations were based on the room temperature phosphorescence (RTP) quenching of a composite Ph-QDs consisting of phenobarbital-containing polymer/silica coated Mn-doped ZnS quantum dots. Under optimum conditions (fish extract pH of 8.0, Ph-QDs concentration of 20 mg L^{-1}, and an interaction time of 12 min), the material offers high selectivity for inorganic mercury and methyl-mercury over other common ions present in the fish matrix. Moreover, good linearity was obtained for mercury concentrations within the 0-100 µg L^{-1} range, and the obtained limit of detection (68.2 µg kg^{-1}) is low enough for a reliable assessment of total mercury in fish and seafood samples. The developed method was found to be free of matrix effects, and offers the advantage that the fish extracts can be directly analysed even at a 1:10 dilution. The method was found to be accurate after analysing a fish certified reference material, and after comparing total mercury levels in a set of fish samples analysed by the proposed chemosensor probe and by inductively coupled plasma mass spectrometry after an acid decomposition sample pre-treatment.

Keywords: Mercury, fish, room temperature phosphorescence, phenobarbital, quantum dots

4.1. INTRODUCTION

The increase of the presence of heavy metals, especially mercury (Hg), due to natural (weathering of rocks, degassing of the earth's crust and volcanism) and anthropogenic (coal combustion, mining industry and by-products, agriculture fertilizers, and waste incineration) activities is becoming one of the most serious problems in the world [1-3]. According to the World Health Organization (WHO), Hg is "one of the top ten chemicals or groups of chemicals of major public health concern" [4]. Moreover, the Government Agency for Toxic Substances and Disease Registry (ATSDR) of the United States ranked Hg as third on their substances priority list in 2017 [5]. After the release of Hg into the environment, it becomes a part of the biogeochemical cycle, with transformation of the species and transpositions between the atmosphere, soil and aquatic ecosystems [6,7]. In the atmosphere, elemental Hg (Hg^0) is the most common species, and it can travel long distances before being deposited far from its original source [8]. The deposited inorganic Hg can be transformed by anaerobic bacteria, mainly forming methyl mercury (MeHg) or dimethyl mercury (Me_2Hg) in the aquatic environment. MeHg can be readily bioaccumulated in aquatic biota and even biomagnified in higher trophic levels of the aquatic food chain; hence, fish and seafood are one of the main pathways of Hg exposure for humans [9,10].

Mercury concern in the environment and human health has led to the development of several strategies for mercury species isolation and the assessment of total mercury as well as mercury species (speciation studies). Critical reviews regarding sample pre-treatment methods [11,12] and analytical techniques, mainly high performance liquid chromatography (HPLC) hyphenated with inductively coupled plasma – mass spectrometry (ICP-MS), for mercury species assessment [12,13] can be found in recent literature. Although these methods are highly sensitive, they have a number of disadvantages, such as the fact that most of them require sophisticated and high-cost

instrumentation as well as staff with technical expertise. The development of fast and low cost analytical methodologies is therefore desired not only for screening purposes but also for reliable quantification of mercury species in complex matrices.

Nanoparticles (NPs), mainly quantum dots (QDs), have received much attention because of their potential for bio-imaging and sensor development [14,15]. The unique photo-physical and photochemical properties of QDs, such as high luminescence quantum yields, size-dependent narrow emission bands, stability against photo-bleaching, and high selectivity and sensitivity [16,17], are responsible for the great QDs' capabilities for sensor probe development. Sensing is based on the changes in QD luminescence after analyte-QDs' surface interactions. QDs' fluorescence has been commonly used in many applications, but room temperature phosphorescence (RTP) has recently been reported to offer better performances than fluorescence due to its reliability, longer lifetime, and absence of auto-fluorescence and scattered light [18,19]. Selectivity of luminescent-based QD methods can be achieved by coating the QDs' surface with a reagent with selective properties through the target (analyte), and the use of molecularly imprinted polymers (MIPs) to enhance selectivity. This is an appealing approach for preparing the so-called molecularly imprinted optosensing materials (MIOM) [20].

There are some reported QD-based fluorescence chemosensors for mercury (mainly inorganic mercury) detection/quantification which use carbon dots (CDs) [21], surface modified CDs with poly(ethylene glycol) (PEG-CDs) [22], and carbon nitride quantum dots (CNQDs) or nitrogen doped CDs (N-CDs) [23,24], the latter synthesized using a nitrogen containing reagent together with the carbon source. A CNQDs chemosensor based on the chemiluminescence of the CNQDs-potassium ferricyanide system has also been reported for inorganic mercury detection since mercury ions form a stable non-luminescent CNQD-Hg(II) complex and diminish the chemiluminescence CNQDs-potassium ferricyanide reaction [25]. Other QDs-based chemosensors for mercury detection consist of CdTe [26], CdTe@CdS QDs [27], ZnS QDs [28], Mn doped ZnSe/ZnS QDs [29], Mn-doped ZnS QDs [30], and QDs derived from fluorescent

semiconducting polymers (pQDs) such as poly(3,4-ethylenedioxythiophene) (PEDOT) [31]. Selectivity of the prepared QD probes can be poor, and luminescence quenching can be attributed to the present of several ions such as those reported for chitosan-stabilized ZnS QDs [28]. Selectivity improvements can be attained by attaching certain ligands to the QDs' surface, ligands which offer specificity for a certain ion. Therefore, mercaptopropionic acid (MPA) capped Mn-doped ZnSe/ZnS QDs [29], thioglycolic acid (TGA)-capped Cd-Te QDs [26], and L-cysteine-capped Mn-doped ZnS QDs [30] have been found to be quite selective for the fluorescence detection of Hg(II) in water. However, TGA-capped CdTe QDs were further coated by denatured bovine serum albumin (dBSA) to avoid quenching by other ions such as Cu(II) and Ag(I) [26].

On other occasions, Fe_3O_4@SiO_2/dendrimers/Cd-Te-QD systems have been proposed for developing an ultrasensitive electrochemiluminescence (ECL) aptasensing assay for selective detection of Hg(II) [27]. Biological materials such as fish and seafood have been successfully analysed by applying some of the proposed chemosensor probes after convenient extraction procedures [22] for determining MeHg, or after acid decomposition of the sample for detecting inorganic mercury [21,25,27].

All developed QD probes have been proved to be more or less selective for one mercury species (mainly Hg(II)), but the simultaneous recognition/detection of both inorganic (Hg(II)) and organic (MeHg) mercury species has not been yet addressed. One of the objectives of this research is the combination of the RTP response of Mn-doped ZnS QDs with the selectivity provided by a polymer that includes a non-vinylated ligand (phenobarbital) that has shown to give an strong affinity for inorganic (Hg(II)) and organic (MeHg and ethyl-mercury, EtHg) mercury species [32]. The prepared phenobarbital containing polymer/silica coated Mn-doped ZnS quantum dot composite (Ph-QDs) has been found to be quite selective for both Hg(II) and MeHg, providing a reliable RTP quantification of total mercury in fishery products.

4.2. MATERIAL AND METHODS

4.2.1. Reagents

Zinc sulfate heptahydrate [$ZnSO_4.7H_2O$] was from Panreac (Barcelona, Spain); whereas, manganese dichloride [$MnCl_2$], and N,N-dimethylformamide (DMF) [$HCON(CH_3)_2$] were purchased from Merck (Darmstadt, Germany). Sodium sulfide hydrate [$Na_2S.xH_2O$], 2,2′-azobis(2-methyl propionitrile) (AIBN) [$C_8H_{12}N_4$], (3-aminopropyl)-triethoxysilane (APTES) [$H_2N(CH_2)_3Si(OC_2H_5)_3$], tetraethyl orthosilicate (TEOS) [$Si(OC_2H_5)_4$], methacrylic acid [$H_2C=C(CH_3)COOH$], phenobarbital sodium salt [$C_{12}H_{11}N_2NaO_3$], and methylmercury chloride (CH_3ClHg) were from Sigma Aldrich (St. Louis, MO, USA). Element standard solutions (Hg measurements and cross-reactivity studies) were prepared by using single element standards of Hg, Cr, K, Na, K, P, Pb and Zn (stock standard solutions of 1000 mg L^{-1}) from Scharlab (Barcelona, Spain), Cd, Cu, Fe and Na (stock standard solutions of 1000 mg L^{-1}) from Perkin Elmer (Shelton, CT, USA), Ca, Co and Mg (stock standard solutions of 1000 mg L^{-1}) from Merck, and As(III) and As(V) stock solutions (stock standard solutions of 1000 mg L^{-1}) from Panreac). Arsenobetaine (AsB) stock solution (1000 mg L^{-1}) was prepared by dissolving appropriate amounts of $AsC_5H_{11}O_2$ from Tri Chemical Laboratory Inc. (Yamanashi, Japan). Other chemicals such as nitric acid (Hyperpur, 69 %), and 33% hydrogen peroxide were supplied by Panreac. NexIon Setup Solution (10 µg L^{-1} of Be, Ce, Fe, In, Li, Mg, Pb, and U in 1 % HNO_3) was purchased from Perkin Elmer. The BCR-463, tuna fish certified reference material (CRM), was from the European Commission Joint Research Centre, Institute for Reference Materials and Measurements (Geel, Belgium).

All chemical and reagents were of analytical grade or better and used as purchased, except for 2,2'-azobisisobutyronitrile (AIBN) which was purified by crystallization at -20 °C after dissolving the reagent in methanol at 50-60 °C. All aqueous solutions were prepared with ultrapure water with a resistivity of 18.2 MΩ/cm obtained from a Milli Q-A10 device (Millipore Co., Bedford, MA, USA).

4.2.2. Instrumentation

RTP measurements were carried out using a Cary Eclipse fluorescence spectrophotometer (Varian, Victoria, Australia) equipped with a xenon flash lamp as an excitation light source and 1 cm standard quartz cells. Phenobarbital coated QD composites were characterized by transmission electron microscopy – energy-dispersive spectroscopy (TEM-EDS) using a JEM-2010F (JEOL, Tokyo, Japan) equipped with an IncaEnergy TEM detector (Oxford Instruments, High Wycombe, United Kingdom), by X-ray diffraction spectrometry (XRD) using an EMPYREAM instrument from PaNalytical (Almelo, Netherlands), and by Fourier transform infrared spectrometry (FTIR) using a Spectrum-Two FT-IR spectrometer (Perkin Elmer, Waltham, MA, USA) operating at the attenuated total reflectance (ATR) mode. Total Hg level was measured by using a Perkin Elmer NexIon 300X ICP–MS equipped with SeaFast SC2 DX autosampler (Elemental Scientific, Omaha, NB, USA). An Ethos Plus microwave accelerated system (Milestone, Sorisole, Italy) equipped with 100-mL closed Teflon vessels was used for sample preparation previous to the measurement of total Hg concentration. The pH measurements were taken on a XS-pH50+DHS pH meter (Labbox, Barcelona, Spain). Other equipment included a USC60TH ultrasonic cleaner bath (45 kHz, 120 W) from VWR (Leuven, Belgium), an ultracentrifuge (Sigma 2K15, Osterode, Germany), a domestic Taurus blade grinder (Taurus, Barcelona, Spain), and an analytical balance (Mettler Toledo, Columbus, OH, USA).

4.2.3. Ph-QDs synthesis

Mn-doped ZnS QDs were encapsulated using APTES and TEOS and modified with a polymer containing phenobarbital. All synthesis steps were performed at room temperature as follows:

(1) 12.5 mmol of $ZnSO_4$, 1 mmol of $MnCl_2$ and 40 mL of ultrapure water were introduced into a three-necked flask, under ultrasonication and a nitrogen stream. After 10 min, a volume of 10 mL of 1.25 mmol Na_2S solution was added dropwise using an addition funnel, and the mixture was ultrasonicated (37 kHz, 325 W) for 30 min [33]. Afterward, 2 mL of TEOS and 2.5 mL APTES were added, and the

mixture was ultrasonicated for 4.5 h under an N_2 stream. The resulting silica coated Mn-doped ZnS QDs [Figure 1(A, B)] were centrifuged at 3000 rpm for 20 min. Centrifugation was repeated 3 times, and the material was rinsed with 5 mL of ethanol between each step. Finally, nanoparticles were dried in a desiccator and stored at 4 °C.

(2) A pre-polymerization mixture was prepared by dissolving 0.3 mmol of phenobarbital and 0.75 mmol of MMA in 4 mL of DMF, and sparged with N_2.

(3) A mass of 0.5 g of the previously prepared silica coated QDs were introduced in a conical flask and mixed with the pre-polymerization mixture (step 2), 25 mL of ultrapure water, 4.5 mL of EDMA and 50 mg of AIBN [Figure 1(C)]. The mixture was ultrasonicated (37 kHz, 325 W, 4 h) to favour EDMA and AIBN transfer to the pre-polymerization mixture (DMF containing MMA and phenobarbital) and to allow dispersion of the pre-polymerization mixture droplets in water and over the dispersed QDs. Afterwards the composite was centrifuged (3000 rpm, 20 min), washed with ethanol, dried and stored as explained in step 1. Phenobarbital trapped into the polymeric matrix ensures specificity towards mercury by interaction through the N functionalities [Figure 1(D)].

The prepared powder Ph-QD composites were stored in amber glass bottles at 4°C. Similarly, Ph-QD suspensions prepared in 0.1M KH_2PO_4 (pH 8) were also kept in amber glass bottles at 4°C.

4.2.4. Analysis of fish samples

Fish species such as yellowfin tuna (*Thunnus albacares*), swordfish (*Xiphias gladius*), bluefin tuna (*Thunnus thynnus*), and blue shark (*Prionace glauca*) were purchased from local fish markets. Fish entrails were removed, and the fish flesh was separated from the bones and skin. Isolated flesh was homogenized, and each sample (wet weight ranging from 0.2 to 1.0 kg) was stored in polyethylene vials with hermetic seals at –20 °C before analysis.

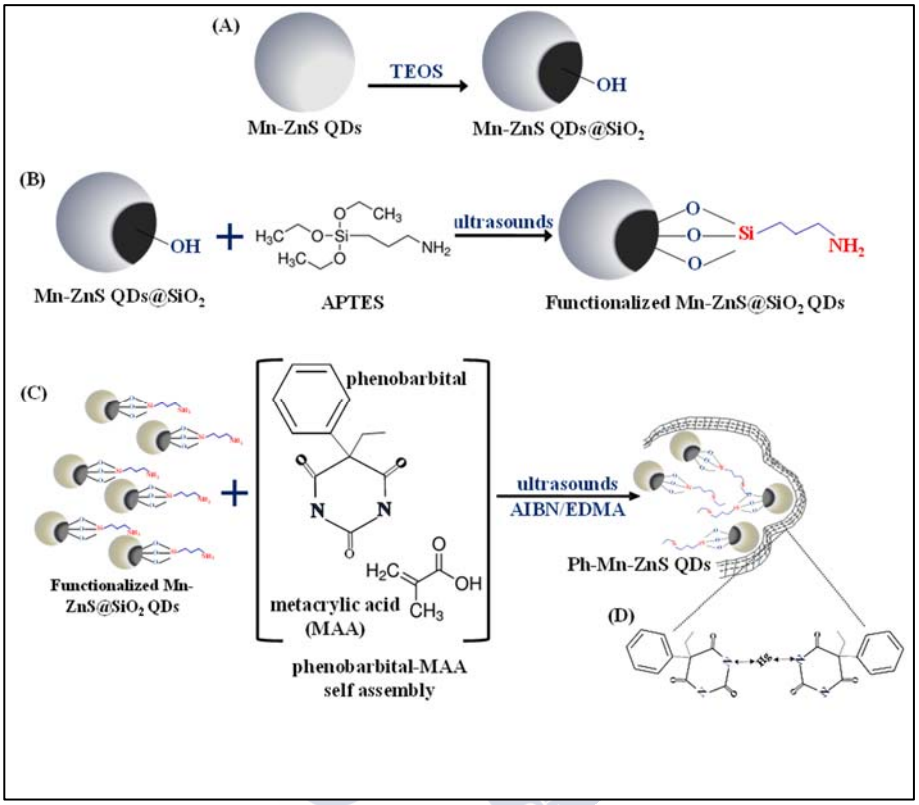

Figure 1. Schematic procedure for the synthesis of Mn-ZnS@SiO_2 QDs (A, B), Ph-Mn-ZnS@SiO_2 QDs (C), and Hg (II)-Ph-Mn-ZnS@SiO_2 QDs interaction (D)

4.2.4.1. Ultrasound assisted acid extraction

Total mercury extraction (inorganic mercury and methyl-mercury) from wet fish tissues was performed according to [34] with some modifications for RTP measurement. Briefly, 1.0 g of wet fish flesh (or 0.3 g of CRM) was weighted into a screw-capped vial and 5 mL of 5.0 M HCl were added. Mixtures were then ultrasonicated (ultrasound water bath, 45 kHz, 120 W, 5 min), and the extracts were separated by centrifugation (3500 rpm, room temperature, 10 min). Finally, extract pH was adjusted to 8.0 by adding small volumes of 12.5% (v/v) ammonium hydroxide. The fish extract was finally made up to 25 mL with ultrapure water. Each sample was subjected to the

extractive procedure in triplicate, and at least two blanks were prepared in each ultrasound assisted acid extraction set.

4.2.4.2. Microwave assisted acid digestion

A reference sample pre-treatment method based on microwave assisted acid digestion in combination with ICP-MS was used for comparative purposes. Briefly, 1.0 g of wet homogenized fish (or 0.3 g of CRM), was weighted in Teflon reactors, and pre-digested with 4.0 mL of 69 % (v/v) HNO_3, 2.0 mL of ultrapure water, and 2.0 mL of H_2O_2 for 15 min at room temperature. The reactors were subjected to microwave energy by increasing the temperature from room temperature to 200 °C for 13.5 min, followed by a treatment at this temperature for 10 min [35]. The digests were made up to 25 mL with ultrapure water and stored in polyethylene bottles at room temperature. Three acid digests were prepared from each sample, and at least two blanks were prepared for each microwave assisted acid digestion set.

4.2.4.3. RTP measurements

RTP measurements were carried out at room temperature (20-25 °C). The excitation wavelength was set at 289 nm, and emission was scanned between 520 and 720 nm. The excitation and emission slits were set as 10 and 20 nm, respectively. Other optimized parameters were: total decay time 0.003 s, number of flashes 1, delay time 0.1 ms, gate time 2.0 ms, and a photomultiplier tube (PMT) voltage operating at medium mode.

All measurements were based on peak area and were carried out using a constant volume of 1.5 mL of 20 mg L^{-1} Ph-QDs dispersion (0.1M KH_2PO_4, pH 8.0, as a solvent). Ph-QDs dispersion was mixed with 200 µL of fish extract and 300 µL of buffer (0.1M KH_2PO_4, pH 8), which implies a 1:10 sample dilution. RTP measurement was performed after an interaction time of 12 min. Total Hg assessment was based on the changes produced in the phosphorescence intensity (quenching effect) when inorganic mercury and methylmercury are present.

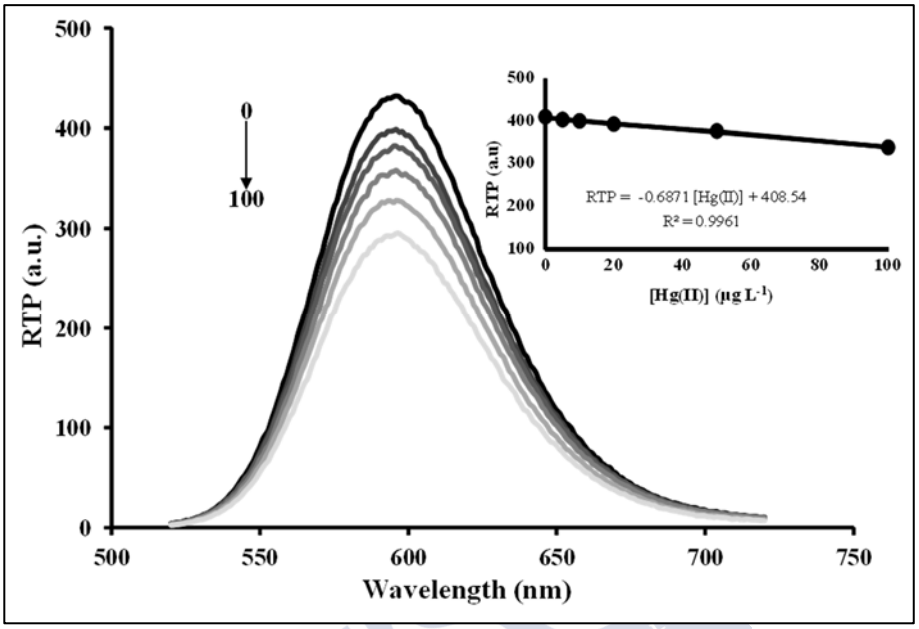

Figure 2. RTP quenching in presence of increasing concentrations of Hg (II)

The absence of matrix effect allowed a buffered calibration (0.1M KH_2PO_4, pH 8.0) using 20 mg L^{-1} of Ph-QDs and varying the Hg^{2+} concentration within the 0-100 µg L^{-1}. Figure 2 shows the overlaid phosphorescence spectra when increasing Hg (II) concentrations.

Finally, Ph-QDs were of single used, and nanocomposites contained in each 1.5 mL of the 20 mg L^{-1} Ph-QDs dispersion were discharged after the RTP measurement.

4.2.4.4. ICP-MS measurements

ICP-MS parameters (nebulization gas flow, torch position, optical lens, and quadrupole voltages) were adjusted to achieve high sensitivity and accuracy. The m/z ratio monitored was ^{202}Hg (Table S1, Electronic Supplementary Information, ESI), and rhodium (m/z ratio of ^{103}Rh, and at 5.0 µg L^{-1}) was used as an internal standard. Measurements were performed in kinetic energy discrimination (KED) mode using He as a collision gas at a flow rate of 1.0 mL min^{-1}. Acid digests from fish were 1:25 diluted with ultrapure water before ICP-MS

measurement by using the standard addition technique (0-10 μg L^{-1} range) to make up for matrix effects.

4.3. RESULTS AND DISCUSSION

4.3.1. Ph-QDs characterization

The morphological TEM characterization of Ph-QDs shows agglomerated spheres covered with the Ph-based polymer (Figure 3A). EDS analysis (Figure 3B) reveals the presence of Zn, S, and Mn (core of the composite), and Si, thus confirming an efficient Si coating over the metallic nanoparticles.

The crystalline structure of the prepared nanocomposites was studied by XRD. Figure 3C shows the X-ray diffraction pattern of QDs (silica-Mn ZnS QDs) and Ph-QDs which consist of broad diffraction β-ZnS peaks at 2θ values of 28.74°, 47.7° and 56.5°, and indicate a cubic structure with peaks assigned to 111, 220 and 311. Results agree with those previously reported for $Zn_{1-x}Mn_xS$ QDs [36] and give mean crystallite sizes of 19.2±2.3 Å (1.9±0.2 nm) for silica-Mn ZnS QDs, and 20.2±5.1 Å (2.0±0.5 nm) for Ph-QD.

The FTIR spectrum of the silica coated QDs and the Ph-QDs composite (Figure 3D) show the characteristic peak at 610 cm^{-1}, which can be assigned to the ZnS band [37], and bands within the 1000-1150 cm^{-1} range which are attributed to the asymmetric and symmetric stretching vibration of Si-O-Si. These findings bear out the presence of a ZnS core and an effective Si coating. In addition, the increase of the bands at 2926 cm^{-1} ($-CH_2$) and 1412 cm^{-1} (-CO) observed in the Ph-QD composite indicate that the phenobarbital containing polymer has been capped to the surface of the silica coated QDs.

The phosphorescence spectrum of the synthesized Ph-QDs is shown in Figure 2. The emission spectrum exhibits a symmetric peak with a maximum at 597 nm, observed when Ph-QDs are excited at 289 nm. The emission spectrum is assigned to the transition of Mn^{2+} from the triplet state to the ground state [15, 38]. Therefore, throughout the study, the excitation wavelength of 289 nm was used, with 10 and 20 nm as excitation and emission slits.

The luminescence and recognition capacities of the synthesized Ph-QD prepared in two different days (two different Ph-QD batches)

were found to be similar. The material from both batches was used interchangeably for approximately ten months, finding repeatable results. The storage of the powdered Ph-QD composite and Ph-QD suspensions (amber glass bottles, 4°C) guarantees stability of the material and RTP reproducibility during at least ten months.

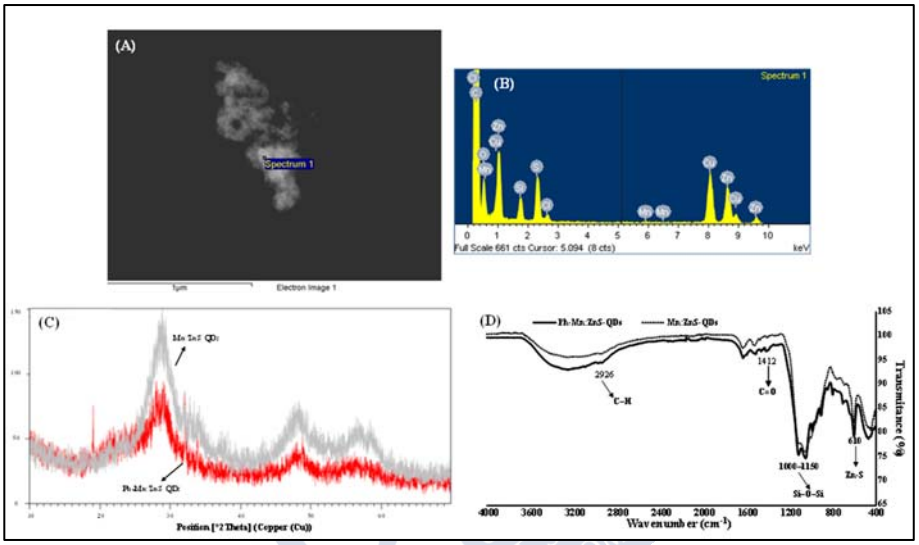

Figure 3. TEM image for Ph-Mn-ZnS QDs (A), EDS spectra for a selected point in the TEM image (B), XRD spectra for Mn-ZnS QDs and Ph-Mn-ZnS QDs (C), and Fourier transform infra-red spectra for Mn-ZnS QDs and Ph-Mn-ZnS QDs (D)

4.3.2. RTP operating conditions

4.3.2.1. Effect of interaction time

The influence of the interaction time between Ph-QDs and inorganic mercury (Hg^{2+}) was investigated by mixing 1.5 mL of Ph-QDs (100 mg L^{-1}, prepared in 0.1 M KH_2PO_4, pH 8) with 40 µL of 500 µg L^{-1} Hg(II), and 460 µL of buffer (0.1 M KH_2PO_4, pH 8.0), which leads to a final Hg(II) concentration of 10 µg L^{-1}. Emission intensity (peak area) was measured at two-min intervals. As shown in Figure 4, there was an immediate decrease in the RTP intensity within the first 6.0 min. After 12 min, the signal was found to be constant,

which indicates stabilization of Hg (II)-Ph-QDs interaction (Figure 4). A stabilization time of 12 min was therefore set for further studies.

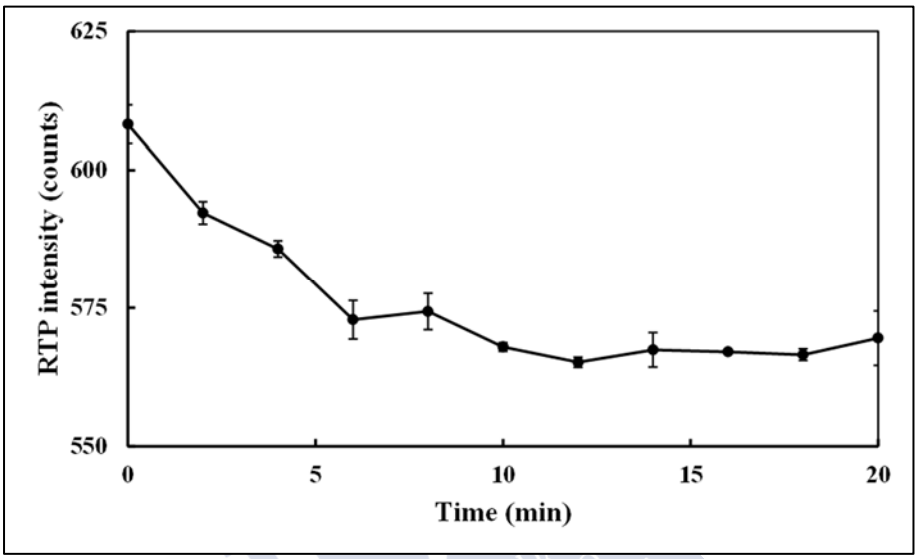

Figure 4. Effect of the interaction time between Ph-QDs and Hg^{2+} ions on the RTP intensity

4.3.2.2. Effect of the pH

The influence of pH on the Ph-QDs' RTP quenching when Hg(II) ions are present was evaluated by fixing the Ph-QDs concentration at 100.0 mg L^{-1} (material dispersed in 0.1 M KH_2PO_4 buffers at the tested pH of 6.0, 7.0, 8.0 and 9.0). Aliquots of 1.5 mL of the Ph-QDs buffered solutions were mixed with several volumes of the selected buffer and Hg (II) standard solution (500 µg L^{-1}) to obtain Hg (II) concentrations within the 0 - 100.0 µg L^{-1} range (final volume of 2 mL). RTP intensities were measured in triplicate after 12 min. The slopes (absolute values) of the calibration curves are plotted in Figure 5A. The highest slopes of the calibration curves (the highest RTP quenching) were observed when a slightly alkaline pH was used (-0.465±0.03 for pH 8.0, and -0.448±0.04 for pH 9.0). These findings agree with the N atoms deprotonation in the pyrimidine heterocyclic skeleton, which is favoured at alkaline pH. Deprotonated N atoms in

the phenobarbital residues promote a better Ph-QDs-mercury interaction and hence higher quenching. Buffered Ph-QDs and Hg (II) solutions at pH 8.0 were therefore selected for further experiments.

4.3.2.3. Effect of Ph-QD concentration

Ph-QDs dispersions were prepared in 0.1 M KH_2PO_4 (pH 8.0) using several Ph-QDs concentrations (10.0, 20.0, 50.0, 100.0, and 200.0 mg L^{-1}), and 1.5 mL aliquots were mixed with the required volume of the Hg^{2+} standard (500 µg L^{-1}, also prepared in 0.1 M KH_2PO_4, pH 8.0), and additional buffer volumes to 2.0 mL. Recorded RTP intensities after 12 minutes (Figure 5B) show that RTP quenching increased up to a Ph-QDs concentration of 20.0 mg L^{-1}. The use of Ph-QDs at higher concentrations than 20 mg L^{-1} led to a weak RTP quenching effect when mercury ions are present, although the magnitude of the RTP quenching is quite similar within the 50 – 200 mg L^{-1} range). These findings have been attributed to inner-filter effects as proposed by Tan *et al.* [30]. Considering these two phenomena and the higher slope (Figure 5B), a Ph-QDs concentration of 20.0 mg L^{-1} was selected to carry out further analysis.

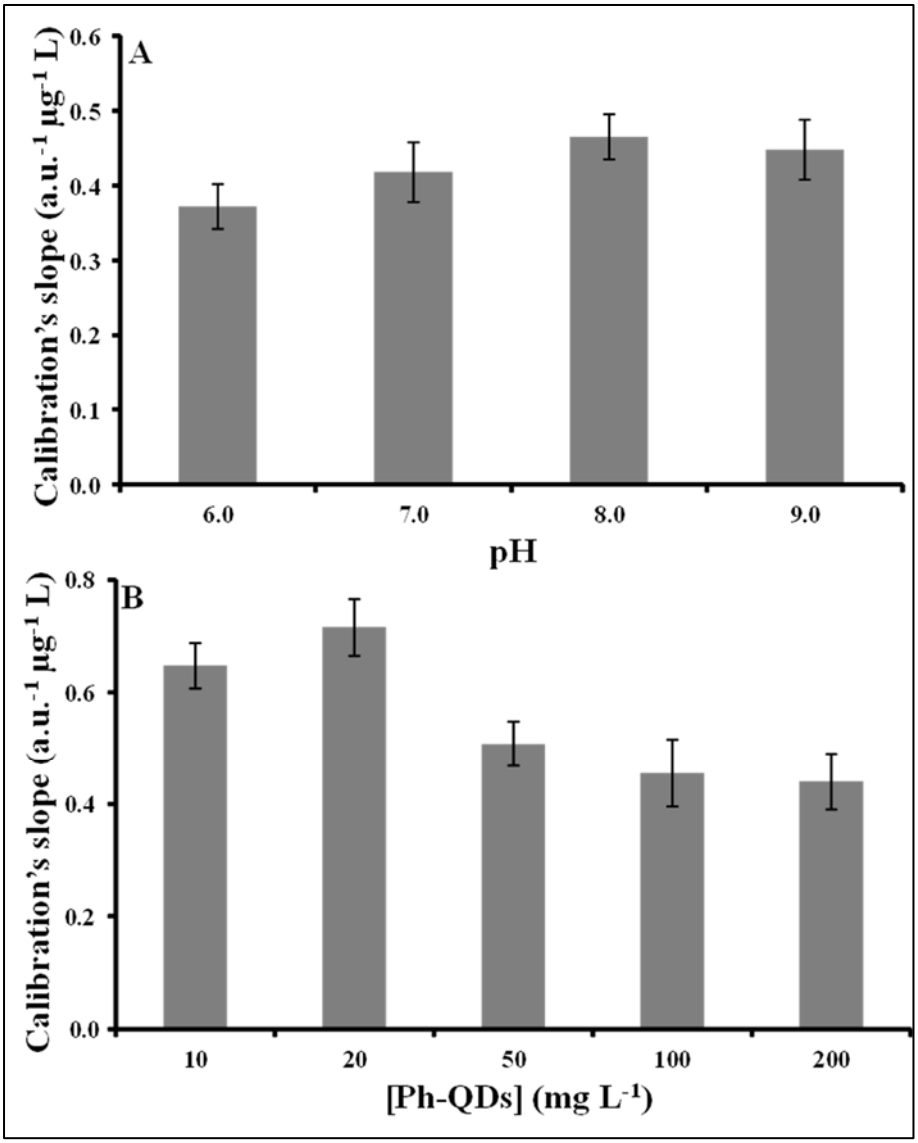

Figure 5. Effect of the pH (A) and Ph-Mn-ZnS QDs concentration (B) on the calibration's slope (Hg (II) concentration from 0 to 100 µg L^{-1})

4.3.3. Selectivity. Quenching effect from coexisting ions and compounds

The quenching effect of methylmercury and inorganic mercury (Hg(II)), and other ions [As(V), Ca(II), Cd(II), Co(II), Cu(II), Fe(III), K(I), Mg(II), Na(I), P(III), Pb(II), and Zn(II)] and compounds (arsenobetaine, AsB) on the response of Ph-QDs phosphorescence was examined. The RTP quenching was calculated according to the Stern–Volmer equation.

$$\frac{P_0}{P} = 1 + K_{SV}[Q] \quad (1)$$

where P_0 and P are the RTP intensities of the Ph-QDs in the absence and presence of the quencher (Hg(II), MeHg, or other tested ions), [Q] is the concentration of Hg (II), MeHg or other tested ions, and K_{SV} is the Stern-Volmer constant. Hg (II) and MeHg concentrations, as well as the concentrations of other potential quenchers, varied within the 0 – 100 µg L^{-1} range.

As shown in Table 1, the same K_{SV} value was obtained for Hg (II) and MeHg, which means that the same response of the Ph-QDs is achieved for both mercury species. Therefore, the prepared material is useful for total mercury assessment since MeHg and Hg (II) are the main mercury species in seafood and fish.

The selectivity factors of the prepared material were calculated as the ratios of the Stern-Volmer constant calculated for mercury to the respective Stern-Volmer constants of the other quenchers [K_{sv}(Hg)/K_{sv}(Q)]. The selectivity factors, also listed in Table 1, confirm that the prepared material is highly selective for MeHg and Hg (II), and the RTP of the prepared material is not affected by the presence of other co-existing ions in the fish extracts.

4.3.4. Method validation

4.3.4.1. Calibration and matrix effect

Matrix effect could be a serious drawback when using rapid detection methods such as luminescent based-QDs because of the presence of concomitants in the sample (extract) when a direct analysis is performed. Due to the complex matrix of fish extracts (large amounts of fats, proteins, vitamins and various minerals),

matrix effect was evaluated by comparing the slopes of the standard addition curves obtained using several dilutions of the sample extracts (1:10, 1:20 and 1:40, which implies the use of 200, 100 and 50 µL of fish extract, respectively) with the slope of the calibration. The slopes achieved (experiments in triplicate) were -0.65±0.02, -0.65±0.02 and -0.68±0.06 au μg^{-1} L for 1:10, 1:20 and 1:40 dilution, respectively. There were no significant differences (95% confidence interval) between these slopes and the slope of calibration curves (-0.68±0.03, n=3) after applying an ANOVA test (Table S2, Electronic Supplementary Information, ESI). Hence, the lowest dilution tested (1:10) was selected for sample analysis, and measurements (total mercury assessment) were performed using buffer calibration.

Table 1. Stern-Volmer constants and selectivity factors for Hg (II), MeHg, and other potential quenchers

Element	K_{sv} (Ph-QDs)	Selectivity factor (K_{sv}(Hg)/K_{sv}(Q))[a]
Hg(II)	0.007	1.0
MeHg	0.007	1.0
Pb(II)	0.00006	117
Cd(II)	0.0002	35
Co(II)	0.00007	100
Mg(II)	0.0002	35
Ca(II)	0.00008	88
Na(I)	0.00006	117
Zn(II)	0.00002	350
Cu(II)	0.0001	70
Fe(III)	0.00008	88
Arsenobetaine	0.0001	70
As(V)	0.00007	100
P(III)	0.0002	35
K(I)	0.0003	23

(a) Selectivity factor defined as the ratio between the Stern-Volmer constant for Hg (II) and the Stern-Volmer constant for the tested quencher

In addition, buffer calibrations were prepared using inorganic mercury (Hg(II)) and MeHg as calibrants (0-100 μg L^{-1} range), and similar slopes (experiments in triplicate) were obtained for both calibrants (-0.65±0.02 and -0.66±0.01 au μg^{-1} L for Hg(II) and MeHg, respectively). These findings imply that the prepared QD-based material gives similar responses for inorganic and organic mercury, and can thus be used for total mercury assessment in fish extracts. Inorganic mercury (Hg (II)) was finally selected as a calibrant for further studies.

4.3.4.2. Limit of detection and limit of quantification

The sensitivity of the method was estimated by calculating the limit of detection (LOD) of the method. This parameter was determined by the 3σ/k equation, where σ is a standard deviation of 11 reagent blanks, and k is the slope of the calibration curve. Similarly, the limit of quantification (LOQ) was calculated by 10σ/k. The instrumental LOD and LOQ were 0.27 and 0.91 μg L^{-1}, respectively, whereas, the method LOD and LOQ were 68.2 and 227 μg kg^{-1}, respectively. The LOD and LOQ obtained indicate that the current method is sensitive enough to measure total mercury levels in fish. The obtained LOD is quite lower than the maximum allowable limits for Hg in fish (0.5 or 1 mg kg^{-1}, depending on the fish species) established by the European Union [39].

4.3.4.3. Precision and accuracy

The inter-day precision and analytical recovery of the method were evaluated at three Hg (II) concentration levels (5.0, 20.0, 100 μg L^{-1}) measured seven times (each concentration level was studied in several consecutive days). Similarly, intra-day precision and analytical recovery were examined at all calibration levels (5.0, 10.0, 20.0, 50.0, 100 μg L^{-1}) measured in triplicate in seven consecutive days. Results (Table 2) show RSD values below 16%, confirming that the proposed RTP method offers excellent precision because they were below 20%, which is the value assigned by European method validation procedures [40]. Regarding analytical recovery, values were close to 100%, ranging from 95 to 117% (Table 2).

Finally, a CRM (BCR-463, tuna fish) was also analysed for total mercury by the proposed RTP method (ultrasound assisted acid extraction performed in triplicate, and each acid extract was measured by RTP based Ph-QDs, also in triplicate). Total Hg concentration found after applying the proposed methodology (3.07±0.013 mg kg^{-1}) agrees with the certified total Hg concentration in the CRM (3.04±0.16 mg kg^{-1}). These findings, together with good analytical recovery, mean that the proposed RTP method is accurate.

Table 2. Inter-day and intraday precision and analytical recovery of the method

	Concentration (μg L^{-1})	Analytical recovery (%)	RSD (%)
Inter-day (n=7)	5	116±1	16
	50	117±3	13
	100	95±4	5
Intraday (n=7)	5	115±1	10
	10	111±1	11
	20	112±1	5
	50	98±3	6
	100	101±6	6

4.3.4.4. Comparison to other QD-based chemosensors for mercury detection

Ph-Mn doped ZnS QDs synthesis is quite easier and safer (room temperature and absence of toxic reagents) than those required for other QDs such as CdS, CdTe, and CdTe@CdS (hydrothermal method at 90°C and/or boiling under reflux) [14, 26, 27]. In addition, special devices (microwave ovens) required for CD synthesis [21, 23, 25] are not needed. Sensitivity of the prepared material is comparable or better than the sensitivity reported for other authors (others CDs/QDs based chemosensors) for mercury assessment (Table 4). However, most screening procedures based on chemosensors (Table 4) allow the assessment of only one mercury species. The proposed Ph-QD-based chemosensor allows the simultaneous assessment of both mercury species (inorganic mercury and methyl-mercury). The simultaneous assessment of both mercury species is an advantage over other

proposed chemosensor screening procedures because inorganic mercury and methyl-mercury are both highly toxic, and the total mercury content should be screened.

4.3.5. Application

The proposed RTP based Ph-QDs method was applied to five commercial fish samples. The same samples were also analysed by ICP-MS after a microwave assisted acid digestion process for comparative purposes (total mercury concentration). Found concentrations are given in Table 3. After applying a paired sample t-test (p>0.05), total mercury concentrations by RTP Ph-QDs and ICP-MS were not found to be statistically significant different (t_{cal} of 1.97 lower from the t_{tab} of 2.78 for 95% confidence interval and four degrees of freedom).

Table 3. Total mercury concentrations in fish samples by RTP and ICP-MS

Sample	[Hg] (mg kg^{-1})[a]	[Hg] (mg kg^{-1})[b]	t_{cal} (Paried t test)
Swordfish-1	0.60±0.03	0.59±0.01	
Swordfish-2	0.16±0.04	0.14±0.01	
Yellowfin tuna	0.28±0.02	0.26±0.02	
Bluefin tuna	1.51±0.05	1.47±0.07	
Blue shark	0.96±0.01	0.97±0.15	1.97[c]

(a) Ultrasound assisted extraction and RTP (1:10 dilution) determination
(b) Microwave assisted acid digestion and ICP-MS determination
(c) $t_{tab\ (95\%,\ 4\ degrees\ of\ freedom)}$ = 2.78

Table 4. Comparison of characteristic performance obtained by using the proposed RTP-Ph-QDs chemosensor and other CDs/QDs based chemosensors for mercury assessment.

Analyte	Sample	QDs	Luminescence technique	Linear range	LOD	Ref.
Hg (II)	Water	TGA-capped CdTe	Fluorescence	0.012–1.5 μM	4.0×10^{-3} μM.	[26]
Hg (II)	Water	L-cysteine-capped Mn-doped ZnS	Room temperature phosphorescence	0.020–4.5 μM	3.8×10^{-3} μM	[30]
Hg (II)	Metal removal from polluted waters	ZnS impregnated Chitosan	---[a]	---[a]	---[a]	[28]
MeHg	Fish	CDs	Fluorescence	23–278 nM	5.9 nM	[22]
Hg (II)	Fish	AuAgS/Ag_2S nanoclusters	Fluorescence	---	10^{-4} nM	[41]
Hg (II)	Water	MPA coated Mn doped ZnSe/ZnS	Fluorescence	0–20 nM	0.1 nM	[29]
Hg (II)	---[a]	PEDOT-QD	Fluorescence	---[a]	---[a]	[31]
Hg (II)	Water	N-CDs	Fluorescence	0.1–10 μM	0.14 μM	[23]
Hg (II)	Water	N-CDs	Fluorescence	0–150 μM	0.089 μM	[24]
Hg (II)	Canned tuna	N-CDs	Chemiluminescence	0.25–10 ng mL^{-1}	0.08 ng mL^{-1}	[25]
Hg (II)	Fish	CDs	Fluorescence	0.1-20 μM	62 nM	[21]
Hg (II)	Water, fish	Fe_3O_4@SiO_2/dendrimer /CdTe@CdS	Electrochemiluminescence	20 aM–2 μM	2 aM	[27]
Total Hg	Fish	Ph-Mn-doped ZnS	Room temperature phosphorescence	0.27-100 μg L^{-1} (1.34–500 nM[b])	68.2 μg kg^{-1}	This study

(a) Not applicable; (b) nM concentration referred to Hg (II)

4.4. CONCLUSIONS

Phenobarbital has been novelty demonstrated to confer highly selective properties throughout mercury species (Hg (II) and MeHg). A phenobarbital-based polymer for coating Mn-doped ZnS QDs has resulted in a sensitive and selective RTP chemosensor for assessing total mercury in fish extracts. The RTP method was found to offer results comparable to those obtained using more sophisticated analytical techniques such as ICP-MS. The proposed method, however, requires low-cost instrumentation and can thus be implemented worldwide. The method was found to be precise and accurate. It offers LOD/LOQ lower than the European Union maximum allowable limits for total mercury in fish. In conclusion, this method is a highly selective, sensitive, reliable and cost-effective option for quality control of total mercury in fishery products.

4.5. ACKNOWLEDGEMENTS

This work was supported by the *Xunta de Galicia* (*Grupo de Referencia Competitiva*, grant numbers 6RC2014/2016 and ED431C2018/19; *Program for Development of a Strategic Grouping in Materials – AEMAT*, grant number ED431E2018/08). The authors are grateful to Dr. Bruno Dacuña-Mariño (*Unidade de Raios X*) at *Rede de Infraestruturas de Apoio á Investigación e ao Desenvolvemento Tecnolóxico* – University of Santiago de Compostela) for XRD technical support, and to Eugenio Solla (*Servicio de Microscopía Electrónica*) at CACTI–University of Vigo for TEM/EDS technical support.

4.6.REFERENCES

[1] B. Piršelová, Monitoring the sensitivity of selected crops to lead, cadmium and arsenic, J. Stress Physiol. Biochem. 7 (2011) 31–38.

[2] S.C.T. Nicklisch, L.T. Bonito, S. Sandin, A. Hamdoun, Mercury levels of yellowfin tuna (*Thunnus albacares*) are associated with capture location, Environ. Pollut. 229 (2017) 87–93.

[3] A. Ordiano-Flores, F. Galván-Magaña, R. Rosiles-Martínez, Bioaccumulation of mercury in muscle tissue of yellowfin tuna, *Thunnus albacares*, of the Eastern Pacific Ocean, Biol. Trace Elem. Res. 144 (2011) 606–620.

[4] WHO, Mercury and Health. https://www.who.int/news-room/fact-sheets/detail/mercury-and-health, 2017 (accessed 19 December 2018).

[5] ATSDR, ATSDR's Substance Priority List, Agency for Toxic Substances and Disease Registry. https://www.atsdr.cdc.gov/SPL/, 2017 (accessed 20 December 2018).

[6] M.C. Sheehan, T.A. Burke, A. Navas-Acien, P.N. Breysse, J. McGready, M.A. Fox, Global methylmercury exposure from seafood consumption and risk of developmental neurotoxicity: A systematic review, Bull. World Health Organ. 92 (2014) 254–269.

[7] K.M. Rice, E.M. Walker, Jr., M. Wu, C. Gillette, E.R. Blough, Environmental mercury and its toxic effects, J. Prev. Med. Public Health 47 (2014) 74–83.

[8] W.F. Fitzgerald, D.R. Engstrom, R.P. Mason, E.A. Nater, The case for atmospheric mercury contamination in remote areas, Environ. Sci. Technol. 32 (1998) 1–7.

[9] M. Arcagni, L. Campbell, M.A. Arribére, M. Marvin-DiPasquale, A. Rizzo, S. Ribeiro Guevara, Differential mercury transfer in the aquatic food web of a double basined lake associated with selenium and habitat, Sci. Total Environ 454–455 (2013) 170–180.

[10] B.K.K.K. Jinadasa, G.S. Chathurika, C.D. Jayaweera, G.D.T.M. Jayasinghe. Mercury and cadmium in swordfish and yellowfin tuna and health risk assessment for Sri Lankan consumers. Food Addit. Contam. B. (2018) https://doi.org/10.1080/19393210.2018.1551247.

[11] S.L.C. Ferreira, V.A. Lemos, L.O.B. Silva, A.F.S. Queiroz, A.S. Souza, E.G.P. da Silva, W.N.L. dos Santos, C.F. das Virgens, Analytical strategies of sample preparation for the determination of mercury in food matrices – A review, Microchem. J. 121 (2015) 227–236.

[12] M. Amde, Y. Yin, D. Zhang, J. Liu, Methods and recent advances in speciation analysis of mercury chemical species in environmental samples: A review, Chem. Spec. Bioavailab. 28 (2016) 51–65.

[13] M. Marcinkowska, D. Barałkiewicz, Multielemental speciation analysis by advanced hyphenated technique – HPLC/ICP-MS: A review, Talanta 161 (2016) 177–204.

[14] Y. Chen, Z. Rosenzweig, Luminescent CdS quantum dots as selective ion probes, Anal. Chem. 74 (2002) 5132–5138.

[15] P. Wu, X.-P. Yan, Doped quantum dots for chemo/biosensing and bioimaging, Chem. Soc. Rev. 42 (2013) 5489–5521.

[16] W.R. Algar, A.J. Tavares, U.J. Krull, Beyond labels: A review of the application of quantum dots as integrated components of assays, bioprobes, and biosensors utilizing optical transduction, Anal. Chim. Acta 673 (2010) 1–25.

[17] H. Kuang, Y. Zhao, W. Ma, L. Xu, L. Wang, C. Xu, Recent developments in analytical applications of quantum dots, Trends Anal. Chem. 30 (2011) 1620–1636.

[18] L. Dan, H.-F. Wang, Mn-doped ZnS quantum dot imbedded two-fragment imprinting Silica for enhanced room temperature phosphorescence probing of domoic acid, Anal. Chem. 85 (2013) 4844–4848.

[19] Y.Q. Wang, W.S. Zou, 3-Aminopropyltriethoxysilane-functionalized manganese doped ZnS quantum dots for room-temperature phosphorescence sensing ultratrace 2,4,6-trinitrotoluene in aqueous solution, Talanta 85 (2011) 469–475.

[20] A. Moreda-Piñeiro, J. Sánchez-González, M.P. Chantada-Vázquez, A.M. Bermejo, P. Bermejo-Barrera, MIPs as a versatile tool for micro-solid-phase extraction and probe sensing, Curr. Chem. Biol. 12 (2018) 114–134.

[21] R. Tabaraki, N. Sadeghinejad, Microwave assisted synthesis of doped carbon dots and their application as green and simple turn off–on fluorescent sensor for mercury (II) and iodide in environmental samples, Ecotox. Environ. Safe. 153 (2018) 101–106.

[22] I. Costas-Mora, V. Romero, I. Lavilla, C. Bendicho, In situ building of a nanoprobe based on fluorescent carbon dots for methylmercury detection, Anal. Chem. 86 (2014) 4536–4543.

[23] X. Cao, J. Ma, Y. Lin, B. Yao, F. Li, W. Weng, X. Lin, A facile microwave-assisted fabrication of fluorescent carbon nitride quantum dots and their application in the detection of mercury ions, Spectrochim. Acta A 151 (2015) 875–880.

[24] S. Yu, K. Chen, F. Wang, Y. Zhu, X. Zhang, Polymer composite fluorescent hydrogel film based on nitrogen-doped carbon dots and their application in the detection of Hg^{2+} ions, Luminescence 32 (2017) 970–977.

[25] H. Abdolmohammad-Zadeh, E. Rahimpour, A novel chemosensor based on graphitic carbon nitride quantum dots and potassium ferricyanide chemiluminescence system for Hg(II) ion detection, Sensor. Actuat. B Chem. 225 (2016) 258–266.

[26] Y.S. Xia, C.Q. Zhu, Use of surface-modified CdTe quantum dots as fluorescent probes in sensing mercury (II), Talanta 75 (2008) 215–221.

[27] B. Babamiri, A. Salimi, R. Hallaj, Switchable electrochemiluminescence aptasensor coupled with resonance energy transfer for selective attomolar detection of Hg^{2+} via CdTe@CdS/dendrimer probe and Au nanoparticle quencher, Biosens. Bioelectron. 102 (2018) 328–335.

[28] A. Jaiswal, S.S. Ghsoh, A. Chattopadhyay, Quantum dot impregnated-chitosan film for heavy metal ion sensing and removal, Langmuir 28 (2012) 15687–15696.

[29] J. Ke, X. Li, Q. Zhao, Y. Hou, J. Chen, 2014. Ultrasensitive quantum dot fluorescence quenching assay for selective detection of mercury ions in drinking water. Sci. Rep. 4, 5624.

[30] L. Tan, Y. Li, Y. Tang, C. Kang, Z. Yu, S. Xu, Room temperature phosphorescence sensor for Hg^{2+} based on Mn-doped ZnS quantum dots, J. Nanosci. Nanotechnol. 12 (2012) 7788–7795.

[31] K.P. Prasad, Y. Chen, M.A. Sk, A. Than, Y. Wang, H. Sun, K.-H. Lim, X. Dong, P. Chen, Fluorescent quantum dots derived from PEDOT and their applications in optical imaging and sensing, Mater. Horiz. 1 (2014) 529–534.

[32] M.P. Rodríguez-Reino, R. Rodríguez-Fernández, E. Peña-Vázquez, R. Domínguez-González, P. Bermejo-Barrera, A. Moreda-Piñeiro, Mercury speciation in seawater by liquid chromatography-inductively coupled plasma-mass spectrometry following solid phase extraction pre-concentration by using an ionic imprinted polymer based on methyl-mercury–phenobarbital interaction, J. Chromatogr. A 1391(2015) 9–17.

[33] M.P. Chantada-Vázquez, J. Sánchez, E. Peña-Vázquez, M.J. Tabernero, A.M. Bermejo, P. Bermejo-Barrera, A. Moreda-Piñeiro, Simple and sensitive molecularly imprinted polymer–Mn-doped ZnS quantum dots based fluorescence probe for cocaine and metabolites determination in urine, Anal. Chem. 88 (2016) 2734–2741.

[34] A.I. Cabañero Ortiz, Y. Madrid Albarrán, C. Cámara Rica, Evaluation of different sample pre-treatment and extraction procedures for mercury speciation in fish samples, J. Anal. At. Spectrom. 17 (2002) 1595–1601.

[35] A. Moreda-Piñeiro, E. Peña-Vázquez, P. Hermelo-Herbello, P. Bermejo-Barrera, J. Moreda-Piñeiro, E. Alonso-Rodríguez, S. Muniategui-Lorenzo, P. López-Mahía, D. Prada-Rodríguez, Matrix solid-phase dispersion as a sample pretreatment for the speciation of arsenic in seafood products, Anal. Chem. 80 (2008) 9272–9278.

[36] E. Mohagheghpour, F. Moztarzadeh, M. Rabiee, M. Tahriri, M. Ashuri, H. Sameie, R. Salimi, S. Moghadas, Micro-emulsion synthesis, surface modification and photophysical properties of $Zn_{1-x}Mn_xS$ nanocrystals for biomolecular recognition, IEEE T. Nanobiosci. 11 (2012) 317–323.

[37] B.S. Rema Devi, R. Raveendran, A.V. Vaidyan, Synthesis and characterization of Mn^{2+}-doped ZnS nanoparticles, Pramana 68 (2007) 679–687.

[38] J.H. Chung, C.S. Ah, D.-J. Jang, Formation and distinctive decay times of surface- and lattice-bound Mn^{2+} impurity luminescence in ZnS nanoparticles, J. Phys. Chem. B 105 (2001) 4128–4132.

[39] EU/EC-1881, Setting maximum levels for certain contaminants in foodstuffs. Official Journal of the European Union, 2006.

[40] SANTE, (11813) Guidance document on analytical quality control and method validation procedures for pesticide residues and analysis in food and feed, European Commission, 2017.

[41] Q. Zhao, S. Chen, L. Zhang, H. Huang, F. Liu, X. Liu, 2014. Synthesis of biocompatible AuAgS/Ag_2S nanoclusters and their applications in photocatalysis and mercury detection. J. Nanopart. Res. 16, 2793. https://doi.org/10.1007/s11051-014-2793-4.

4.7. ELECTRONIC SUPPLEMENTARY INFORMATION (ESI)

Table S1. Operating ICP-MS conditions for total Hg determination in acid digests from fish samples.

Operating ICP-MS conditions		
Radiofrequency power		1600 W
Gas flows	Nebulization	0.92 mL min^{-1}
	Auxiliary	1.2 mL min^{-1}
	Plasma	16 mL min^{-1}
KED mode: He flow rate		1.0 mL min^{-1}
Analytes		^{202}Hg
Internal standards		^{103}Rh

Table S2. ANOVA output when comparing the slopes of calibration and standard addition (1:10, 1:20, and 1:40 dilution) graphs

Source	Sum of squares	Degree of freedom	Mean square	F ratio	p-value
Between groups	0.007425	3	0.002475	1.87	0.2134
Within groups	0.0106	8	0.001325		
Total (Corr.)	0.018025	11			

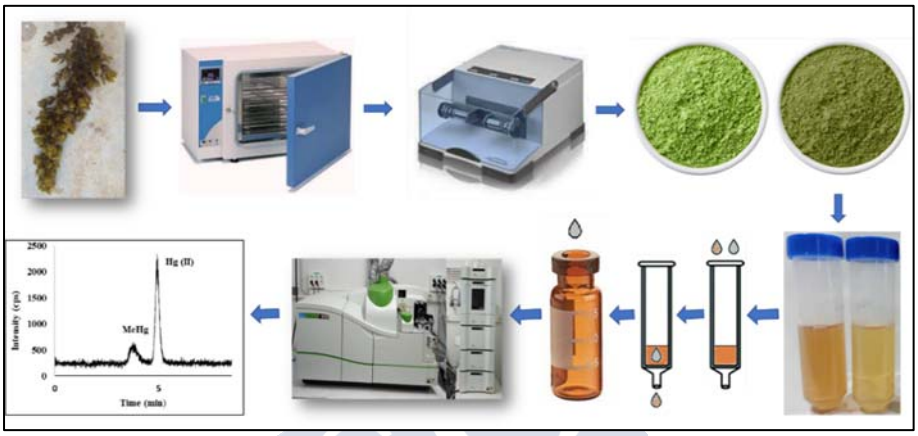

CHAPTER 5

MOLECULARLY IMPRINTED POLYMER-SOLID PHASE EXTRACTION AND HIGH-PERFORMANCE LIQUID CHROMATOGRAPHY - INDUCTIVELY COUPLED PLASMA MASS SPECTROMETRY FOR MERCURY SPECIATION IN SEAWEED

KAMAL K. JINADASA, PALOMA HERBELLO HERMELO, ELENA PEÑA-VÁZQUEZ, PILAR BERMEJO-BARRERA, ANTONIO MOREDA-PIÑEIRO

USC
UNIVERSIDADE
DE SANTIAGO
DE COMPOSTELA

Molecularly imprinted polymer-solid phase extraction and high-performance liquid chromatography - inductively coupled plasma mass spectrometry for mercury speciation in seaweed

Kamal K. Jinadasa, Paloma Herbello Hermelo, Elena Peña-Vázquez, Pilar Bermejo-Barrera, Antonio Moreda-Piñeiro

Trace Element, Spectroscopy and Speciation Group (GETEE), Strategic Grouping in Materials (AEMAT), Department of Analytical Chemistry, Nutrition and Bromatology. Faculty of Chemistry. Universidade de Santiago de Compostela. Avenida das Ciencias, s/n. 15782, Santiago de Compostela. Spain

Abstract

In contrast to most of essential and heavy metals, mercury levels in seaweed are very low, and pre-concentration methods are required for an adequate determination, and also methylmercury and inorganic mercury speciation in edible seaweed. A molecularly imprinted polymer-based solid phase extraction (on column) pre-concentration procedure has been optimized for mercury species enrichment before high performance liquid chromatography hyphenated with inductively coupled plasma mass spectrometry determination. The polymer has been synthesised by using a ternary pre-polymerization mixture containing the template (methylmercury), a non-vinylated monomer (phenobarbital), and a vinylated monomer (methacrylic acid), and by the precipitation polymerization method. Factors affecting the adsorption/desorption of Hg species (extract pH, loading and elution flow rates, volume of eluent, etc.), and parameters such as breakthrough volume and reusability, were fully studied. Mercury species were first isolated from seaweed by ultrasound assisted extraction using 0.1% (v/v) HCl, 0.12% (w/v) L-cysteine, 0.1% (v/v) mercaptoethanol as an extractant mixture. Under optimized conditions, the limits of detection were 0.007 and 0.02 μg kg^{-1} dw for methylmercury and Hg (II), respectively. The pre-concentration factor (volume of 10 mL of seaweed extract) was 50. Repeatability and reproducibility of the method were satisfactory with relative standard deviations (RSDs)

lower than 16%. The proposed methodology was finally applied for the selective pre-concentration and determination of methylmercury and Hg (II) in a BCR-463 certified reference sample and several edible seaweeds.

Keywords: Molecularly imprinted polymer, **s**olid-phase extraction, mercury speciation, edible seaweed

5.1. INTRODUCTION

Seaweed (benthic marine algae or macroalgae) are a source of food for humans since ancient times, and they have been also used in medicine and as animal fodder [1]. Seaweed can be classified into three main groups according to their dominant pigmentation: red (*Rhodophyta*), brown (*Phaeophyta*), and green (*Chlorophyta*) seaweed. According to the Food and Agriculture Organization (FAO) statistics, world seaweed mariculture production reached 24.9 million tons (valued about six billion USD) in 2014 [2]. As a food source, edible seaweed are rich in polysaccharides, proteins, dietary fibre, polyunsaturated fatty acids, vitamins (A, C, B2 and B12), iodine, and minerals (magnesium, sodium, and iron) [3,4]. Additionally, seaweed are used as low-calorie food (body weight control), and their consumption has been reported to prevent cancer, and gastrointestinal and cardiovascular diseases [4,5]. Another important application of seaweed is the production and extraction of derivatives such as agar, carrageenan, and alginate, and bio-active compounds [5]. However, some studies are showing the safety hazard of seaweed due to their content of non-essential trace metals (Hg, Cd, Pb, As, etc.), radioactive isotopes, dioxins, and pesticides [6-8].

Mercury (Hg) is a highly toxic element that can be bio-accumulated and biomagnified through the food chain, especially in the marine environment [9]. The World Health Organization (WHO) has classified Hg as “one of the top ten chemicals or groups of chemicals of major public health concern” [10], and the Agency for Toxic Substances and Disease Registry (ATSDR) of the United States (US) ranked Hg on the third place of their substance’s priority list [11]. The sources of Hg in the aquatic environment originate from

several natural processes such as volcanism, weathering of rocks and degassing of the earth's crust; and several anthropogenic activities that are a consequence of rapid urbanization and industrialization (e.g. coal combustion, mining industry and by-products, use of agriculture fertilizers, and waste incineration) [12,13]. The toxicity of Hg is related to the chemical form, and the path of entry into the organism. As an example, in the digestive tract methyl mercury (MeHg) has the greatest impact and has shown the ability to affect the nervous system [14].

The levels of heavy metals in seaweed depend on several factors i.e. pH, salinity, presence of complex organic-inorganic molecules, temperature, light irradiation, oxygen, and nutrient concentration. According to the published scientific data, Hg concentration present in seaweed varies with the type of seaweed and sampling location, and in contrast to other non-essential metals, Hg levels in seaweed are low [15]. Therefore, many investigations have reported the Hg content as total Hg concentration (tHg), and the levels were frequently below the limits of detection of most of conventional instrumental techniques [6,16-18].

An adequate sample pre-treatment is very important when assessing ultra-trace levels of Hg (and Hg species), and accurate quantification of Hg and/or mercury species in seaweed usually requires a pre-concentration technique before instrumental analysis. Microwave assisted acid digestion has been typically used for seaweed solubilization when total Hg is assessed [19-22]. Other authors have performed alkaline treatments by using aqueous KOH or KOH/methanol for MeHg isolation [23-25] when applying the US Environmental Protection Agency (USEPA) 1630 method [26] with cold vapour – atomic fluorescence spectrometry (CV-AFS) quantification (total mercury assessment, MeHg assessment, and inorganic Hg by difference) [24,25]. On other occasions, organic solvents such as toluene [27] and HCl/toluene mixtures [28] have been proposed, although several additional stages (back extraction step with sodium thiosulfate and a final oxidation of MeHg with acidified BrCl for total Hg determination by CV-AFS) are required [27]. CV-AFS hyphenated with high performance liquid chromatography (HPLC) has been used by Brombach *et al.* for Hg speciation in seaweeds [23].

Although a first microwave assisted extraction was performed with aqueous KOH as an extractant, a further treatment with concentrated HCl was needed for a quantitative extraction of mercury species.

In order to pre-concentrate and/or cleaning the extracts/digests from seaweed, some procedures, mainly based on solid phase extraction (SPE), have been proposed. Because of the great affinity of mercury ions for thiol groups, sulfydryl-based absorbents such as laboratory made sulfydryl cotton fiber (SCF) for total Hg determination by coul vapour atomic absoroption spectrometry (CV-AAS) [19], and thiol-thiourea on silica by HPLC-CV-AFS [23]. Molecularly imprinted polymers (MIPs) and ionic imprinted polymers (IIPs) are promising absorbents for selective pre-concentration, matrix removal, and medium exchange [29], and some few applications have been developed for Hg determination/speciation [30]. Selective MIP-based SPE has been applied for pre-concentrating mercury species from seawater before HPLC-inductively coupled plasma – mass spectrometry (ICP-MS) [31], although most of MIP/IIP applications have been focused on total Hg determination or the assessment of a specific species (MeHg) in fish [20,21,28], wine [32], human hair [21,22], and human serum [33]. Similarly, IIPs have been also used for developing selective electrodes for potentiometric/voltammetric determination of total mercury in freshwater [34,35]. However, to the best of authors' knowledge, there are not developments of MIPs for ultra-trace pre-concentration of Hg species from extracts from complex materials such as seaweed. In this work, a selective MIP for mercury species has been synthesized by the precipitation polymerization method, and a on column pre-concentration method combined with HPLC-ICP-MS has been optimized for assessing low concentrations of Hg(II) and MeHg in edible seaweeds.

5.2. MATERIALS AND METHODS

5.2.1. Reagents

Methylmercury stock solution (1000 mg L^{-1}) was prepared from methylmercury chloride from Sigma Aldrich (St. Louis, MO, USA). This reagent was also used when preparing the MIP (MeHg as a template). The Hg (II) stock solution (1000 mg L^{-1}) was from Scharlab

(Barcelona, Spain). Working standard solutions of MeHg and Hg (II) were prepared daily by appropriate dilution of the stocks. Hydrochloric acid from Panreac (Barcelona, Spain) and ammonia solution from Merck (Darmstadt, Germany) was used for pH adjustment of extracts. The ammonium chloride/ammonium hydroxide (NH_4Cl/NH_4OH) buffer solution was prepared from NH_4Cl and NH_4OH from Merck. Ultrapure water (18.2 MΩ/cm resistivity) was obtained from a Milli-QA10 water purification system (Millipore Co., Bedford, MA, USA) and was used for the preparation of all solutions and for extracts dilution.

The following reagents were used for the synthesis of MIPs: phenobarbital sodium salt, methacrylic acid (MA), and ethylene glycol dimethacrylate (EGDMA) from Sigma Aldrich (St. Louis, MO, USA), 2,2′-azobis(2-methyl propionitrile) (AIBN) from Fluka (Steinheim, Germany), and acetonitrile from Merck. Thiourea (Sigma Aldrich) and HCl (Fluka) were used for template removal. Multi-element standard solutions for the cross-reactivity study were prepared by combining single As, Ca, Co and Mg stock standard solutions (1000 mg L^{-1}) from Merck, single Cr, K, P, Pb and Zn stock standard solutions (1000 mg L^{-1}) from Scharlab, and single Cd, Cu, Fe and Na stock standard solutions (1000 mg L^{-1}) from Perkin Elmer (Shelton, CT, USA). Internal standard solutions (Ge, Sc, and Rh) were prepared from single-element standards (1000 mg L^{-1}) purchased from Perkin Elmer. Nitric acid (Hyper pure, 69%), and 33% of hydrogen peroxide were supplied by Panreac (Barcelona, Spain). Due to the non-availability of Hg certified reference material for Hg species in seaweed, a tuna fish certified reference material (BCR-463) from the European Commission Joint Research Centre, Institute for Reference Materials and Measurements (Geel, Belgium) was used to evaluate the accuracy of the method.

To avoid contamination with Hg throughout the study, all glassware and plastic-ware were thoroughly rinsed with ultrapure water, soaked 2 days in 10% (v/v) nitric acid, and finally rinsed several times with ultrapure water.

5.2.2. Instrumentation

A Perkin Elmer Nex-Ion 300X ICP–MS (Waltham, MA, USA), coupled with a Flexar LC HPLC (LC pump, column oven, and LC autosampler) from Perkin Elmer, was used for Hg speciation. A Kinetex C-18 100 Å analytical column (100 mm × 2.10 mm, 5 µm particle diameter) connected with a C-18 guard column from Phenomenex (Torrance, USA) was used for reverse-phase chromatographic separation.

Polymerization was performed in a Boxcult temperature-controlled chamber (Stuart Scientific, Surrey, UK), with the support of a low-profile roller (Stovall, Greensboro, NC, USA). The MIP sorbent was packed into 5 mL syringes (Dispomed Witt OHG, Gelnhausen, Germany) between two Teflon frits (Supelco, Bellefonte, USA). SPE was performed by using an 8 channel Minipuls-3 (Gilson, Middleton, WI, USA) peristaltic pump equipped with PVC 2-stop tubing (1.52 mm i.d.) from SCP Sciences (Baie-D'Urfe, Quebec, Canada). MIPs characterization was performed by Fourier transform infrared spectrometry (FT-IR) using a Spectrum-Two FT-IR (Perkin Elmer) operating in ATR mode.

Other general instrumentation such as an USC60TH ultrasonic cleaner bath (45 kHz, 120 W) from VWR (Leuven, Belgium), an ultracentrifuge (Sigma 2K15, Osterode, Germany), a pH meter with a glass combined electrode (Crison Basic 20, Barcelona, Spain), a vibrating zircon ball mill (Retsch, Haan, Germany), an oven model 207 from Selecta (Barcelona, Spain), and a Classic ML analytical balance (Mettler Toledo, Columbus, OH, USA) were used throughout this research.

5.2.3. Preparation of the MIPs

The MIPs were synthesized following a three step-procedure developed by Rodríguez-Reino *et al.* [31], with minor changes. To prepare the pre-polymerization mixture, 0.053 g of CH_3ClHg, 0.097 g of phenobarbital salt, 71 µL of MA, and 25 mL of porogen (18.75 mL ACN and 6.25 mL H_2O) were mixed into a glass tube. The mixture was then stirred for 5 min and kept into a dark place overnight. Afterward, 1.13 mL of EGDMA and 55 mg of purified AIBN were

added into the test tube. The mixture was again stirred for 1 min, purged with argon for 10 min, placed into the low-profile roller (33 rpm) and incubated at 60 °C for 24 h inside of the temperature-controlled incubation chamber. After finishing the polymerization, the synthesized material was vacuum filtered, washed 3 times with an acetonitrile/water mixture (3:1), and oven-dried at 40 °C overnight. NIPs (non-imprinted polymers) were prepared in the same manner, without adding the template ion.

The template (methylmercury ion) was leached by passing 400 mL of 1.0 M thiourea solution in 1.0 M HCl through a syringe containing 0.5 g of MIPs at a flow rate of 0.5 mL min^{-1}. The polymer was then washed with ultrapure water, dried at 40 °C in an oven (12 h), and stored in sealed bottles until use in further analysis.

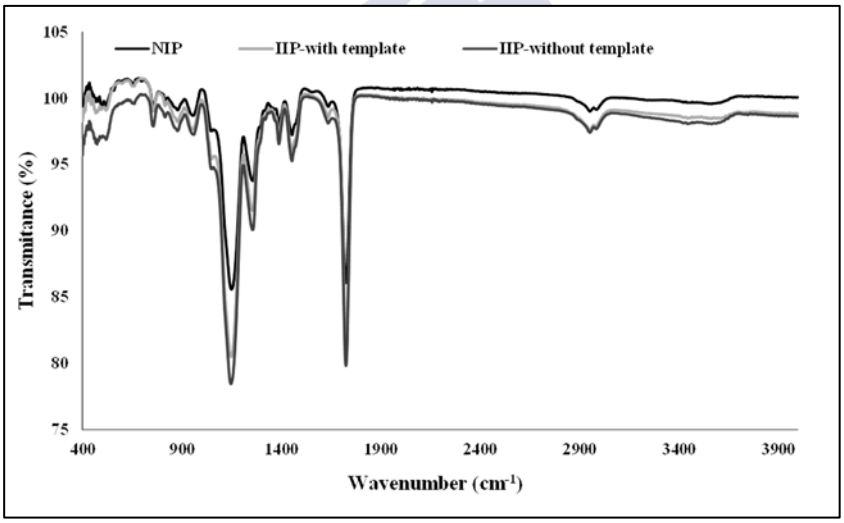

Figure 1. FT-IR spectra of MIP (before and after template removal) and NIP

In accordance with previous works [31], scanning electron microscopy (SEM) characterization of MIP and NIP showed agglomeration of spherical particles of diameters lower than 10 μm. Characterization by FT-IR spectrometry (FT-IR spectra of MIPs after template removal and before template removal, and NIP in Figure 1 shows similar characteristic peaks for all cases: 3584 cm^{-1} (stretching peak of O-H), 2986 cm^{-1} (stretching vibration of C-H_3), 1732 cm^{-1}

(stretching vibration of C=O), 1456 cm^{-1} (bending vibration of C=C, C=N), 1389 cm^{-1} (bending vibration of C-H_3), 1254 cm^{-1} (bending vibration of N-H), and 1148 cm^{-1} (stretching vibration of C-O). All these bands confirmed that the MIP has been successfully formed, and the presence of prominent C=N-, N-H bands confirm that the complexing agent phenobarbital trapped into the polymeric matrix.

5.2.4. Ultrasound assisted extraction of mercury species from seaweed

Dehydrated seaweed samples were pulverized using a ball mill and dried in an oven at 70 °C for 24 h. Then, seaweed samples and the CRM were prepared according to published methods [36,37] with small modifications. Homogenized dried seaweed samples (0.2 g portions) were weighed in triplicate into polypropylene centrifuge tubes, and a volume of 10 mL of the extractant solution [0.1% (v/v) HCl, 0.12% (w/v) L-cysteine, 0.1% (v/v) mercaptoethanol] was added. These suspensions were ultrasonicated at 45 kHz and room temperature for 30 min. After centrifugation (5000 rpm, 30 min), supernatants (extracts) were separated, and these extracts used in further experiments.

5.2.5. MIP-based solid phase extraction procedure

Sorbent particles (200 mg of MIP) were placed between two Teflon frits into 5 mL syringes and the sorbent was conditioned by passing volumes of 20 mL of NH_3/NH_4Cl buffer solution (pH 9.0) at a 2 mL min^{-1}. Loading stage consisted of passing 10 mL of seaweed extract (pH adjusted to 9.0) at 2 mL min^{-1} flow rate, which was followed by a cleaning step with 10 mL of pH 9.0 NH_3/NH_4Cl buffer solution also at a flow rate of 2 mL min^{-1}. The retained Hg ions were subsequently eluted with 2 mL of a solution containing 0.8% (v/v) 2-mercaptoethanol and 20% (v/v) methanol (pH adjusted to 4.5) at a flow rate of 1.0 mL min^{-1}. The eluate was dried under N_2 gas, and then re-dissolved in 200 µL of mobile phase solution (0.4% (v/v) 2-mercaptoethanol and 10% (v/v) methanol, pH 2.0) for HPLC-ICP-MS analysis. A pre-concentration factor of 50 was achieved by the previous treatment.

First attempts for total Hg determination in seaweed after a microwave assisted acid digestion procedures led to undetected total

Hg concentrations in the tested seaweed samples because of the strong matrix effect of the acid matrix. Therefore, the same extraction procedure (section 5.2.4) followed by the MIP-based SPE (but re-dissolving the residues in 5-10 mL of ultrapure water after N_2 stream drying) was used for total Hg determination by ICP-MS.

5.2.6. Determinations by HPLC-ICP-MS and ICP-MS

Operating conditions for Hg (II) and MeHg species separation and determination (reverse-phase chromatography) are listed in Table 1. Quantification of both Hg species was achieved by using calibration matched with the mobile phase an covering the 0-50 µg L^{-1} and 0-20 µg L^{-1} range for Hg (II) and MeHg, respectively (chromatograms in Figure 2 show signals at a retention time of 3.5 min for MeHg, and at 4.8 min for Hg (II)).

Total Hg determination were assessed by ICP-MS following the operating conditions listed in Table 1 (^{103}Rh at 10 µg L^{-1} as an internal standard) and using aqueous calibration covering the 0-10 µg L^{-1} concentration range. Elements involved in cross-reactivity studies (Ca, As, Cd, Co, Cr, Cu, Fe, Hg, K, Mg, Na, P, Pb, and Zn) were also measured by ICP-MS by using suitable aqueous calibrations and internal standards (^{74}Ge, ^{54}Sc and ^{103}Rh, all at 10 µg L^{-1}).

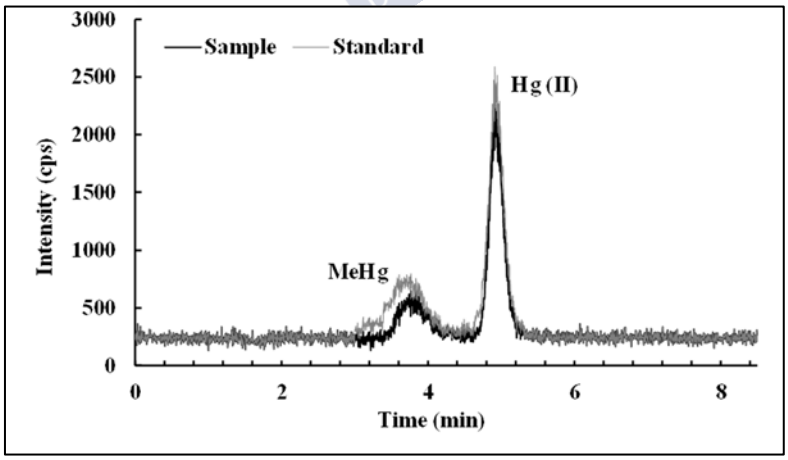

Figure 2. HPLC-ICP-MS chromatograms for a 5.0 µg L^{-1} Hg (II) and 2.0 µg L^{-1} MeHg aqueous standard and a pre-concentrated extract from a Sea-spaghetti sample.

Table 1. Operating ICP-MS conditions for total Hg determination and cross reactivity studies and operating HPLC-ICP-MS conditions for Hg speciation

Operating ICP-MS conditions		
Radiofrequency power		1600 W
Gas flows	Nebulization	0.92 mL min^{-1}
	Auxiliary	1.2 mL min^{-1}
	Plasma	16 mL min^{-1}
Standard mode		Ca, Cu, K, Mg, Na, P
KED mode: He flow rate/ 4.0 mL min^{-1}		As, Cd, Co, Cr, Fe, Hg, Pb, Zn
Analytes		^{75}As, ^{43}Ca, ^{111}Cd, ^{59}Co, ^{53}Cr, ^{63}Cu, ^{57}Fe, ^{39}K, ^{202}Hg, ^{26}Mg, ^{23}Na, ^{31}P, ^{208}Pb, ^{66}Zn
Internal standards		^{74}Ge (As, Co, Cr, Fe, and Zn) ^{54}Sc (Ca, K, Mg, Na, and P)
Operation HPLC conditions		
Column		Kinetex C-18 100 A (100×2.10 mm, 5 µm)
Mobile phase		0.4% mercaptoethanol, 10% methanol, pH 2.0
Flow rate		0.3 mL min^{-1}, 8.5 min
Injection volume		50 µL

(a) Auxiliary O_2 only when operating as HPLC-ICP-MS

5.3. RESULTS AND DISCUSSION

5.3.1. MIP-based solid phase extraction

5.3.1.1. Loading conditions: extract pH and loading flow rate

The hydrogen ion amount and the charge distribution on the absorbent surface play an important role in the adsorption of target ions, especially in metal ion speciation [38]. The effect of varying the pH of the extract on the absorption process was investigated in the range from pH 5.0 to 11.0, performing the experiments in triplicate. Briefly, a volume of 10 mL of seaweed extract was spiked with 0.5 µg L^{-1} MeHg standard (pH adjusted with 0.1 M HCl and 0.1 M NH_3OH) and passed through the syringe under non optimized conditions

(loading/elution flow rate of 1.0 mL min^{-1}) and 2.0 mL of 0.8% (v/v) 2-mercaptoethanol and 20% (v/v) methanol (pH 4.5) as an eluting solution [31]. The Hg (II) concentration measured in the eluates and the analytical recovery of MeHg under several pHs are shown in Figure 3(a), and low mercury species retention was observed when the extracts were adjusted at the lowest (acid) pHs. These findings are probably because of the hindrance of H^+ ions. Moreover, the absorption of both Hg(II) and MeHg diminishes at when adjusting the extracts' pHs at the highest values (10 and 11), which might be due to the increase in the concentration of OH^- ions. Hence, a pH 9.0 was selected and used for further optimization of other loading and elution variables. Previous results when pre-concentrating Hg species from seawater revealed optimum pHs within the 8.0-9.0 range [31].

Seaweed extracts (10 mL spiked with 0.5 µg L^{-1} MeHg) at pH 9.0 were loaded at several loading flow rates (0.5, 1.0, and 2 mL min^{-1}) in triplicate (non-optimized elution conditions as shown above were used). Figure 3(b) shows that there were not retention differences in Hg (II) under all tested loading flow rates but improved analytical recoveries for MeHg were obtained at higher loading flow rates. Since flow rates higher than 2.0 mL min^{-1} were not possible with the peristaltic pump used, a flow rate of 2.0 mL min^{-1} was selected.

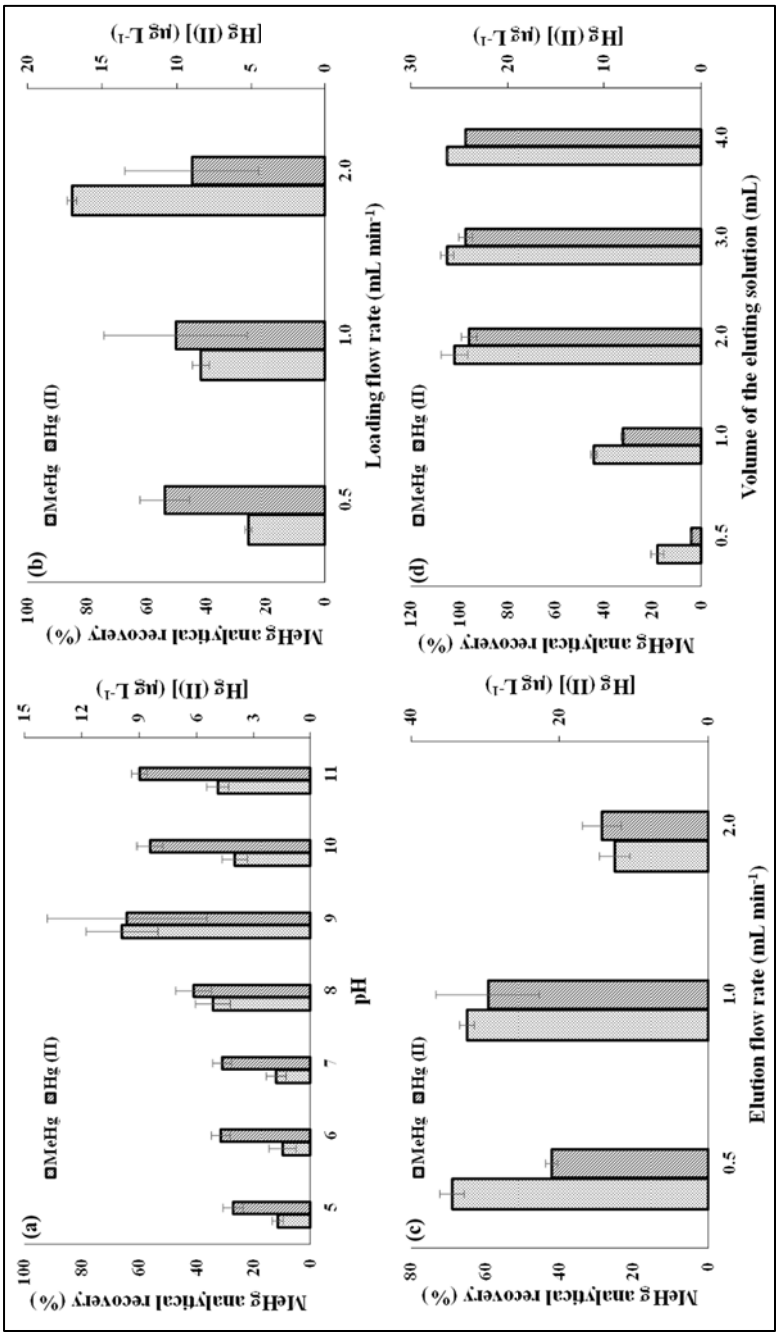

Figure 3. Influence of pH of the seaweed extract (a), loading flow rate (b), elution flow rate (c), and elution volume (d) on the MIP-based SPE of Hg(II) and MeHg

5.3.1.2. Eluting conditions: eluting flow rate and volume of the eluting solution

Several elution speeds (0.5, 1.0 and 2 mL min^{-1}) and elution volumes (0.5, 1.0, 2.0, 3.0 and 4.0 mL) of a 0.8% (v/v) 2-mercaptoethanol and 20% (v/v) methanol (pH 4.5) eluting solution were evaluated. Analytical recoveries of MeHg were similar at 0.5 and 1.0 mL min^{-1} elution flow rates (Figure 3(c)), but the concentration of Hg (II) in the eluate decreased when eluting at 0.5 mL min^{-1}.The highest elution flow rate (2.0 mL min^{-1}) led to poor retention for both MeHg and Hg(II). Therefore, 1.0 mL min^{-1} was selected as the best elution speed for further studies.

Finally, the influence of the volume of the eluting solution has been demonstrated to be quite important (Figure 3(d)) and analytical recoveries of MeHg, and also Hg(II) concentrations are increased for volumes of the eluting solution of 2.0 mL or higher (analytical recovery for MeHg is close to 100% when using the highest volumes). A volume of the eluting solution of 2.0 mL was therefore selected.

5.3.2. Breakthrough volume, mass capacity and reusability

In order to find the maximum volume that can be loaded into the MIP syringes without a breakthrough of the analyte (breakthrough volume), the optimum SPE conditions were applied with varying loading volumes. Aqueous solutions (10, 25, 37.5, 50, and 100 mL at pH 9.0) were spiked with 1 μg L^{-1} of MeHg and Hg (II) standards and were passed through the syringes in triplicate. It was proved that no significant losses of MeHg and Hg (II) took place, not even when a volume of 100 mL of sample was loaded (Figure 4(a)). This finding implies that the MIP could be successfully used as an SPE sorbent for loading high volumes of extracts, and the pre-concentration factor can therefore be quite high.

Mass capacity of the MIP sorbent was calculated by loading volumes of 50 mL (5 aliquots of 10 mL) of aqueous solution (pH 9.0) containing 100 μg L^{-1} of MeHg in triplicate under the optimum conditions. After passing through the syringe, each 10 mL aliquots were collected and analyzed for MeHg. No chromatographic signals were recorded for MeHg in the solutions after being loaded until the

fourth 10 mL aliquot. Taking into account a volume of 30 mL and the amount of MIP used in the experiment, the mass capacity of the MIP was found to be 20±0.13 μg g^{-1}.

The reusability of the MIP absorbent was evaluated with the same set of three syringes and using aqueous standards of 1.0 μg L^{-1} of MeHg and Hg (II) (50 μg L^{-1} after pre-concentration). As shown in Figure 4(b), the analytical recovery of MeHg and Hg (II) was found between 80-100 % at least after performing 15 absorption/desorption cycles. These findings suggest that the same MIP syringe (the same MIP portion) can be reused 15 times without losing its recognition/sorption properties.

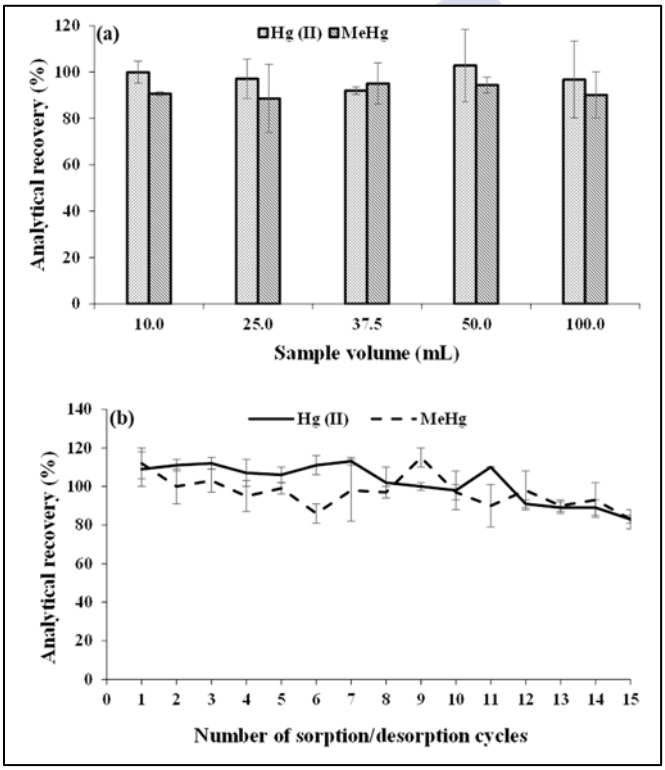

Figure 4. Effect of the sample volume (breakthrough volume of the MIP-based SPE procedure) on the analytical recovery of Hg(II) and MeHg (a), and analytical recovery of Hg(II) and MeHg after several loading/elution cycles (reusability of each MIP portion) (b)

5.3.3. Cross-reactivity

The selectivity of the prepared MIP and NIP for the target compounds (Hg (II) and MeHg) was evaluated by comparing their extraction efficiencies with those of several foreign metal ions. An aqueous 0.1% (v/v) HCl, 0.12% (w/v) L-cysteine, 0.1% (v/v) mercaptoethanol solution (pH 9.0) spiked with 0.04 μg L^{-1} of MeHg and 0.1 μg L^{-1} of Hg (II), As(III), Cd(II), Pb(II), Cr(III), and Co(II) at 2 μg L^{-1}, and Ca(II), Mg(II), Fe(III), Cu(II), Na(I), K(I), and Zn(II)) at 20 μg L^{-1}, was prepared and subjected to the optimized MIP-SPE in triplicate. After eluate evaporation to dryness, the residues were re-dissolved in 600 μL of ultrapure water and analyse by ICP-MS (operating conditions in Table S1, electronic supplementary information). The selectivity was studied by calculating extraction efficiencies, distribution ratios, and selectivity coefficients as shown in Table 2.

According to the results, MIP sorbent favoured the extraction of MeHg and Hg (II) ions and high extraction efficiencies (97% and 95%, respectively) were obtained (Table 2). NIP material showed a low extraction efficiency for target analytes (12% for MeHg and 10% for Hg (II)), which indicates that Hg(II) and MeHg interaction with MIP occurs through the recognition cavities in MIP and not surface absorption (unspecific interactions in NIP). The distribution coefficients for MeHg and Hg (II) have been found to be higher (30 and 19, respectively) than those found for the foreign ions (Table 2), which implies that the imprinting process produces cavities with adequate conformations for the interactions between the target ions (Hg(II) and MeHg) and MIP particles. As a conclusion, the synthesized MIP showed excellent recognition ability and selectivity for MeHg and Hg (II) species.

Table 2. Extraction efficiency, distribution ratio and selectivity coefficients for the IIP and the NIP applied to the SPE of seaweed extract

Ions	Extraction efficiency (E) /%[a]		Distribution ratio (D)[b]		Selectivity coefficient (S)[c]	
	MIP	NIP	MIP	NIP	MIP	NIP
MeHg	96.8	11.7	30	0.13	_	226
Hg (II)	95.0	9.6	19	0.11	2	282
Cd(II)	78.3	0.2	3.61	0.00	8	---[d]
Pb(II)	26.0	0.2	0.35	0.00	85	---[d]
Al(III)	35.6	10.4	0.55	0.12	54	258
Cr(II)	0.9	0.1	0.01	0.00	3249	▫
Fe(III)	5.8	1.2	0.06	0.01	491	2394
Co(II)	0.7	0.2	0.01	0.00	4301	---[d]
Ni(II)	3.1	0.2	0.03	0.00	940	---[d]
Cu(II)	0.4	0.0	0.00	0.00	---[d]	---[d]
Zn(II)	0.5	0.0	0.00	0.00	---[d]	---[d]
As(III)	1.4	0.6	0.01	0.01	---[d]	4654
Na(I)	0.0	0.3	0.00	0.00	---[d]	---[d]
K(I)	0.0	1.7	0.00	0.02	---[d]	1770
Ca(II)	2.5	0.0	0.03	0.00	1174	---[d]
Mg(II)	1.0	0.8	0.01	0.01	3014	3627

(a) $E(\%)=\frac{A_2}{A_T}x100$

(b) $D=\frac{A_2}{A_1}$

(c) $S_{MeHg/M}=\frac{D_{MeHg}}{D_M}$

(d) Not calculated

A_1 = Analyte concentration at equilibrium

A_2 = Analyte concentration enriched by IIP/NIP SPE at equilibrium

A_T = Total analyte concentration

M = Hg(II), Cd(II), Pb(II), Al(III), Cr(III), Fe(III), Co(II), Ni(II), Cu(II), Zn(II), As(III), Na(I), K(I), Ca(II), Mg(II)

5.3.4. Calibration and matrix effect

Many studies on analytical troubleshooting have focused on the problems which arise due to matrix effects, mainly signal suppression/enhancement in the presence of matrix concomitants. Matrix effects on MeHg and Hg (II) have been estimated by comparing the slopes of mobile phase (0.4% (v/v) 2-mercaptoethanol and 10% (v/v) methanol, pH 2.0) matched calibration curves and standard addition curves (solutions prepared from seaweed extracts spiked with variable MeHg and Hg(II) concentrations and subjected to the MIP-based SPE procedure described in section 5.2.5.). Matched calibrations and standard addition calibrations cover five concentration levels within the 0-20 μg L^{-1} range for MeHg and 0-50 μg L^{-1} range for Hg (II) (regarding standard addition calibrations, the MeHg and Hg(II) concentrations have been calculated taking into account a pre-concentration factor of 50). The mean slopes obtained for calibrations (experiments in triplicate) were 3012±547 and 4987±166 for MeHg and Hg (II), respectively; whereas, mean slopes for the standard addition calibration were 3048±142 for MeHg and 5322±174 for Hg (II). There was not a statistically significant differences between the slopes of the standard addition calibration graphs and the slopes of aqueous standard calibration graphs ($p>0.05$), which means that the matrix effect is negligible in this procedure.

The EU has established that a correlation coefficient higher than 0.9980 is required to obtain satisfactory linearity using confirmatory methods [39]. Acceptable linearity was obtained for the aqueous calibration and standard addition curves for both Hg (II) and MeHg (correlation coefficients higher than 0.999).

5.3.5. Limit of detection and limit of quantification

The limit of detection (LOD) was calculated as 3 times the standard deviation (3 σ) of eleven replicate measurements of the blank sample, while the limit of quantification (LOQ) was calculated as 10 times the standard deviation (10 σ). Therefore, eleven reagent blank samples were prepared and treated as described in section 5.2.5, and the analytical responses were then expressed as concentrations dividing by the mean slope of the calibration graph. LOD and LOQ values

referred to the mass sample (seaweed) were calculated after considering the pre-concentration factor of 50 of the MIP-based SPE process. The calculated LODs were 0.007 and 0.02 μg kg^{-1} dw (dry weight) for MeHg and Hg (II), respectively, whereas, LOQs were 0.02 and 0.07 μg kg^{-1} dw for MeHg and Hg (II), respectively. These LODs are much better than some published LODs for Hg assessment in seaweed such as 0.120 μg kg^{-1} for MeHg by pre-concentration and HPLC-CV-AFS [23], 1.3 μg kg^{-1} for MeHg in cyanobacteria [40], and 0.01 mg kg^{-1} dw for MeHg using an automatic Hg analyzer [41]. The LOD obtained by Morrison *et al.* [24] was 0.435 μg kg^{-1} ww using the 1630 USEPA method, while the LOD for biota obtained by Shoham-Frider *et al*. [27] was 0.07 μg kg^{-1} dw.

On the other hand, the Regulation No 464/2018 of the European Parliament and the Council establishes the maximum residue level (MRL) for Hg in algae, prokaryotic organisms, and food products based on seaweed as 0.01 mg kg^{-1} [42], much higher than the LOD value found in the present study which implies that the propose method can be applied to the analysis of commercial edible seaweed.

5.3.6. Repeatability, reproducibility, and accuracy

Reproducibility (inter-day assay) and repeatability (intraday assay) were studied using seaweed extracts spiked with MeHg and Hg (II) at different concentration levels. Inter-day assay was performed by spiking seven seaweed extracts with three concentration levels of MeHg (0.02, 0.1, 0.4 μg L^{-1}; i.e. concentrations of 1, 5, and 20 μg L^{-1} after pre-concentration), and three Hg (II) concentration levels (0.04, 0.2, 1 μg L^{-1}; i.e., 2, 10, 50 μg L^{-1} after pre-concentration) and measuring the seven replicates of each concentration level in the same day. Intraday assay was performed by preparing seven standard addition curves in seven different days by spiking in triplicate several seaweed extract aliquots at five concentration levels of MeHg (1, 2, 5, 10 and 20 μg L^{-1} after pre-concentration) and Hg (II) (2, 5, 10, 20 and 50 μg L^{-1} after pre-concentration). As it can be observed in Table 3, good analytical recovery and precision is obtained since all analytical recoveries ranged between 89-112% for MeHg and 86-108% for Hg (II),

and the relative standard deviations (RSDs) were lower than 20% (13% for MeHg and 16% for Hg (II) for all concentration levels).

Table 3. Inter-day and intraday analytical recovery and precision (RSD)

	MeHg			Hg(II)		
	Concentration μg L^{-1}	Analytical recovery %	RSD %	Concentration μg L^{-1}	Analytical recovery %	RSD %
Interday	1	112±8	8	2	86±10	12
	5	97±13	13	10	108±18	16
	20	98±10	10	50	102±8	8
Intraday	1	94±7	6	2	98±8	8
	2	92±9	9	5	100±7	7
	5	89±7	9	10	102±10	10
	10	89±8	9	20	102±4	4
	20	95±6	6	50	97±5	4

In addition to the analytical recovery, accuracy of the developed method was also tested by analysing a BCR 463 (tuna fish) CRM (a CRM for total Hg and/or Hg species in seaweed is not commercially available). After BCR 463 UAE and MIP-based SPE (section 5.2.4 and 5.2.5) and ICP-MS determination, a total Hg content of 3.01±0.06 mg kg^{-1} was obtained, which is in good agreement with the certified value (2.85±0.16 mg kg^{-1}). HPLC-ICP-MS analysis gave a Hg(II) concentration of 0.01±0.001 mg kg^{-1}, and a MeHg concentration of 2.86±0.05 mg kg^{-1}. The found MeHg concentration is in good agreement with certified MeHg content in BCR 463 (3.01±0.06 mg kg^{-1}). In addition, the total Hg concentration as a sum of Hg(II) and MeHg concentrations after HPLC-ICP-MS (2.87±0.07 mg kg^{-1}) also agrees with the certified total Hg content in BCR 463 (2.85±0.16 mg kg^{-1}).

5.3.7. Applications

Three edible seaweed samples were subjected to the optimized MIP-based SPE after UAE extraction and before HPLC-ICP-MS (Hg(II)

and MeHg assessment) and ICP-MS (total Hg assessment) analysis. Results are given in Table 4 and it can be observed that the results obtained by HPLC-ICP-MS (sum of the species) are in good agreement with the total Hg concentration levels measured directly in the eluates by ICP-MS. Hg (II) is the major species in the tested seaweed sample, and the highest Hg (II) content was recorded in sea spaghetti species (0.11±0.02 mg kg^{-1} dw).

Table 4. Mercury species concentration in BCR-463 and in commercial seaweed samples

Sample	Hg (II) mg kg^{-1a}	MeHg mg kg^{-1a}	tHg mg kg^{-1b}	tHg mg kg^{-1c}
Wakame	0.06±0.01	0.01±0.002	0.07±0.01	0.07±0.01
Sea-spaghetti	0.11±0.02	0.06±0.02	0.17±0.03	0.19±0.02
Hijiki	0.06±0.01	0.01±0.002	0.07±0.01	0.06±0.003

(a) Hg(II) and MeHg concentrations after MIP-based SPE and HPLC-ICP-MS determination
(b) Total Hg expressed as the sum of Hg (II) and MeHg concentrations after MIP-based SPE and HPLC-ICP-MS determination
(c) Total Hg after MIP-based SPE and ICP-MS determination

5.4. CONCLUSIONS

The molecularly imprinted polymer based on the interaction between MeHg (template) and phenobarbital (complexing agent) was found to offer excellent recognition capabilities for MeHg and Hg(II). The MIP-based SPE procedure is robust since large sample volumes (seaweed extracts) can be loaded without impairment of the analytical performance. High pre-concentration factors can be therefore achieved, which implies quite sensitive determinations. The prepared material has demonstrated a large absorption capacity and stability, and each 200 mg portions can be reused at least fifteen times (fifteen absorption/desorption cycles). The optimized MIP-based SPE combined with HPLC-ICP-MS allows low limits of detection, and the methodology can be successfully applied for quantifying mercury

species (MeHg and Hg(II)) at very low concentrations in complex samples such as seaweeds.

5.5. ACKNOWLEDGEMENTS

This work was supported by the *Dirección Xeral de I + D –Xunta de Galicia*: *Grupos de Referencia Competitiva*, project number ED431C2018/19; and Development of a Strategic Grouping in Materials – AEMAT, grant ED431E2018/08.

5.6. REFERENCES

[1] C.S. Kumar, P. Ganesan, P. Suresh, N. Bhaskar, Seaweeds as a source of nutritionally beneficial compounds-a review, Journal of Food Science and Technology 45 (2008) 1-13.

[2] F. Ferdouse, S.L. Holdt, R. Smith, P. Murua, Z. Yang, The global status of seaweed production, trade and utilization, Food and Agriculture Organization of the United Nations, 124 (2018). http://www.fao.org/in-action/globefish/publications/details-publication/en/c/1154074/, Accessed February 19th 2020.

[3] C. Dawczynski, R. Schubert, G. Jahreis, Amino acids, fatty acids, and dietary fibre in edible seaweed products, Food Chemistry 103 (2007) 891-899.

[4] A. Bocanegra, S. Bastida, J. Benedi, S. Rodenas, F.J. Sanchez-Muniz, Characteristics and nutritional and cardiovascular-health properties of seaweeds. Journal of Medicinal Food 12 (2009) 236-258.

[5] M.C. Taboada, R. Millán, M.I. Miguez, Nutritional value of the marine algae wakame (*Undaria pinnatifida*) and nori (*Porphyra purpurea*) as food supplements, Journal of Applied Phycology 25 (2013) 1271-1276.

[6] V. Besada, J.M. Andrade, F. Schultze, J.J. González, Heavy metals in edible seaweeds commercialised for human consumption, Journal of Marine Systems 75 (2009) 305-313.

[7] C. van Netten, S.A. Hoption Cann, D.R. Morley, J.P. van Netten, Elemental and radioactive analysis of commercially available seaweed, Science of the Total Environment 255 (2000) 169-175.

[8] D. García-Rodríguez, A.M. Carro, R. Cela, R.A. Lorenzo, Microwave-assisted extraction and large-volume injection gas chromatography tandem mass spectrometry determination of multiresidue pesticides in edible seaweed, Analytical and Bioanalytical Chemistry 398 (2010) 1005-1016.

[9] M.M. Chen, L. Lopez, S.P. Bhavsar, S. Sharma, What's hot about mercury? Examining the influence of climate on mercury levels in Ontario top predator fishes, Environmental Research 162 (2018) 63-73.

[10] World Health Organization, Mercury and health (2017), https://www.who.int/news-room/fact-sheets/detail/mercury-and-health. Accessed February 19th 2020.

[11] Agency for Toxic Substances and Disease Registry. ATSDR's Substance Priority List (2017). https://www.atsdr.cdc.gov/SPL/. Accessed February 19th 2020.

[12] S.C.T. Nicklisch, L.T. Bonito, S. Sandin, A. Hamdoun, Mercury levels of yellowfin tuna (*Thunnus albacares*) are associated with capture location, Environmental Pollution 229 (2017) 87-93.

[13] B.K.K.K. Jinadasa, S.W. Fowler, Critical review of mercury contamination in Sri Lankan fish and aquatic products, Marine Pollution Bulletin 149 (2019) 110526.

[14] S. Paz, C. Rubio, I. Frías, Á.J. Gutiérrez, D. González-Weller, V. Martín, C. Revert, A. Hardisson, Toxic metals (Al, Cd, Pb and Hg) in

the most consumed edible seaweeds in Europe, Chemosphere 218 (2019) 879-884.

[15] M.Y. Roleda, H. Marfaing, N. Desnica, R. Jónsdóttir, J. Skjermo, C. Rebours, U. Nitschke, Variations in polyphenol and heavy metal contents of wild-harvested and cultivated seaweed bulk biomass: Health risk assessment and implication for food applications, Food Control 95 82019) 121-134.

[16] R. Fernández-Martínez, I. Rucandio, I. Gómez-Pinilla, F. Borlaf, F. García, M.T. Larrea, Evaluation of different digestion systems for determination of trace mercury in seaweeds by cold vapour atomic fluorescence spectrometry, Journal of Food Composition and Analysis 38 (2015) 7-12.

[17] G.D.T.M Jayasinghe, B.K.K.K. Jinadasa, S.D.M. Chinthaka, Nutritional composition and heavy metal content of five tropical seaweeds, Open Science Journal of Analytical Chemistry 3 (2018) 17-22.

[18] A. Moreda-Pineiro, E. Peña-Vázquez, P. Bermejo-Barrera, Significance of the presence of trace and ultratrace elements in seaweeds. In S.-K. (Ed) Kim, Handbook of Marine Macroalgae: Biotechnology and Applied Phycology, Wiley-Blackwell (2012), Chichester, UK, pages 116-170.

[19] A.M. Fernández-Fernández, A. Moreda-Piñeiro, P. Bermejo-Barrera, On-line preconcentration cold vapour atomic absorption spectrometry for the determination of trace mercury in edible seaweeds, Journal of Analytical Atomic Spectrometry 22 (2007) 573-577.

[20] E. Najafi, F. Aboufazeli, H.R. Lotfi Zadeh Zhad, O. Sadeghi, V. Amani, A novel magnetic ion imprinted nano-polymer for selective separation and determination of low levels of mercury(II) ions in fish samples, Food Chemistry 141 (2013) 4040-4045.

[21] Z. Zhang, J. Li, X. Song, J. Ma, L. Chen, Hg^{2+} ion-imprinted polymers sorbents based on dithizone–Hg^{2+} chelation for mercury speciation analysis in environmental and biological samples, RSC Advances 4 (2014) 46444-46453.

[22] H.R. Rajabi, M. Shamsipur, M.M. Zahedi, M. Roushani, On-line flow injection solid phase extraction using imprinted polymeric nanobeads for the preconcentration and determination of mercury ions, Chemical Engineering Journal 259 (2015) 330-337.

[23] C.C Brombach,. Z. Gajdosechova, B. Chen, A. Brownlow, W.T. Corns, J. Feldmann, E.M. Krupp, Direct online HPLC-CV-AFS method for traces of methylmercury without derivatisation: A matrix-independent method for urine, sediment and biological tissue samples, Analytical and Bioanalytical Chemistry 407 (2015) 973-981.

[24] R.J. Morrison, P.J. Peshut, R.J. West, B.K. Lasorsa, Mercury (Hg) speciation in coral reef systems of remote Oceania: Implications for the artisanal fisheries of Tutuila, Samoa Islands, Marine Pollution Bulletin 96 (2015) 41-56.

[25] M. Meng, R.Y. Sun, H.W. Liu, B. Yu, Y.G. Yin, L.G. Hu, J.B. Chen, J.B. Shi, G.B. Jiang, Mercury isotope variations within the marine food web of Chinese Bohai Sea: Implications for mercury sources and biogeochemical cycling, Journal of Hazardous Materials 384 (2020) 121379.

[26] United States Environmental Protection Agency, Methyl mercury in water by distillation, aqueous ethylation, purge and trap, and CVAFS. Method 1630 (2001).

[27] E. Shoham-Frider, Y. Gertner, T. Guy-Haim, B. Herut, N. Kress, E. Shefer, J. Silverman, Legacy groundwater pollution as a source of mercury enrichment in marine food web, Haifa Bay, Israel, Science of the Total Environment 714 (2020) 136711.

[28] R. Rodríguez-Fernández, E. Peña-Vázquez, P. Bermejo-Barrera, Synthesis of an imprinted polymer for the determination of methylmercury in marine products, Talanta 144 (2015) 636-641.

[29] T.P. Rao, R. Kala, S. Daniel, Metal ion-imprinted polymers - Novel materials for selective recognition of inorganics, Analytica Chimica Acta 578 (2006) 105-116.

[30] B.K.K.K. Jinadasa, E. Peña-Vázquez, P. Bermejo-Barrera, A. Moreda-Piñeiro, New adsorbents based on imprinted polymers and composite nanomaterials for arsenic and mercury screening/speciation: A review, Microchemical Journal 156 (2020) 104886.

[31] M.P. Rodríguez-Reino, R. Rodríguez-Fernández, E. Peña-Vázquez, R. Domínguez-González, P. Bermejo-Barrera, A. Moreda-Piñeiro, Mercury speciation in seawater by liquid chromatography-inductively coupled plasma-mass spectrometry following solid phase extraction pre-concentration by using an ionic imprinted polymer based on methyl-mercury–phenobarbital interaction, Journal of Chromatography A 1391 (2015) 9-17.

[32] I. Dakova, T. Yordanova, I. Karadjova, Non-chromatographic mercury speciation and determination in wine by new core–shell ion-imprinted sorbents. Journal of Hazardous Materials 231-232 (2012) 49-56.

[33] M. Andaç, S. Mirel, S. Şenel, R. Say, A. Ersöz, A. Denizli, Ion-imprinted beads for molecular recognition based mercury removal from human serum, International Journal of Biological Macromolecules 40 (2007) 159-166.

[34] M. Karimi, F. Aboufazeli, H.R.L.Z. Zhad, O. Sadeghi, E. Najafi, Potentiometric determination of mercury ions by ion imprinted polymer coated multiwall carbon nanotube: High selective sensor for

determination of trace amounts of mercury ions in biological samples, Oriental Journal of Chemistry 28 (2012) 1557-1566.

[35] H.R. Rajabi, M. Roushani, M. Shamsipur, Development of a highly selective voltammetric sensor for nanomolar detection of mercury ions using glassy carbon electrode modified with a novel ion imprinted polymeric nanobeads and multi-wall carbon nanotubes, Journal of Electroanalytical Chemistry 693 (2013) 16-22.

[36] C. Rubio, G. Napoleone, G. Luis-González, A.J. Gutiérrez, D. González-Weller, A. Hardisson, C. Revert, Metals in edible seaweed, Chemosphere 173 (2017) 572-579.

[37] H. Liu, J. Luo, T. Ding, S. Gu, S. Yang, M. Yang, Speciation analysis of trace mercury in sea cucumber species of *Apostichopus japonicus* using high-performance liquid chromatography conjunction with inductively coupled plasma mass spectrometry, Biological Trace Element Research 186 (2018) 554-561.

[38] A. Mollahosseini, A. Khadir, J. Saeidian, Core–shell polypyrrole/Fe_3O_4 nanocomposite as sorbent for magnetic dispersive solid-phase extraction of Al^{+3} ions from solutions: investigation of the operational parameters, Journal of Water Process Engineering 29 (2019) 100795.

[39] Directive, I. C. 2002. 96/23/EC concerning the performance of analytical methods and the interpretation of results. Off J Eur Communities, 221, 8-36.

[40] L.A. Mendes, M.W. Franco, F.A.R. Barbosa, P.I.A. de Carvalho, J.C. de Lena, C.C. Windmöller, Determination of methylmercury in sediment and cyanobacteria samples: method validation and application to methylation investigation, Analytical Methods 10 (2018) 91-100.

[41] A.L. Maulvault, P. Anacleto, V. Barbosa, J.J. Sloth, R.R. Rasmussen, A. Tediosi, M. Fernandez-Tejedor, F.H.M. van den Heuvel, M. Kotterman, A. Marques, Toxic elements and speciation in seafood samples from different contaminated sites in Europe, Environmental Research 143 (2015) 72-81.

[42] EU/EC 2018. Commission Regulation (EU) No 464/2018 of 19 March 2018 on the monitoring of metals and iodine in seaweed, halophytes and products based on seaweed. Official Journal of the European Union, 78, 16-18.

5.7. ELECTRONIC SUPPLEMENTARY INFORMATION (ESI)

Table S1. Operating ICP-MS conditions for total As determination in acid digests from fish samples, and for P, K, Ca, Mg, Na, Zn, Co, Fe, Cr, Pb, Hg, Cd, and Cu determination in cross reactivity studies.

Operating ICP-MS conditions		
Radiofrequency power		1600 W
Gas flows	Nebulization	0.92 mL min^{-1}
	Auxiliary	1.2 mL min^{-1}
	Plasma	16 mL min^{-1}
Standard mode		Ca, Cu, K, Mg, Na, P
KED mode: He flow rate/ 4.0 mL min^{-1}		As, Cd, Co, Cr, Fe, Hg, Pb, Zn
Analytes		^{75}As, ^{43}Ca, ^{111}Cd, ^{59}Co, ^{53}Cr, ^{63}Cu, ^{57}Fe, ^{39}K, ^{202}Hg, ^{26}Mg, ^{23}Na, ^{31}P, ^{208}Pb, ^{66}Zn
Internal standards		^{74}Ge (As, Co, Cr, Fe, and Zn) ^{54}Sc (Ca, K, Mg, Na, and P) ^{103}Rh (Cd, Hg, and Pb)

IV. CONCLUSIONS

USC
UNIVERSIDADE
DE SANTIAGO
DE COMPOSTELA

Development of fast methodology for analysis and speciation of mercury and arsenic in foodstuff

Considering the initial objectives of this Thesis, the general conclusions that can be outlined are the following:

1. Development of fast and low-cost analytical methodologies for assessing total inorganic arsenic (iAs) by using Quantum Dots (QDs) and Ionic Imprinted Polymer (IIP) based Solid Phase Extraction (SPE) methodologies for iAs speciation in foodstuff

1.1. There are several difficulties to use high-end technological instrumentation mainly due to these pieces of equipment are associated with high cost, need for training people to handle the equipment, and need for maintaining special environmental conditions to achieve the best performance. Therefore, simple and low-cost screening techniques to detect and quantify toxic trace elements such as As in food samples are needed. Quantum Dots (QDs) exhibit luminescent properties which can be used as a sensing probe.

In **Chapter 1**, a nanosensor probe based on IIP-QDs has been used to assess iAs contents in fish samples by Room Temperature Phosphorescence (RTP). The synthesized IIP over the Mn-doped ZnS QDs enhances selectivity for As(III) and As(V) and the analytical response (RTP quenching) is only attributed to the presence of iAs. In addition, the use of siliceous materials during the synthesis of the IIP-QD composite has found to give robustness to the prepared material under drastic acid conditions (required for template removal). The developed method was successfully applied for iAs assessment in fish, and the obtained results were comparable to those obtained after confirmatory analysis (iAs speciation by High Performance Liquid Chromatography – Inductively Coupled Plasma – Mass Spectrometry, HPLC-ICP-MS).

1.2. The synthesized IIP as an absorbent in SPE procedures has been found to be quite selective for iAs. Since iAs concentration in fish is very low (the major As species concentration in fish is the non-toxic arsenobetaine) the selective enrichment of iAs by the prepared IIP has allowed a reliable assessment of As(III) and As(V) species by HPLC-ICP-

MS without interferences of the major As species. Two different pre-concentration schemes have been developed: a conventional column SPE procedure which was applied for iAs assessment in fish (**Chapter 2**), and a micro-solid phase extraction (μ-SPE) procedure (a vortex assisted dispersive micro solid-phase extraction, VA-D-μ-SPE) which was used for iAs speciation in rice (**Chapter 3**). The developed procedures offer the advantages of SPE (μ-SPE) techniques (green process since the low amounts of organic solvents/reagents are required). Moreover, the use of IIPs provides high selectivity for As (III) and As (V). The vortex assisted D-μ-SPE offers as an advantage the quick extraction process as well as the possibility of reusing several times the absorbent.

2. Development of fast and low-cost analytical methodologies for assessing total Hg (tHg) by using Quantum Dots (QDs) and Molecularly Imprinted Polymer (MIP) based Solid Phase Extraction (SPE) methodologies for Hg speciation in foodstuff

2.1. In **Chapter 4**, a nanosensor probe based on a phenobarbital-based MIP – silica coated Mn doped ZnS QDs composite has been developed for selective recognition of tHg (Hg(II) plus MeHg) in fish samples. The strategy was based on covering the QDs with a specific ligand (phenobarbital) for recognizing Hg ions. Phenobarbital was used as a ligand that shows a high and selective affinity for Hg ions. The developed RTP nanoprobe allows a low-cost assessment of tHg in fish, and the obtained results are comparable with those obtained after ICP-MS determinations.

2.2. A MIP has been synthesized by using a ternary pre-polymerization mixture containing the template (MeHg), a non-vinylated monomer (phenobarbital), and a vinylated monomer (methacrylic acid), and a selective column SPE process was optimized for Hg speciation in seaweed by HPLC-ICP-MS (**Chapter 5)**. The optimized MIP-SPE procedure allowed the selective pre-concentration of low amounts of Hg species (Hg(II) and MeHg) from seaweed extracts, and has been found to be robust since large sample volumes (seaweed extracts) can be loaded without impairment of the analytical performance. In addition, the prepared MIP exhibits a large adsorption capacity and stability, and each 200 mg MIP

portions can be reused at least fifteen times. The MIP-based SPE – HPLC-ICP-MS allows low limits of detection, and the methodology can be successfully applied for quantifying MeHg and Hg(II) at very low concentrations in complex samples such as seaweeds

USC
UNIVERSIDADE
DE SANTIAGO
DE COMPOSTELA

V. ANNEX I

RESUMEN Y DISCUSIÓN

Resumen y discusión

Los alimentos son la principal fuente de exposición a los metales esenciales y no esenciales (metales pesados) en los seres vivos. El comercio internacional y la globalización de las fuentes de alimentos, junto con el desarrollo industrial de fertilizantes y la contaminación de las aguas de riego, ha incrementado la presencia de metales pesados en los alimentos, y por tanto, el potencial riesgo para la salud tanto en países desarrollados como en países en desarrollo. Ciertos metales, como el arsénico (As) y el mercurio (Hg), no tienen ninguna actividad biológica en los seres vivos; y por el contrario, se ha demostrado que provocan un deterioro de la salud y enfermedades que pueden desembocar en la muerte. Sin embargo, la toxicidad y la biodisponibilidad de estos elementos dependen de varios factores, incluida la concentración y la forma química (especie química).

El mercurio se considera uno de los contaminantes ambientales de mayor prioridad a escala mundial. La toxicidad del mercurio es conocida desde la antigüedad, y la toxicidad del metilmercurio (MeHg) en humanos se observó por primera vez en Minamata (Japón) en 1955, y después en Niigata (Japón), tras el consumo de pescado contaminado con metilmercurio (MeHg). El origen de esta contaminación por MeHg se debió en ambos casos a descargas de Hg (hasta el 70% de mercurio estaba en forma metilada) a las aguas de los estuarios por parte de fábricas químicas tras el empleo de mercurio inorgánico (Hg(II)) durante el proceso tecnológico para producción de acetaldehído. Posteriormente, se comprobó también la biometilación del Hg(II) por parte del plancton marino. La contaminación de los sistemas terrestres por compuestos de Hg utilizados en la agricultura como fungicidas y desinfectantes de semillas representa también un problema a gran escala. Así, existen evidencias de intoxicaciones por ingestión de semillas tratadas con fungicidas a base de alquilmercurio. Durante la década de 1960 se observó acumulación de Hg en la biota terrestre y marina, haciendo evidente que el problema de la contaminación por Hg era mucho más extenso que una situación local aguda aislada, como Minamata y Niigata. De esta forma, y ya en la década de 1970, países como Estados Unidos y Canadá establecieron restricciones a la comercialización y consumo de pescado con niveles

de Hg superiores a 0,5 mg kg^{-1} en peso húmedo. El mercurio es uno de los metales traza que presenta uno de los más altos niveles de biomagnificación en la cadena trófica, y muchas directivas de agencias y organizaciones internacionales, nacionales y regionales regulan las emisiones de Hg. Debe enfatizarse que el papel del desarrollo de métodos sensibles y específicos para la especiación y análisis de Hg jugó un papel importante para una mejor comprensión de los efectos del Hg en los seres vivos.

Durante muchos siglos, la palabra "arsénico" tuvo el significado de "veneno", connotación que cambió a finales del siglo XX debido, en parte, a la introducción de ciertos medicamentos que contenían arsénico (As). La Agencia para el Registro de Sustancias Tóxicas y Enfermedades de los Estados Unidos (*Agency for Toxic Substances and Disease Registry*, ATSDR) sigue clasificando al As dentro de la lista de sustancias toxicas prioritarias (actualización de 2017), mientras que la Agencia Internacional para la Investigación del Cáncer (*International Agency for Research on Cancer*, IARC) ha clasificado el arsénico como un carcinógeno humano. Las diferentes toxicidades de los compuestos que contienen As se hicieron evidentes cuando se demostró que los compuestos organoarsénicos (oAs), que son las principales especies de As en alimentos de origen marino, son casi 100 veces menos tóxicas que el arsénico inorgánico (iAs). El arsénico está presente de forma natural a niveles traza en el aire, el agua, el suelo y en la biota. Sin embargo, las concentraciones naturales de As pueden elevarse principalmente por actividades humanas y ciertos fenómenos naturales, los cuales pueden plantear serios problemas de salud pública. Los compuestos arsenicales utilizados en la industria agroquímica comenzaron en la década de 1970, y sus usos se focalizaron en la conservación de la madera y en la formulación de insecticidas, pesticidas y herbicidas. Actualmente, el As se utiliza ampliamente en la industria electrónica como arseniuro de galio y gas arsina en la preparación de semiconductores. Además, se emplea como alguicida, como agente desecante en la cosecha mecánica de algodón, en la fabricación de vidrio y aleaciones no ferrosas, y en la industria de piensos como aditivo. En general, el iAs [las especies de As en estados de oxidación +3 y +5 (As (III) y As (V)), es más tóxico

que el oAs. Además, el As (III) es más tóxico que As (V). Sin embargo, el ácido dimetil arsónico (DMA) y el ácido monometil arsónico (MMA) son más tóxicos que las especies de As de partida. Por el contrario, compuestos como la arsenobetaína (AB), la arsenocolina (AC), los arsenoazúcares (*arsenosugars*, ASs) y los arsenolípidos (*arsenolipids*, ALs), que contribuyen con aproximadamente el 80% del total de As en productos marinos, son inocuos. Por lo tanto, la determinación de las distintas especies o formas de As en alimentos es un factor importante a considerar en los estudios de evaluación de riesgos y salud humana.

El análisis de especiación es una actividad habitual en muchos laboratorios especializados. La Unión Internacional de Química Pura y Aplicada (*International Union of Pure and Applied Chemistry*, IUPAC) define el término especiación como "la actividad analítica de identificar y medir la cantidad de una o más especies químicas individuales en una muestra". Se han desarrollado varios métodos de especiación empleando distintas técnicas instrumentales; entre éstas, destacan las técnicas híbridas que implican la combinación de una técnica de separación cromatográfica o electroforética y una técnica de espectrometría, fundamentalmente de espectrometría de masas atómicas. En general, estas técnicas ofrecen una especiación elemental rápida y con límites de detección muy bajos; sin embargo, la mayoría implican una instrumentación de alto coste y especialización técnica. Este inconveniente ha llevado al desarrollo de métodos de cribado (*screening*) empleando instrumentación analítica más accesible y económica; y en este sentido, el desarrollo de nanomateriales se ha convertido en una pieza clave. Además de los nanomateriales con propiedades electroquímicas para el desarrollo de métodos eléctricos de análisis, los nanocristales coloidales semiconductores (denominados quantum dots, QDs) se han constituido como fase sensoras ideales para el desarrollo de sensores químicos luminiscentes. La alta sensibilidad analítica de las técnicas luminiscentes combinada con el incremento de selectividad de los QDs al modificarlos en superficie con determinados compuestos ofrece una posibilidad económica para llevar a cabo determinaciones de metales y especies organometálicas. Los polímeros sintéticos basados en las

técnicas de impronta molecular/iónica (*molecularly imprinted polymers/ionic imprinted polymers*, MIPs/IIPs) ofrecen una alta selectividad debido a las cavidades de reconocimiento específicas generadas en los mismos hacia el analito plantilla, y de esta forma la detección luminiscente (fundamentalmente espectrofluorimetría) empleando compositos MIP/IIP-QDs como fases quimiosensoras está en pleno desarrollo.

Los procedimientos para la determinación del contenido total de un elemento y de los niveles de sus distintas especies químicas requiere de tres etapas principales que incluye (1) aislamiento de las especies de interés con o sin etapa de preconcentración; (2) separación de las distintas formas químicas; y (3) cuantificación de cada especie. Existen muchos enfoques para la extracción y preconcentración previa de metales/especies metálicas en distintos tipos de muestras. Mientras que los procedimientos de descomposición de la muestra, fundamentalmente aquellos basados en digestiones ácidas, son los más empleados para una posterior determinación del contenido total del elemento, los métodos de extracción y preconcentración clásicos más comunes para especies organometálicas en muestras sólidas son la extracción asistida por ultrasonidos (*ultrasound assisted extraction*, UAE), la extracción asistida por Soxhlet (*Soxhlet assisted extraction*, SAE), la extracción acelerada con solventes (*accelerated solvent extraction*, ASE) y la extracción asistida por microondas (*microwave assisted extraction*, MAE). Para muestras líquidas, o bien para extractos obtenidos de muestras sólidas, las técnicas de extracción y/o preconcentración más habituales son la extracción en fase sólida (*solid phase extraction*, SPE) y la extracción líquida basada en solventes (*solvent based liquid extraction*, SBLE). Las técnicas de microextracción (*microextraction techniques*, MET) se introdujeron en la década de 1990 con el desarrollo de la microextracción en fase sólida (*solid phase microextraction*, SPME). A partir de la introducción de la técnica SPME, se desarrollaron distintos enfoques encaminados a la miniaturización de las técnicas convencionales de extracción. El conjunto de estas técnicas presenta como ventajas una alta reducción del tiempo de operación, una mayor facilidad de automatización, y una reducción considerable de los volúmenes

(masa) de muestras y, fundamentalmente, de los volúmenes de disolventes extractantes. Este último aspecto es importante en el concepto de Química Verde, siendo un conjunto de prácticas a implementar en los laboratorios analíticos. La hibridación o combinación de distintos procedimientos MET entre sí o con técnicas de extracción convencionales (*combined microextraction techniques*, CMET) es otra área importante de trabajo de cara al desarrollo de procedimientos de pretratamiento de la muestra modernos y robustos.

En la presente memoria de Tesis Doctoral se presenta una discusión crítica de nuevos materiales basados en MIPs e IIPs y en nanopartículas, empleados como absorbentes en SPE o como fases sensoras, para la determinación/especiación de As y Hg en alimentos (Introducción 2). Posteriormente, se discuten los resultados obtenidos en la síntesis y empleo de compositos MIP/IIP-QDs como fases sensoras para el cribado de iAs (Capítulo 1) y Hg total (Capítulo 4) por espectrometría de fosforescencia a temperatura ambiente (*room temperature phosphorescence*, RTP). La preparación de nuevos absorbentes para la preconcentración selectiva de iAs basada en IIPs, así como la especiación de iAs por cromatografía líquida hibridada a espectrometría de masas con plasma acoplado por inducción (*high performance liquid chromatography – inductively coupled plasma – mass spectrometry*, HPLC-ICP-MS) se detallan en el Capítulo 2 (procedimiento SPE en columna para la especiación de iAs en productos de la pesca) y en el Capítulo 3 (procedimiento de microextración dispersiva para la especiación de iAs en arroz). Finalmente, en el Capítulo 5 se muestra la metodología IIP para la especiación de Hg (Hg(II) y MeHg) en algas comestibles.

En la Introducción se discute la bibliografía existente sobre el empleo de MIPs e IIPs como absorbentes para la preconcentración de As y Hg haciendo especial hincapié en las metodologías de eliminación del ion plantilla y su relación con el tipo de monómero empleado (monómero bifuncional o monómero vinilado asociado a un reactivo complejante). Se revisa también la bibliografía relativa a nanopartículas de oro y plata en el desarrollo de métodos de cribado colorimétricos, basados fundamentalmente en mecanismos de agregación-dispersión; y en el empleo de nanomateriales a base de

carbono (*carbon dots*, CDs) y QDs en el desarrollo de fases sensoras para cribado luminiscente. En relación a los QDs, se discute la mejora de la selectividad de la respuesta luminiscente en función de la modificación en superficie de estas nanopartículas, proponiendo las ventajas de una modificación con MIPs/IIPs.

El método de cribado luminiscente desarrollado para iAs (Capítulo 1) se basa en un composito IIP-QDs cuya preparación requirió la síntesis de QDs de base ZnS dopado con Mn (Mn-ZnS QDs) modificados en superficie con un IIP (arseniato como ion plantilla y 1-vinil imidazol como monómero) previa funcionalización de la superficie de las nanopartículas con grupos $–NH_2$ [recubrimiento con (3-aminopropil)trietoxisilano (APTES)]. El nanomaterial preparado presenta un máximo de RTP a 595 nm tras la excitación a 289 nm. El sensor químico de cribado luminiscente resulto ser selectivo para iAs, no observando atenuación de la RTP en presencia de especies orgánicas de As y de otros iones mayoritarios en extractos de productos marinos. El método de cribado desarrollado ofrece un límite de detección de 29,6 $\mu g\ kg^{-1}$, valor inferior al máximo permitido por la UE en relación al contenido de iAs en alimentos (arroz). Por otra parte, los resultados de cribado para iAs son comparables a los obtenidos tras aplicar metodologías avanzadas como HPLC-ICP-MS a muestras de pescado y a materiales de referencia certificados (CRMs) después de un procedimiento UAE con metanol y agua como mezcla extractante para extraer las especies de As.

Una metodología similar de trabajo se llevó a cabo para un cribado luminiscente (RTP) de Hg total en productos de la pesca (Capítulo 4). Se empleó igualmente un núcleo luminiscente de Mn-ZnS QDs recubiertos en superficie con una doble capa de sílice [empleo de tetraetoxisilano (TEOS) para una funcionalización con grupos –OH, y APTES para una funcionalización con grupos $–NH_2$]. Se llevaron a cabo distintas síntesis de IIPs sobre la superficie modificada del QD, siendo la más prometedora aquella que empleaba fenobarbital como monómero funcional y ácido metacrílico (MMA) como monómero vinilado (técnica de atrapamiento del ion plantilla, en ese caso MeHg). Sin embargo, el fuerte enlace del ion plantilla con

el monómero auxiliar dificultó enormemente la etapa de la eliminación del mismo (procedimiento necesario para que queden disponibles las cavidades de reconocimiento iónico). En condiciones suaves de eliminación, la cantidad de ion plantilla eliminada fue insignificante; por el contrario, empleando condiciones de extracción enérgicas y disoluciones fuertemente ácidas, se lograba extraer la plantilla pero se perdía parte del polímero sobre la superficie del QD. Además, las propiedades luminiscentes del QD se alteraban tras estos procedimientos drásticos de eliminación del ion plantilla. La estrategia que se propuso fue la de llevar a cabo una síntesis del polímero en ausencia del ion plantilla (MeHg), formalmente sintetizar un MIP para el fenobarbital (molécula plantilla). Dado que el fenobarbital es muy selectivo tanto para el ion Hg(II) como para el MeHg, se decidió emplear el composito generado con este MIP (sin eliminación de la molécula plantilla de fenonarbital) para el reconocimiento selectivo de Hg(II) y MeHg.

Igualmente que en la fase sensora diseñada para iAs (Capítulo 1), el composito presenta un máximo de RTP a 595 nm tras la excitación a 289 nm, pero en este caso la atenuación de la RTP se observa únicamente cuando los iones Hg(II) y MeHg están presentes. El sensor RTP desarrollado ofrece un límite de detección de 68,2 μg kg^{-1}, valor inferior al límite máximo permitido por la UE (entre 0,5 y 1,0 mg kg^{-1} según la especie de pescado). Los resultados de Hg total obtenidos en muestras de pescado y en CRMs por el método RTP (UAE con ácido clorhídrico 5,0 M como extractante) son similares a los medidos tras aplicar una metodología ICP-MS (digestión ácida asistida por microondas como pretratamiento de la muestra).

La proporción de iAs en los productos de la pesca es muy pequeña en comparación con las especies orgánicas de As, especialmente la AB, que puede llegar a representar el 90% del As total. Al llevar a cabo la especiación de As por HPLC las elevadas señales cromatográficas para AB a menudo dificultan la integración de las pequeñas señales de las especies As(III) y As(V), y en muchas de las aplicaciones apenas se determinan las concentraciones de estas especies inorgánicas minoritarias. En el Capítulo 2 se describe la síntesis de un IIP para su empleo como nuevo absorbente en SPE para

iAs. La alta selectividad esperada para este absorbente hace que únicamente las especies minoritarias de iAs sean preconcentradas, facilitando su detección por HPLC-ICP-MS e impidiendo que las señales debidas a los compuestos mayoritarios de As interfieran. La síntesis del IIP se llevó a cabo mediante un procedimiento de polimerización mixto entre la polimerización por bloque y la polimerización por precipitación (exceso de porogen con respecto a lo requerido para la polimerización por bloque, pero porogen en defecto respecto al requerido para la polimerización por precipitación). Las condiciones para una polimerización por precipitación requerían un volumen de porogen para el cual la síntesis del IIP mostró muy poco rendimiento. Por el contrario, a medida que se disminuía el volumen de porogen el rendimiento de la síntesis era mayor. El volumen de porogen seleccionado, considerablemente mayor que el requerido para la polimerización en bloque, permitió obtener partículas dispersas de IIP, de forma similar a una polimerización por precipitación. En la síntesis se empleó arseniato como ion plantilla y 1-vinil imidazol como monómero bifuncional. El absorbente preparado se utilizó en el desarrollo de un procedimiento SPE en columna para preconcentrar selectivamente iAs en extractos de pescado (previa extracción por UAE). El procedimiento de preconcentración con el IIP sintetizado resultó altamente selectivo para iAs, obteniéndose cromatogramas donde solamente aparecen dos señales cromatográficas, las debidas a las especies iAs (As(III) y As(V)). El procedimiento, además, es altamente sensible, obteniéndose límites de detección de 0,32 and 0,39 $\mu g\ kg^{-1}$ para As(III) y As(V), respectivamente (valores por debajo de los límites máximos establecidos en la UE para arroz).

El IIP previamente descrito en el Capítulo 2 se ha utilizado también en la optimización de una metodología de microextracción para iAs en arroz (Capítulo 3). En concreto, se desarrolló una técnica de microextracción dispersiva asistida por agitación vórtex y empleando una pequeña cantidad de IIP (*ionic imprinted polymer – vortex assisted dispersive micro-solid phase extraction*, IIP-VA-D-μ-SPE). La extracción de las especies de As se optimizó empleando sonda de ultrasonidos, que resultó ser más eficaz que el baño de ultrasonidos para la matriz de arroz. El procedimiento IIP-VA-D-μ-

SPE requirió tan solo 50 mg del absorbente, pudiendo cada porción de 50 mg ser reutilizada al menos 20 veces sin perder las capacidades de absorción selectiva. El límite de detección obtenido con esta técnica de preconcentración fue menor para la especie As(III) (0,20 μg kg^{-1}) en comparación con la metodología SPE (0,32 μg kg^{-1}); sin embargo, el límite de detección para la especie As(V) (0,41 μg kg^{-1}) fue similar al obtenido con el procedimiento convencional (0,39 μg kg^{-1}).

A diferencia de los moderados niveles de Hg en productos marinos como el pescado y los mariscos, el Hg se encuentra a niveles ultratraza en las algas marinas. Por tanto, para evaluar la presencia de este elemento altamente tóxico en este tipo de alimento, y a diferencia de lo que ocurre en pescados y mariscos, se requiere el desarrollo de procedimientos previos de preconcentración de las especies mercuriales. De esta forma, en el Capítulo 5 se describe la síntesis de un IIP selectivo a Hg (Hg(II) y MeHg) el cual se ha empleado como absorbente selectivo para SPE en columna en la preconcentración de trazas de Hg(II) y MeHg en algas marinas comestibles (previa extracción de las especies de Hg por UAE empleando una mezcla de ácido clorhídrico 0,1% (v/v), L-cisteína al 0,12% (m/v) y mercaptoetanol al 0,1% (v/v)). La síntesis del IIP se llevó a cabo con la técnica de la polimerización por precipitación y atrapamiento del ion plantilla (MeHg), empleando fenobarbital como monómero funcional y MAA como monómero vinilado. En este caso, la eliminación del ion plantilla requirió de condiciones moderadas (disolución de ácido clorhídrico 1,0 M y tiourea 1,0 M) que no dañaron los sitios de reconocimiento iónico generados en el polímero. El IIP sintetizado resultó ser selectivo para especies de Hg teniendo además una alta capacidad de carga. El procedimiento IIP-SPE desarrollado junto con la instrumentación HPLC-ICP-MS ha permitido llevar a cabo una determinación altamente sensible, consiguiendo límites de detección de 0,007 y 0,02 μg kg^{-1} para Hg(II) y MeHg, respectivamente. Los resultados obtenidos en el análisis de un CRM para pescado fueron concordantes tanto para el contenido de Hg total como para el contenido de MeHg. Las muestras de algas analizadas arrojaron niveles de Hg total (como suma de las concentraciones de Hg(II) y MeHg, tras el proceso de extracción UEA, preconcentración

IIP-SPE y HPLC-ICP-MS) similares a las obtenidas tras el proceso de extracción UEA, preconcentración IIP-SPE e ICP-MS.

USC
UNIVERSIDADE
DE SANTIAGO
DE COMPOSTELA

VI. ANNEX II

LIST OF PUBLICATIONS

USC
UNIVERSIDADE
DE SANTIAGO
DE COMPOSTELA

List of publications

1. K.K. Jinadasa, E. Peña-Vázquez, P. Bermejo-Barrera, A. Moreda-Piñeiro, New adsorbents based on imprinted polymers and composite nanomaterials for arsenic and mercury screening/speciation: A review, Microchemical Journal, 156 (2020) 104886.
   DOI: https://doi.org/10.1016/j.microc.2020.104886

2. K.K. Jinadasa, E. Peña-Vázquez, P. Bermejo-Barrera, A. Moreda-Piñeiro, Synthesis and application of a surface ionic imprinting polymer on silica-coated Mn-doped ZnS quantum dots as a chemosensor for the selective quantification of inorganic arsenic in fish, Analytical and Bioanalytical Chemistry, (2020).
   DOI: https://doi.org/10.1007/s00216-020-02405-1

3. K.K. Jinadasa, E. Peña-Vázquez, P. Bermejo-Barrera, A. Moreda-Piñeiro, Ionic imprinted polymer solid-phase extraction for inorganic arsenic selective pre-concentration in fishery products before high-performance liquid chromatography – inductively coupled plasma-mass spectrometry speciation, Journal of Chromatography A, (2020) 460973.
   DOI: https://doi.org/10.1016/j.chroma.2020.460973

4. K.K. Jinadasa, E. Peña-Vázquez, P. Bermejo-Barrera, A. Moreda-Piñeiro, A phenobarbital containing polymer/ silica coated quantum dot composite for the selective recognition of mercury species in fish samples using a room temperature phosphorescence quenching assay, Talanta, 216 (2020) 120959.
   DOI: https://doi.org/10.1016/j.talanta.2020.120959

USC
UNIVERSIDADE
DE SANTIAGO
DE COMPOSTELA